Acta Universitatis
Lappeenrantaensis
805

Emmanuel Afrane Gyasi

ON ADAPTIVE INTELLIGENT WELDING: TECHNIQUE FEASIBILITY IN WELD QUALITY ASSURANCE FOR ADVANCED STEELS

LUT
Lappeenranta
University of Technology

Emmanuel Afrane Gyasi

ON ADAPTIVE INTELLIGENT WELDING: TECHNIQUE FEASIBILITY IN WELD QUALITY ASSURANCE FOR ADVANCED STEELS

Thesis for the degree of Doctor of Science (Technology) to be presented with due permission for public examination and criticism in the lecture hall 2305 at Lappeenranta University of Technology, Lappeenranta, Finland, on the 28th of August, 2018, at noon.

Acta Universitatis
Lappeenrantaensis 805

Supervisors Associate Professor, Docent Paul Kah
LUT School of Energy Systems
Lappeenranta University of Technology
Finland

Professor Heikki Handroos
LUT School of Energy Systems
Lappeenranta University of Technology
Finland

Reviewers Professor Suck-Joo Na
Department of Mechanical Engineering
Korea Advanced Institute of Science and Technology
South Korea

Professor Victor A. Karkhin
Department of Mechanical Engineering
Peter the Great St. Petersburg Polytechnic University
Russia

Opponents Professor Suck-Joo Na
Department of Mechanical Engineering
Korea Advanced Institute of Science and Technology
South Korea

Professor Victor A. Karkhin
Department of Mechanical Engineering
Peter the Great St. Petersburg Polytechnic University
Russia

ISBN 978-952-335-251-3
ISBN 978-952-335-252-0 (PDF)
ISSN-L 1456-4491
ISSN 1456-4491

Lappeenrannan teknillinen yliopisto
Yliopistopaino 2018

Abstract

Emmanuel Afrane Gyasi
On adaptive intelligent welding: technique feasibility in weld quality assurance for advanced steels
Lappeenranta 2018
100 pages
Acta Universitatis Lappeenrantaensis 805
Diss. Lappeenranta University of Technology
ISBN 978-952-335-251-3, ISBN 978-952-335-252-0 (PDF), ISSN-L 1456-4491, ISSN 1456-4491

The welding industry has a need to utilize lightweight steels in welded applications while maintaining acceptable weld quality. This goal can be achieved through effective quality assurance, efficient weld parameter decision-making systems, and careful choice of steel grades. Consequently, there is a need for: i) knowledge enabling manufacturers to select appropriate lightweight material to meet the requirement for reduced structural weight and attain cost reduction in welding manufacturing; and ii) new ways to assure weld quality in real-time, ideally with welding systems that are self-adjusting and able to eliminate welding flaws during welding. Concurrent with this evolution towards lighter structures, the next phase in modern manufacturing, Industry 4.0, is also driving welding industries to digitization of manufacturing using advanced welding technologies. The Industry 4.0 concept aims to harness emerging digital technologies for enhanced quality, connectivity, productivity, and environmental and economic gain via improved reliability in manufacturing and production. Greater integration of evolving technologies in automation, digitization and artificial intelligence (AI) are required in welding manufacturing to realize a sustainable future industry.

The objectives of this thesis are to provide an overview of weld integrity aspects of advanced steels, that is, high strength steels (HSS) and ultra high strength steels (UHSS), and through experimental study to explore the applicability of adaptive intelligent robotic gas metal arc welding (GMAW) of UHSS for structural applications. Additionally, the study aims to utilize the findings from experimental work in the design of a new weld quality assurance model based on adaptive intelligence. This aspect is grounded on the concept of Industry 4.0 and the "big data" involved in systems integration processes (automation, robotics, sensory, monitoring and artificial intelligent systems).

The thesis is an article-based study comprising the outcome of five research articles. Research methods used include both review of previous work and experimental study. Review of the weldability of HSS and UHSS showed that these steels have high susceptibility to heat affected zone (HAZ) softening when they are welded at elevated temperatures and with imprecisely controlled heat input. Additionally, a risk of cold cracking and a propensity to weld integrity problems arises when the steels are welded with filler materials having high hydrogen content and varying strength. The experimental studies indicated the feasibility of effectively welding these steels with accurately modelled and controlled welding heat conditions. The welding of direct-quenched UHSS

S960QC material in fillet joint configurations in different welding positions with an adaptive intelligence welding system demonstrated the possibility of real-time process monitoring, process outcome prediction, and control of welding parameters and variables in robot welding with the aim of achieving desired weld quality. The behaviour of welding parameter control and adaptation and their effects correlate with the consequential changes in the macrostructure, mechanical properties and microstructure of the weldments.

A new weld quality assurance model based on adaptive intelligence systems is examined and presented with detailed steps. The model aims to assist welding companies, large and small and medium-sized enterprises (SMEs), in their decision-making, and to contribute to efforts to integrate and advance the implementation of adaptive welding systems in manufacturing and production networks. The new weld quality assurance model facilitates digitization of weld quality and quality assurance processes to improve weld quality, eliminate or reduce already at the commissioning stage weldments with defects, maintain a digital history of the welding operation for optimization and development purposes, reduce rework, trace weld defects digitally and in real-time, and define and approve welding procedure specification (WPS) in digital formats. In addition to the fundamental aim of weld quality assurance, additional benefits for welding companies include opportunities to network with other robot cells in other companies and firms and synchronize adaptive welding systems on a global level for common welding production throughput.

Keywords: High strength steels, ultra high strength steels, robotic GMAW process, adaptive welding, artificial neural network, weld quality assurance, intelligent systems.

Preface

Having the privilege to do doctoral studies is the opportunity of a lifetime. Such work enables continuous personal growth and the development of knowledge in a specific field of endeavour. It helps broaden horizons and gives a platform to connect with other experts, which might otherwise not be possible. A doctoral degree brings the holder increased status in the area of specialization, as a result of improved expertise, but also brings the obligation to contribute to society, industry and the world as a whole. My journey through doctoral study has been an eye opener for both personal and career development. It has provided the basis for my understanding of entrepreneurial thinking, which is informed by the requirement for effective and innovative decision-making, and sustainable value creation. Throughout this journey, I have endeavoured to share my knowledge and contribute in diverse ways. In Finland, I have acted as a bridge for the transfer of ideas on technology-related business between Finland and Ghana. In Ghana, I have endeavoured to contribute by helping to develop welding training programs in local companies and educational institutions. As the founder of a non-governmental and not-for-profit organization, my vision has been to promote and accelerate the development of welding training and learning in West Africa, and to advocate for greater appreciation in the region of the importance of health, safety and environmental issues in welding. The organization aims to familiarize about 1000 new welders, many of them women, with internationally established welding norms and expose them to international welding practices. My doctoral studies are a collection of experiences from both the academic and the industrial world. My industrial experience stared in the latter part of 2014 when I had the opportunity to do a doctoral internship in Canada. I worked as a structural welder in a fabrication company producing welded structures for the oil and gas industry. Conventional steels were mostly used in the fabrication of the oil and gas production units, sand filtration units, etc. As most of the oil production units were mounted on trailers, the need to use lightweight steels to reduce weight on the trailers and to minimize fuel consumption became a concern. Having become aware of the importance of this issue, I was motivated to investigate lightweight steels as a part of my doctoral studies. Returning to Finland in 2015, I made several visits to local fabrication companies to identify the extent of the need for greater use of lightweight steels in their product manufacturing. Similar concerns to their Canadian colleagues were expressed. During the latter part of 2015, I had the opportunity to use industrial robots in welding of lightweight steel plates. During this work, I identified some drawbacks in present-day industrial robots, in particular the inability of current welding robots to adapt in real-time to changes in the welding environment. Repeated precision errors sometimes occurred, which led to the production of bad quality welds. My interest in adaptive welding systems encouraged me to maintain and strengthen my contacts with original equipment manufacturers (OEM) of welding equipment, robots, lasers and sensors. I then had the privilege to work for an adaptive welding project at the Laboratory of Welding Technology, Lappeenranta University of Technology (LUT) in mid-2017 and the Manufacturing 4.0 project of the Laboratory of Intelligent Machines in 2018.

I remain grateful and thankful to you all who encouraged and helped me travel this far.

Acknowledgements

My profound thanks go to my supervisor, Associate Professor Paul Kah, for his encouragement and sincere support throughout this work. I call you "Prof" because of your selfless attitude, professionalism in research, patient and attentive attitude, international outlook, and willingness to help regardless of time. Thanks for devoting your precious time to my concerns and my research work. You shared ideas with me at all times, and sometimes even at dawn. Can any supervisor be as motivating as you are? The relationship we have built over these years has become as hard as steel, and our hearts are welded together. I have learned so much from you "Prof". I am grateful you took me as one of your protégés. Truly, mentorship is your flagship. "*Merci beaucoup"*.

My sincere thanks go to my second supervisor, Professor Heikki Handroos, whose financial support has helped me to complete my studies. Dear Professor Heikki, I am very grateful to you. I am very glad for the trust we are building together. "*Kiitos paljon*".

Special thanks to Peter Jones. Sir, you have played an important role as an internal reviewer in many ways. Your comments and English language checks on my scripts are revealing and profound. Also, thanks to the external reviewers of this work, Professor Suck-Joo Na and Professor Victor A. Karkhin. I am very grateful that you agreed to review my work and thank you for taking the time to help me complete my apprenticeship as a researcher.

I would like to thank Professor Emeritus Jukka Martikainen for his support during the early years of my research. My thanks go to all the staff of the Laboratory of Welding Technology and my colleagues from the Department of Mechanical Engineering, whose assistance made this work a reality. I would like to express my gratitude to Esa Hiltunen, Docent Huapeng Wu, Dr. Markku Pirinen, Raimo Suoranta and Dr. Juho Ratava. To my research colleagues and friends, Dr. Eric Mvola Belinga and Dr. Pavel Layus, I have learnt from you how to be patient in research. I say thanks for this and for the support you have given me in many other ways. Many thanks to Sakari Penttilä, François Njock Bayock and Charles Nutakor for their support.

Special thanks to my friend Martin Appiah Kwame Kesse for his encouragement and support throughout my journey on this work. Kwame, we have been in this struggle together, in the snow, rain and sunshine. It seems that I am nearing the end of this particular journey, but your destination is still ahead. I will not leave you to travel alone. Also, special thanks to my brother Enoch Afrane Gyasi and to my long standing friend Dennis Mireku Sasu for their encouragement and unflinching support.

To Antero Jernberg from the Lappeenranta Employment and Economic Development Office (TE Office), thanks so much for your encouragement and support. Thanks to Jukka Vasara from Sampo Saimaa Adult Vocational College and Jouni Verhelä for taking me through practical training in welding and robotics respectively. Also, thanks to Markus Melander, Ilkka Rautianen, Hannu Ylisiurua and Jarmo Ihalainen for their encouragement.

To my fathers – Mr. Peter Afrane Gyasi (deceased), Mr. John Ofori Gyasi, Mr. Kwasi Gyamfi Gyasi, Mr. Kojo Anyimadu, and Mr. Kofi Karikari Gyasi. I say thank you all for your fatherly love and contribution in my life.

I would like to say a big thanks to my Mother, Susuana Baidoo, for her love, care and constant encouragement on my journey in this work. Oh "Mama Suzzy", words cannot describe my appreciation to you. This hard-earned piece of work is for you.

To my beloved wife, Johanna Mustonen-Gyasi, and my beautiful daughters, Jenni Riina Susuana Gyasi and Adiella Petra Alina Gyasi, I say special thanks to you all. You are the last on my list but you are also the first – the foundation and source of energy for this work. Without your support and love, I would not have made it this far. To God be the glory. God bless you all.

Emmanuel Afrane Gyasi
August 2018
Lappeenranta, Finland

Dedication

To my mother Susuana Baidoo
And
To the entire Gyasi & Mustonen family

Contents

List of publications

This thesis is based on the following scientific publications. The rights have been granted by the publishers to include the publications in the dissertation.

I. Gyasi, E.A., Kah, P. (2016). Structural integrity analysis of the usability of High Strength Steels (HSS). *Reviews on Advanced Materials Science*, 46, pp. 39-52.

II. Gyasi, E.A., Kah, P., Wu, H., Kesse, M.A. (2017). Modelling of an artificial intelligence system to predict structural integrity in robotic GMAW of UHSS fillet welded joints. *The International Journal of Advanced Manufacturing Technology*, 93 (1-4), pp. 1139-1155.

III. Gyasi, E.A., Kah, P., Ratava, J., Kesse, M.A., Hiltunen, E. (2017). Study of adaptive automated GMAW process for full penetration fillet welds in offshore steel structures. *Proceedings of the Twenty-seventh (2017) International Ocean and Polar Engineering Conference, San Francisco, CA, USA, June 25-30*, pp. 290-297.

IV. Gyasi, E.A., Kah, P., Handroos, H., Layus, P., Lin, S (2018). Adaptive welding of S960QC UHSS for Arctic structural applications. *International Review of Mechanical Engineering*, 12 (4).

V. Gyasi, E.A., Pirinen, M., Martikainen, J., Nallikari, M (2015). Transforming Arctic welding with Finnish technological know-how. *Canadian Welding Association (CWA) Conference and the International Institute of Welding (IIW) International Congress*, Vancouver, Canada, September 28-October 1, 2014.

Author's contribution

Emmanuel Afrane Gyasi is the principal author and investigator in papers I – V. The ideas and experiments for all the papers were generated and constructed by the author. The co-authors assisted in performing the experiments and evaluation of the findings as well as reviewing and improving the papers.

Other scientific publications

- Layus, P., Kah, P., Kesse, M., Gyasi, E.A. (2017). Submerged arc welding productivity in welding thick high strength steel plates used for Arctic applications. *Proceedings of the Twenty-seventh (2017) International Ocean and Polar Engineering Conference, San Francisco, USA, June 25-30*, pp. 92-98.
- Kesse, M., Gyasi, E.A., Kah, P. (2017). Usability of laser-TIG hybrid welding processes. *Proceedings of the Twenty-seventh (2017) International Ocean and Polar Engineering Conference, San Francisco, USA, June 25-30*, pp. 42-49.
- Yang, X., Kah, P., Gyasi, E.A., Martikainen, J. (2016). Risk management system and execution in welding for offshore and coastal constructions. *Proceedings of the Twenty-sixth (2016) ISOPE Conference, Rhodes, Greece, July 2*, pp. 92-98.

Nomenclature

In the present work, variables and constants are denoted using *slanted type* and abbreviations are denoted using normal type.

Latin alphabet

A	area	m^2
E	arc energy	kJ/mm
I	arc current	A
U	arc voltage	V
v	welding speed	mm/s
Q	heat input	kJ/mm
c_p	specific heat capacity at constant pressure	J/(kgK)
c_v	specific heat capacity at constant volume	J/(kgK)
d	diameter	m
F	force vector	N
f	frequency	Hz
g	acceleration due to gravity	m/s^2
h	heat transfer coefficient	$W/(m^2K)$
j	flux vector	m/s
L	characteristic length	m
l	length	m
m	mass	kg
p	pressure	Pa
q	heat flux	W/m^2
r	radius	m
T	temperature	K
t	time	s
U_w	material moving speed	kg/s
V	volume	m^3
v	velocity magnitude	m/s
$\boldsymbol{v}$	velocity vector	m/s
x	x-coordinate (width)	m
y	y-coordinate (depth)	m
z	z-coordinate (height)	m

Greek alphabet

α	alfa
β	beta
γ	gamma
Δ	capital delta
δ	delta
ε	emissivity

η	Arc efficiency
θ	theta
ι	iota
κ	kappa
Λ	capital lambda
λ	lambda
μ	mu
π	pi = 3.14159...
ρ	density of metal
Σ	capital sigma
σ	sigma
τ	tau
υ	upsilon
ϕ	phi variant
Ø	oh with stroke
φ	phi
χ	chi
ψ	psi
Ω	capital omega

Dimensionless numbers

Gr	Grashof number
Pe	Peclet number
Fr	Froude number
Rm	Reynolds number
Ma	Surface tension Reynolds number

Abbreviations

AC	Alternating Current
AHP	Analytical Hierarchy Process
AI	Artificial Intelligence
ANFIS	Adaptive Neuro-Fuzzy Inference System
ANN	Artificial Neural Network
API	Application Programming Interface
BM	Base Metal
BOM	Bill of Materials
BP	Back Propagation
BSE	Back Scattered Electron
CAD	Computer Aided Design
CAM	Computer Aided Manufacturing
CCD	Charge-Coupled Device
CEV	Carbon Equivalence
CFD	Computational Fluid Dymanics

CHAZ	Coarsed Grained Heat Affected Zone
CMOS	Complimentary Metal-Oxide Semiconductor
CTWD	Contact-To-Work-Distance
DCEN	Direct Current Electrode Negative
DCEP	Direct Current Electrode Positive
EDS	Energy-Dispersive Spectroscopy
FCAW	Flux Cored Arc Welding
GA	Genetic Algorithm
GMAW	Gas Metal Arc Welding
GTAW	Gas Tungsten Arc Welding
HAZ	Heat Affected Zone
HD	Hydrogen Deuteride
HMI	Human and Machines Interface
HRC	Human Robot Collaboration
HSS	High Strength Steel
HV	Vickers Hardness
IP	Internet Protocol
IRT	Infrared Thermography
ISO	International Organization for Standardization
MAG	Active Gas Metal
MIG	Inert Gas Metal
MLP	Multi-Layer Perceptron
OEM	Original Equipment Manufacturer
QC	Direct Quenched
QT	Quenched and Tempered
PA	Horizontal Flat Welding Position
PB	Horizontal Welding Position
PDM	Product Data Management
PID	Proportional, Integral and Derivation
PSD	Power Spectral Density
PSO	Particle Swarm Optimization
RNN	Recurrent Neural Network
RPC	Remote Procedure Call
SAW	Submerged Arc Welding
SEM	Scanning Electron Microscopy
SMAW	Shielded Metal Arc Welding
SME	Small and Medium-sized Enterprices
TMCP	Thermo-mechanical Controlled Process
TPS	Thermo Profile Sensor
UHSS	Ultra High Strength Steel
UTS	Ultimate Tensile Strength
WM	Weld Metal
WQA	Welding Quality Assurance
WPS	Welding Procedure Specification

1 Introduction

This doctoral thesis describes research that was completed in the Laboratory of Welding Technology of Lappeenranta University of Technology as a part of efforts to contribute to expanding knowledge on adaptive intelligent welding of advanced steels (high strength steels and ultra high strength steels), paying critical attention to the techniques, applications and weld quality assurance issues involved.

This work has received support from Academy of Finland grants for Lappeenranta University of Technology, the Laboratory of Welding Technology project 'Monitoring and Modelling of Advanced Adaptive Welding Process Systems for Ultra High Strength Steel (UHSS), and Laboratory of Intelligent Machines project "Manufacturing 4.0 – Strategies for Technological, Economical, Educational and Social Policy Adoption.

The research methods used in this work are in two parts: review of previous studies as the first part and empirical study as the second part. Review of previous studies on the usability of high strength steels and ultra high strength steels, especially as regards welding conditions is performed. The challenges associated with welding of these advanced steels, in particular UHSS material, are noted. In line with the overall objective of the work of devising a holistic welding quality assurance method to help mitigate the weldability challenges of these advanced steels, the applicability of adaptive welding systems comprising sensors, monitoring devices and an artificial intelligence approach with industrial robots is investigated. The concept of Industry 4.0 is briefly presented to provide the context of the need to use adaptive welding systems in modern factories and to draw attention to trends in modern manufacturing.

The introductory section to this thesis is structured as follows: research background, motivation of the study, research objectives, research questions, overview of the thesis, impact of the work on society and the environment, limitation and scope of the work, and finally the research hypothesis.

This doctoral thesis is valuable for academia and industry as it provides a comprehensive study of the subject of adaptive automated welding systems and artificial intelligence for weld quality prediction, control and assurance when welding advanced steels for structural applications from both the theoretical and empirical perspectives. The theoretical findings can be used to develop and improve knowledge of the subject to gain deeper understanding of welding of advanced steels and the issues involved as well as the applicability of adaptive intelligent welding systems in this era of intelligent manufacturing. Some results of the empirical study can be adopted in welding industry applications, especially the weld quality assurance (WQA) model based on adaptive intelligent systems (AIS), although the model still requires more detailed proof of concept analysis.

1.1 Research Background

Potential structural weight reduction associated with material selection is leading modern welding manufacturing to embrace lightweight materials, because such materials have superior strength-to-weight ratio and mechanical and physical properties. High strength steels (HSS) and ultra high strength steels (UHSS) having tensile strengths between 500–1700 MPa are possible material choices for lightweight manufacturing (Kah, et al., 2014). However, weld quality of these advanced steels remain a subject of concern when considering, for example, structural integrity in the context of usability in welding manufacturing and production (Pirinen, 2013; Kah, et al., 2014; Björk, 2012). These issues noted in welding of such advanced steels are the reasons for investigating the usability of HSS and UHSS for welded joints. In addition, the prevailing industrial and societal environment towards Industry 4.0 is driving welding manufacturing industries to employ evolving welding technologies for efficient, effective and reliable manufacturing and production. This paradigm shift is a result of factors including cost in manufacturing, structural integrity, digitization and other issues. Greater integration of evolving technologies such as digitalized welding systems and artificial intelligence (AI) systems is required to realize the goals of sustainable future industry, especially in the area of solving challenging problems pertaining to weld quality in welding manufacturing and production globally. Figure 1 shows the schematic framework of the research and the approaches considered, with follow up steps from level 1 to level 7, as explained explicitly in subsequent chapters.

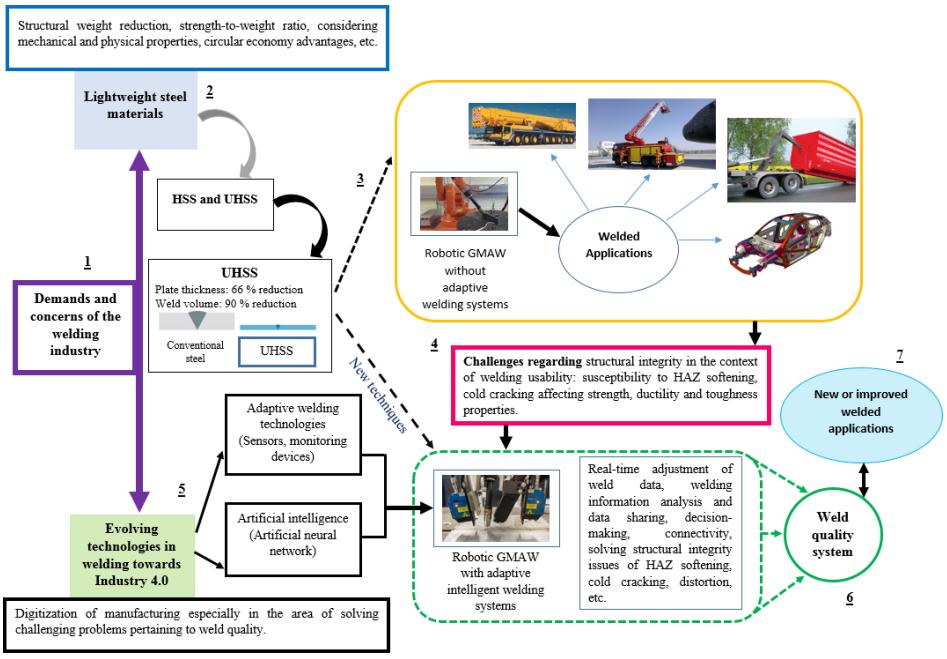

Figure 1. Schematic framework of the research.

1.1.1 Usability of HSS and UHSS for welded joints

High strength steels (HSS) and ultra high strength steels (UHSS), denoted in this work as advanced steels, are in increasing demand because their superior physical and mechanical properties, such as strength-to-weight ratio, and low-temperature properties permit their use in a wide range of industrial applications. Typically, HSSs, which are produced as quenched and tempered steels (QT) and thermomechanical controlled process steels (TMCP), are of yield strength between 500–900 MPa. QT steels are produced through a controlled heating, and a quenching and tempering process, whereas TMCP steels are produced using controlled heating and a controlled or accelerated cooling process. QT steels have higher carbon equivalence and lower alloying elements than TMCP steel of the same yield strength. The microstructure of QT steels is mainly martensitic-bainitic, while that of TMCP steels is ferritic-bainitic. QT and TMCP steels have similar physical properties such as good strength-to-weight ratio, high load carrying capacity, good weldability and improved service life in harsh conditions (Billingham and Sharp, 2003; Hill, 1991). It has been reported that QT steels can operate at very low temperatures down to -40 ^{o}C and have better low-temperature properties than TMCP steels of the same yield strength and thickness (Billingham and Sharp, 2003). QT steels possess higher toughness and good ductility properties at very low temperatures between -50 to -60 ^{o}C, at minimum impact energy of 27 J (WTIA TN 15, 1999). The physical behaviour of QT and TMCP steels to withstand low temperatures shows improved mechanical strength when compared with conventional steels. *Publications I* and *V* give more detailed descriptions of these steels.

HSS and UHSS steels have predominantly been used in the automotive industry for strength reinforcement. Nowadays, however, the material is being utilized in many different industries, for example, in crane manufacturing, frames of lumber carriers (Pirinen, 2013), and in Arctic structural constructions and shipbuilding (Layus, 2017). UHSS is produced through hot strip rolling, direct quenching and levelling (Porter, 2006). UHSS has higher yield strength, up to 1700 MPa, and offers a unique combination of qualities for specialist applications in the lightweight automotive industry and mobile heavy equipment manufacturing (Kah, et al., 2014). The usability of UHSS has also received attention in the research area of fatigue and fracture of welded UHSS components (Dabiri et al., 2016; 2017; Dabiri and Björk, 2017).

Although the potential application area of such advanced steels is enormous, and they extend possible utilization of steel structures to applications for which conventional steels are of less advantage, there are challenges in their usage when welding conditions are not controlled sufficiently accurately. It has been reported that manufacturing methods, types of alloying elements, material properties and quantity of alloying elements, type of filler materials, heat input and cooling time, welding methods and automation need to be carefully considered and specifications, limits and parameters strictly observed when welding advanced steels (Pirinen, 2013; Kah, et al., 2014; Björk, 2012). Improper combinations of these factors, especially heat inputs and filler materials, lead to susceptibility to heat affected zone (HAZ) softening and cold cracking, thus affecting the

strength, ductility and toughness properties of the welded joints (Pirinen, 2013; Kah, et al., 2014; Björk, 2012; Wang, et al., 2003; Juan, et al., 2003).

It is claimed that high heat input decreases impact toughness and reduces strength and ductility, as it promotes grain growth (coarse lath bainite and soft ferrite) in the coarse grained HAZ (CGHAZ) (Liu et al. 2007). Figure 2 shows the temperature curve, the various weld zones and microstructure during welding of steels (Pirinen, 2013). It is reported that S960QC UHSS HAZ softening is caused by HAZ peak temperatures in the range of 450–850 °C (Hemmilä, et al., 2010), as depicted in Figure 2.

High heat input has the tendency to diffuse alloying elements and consequently produces slower cooling rates. For HSS, the following heat inputs and cooling rates have been suggested for plate thickness ≥ 8 mm: 1.31–1.86 kJ/mm ($t_{8/5}$ between 10–20 s) (Wang et al. 2003; Juan et al. 2003); and 0.5–1.7 kJ/mm ($t_{8/5}$ between 5–20 s) (Pirinen, 2013). For UHSS, the following heat inputs and cooling rates have been suggested for plate thickness ≥ 5 mm: 0.5 kJ/mm ($t_{8/5}$ not exceeding 15 s) (Ruukki, 2007); and plate thickness ≥ 8 mm: 0.6 kJ/mm ($t_{8/5}$ not exceeding 10 s) (Björk, 2012). Correspondingly, using filler material of high hydrogen content can yield hydrogen induced cracking in the HAZ when welding HSS and UHSS (Ruukki, 2007).

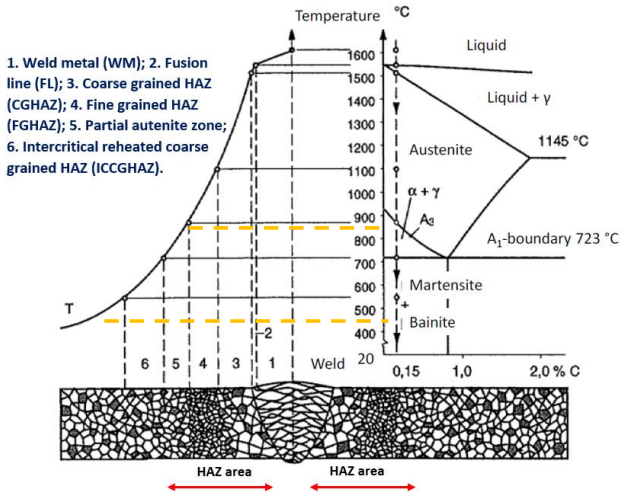

Figure 2. Temperature curve, the various weld zones and microstructure during welding of steels. Modified (Pirinen, 2013).

Notably, the use of undermatched filler material is preferred in welding of HSS and UHSS to matched and overmatched filler materials (Porter, 2006). Undermatched filler materials produce weld metal of lower micro-hardness (mismatch) than the hardness of the base metal. Undermatched filler metal thus produces weld metal whose strength is less than the strength of the base metal. Undermatched filler metals are used in applications where

bending, compression, shear and cracks are major operating factors due to the ability of undermatched filler to mitigate such phenomena and minimize hydrogen induced cracking. Undermatched fillers are mostly suitable for partial joint penetration welds like fillet welds, since they produce low yield points having less residual stress on the base metal, while matched filler metals are suitable for complete joint penetration in tension applications (Miller, 1997). The properties of undermatched filler materials correlate with higher elongation, higher impact toughness and better ductility properties. When using undermatched filler materials, the weakest point of the welded joint is in the weld metal and not in the HAZ. Matched and overmatched filler materials, on the other hand, produce the weakest point in the HAZ, which is undesirable (Björk, 2012).

Figure 3 presents a graph of yield and tensile strengths for three different welds of direct-quenched UHSS S960QC made with matched filler material (X96), slightly undermatched filler material (OK 13.31) and undermatched filler material (OK 12.64). The same heat input range of 0.6 kJ/mm was used for all welds. It can be observed that the welds with slightly matched and matched filler materials have the lowest ultimate tensile strength (UTS) in the HAZ, while the lowest tensile strength of the welds with undermatched filler material is located near the weld metal. It can be suggested that high heat input above 0.6 kJ/mm could have a detrimental effect on undermatched, matched and overmatched filler materials when welding UHSS. Heat input values for matched and overmatched filler materials must not be used for undermatched filler materials since the mechanical properties across the weld joint deteriorate. It is recommended that when using undermatched welds in joints where load carrying capacity is required, the throat thickness must be large, taking into consideration the thickness of the base metal (BM) (Björk, 2012). Matched and overmatched welds are in most cases suitable for load carrying purposes but the effects of the softened HAZ must be considered (Björk, 2012).

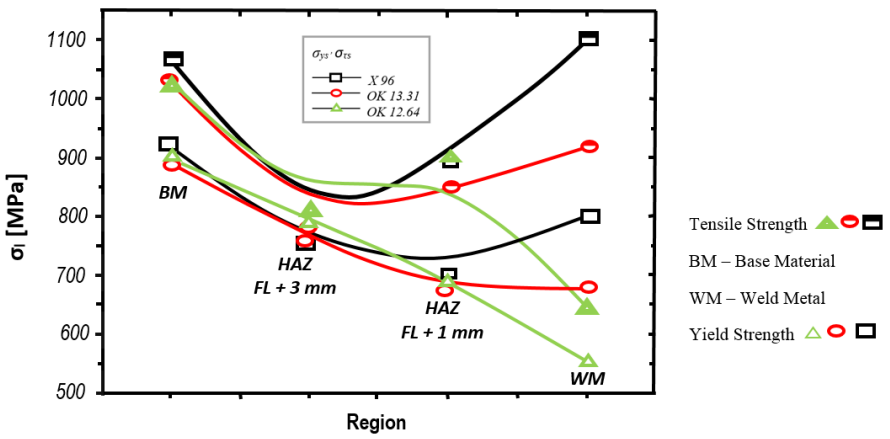

Figure 3. Strength of filler materials in terms of joint region of S960 UHSS weld. Modified (Björk, et al., 2012).

Welding of these lightweight advanced steels seems cumbersome due to several nonlinear factors that need to be considered. Furthermore, information on automation aspects of welding of advanced steels, especially UHSS, is somewhat limited. In a context of vastly increased usage of advanced steels, it is clear that the potential of automated adaptive welding systems should be harnessed. A robust weld quality assurance system based on automated adaptive systems to monitor and adjust the performance of the process to achieve precise welding outputs toward obtaining desired mechanical properties and service requirements of weldments should also be developed. Considerations for such developments are presented in subchapter 1.1.2.

1.1.2 Adaptive welding using industrial robots

In industrial welded product manufacturing and production, industrial robots play an integral role in automated welding, with GMAW being the most frequently used fusion welding process because of its flexibility and adaptability. The advent of better sensor systems has increased the benefits of using robotic welding and has enabled improvements in productivity and repeatability, precision, cost savings and quality in manufacturing and production. Recent developments in process monitoring have included the adoption of techniques like infrared thermography as an adaptive feature for real-time weld quality monitoring in robotic welding. In recent times, the capabilities of intelligent systems like artificial neural networks for control purposes and to handle nonlinear characteristics in welding have been noted. Intelligent systems enable the robot to self-adjust to its operating environment, learn new input and output relationships, adapt to previously unknown conditions and react to changes in parameter and variable settings based on decision-making algorithms generated by the intelligent system (Kah, 2015; Garašić, 2015; Pires, 2006). Integrating these systems having automation, digitization and decision-making capabilities could permit a holistic approach to welding quality assurance and enable a system to be developed that can alleviate weld quality problems of the type identified in the welding of UHSS and other lightweight advanced steels.

Industry 4.0, with its focus on automation and data exchange, envisions the transformation of traditional industrial manufacturing into smart manufacturing where the manufacturing systems are able to: i) digitally monitor physical processes and make adaptive intelligent decisions through real-time connectivity, collaboration and communication with humans, machines and sensors (Wang, et al., 2016); and ii) adjust their behaviour in response to diverse situations and requirements based on past experience and learning capabilities (McFarlane, et al., 2003). The use of adaptive welding systems complements the trends and direction forming the basis of the Industry 4.0 concept and such adaptive systems are therefore worth exploring, especially as regards welding quality assurance. With effective automation and data exchange, welding quality assurance processes could be digitized and upgraded to an intelligent level across small and medium-sized enterprises (SMEs) and within large companies. Such intelligent welding quality assurance can be achieved by taking advantage of evolving technologies, such as leading-edge industrial robots, sensor and monitoring systems, and artificial intelligence strategies underpinning the concept of Industry 4.0 (Zhong, et al., 2017).

1.2 Motivation of the study

Changes in modern manufacturing brought on by innovations in process sensoring systems, process control, and processing of big data form the overall manufacturing context of this work. The desire for greater use of advanced steels because of their superior properties, particularly their good strength-to-weight ratio, and challenges noted in welding of such steels are the grounds for study of HSS and UHSS in particular.

Further motivation for the study is provided by:

- The research gap in scientific literature on the relationship between GMAW process mode factors (heat transfer and fluid flow) and their influence on the weldability of UHSS.

The motivation here is to contribute to scientific literature by providing insights and analysis of the influence of process mode factors associated with heat transfer and fluid flow in robotic GMAW of UHSS under different welding conditions.

- Adaptive welding using industrial robots

The motivation here is to contribute to utilization of adaptive intelligent welding systems (integrated automation, digitization and artificial intelligence) in welding of lightweight steels (UHSS) by investigating aspects related to weld quality assurance, and further to develop a weld quality assurance model as a foundation for future development, and to examine its implementation in welding companies, large enterprises and small and medium-sized enterprises (SMEs).

1.3 Research objectives

The first objective of this study is to provide a review of weld integrity aspects of advanced steels, that is, high strength steels (HSS) and ultra high strength steels (UHSS), and through experimental study to explore the applicability of adaptive intelligent robotic GMAW systems in welding, especially of UHSS, for structural applications. Additionally, the study aims to utilize the findings from the experimental work in design of a new weld quality assurance model based on adaptive intelligence. The aims of the various publications included in this work were crafted to reflect the main objective of the study.

1.4 Research questions

This work aimed to clarify and find solutions to the research questions and problems listed below:

1) What are the criteria to consider when examining the usability of advanced steels (HSS/UHSS) in welding manufacturing and production? [This issue is addressed in *Publication I, II* and *V*.]
2) What are the interactions between the forces in heat transfer and fluid flow during GMAW of UHSS in fillet joint configurations? [This issue is addressed in chapter 2 of the thesis.]
3) What influence does an adaptive robotized welding system have on weld quality? [This issue is addressed in *Publication II, III* and *IV*.]
4) What are the requirements and steps to consider when developing an adaptive intelligent robotized welding system for weld quality assurance? [This issue is addressed in *Publication II, III* and *IV* and in chapter 2 and 4 of the thesis.]
5) Can a weld quality assurance model based on an adaptive intelligent system be developed such that it enhances communication and information sharing, and offers integration of product data systems for reliable manufacturing? [This issue is addressed in chapter 4 of the thesis.]

1.5 Overview of the work

Chapter 1 provides the background of the thesis and the main introduction to the work. Due to the multi-disciplinary nature of the work, the background is described from two points of view: Usability of HSS and UHSS for welded products; and adaptive intelligent welding using industrial robots. The term, advanced steels, is introduced as an umbrella term for HSS and UHSS. The potential use of an adaptive robotic GMAW process to weld these steels is considered. The concept of Industry 4.0 and the benefits it brings to adaptive manufacturing are also presented briefly. Preliminary considerations and initial steps in the development of a welding quality assurance system based on an adaptive welding system are presented. The following subchapters give the motivation of the study, research objectives, research questions, impact of the study on society and environment, limitation and scope, and the research hypothesis of the work.

Chapter 2 describes the state of the art of the GMAW process, robotic welding, sensing and monitoring systems for welding, modelling of robotic GMAW, and artificial intelligent systems for control and decision-making in welding. This chapter supplements and extends the review of previous work in the publications included as part of this thesis.

Chapter 3 presents the research method and procedures used in the publications. The research objectives of the publications are presented with brief descriptions of the approaches used. The adaptive welding systems used in the experimentation are also described, as well as the mechanical and chemical properties of the base metal and consumables. The welding procedures, parameters and variables considered in the empirical study are presented. In addition, material preparation before and after the welding experimental work is described. A summary of the findings of *Publications I, II*

and *V* are given, and the results of *Publication III* and *IV*, including some discussion, are presented.

Chapter 4 presents a new welding quality assurance model based on adaptive intelligent systems. Developing the model required identification and selection of system hardware, system integration protocols and other modelling and system control stages.

Chapter 5 briefly gives suggestions for future research and possible research directions.

Chapter 6 presents the concluding remarks of the thesis, summarizing the results of the theoretical findings and conducted experiments.

1.6 Impact on society and the environment

This study makes a contribution to society and the natural environment from the goal of the work which seeks to evaluate the use of: i) welding of advanced steels and pertinent techniques to mitigate weld quality problems and assure high integrity welded products; and ii) adaptive intelligent systems like robots, sensors and monitoring devices for weld quality assurance purposes and as a way to gain the benefits implicit in the Industry 4.0 concept.

On the societal front, the work contributes to raising greater awareness of quality issues in welding and manufacturing of advanced steels. Assured weld quality and weld integrity when using advanced steels would encourage greater use of such steels and lead to novel designs of high value welded products for both mass production and individualized products. Demand for quality welded products is significant in major industries like automotive manufacturing providing work opportunities and creating jobs. Other welding industries, for example, those involved in heavy manufacturing and fields like shipbuilding and the construction of Arctic structures, would also see a rise in employment opportunities as the demand for strong, lightweight and durable products is considerable. The greater application area resulting from reliable welding of HSS and UHSS would generate new business opportunities.

The importance of addressing adequately the application of adaptive systems is evident in this era of intelligent manufacturing. For example, it has been estimated by the International Federation of Robotics that by 2020 the worldwide stock of operational industrial robots will amount to over 3 million units (IFR, 2017). Making industrial robots more responsive requires the integration of adaptive systems like sensors and monitoring devices. In the specific area of weld quality assurance, the welding industry stands to benefit from welded products of high integrity, improved productivity with shorter lead-time, and uncompromised weld quality due to adaptive robotic systems that have machine learning capabilities.

By addressing the potential of adaptive welding systems, this work provides explicit information to support companies in the welding community on systems integration

aspects related to the framework of Industry 4.0. The future factory, as envisioned in the Industry 4.0 concept, has generated much debate and many innovative suggestions have been made on how to gain maximum benefit from the potential evident in advanced technology. Information about system integration provided in this work can help large companies and SMEs gain a clearer overview of the topic, thus enabling them to strategically plan the implementation of such intelligent systems in their manufacturing and production networks. Requirements from welding contractors keep changing with increasing emphasis on quality, productivity, and effective human robot collaboration (HRC). Meeting these demands would bring greater value to welded products and companies having fully integrated automated intelligent systems, optimized production and improved productivity and efficiency would maintain a high level of competitiveness. By changing traditional production relationships among producers, suppliers and customers and by improving the human machine interface (HMI), adaptive intelligent robotic welding can create substantial numbers of jobs along the value chain.

On the environmental front, the potential of adaptive welding systems can help avert unexpected weld defects which might lead to catastrophic failure in welded products while in operation. The development of advanced welding and adaptive systems make it possible to enhance welding of lightweight materials and improve reliability, quality assurance and weld integrity. Additionally, the concept of a circular economy can be advanced since lightweight welded products can be more easily recycled. The emission of poisonous gases into the atmosphere would be reduced since products made of advanced steels would consume less energy because of their reduced weight. In the automotive industry, the production of lighter weight vehicles would increase and the consumption of fuel per travelled kilometre would decrease. This translates to less pollution of the atmosphere with fumes from vehicle exhausts and the emission of less greenhouse gases. The use of advanced steels and adaptive welding systems can, therefore, support energy saving and drive the agenda of sustainable development and environmental protection.

1.7 Limitation and scope

The findings and conclusions of this work are limited to the advanced steels, welding process, filler materials, sensing devices, monitoring devices and artificial intelligence system studied. The small number of empirical tests, which is a result of a lack of resources, as well as a result of the focus on providing a conceptual overview of key issues and possible approaches, and the absence of computational work are limitations that restrict the outcomes from being generalized. However, the conclusions presented in this work provide a basis for study of other lightweight steels and give an indication of the possible results that could be achieved with adaptive intelligent welding of advanced steels.

The weld quality assurance model presented in this work gives a generalized view for developing case specific models.

1.8 Research hypothesis

Based on the scope of the study, several hypotheses are examined:

a) Advanced steels (structural steels having yield strength between 500–960 MPa and thickness ≥ 5 mm and ≤ 10 mm) can be considered as lightweight steels.
b) When welding advanced steels, selection of welding process and manufacturing setup, heat input levels, cooling rate, filler materials and consumables, weld geometry, weld orientation and control of the fusion process must be carefully considered and critically observed.
c) An adaptive intelligent welding system is capable of providing real-time weld quality assurance data because of the self-monitoring and control features embedded in the system.
d) An adaptive intelligent welding system has the potential to be integrated with engineering design and manufacturing tools (CAD/CAM programs). By creating product data management (PDM) systems for fabrication of welded components, modular adaptive intelligent welding systems can be made for each bill of material (BOM) when fabricating specific products. Routines and modules in the welding process will be the same for each product, and weld quality will be achieved with high assurance.
e) The proposed weld quality assurance model when implemented in factories of SMEs and large companies will serve multiple purposes: weld quality data in digitized format can be acquired, digitized welding procedure specifications (WPS) can be generated, a wide range of modular products can be manufactured, and linking of information to cloud-based systems for effective information sharing in welding operations can be achieved.

2 State of the art of adaptive intelligent GMAW

This chapter presents the state of the art of adaptive welding and reviews previous studies. The information in this section restates and supplements the review studies in *Publication 1*, *II* and *V*. The main aspects considered in this chapter include: the gas metal arc welding (GMAW) process, sensing, monitoring and modelling of the robotic GMAW process for control purposes, and artificial intelligence.

2.1 Gas Metal Arc Welding (GMAW) process

By definition, GMAW, which is also known as MIG (Inert Gas Metal) or MAG (Active Gas Metal), is an arc welding process that produces fusion of metals by heating them with an arc between a continuously fed filler metal electrode. The GMAW process is characterized by a set of equipment that consists of five main units: (1) the power source, (2) the electrode wire feeder and control system, (3) the welding gun and cable assembly for semiautomatic welding or the welding torch for automatic welding, (4) the gas control system for the shielding gas, and (5) a travel mechanism and guidance for automatic welding when used. Figure 4 shows a schematic of GMAW equipment detailing key components of the process equipment and the welding gun unit. The principle of operation, depicted diagrammatically in the equipment and process layout, relies on the generation of heat as a result of electric current producing an arc between a continuously fed filler metal electrode and the material to be welded. Heat generation depends on electrode polarity, either direct current electrode positive (DCEP) or direct current electrode negative (DCEN). DCEP, which also means reverse polarity, is when the electrode is used as the positive terminal while the negative terminal is connected to the base metal. DCEN, which also means direct polarity, is when the electrode is used as the negative terminal while the positive terminal is connected to the base metal (Howard and Scott 2005; Pires, et al., 2006; Nadzam, et al., 2014).

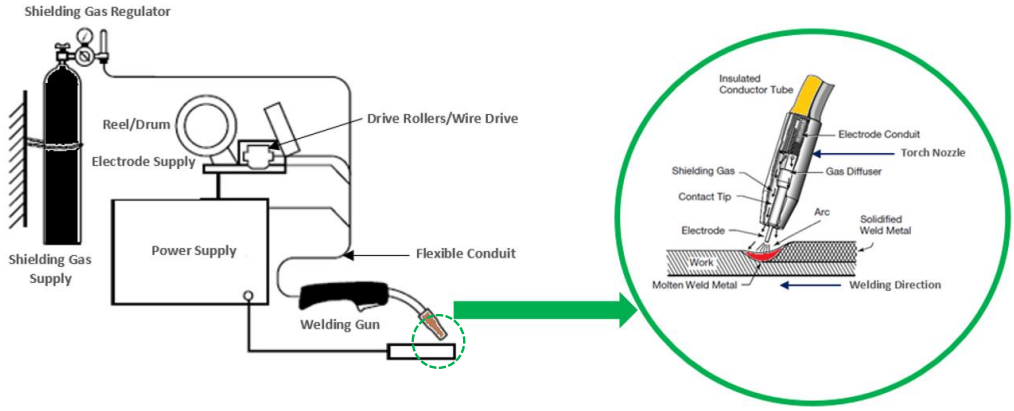

Figure 4. GMAW equipment and process details. Modified (Nadzam, et al., 2014).

Heat transfer and fluid flow is governed by arc plasma and forces in the form of conduction and convection, including the flow of electrons. On reaching the base metal, the heat of the arc melts the surface of the base metal and the end of the electrode, creating a molten pool. The melted tip of the electrode is transferred across the arc to the molten pool, resulting in a weld puddle/weld pool. Considering the magnitude of the wire voltage and current, and size of the wire and the type of shielding gas, four modes of metal transfer can be achieved: short-circuiting, spray, pulse-spray transfer and globular. Table 1 shows key characteristics associated with the GMAW process.

Table 1. Key characteristics of GMAW process (Pires, 2006; Howard and Scott 2005; Nadzam, et al., 2014).

GMAW process	Description
Arc types	In short-circuiting transfer, the metal is deposited during a short-circuiting (low voltage, short arc length and low current) of the weld wire which normally lasts about 10 ms. Globular transfer occurs when voltage and current are increased above the short arc welding and when the droplet diameter is larger than the electrode wire. Spray transfer occurs when the weld droplets are smaller than the electrode wire. The transfer phenomenon is such that, the mean current increases and the metal transfer goes from stubbing, short-circuits, globular and then to spray transfer mode. In pulse-spray transfer, the mean current and the average heat input to the workpiece is lower than in spray transfer. Upon solidification, the weld pool forms a fused joint, termed as the weld metal. An envelope of gas fed through the nozzle shields the arc, molten pool, and the surrounding areas from contamination from the atmosphere. The type of metal transfer mode is a function of the weld current controlled by both the static force balance theory and the pinch instability theory.
Shielding gases	Shielding gases help to stabilize the arc and influence the mode of metal transfers types, formation of weld bead contours and elimination of weld spatter. The European standard EN ISO 14175 classifies welding consumables and gases, and mixture of gases for fusion welding and allied processes. Therefore, shielding gases can be used in their pure state (hydrogen: H_2, oxygen: O_2, carbon dioxide: CO_2, argon: Ar, nitrogen: N_2, Helium: He) or mixed together given a binary blend (Ar + O_2, Ar + He, or Ar + CO_2), ternary blend (Ar + O_2 + He, Ar + CO_2 + O_2), or quaternary blend (Ar + O_2 + He + CO_2, Ar + CO_2 + He + N_2). The most frequently used shielding gases are Ar, He and CO_2, and the other gases blended with these for the purpose of modifying arc characteristics and the weld pool shape and size.
Effects of shielding gas	Pure argon produces a finger-like weld penetration and addition of helium increase thermal conductivity and provides more puddle fluidity, and flatter bead shape. Argon enhances arc starting and promotes cleaning action when welding aluminium. The addition of CO_2 to Ar is suitable for carbon steel welding, as CO_2 increase the heat generated. Oxygen is an oxidizer that reacts with elements in the weld pool to form oxides. Blended with argon, oxygen enhances arc stability and the appearance of the weld bead. The oxides float to the surface of the weld bead to form small islands. The float of oxides is more prominent with CO_2 shielding.
Filler materials	Selecting filler metal electrodes for GMAW process need several considerations. This include the electrode type, electrode diameter, metal to be welded, thickness and joint design of the metal, surface conditions, specification or service condition which should complement the shielding gas to be utilized. The mechanical and chemical properties of the electrode should either match, overmatch or undermatch the properties of the base metal.

Initially, GMAW was developed for welding aluminium using spray mode of metal transfer, argon gas for shielding, and a relatively large diameter electrode. The problem encountered was the large uncontrollable molten weld pool. For steel welding, CO_2

shielding gas and large diameter electrode wire (1.6 mm) were used. The metal transfer was globular and spatter was greater than desired. Beside these problems, the manual setting of welding parameters such as current, wire feed rate, welding speed and gas flow rate were a challenge, thus producing weld joints with a lot of defects and imperfections like weld porosity, irregular repartition, lack of weld penetration, weld embrittlement and softening. These defects were a result of the limited control possibilities of the GMAW process variations that were available at the time (Howard and Scott, 2005).

Recent developments of the GMAW process have seen the addition of microprocessors and digital signal processors to control the process performance and arc stability, which has led to vastly improving joint quality. A large number of proprietary process control options exist (Norrish, 2017). These process control options, which are commonly known as waveform-controlled welding processes, are defined according to ISO/TR 18491 as "welding process modification of the voltage and current wave shape to control characteristics such as droplet shape, penetration, wetting, bead shape or transfer mode(s)" (ISO/TR 18491). Typical examples of GMAW waveform-controlled processes include: pulse-spray transfer; controlled short circuit transfer; modified spray, combined variants and AC operation; and synergic and self-regulation control, although other variants of waveform-controlled processes exist (Mvola, 2017). Synergic and self-regulating control can be seen as voltage control where the wire feed rate and voltage are kept constant. A change in position causes the current to change, which prompts the filler wire output to compensate for the change. GMAW processes can have tandem and multi wire systems. These features produce a significant increase in welding speed and deposition rate, and they influence the strength of the weld geometry.

Application of the GMAW process requires consideration of several parameters and variables, which are inter-related and show nonlinear behaviour. Welding parameters such as arc current, arc voltage, welding speed and gas flow rate are associated with heat input. Welding parameters such as electrode stick-out, arc length, wire feed rate and wire diameter are associated with contact tip to work distance (CTWD). In addition, welding parameters such as torch position, torch travel angle and torch movement techniques are associated with torch angle. If any of these nonlinear attributes of the GMAW process is not appropriately set or controlled, defects associated with heat transfer and fluid flow may occur. Investigation of heat transfer and fluid flow phenomena of the GMAW process assists with understanding of the complexities of GMAW and provides a more solid foundation for utilization of GMAW in adaptive welding of advanced steels.

2.1.1 **Heat transfer and fluid flow**

The GMAW process is complicated and involves nonlinear interaction of multiple welding parameters and variables, and several numerical models have been developed to describe and help understand heat transfer and fluid flow phenomena in GMAW and their effects on weld configuration, welding position, and weld quality. Most of these three-dimensional numerical models capture the dynamics of temperature profiles, weld pool free surface profile, velocity fields, weld pool shape, thermal cycles, cooling rates and the

effects of the tilt angle. Recent developments in computer technology have led to the use of CFD and finite element methods for computation of the welding process by analysing the heat transfer and fluid flow to establish dynamic models between temperature fields and weld pool surface deformation (Cho, et al., 2013;Wahab, 1998; Chen and Wu, 2009).

Modelling of GMAW for fillet joints performed by (Kumar, et al., 2005; Kumar and DebRoy, 2007) provides improved understanding of the underlying scientific principles; such understanding leads to good quality welds in practice. In the model, thermo-physical properties such as thermal diffusivity and the specific heat needed for the computational process are taken at 1745 K as a pre-set value. Additional heat transported by the weld droplets into the weld pool is taken into account using a time-average volumetric heat source term (S_v). The heat flux from the arc is assumed to have a Gaussian distribution on the top surface of the weld pool. With these steady state conditions established, a coordinate system is attached to the heat source in order to compute the heat transfer and fluid flow during the GMAW process using continuity, momentum conservation and energy conservation governing equations.

$$\frac{\partial u_i}{\partial x_i} = 0 \tag{1}$$

$$\rho \frac{\partial (u_i u_j)}{\partial x_i} = \frac{\partial}{\partial x_i}\left(\mu \frac{\partial u_j}{\partial x_i} \right) + S_j \tag{2}$$

$$\rho \frac{\partial (u_i h)}{\partial x_i} = \frac{\partial}{\partial x_i}\left(\alpha \frac{\partial h}{\partial x_i} \right) - \rho L \frac{\partial (u_i f_l)}{\partial x_i} - \rho U_w \frac{\partial h}{\partial x_1} - \rho U_w L \frac{\partial f_l}{\partial x_1} + S_v \tag{3}$$

Equation [1], [2], and [3] are the continuity, momentum conservation and energy conservation equations respectively. The energy conservation equation comprises the arc heat flux, heat dissipation by convection and radiation, and heat loss due to evaporation (Cho, et al., 2013).The subscripts *i* and *j* denote the coordinate direction, *x* is distance, *u* is the liquid metal velocity, ρ is the density, μ is the viscosity, S_j is the source term for the *jth* momentum equation, *h* is the sensible heat, α is the thermal diffusion coefficient (defined as $\alpha = k/C_p$, where *k* is the thermal conductivity and C_p is the specific heat), U_w is the material moving speed (parallel to the positive *x* direction, i.e., *i=1* direction), *L* is the latent heat of fusion, and S_v is a source term accounting for the additional heat from the metal droplets. The source term S_j used in Equation [2] can be written as:

$$S_j = -\frac{\partial p}{\partial x_j} - \rho U_w \frac{\partial u_j}{\partial x_1} - C\left(\frac{(1-f_l)^2}{f_l^3 + B} \right) u_j + F_j^e + F_j^b + F_j^i \tag{4}$$

Where *p* represents pressure; f_l is the liquid metal fraction; and F^e_j, F^b_j and F^i_j correspond to the electromagnetic, buoyancy and inertia forces in the *jth* direction respectively. The third term in Equation [4] represents the frictional dissipation in the mushy zone (a semi-

solid region of the weld) according to the Carman-Kozeny approximation, where *B* and *C* are two constants. The liquid metal fraction, f_l, is assumed to vary linearly with temperature inside the mushy zone:

$$f_\ell = \begin{cases} 1 & T \geq T_\ell \\ \dfrac{T - T_S}{T_\ell - T_S} & T_S < T < T_\ell \\ 0 & T \leq T_s \end{cases} \quad (5)$$

Where T_l and T_s are the liquidus and solidus temperature of the material respectively.

Figure 5 presents an illustration of plots of heat transfer and fluid flow under investigation in GMAW process analysis.

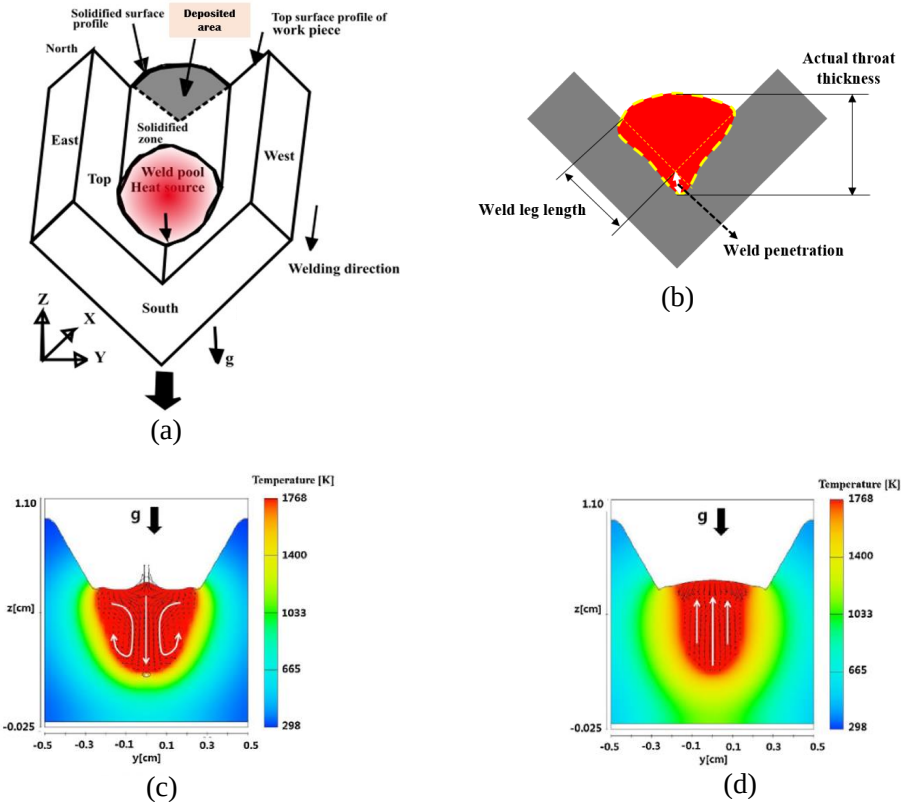

Figure 5. Illustration plots of: a) coordinate transformation from the physical domain; b) nomenclature of GMAW fillet weld geometry (Kumar, et al., 2005); and temperature profiles and fluid flow pattern on a transverse cross-section: c) 1.52 s; d) 2.0 s (Cho, et al., 2013).

In Figure 5(a), a coordinate transformation from the physical domain is shown. Figure 5(b) provides a nomenclature of GMAW fillet weld geometry (Kumar, et al., 2005). Figures 5(c) and 5(d) present a simulated case of calculated temperature profiles and flow patterns on a transverse cross-section when time was varied from 1.52 s and 2.0 s respectively (Cho, et al., 2013). It can be clearly seen from Figure 5(c) and 5(d) that the heat transfer and fluid flow pattern changes with respect to time. Heat transfer assumes a circulation path from the top of the weld pool to the bottom, whereas the metal fluid flows in a laminar pattern. After some few seconds, and depending on the temperature of the fluid, the heat transfer assumes a linear direction from the bottom of the molten weld pool to the top.

2.1.2 Relative effects on weld quality of fillet joints

Non-dimensional properties and driving forces are present in the GMAW process. The relationship between these variables have effects on weld quality, temperature distribution, velocity field, weld bead surface profile, etc. It has been established that during fillet welding, the weld pool top surface under the electrode is depressed by the arc force, which consequently deforms the weld pool surface profile. The energy from the arc is transported from the top surface of the weld pool to the surrounding solid region by both heat conduction and liquid metal convection (Kumar, et al., 2005; Kumar and DebRoy, 2007). Likewise, in the weld pool, heat is transported by convection and conduction (Cho, et al., 2013). The rate of heat transfer in the workpiece determines the shape of the weld pool, peak temperature, and temperature distribution in the HAZ.

The case of GMAW of structural steel A-36 provides a situational example for understanding the various non-dimensional properties and driving forces (Kumar, et al., 2005; Kumar and DebRoy, 2007). Table 2 shows the physical properties of the A-36 steel and other data used in the computational analysis. The values of the non-dimensional properties are shown in Table 3 for a given set of welding parameters: 312.0 A (arc current), 31.0 V (voltage), 4.2 mm/s (welding speed) and 169.3 mm/s (wire feed rate). The equations of the non-dimensional properties including that of the driving forces are shown in Table 4.

Table 2. Physical properties of A-36 and data for computational analysis.

Name	Value
Liquidus temperature, T_l (K)	1785
Solidus temperature, T_s (K)	1745
Density of steel, ρ (kg m^{-3})	7.8 x 10^{3}
Thermal conductivity of solid, k_s (J m^{-1} s^{-1} K^{-1})	21.0
Specific heat of solid, C_{ps} (J kg^{-1} K^{-1})	703.4
Specific heat of liquid, C_{pl} (J kg^{-1} K^{-1})	808.1
Surface tension of liquid metal at melting point, γ (N m^{-1})	1.2
Temperature coefficient of surface tension, $d\gamma/dT$ (N m^{-1} K^{-1})	-3.5 x 10^{-4}
Magnetic permeability, μ_m (N A^{-2})	1.26 x 10^{-6}

Coefficient of thermal expansion, β (K^{-1})	1.0×10^{-5}
Arc efficiency, η	54%
Arc radius, r_b (mm)	5.0
Convective heat-transfer coefficient, h_c ($W\ mm^{-2}K^{-1}$)	42.0
Emissivity, ε	0.7
Ambient temperature, T_a (K)	298
Constant B in the Carman-Kozeny equation	1.0×10^{-7}
Constant C in the Carman-Kozeny equation	1.6×10^{4}

Table 3. Non-dimensional properties of the GMAW process.

Non-dimensional properties	**Value**
Peclet number (PE)	120
Grashof Number (Gr)	11.9
Froude Number (Fr)	0.27
Magnetic Reynold's number (Rm)	3.3×10^{4}
Surface tension Reynold's number (Ma)	2.9×10^{4}

The fluid flow (liquid-metal motion) mechanism in GMAW is quite complex due to the combined effects of the various driving forces: electromagnetic, Marangoni and buoyancy forces. In addition, the forces of inertia, surface tension, gravity and viscosity play major role. In determining the relative significance of convection verses conduction in transfer of heat in the weld pool, the Peclet number (Pe) is used.

Table 4. Driving forces and non-dimensional properties in the GMAW process (Kumar, et al., 2005; Kumar and DebRoy, 2007).

Driving forces	Electromagnetic force	$F^e = J \times B$ (6) Where J and B are the current flux and magnetic field in the workpiece respectively.
and	Buoyancy force	$F^b = -\rho g \cos\left(\frac{\pi}{4} - \theta\right) \cos\varphi\beta(T - T_{ref})$ (7) Using the Boussinesq approximation, the gravity (buoyancy) force is given: where g is the acceleration due to gravity and is in the negative Z direction; θ is the tilt angle or inclination of plates from the horizontal position, φ is the angle of lift from the horizontal plane, β is the thermal expansion coefficient; and T and T_{ref} are the local and arbitrarily selected reference temperatures.
	Inertia force	$F^i = -\rho g \sin\varphi i + \rho g \cos\left(\frac{\pi}{4} - \theta\right) j$ (8) Where i and j are the unit vectors in the x and y directions respectively.
Heat flux	Heat flux	$\alpha \nabla h \cdot n_b = F_b = h_c(T - T_a)$ (9)

		For the bottom surface, the heat flux is given: where n_b is a unit normal vector to the bottom surface, h_c is the convective heat-transfer coefficient, and T_a is the ambient temperature (a value of 298 K is used). The temperature at the other surfaces, i.e., east, west, south, and north surfaces, are set to the ambient temperature.		
Non-dimensional properties	Peclet number	$\mathrm{Pe} = \frac{heat_{convection}}{heat_{conduction}} = \frac{u_R \rho C_{pl} L_R}{k_l}$ (10) Where u_R and L_R are the characteristic velocity and length in the weld pool respectively; p is the density; and C_{pl} and K_l are the specific heat and thermal conductivity of liquid metal respectively.		
	Grashof number	$\mathrm{Gr} = \frac{g\beta L_B^3 \Delta T \rho^2}{u^2}$ (11) Where g is the acceleration due to gravity, β is the thermal expansion coefficient, ΔT is the temperature difference between the peak pool temperature and solidus temperature, ρ is the density of the liquid-metal, μ is the viscosity of the liquid-metal, and L_B is a characteristic length for the buoyancy force in the liquid pool and is approximated by one-eighth of the pool radius.		
	Froude number	$\mathrm{Fr} \equiv \left[\frac{\text{inertia force}}{\text{gravity force}}\right]^{1/2} = \frac{u}{\sqrt{gH}}$ (12) Where u is the average liquid velocity in the weld pool and H is the characteristic depth of the liquid pool and is approximated by the value of weld bead throat dimension.		
	Reynold's number	$\mathrm{Rm} = \frac{\rho \mu_m I^2}{4\pi^2 \mu^2}$ (13) Where μ_m and μ are magnetic permeability and viscosity of the liquid metal respectively.		
	Surface tension Reynolds number	$\mathrm{Ma} = \frac{\rho L_R \Delta T \left\lvert \frac{d\gamma}{dT} \right\rvert}{\mu^2}$ (14) Where L_R is the characteristic length and $d\gamma/dT$ is the surface temperature gradient.		
	Ratio of surface tension force to buoyancy force	$R_{S/B} = \frac{Ma}{Gr}$ (15)	Ratio of electromagnetic force to buoyancy force	$R_{M/B} = \frac{Rm}{Gr}$ (16)

When the Pe number is higher than unity, heat transfer in the weld pool is caused by convection due to high liquid metal velocity and larger weld pool size. Contrarily, when the Pe number is less than unity, heat transfer by conduction is the cause of heat dissipation in the weld pool. Since the Pe number in the case of A-36 steel is higher than unity, the liquid metal convection mechanism is the dominant factor in dissipation of the heat in the weld pool. The ratio of the buoyancy force to the viscous force is determined

by the Grashof number. The Grashof number is much higher than unity, as seen from Table 3, causing the viscous force to be negligible compared to the buoyancy force. The property value of the Froude number (Fr) is much higher than unity, causing the inertia force to dominate the flow in the weld pool. If Fr is much less than unity, the buoyancy or gravity force dominates the liquid metal flow (Kumar et al., 2005; Kumar and DebRoy, 2007).

The magnetic Reynold's number, Rm, expresses the ratio of the electromagnetic force to the viscous force. The Rm value is significantly higher than unity, which suggests that the electromagnetic force is very dominant compared to the viscous force. The surface tension Reynold's number (Ma) is used to describe the ratio of the Marangoni force to viscous force. The value of Ma is of the same order of magnitude as Rm. However, the value of Gr is very low compared to Rm and Ma, which means that the effect of the buoyancy force is very low compared to the electromagnetic and Marangoni forces.

In describing the relative importance of the driving forces, the following dimensionless properties can be formulated. The ratio of the surface tension force to the buoyancy force is defined as $R_{S/B}$, and the ratio of the electromagnetic force to the buoyancy force is given as $R_{M/B}$. However, for GMAW of fillet joints, the values of $R_{S/B}$ and $R_{M/B}$ are found to be 2.4×10^3 and 2.8×10^3 respectively. These values suggest that the liquid metal flow in the molten pool is driven chiefly by the Marangoni and electromagnetic forces, and to a much lesser extent by the force of buoyancy. Furthermore, the electromagnetic force plays a major role during GMAW of fillet joints (Kumar et al., 2005; Kumar and DebRoy, 2007). Figure 6 shows an illustration of the various forces and the flow pattern of the weld pool in GMAW.

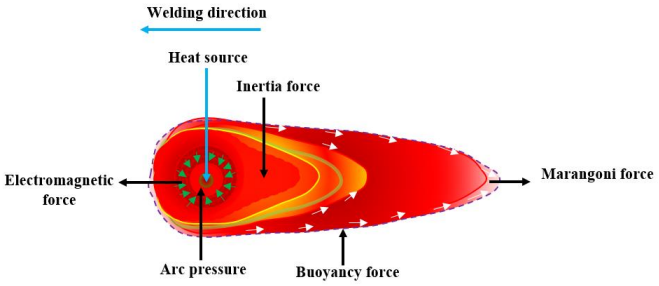

Figure 6. Illustration of the various forces and the flow pattern of the weld pool in GMAW.

In symmetrically V-shape fillet welding, the effect of high arc pressure causes a deep finger penetration, although some research suggests that weld droplet impingement is the dominant reason for fingertip penetration (Mendez and Eagar, 2003; Essers and Walter, 1981).The liquid metal flows downward in the middle of the weld pool driven by the electromagnetic force, assisted by gravity and the plasma drag force (Cheon, et al., 2016). A major counterclockwise circulation loop is formed along the central longitudinal plane.

However, at the top surface of the weld pool, the Marangoni shear stress drives the melt from the center to the edge of the weld pool in the region close to the heat source, where the variation of the surface temperature is relatively high (Kumar et al., 2005).

Due to the difference in flow patterns resulting from the electromagnetic and Marangoni forces, the leg length of the weld pool decreases, while the actual throat is increased due to weld penetration, as shown in Figure 5 (b). However, the situation illustrated in Figure 5 (b) is not a general case, especially when different workpiece orientations and welding positions are used. It is claimed that when weld droplet flight distance increases, weld penetration becomes deeper (Cheon, et al., 2016), which may have a resultant effect on the length of the weld leg and weld pool size. Consequently, it is further asserted that an increase in CTWD causes low arc heat intensity at the surface of the weldment, thus reducing the inert gas density effect on weld penetration as a result of dissipation of the arc heat intensity (Nestor, 1962).

Workpiece orientation and welding position affect the strength and integrity of the welded joint due to changes in the weld bead geometry (Bowditch, 1997). For L-shape fillet welding, the buoyancy and inertia forces affect the temperature distribution and the velocity fields in the workpiece. The depth of weld penetration is not as deep as in the V-shape. With an increase in the tilt angle of the workpiece, weld penetration increases and the width of the weld pool decreases, as shown in Figure 7.

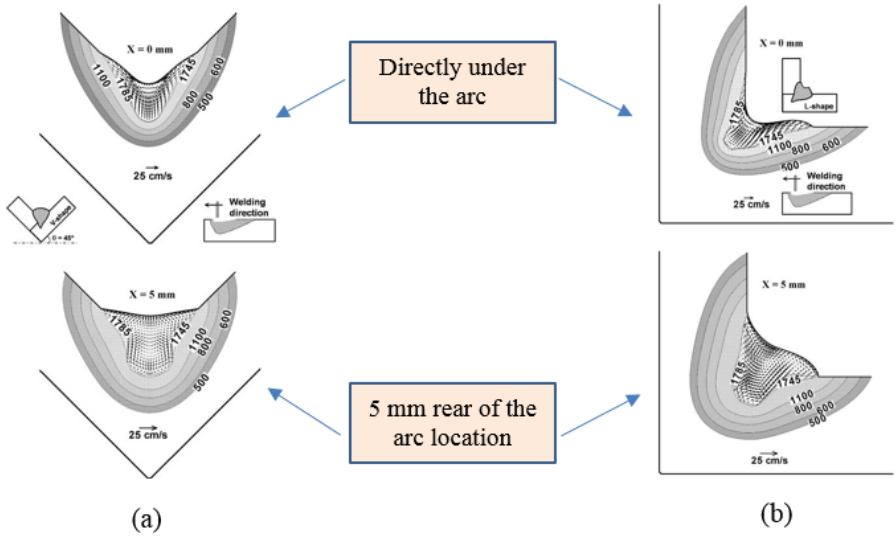

Figure 7. Temperature and velocity fields at different cross-sectional planes in (a) V-shaped joint and (b) L-shaped joint. Modified (Kumar and DebRoy, 2007).

The dynamic behavior and effects of fillet joint orientation on the free surface profile, temperature distribution, velocity field, weld pool shape and size due to the driving forces

and dimensionless properties present some level of justification for automation of the GMAW process in adaptive welding setting. Automation enables the complexities in GMAW welding to be addressed in a more consistent manner, resulting in more dependent weld quality, improved productivity and superior weld quality assurance.

2.1.3 **Automating the manual operation of the GMAW process**

The versatility, flexibility, productivity and adaptability of the GMAW process make it one of the most commonly used fusion welding processes in the welding industry. The GMAW process can be used to weld almost all metallic materials having thickness above 30 mm, it is effective in all welding position, has higher speeds and gives higher deposition rates than manual metal arc welding (stick welding). However, the process is not without its complications. The need to automate its operational functionalities to mimic an experienced welder stem primarily from issues related to positioning the welding torch, controlling the welding parameters, and holding and manoeuvring the welding torch in a precise and controlled manner. Automation is also required to produce more consistent weld quality, reduce production cost, and increase production volume even when operating in non-human friendly environments. Databases and programmable software, IO control and data acquisition systems, communication interfaces and protocols incorporated into robots are available for the purpose of automating the GMAW process.

Automated GMAW processes, referred to herein as robotic GMAW, rely on the kinematics of the robot manipulator and dexterity of the robot end effector for effective operation and performance. Table 5 shows a summary of the characteristics of robot manipulators. The robot manipulator characteristics make it possible to define positions/orientations, define reference systems, parameterize trajectories and other actions, and run the program continuously with high precision and repeatability (Chen and Wu, 2009).

Table 5. Robot manipulators main characteristics (Chen and Wu, 2009).

Repeatability	Up to 0.03 mm (0.1 mm is common)
Velocity	Up to 5 m/s
Acceleration	Up to 25 m/s^2
Payload	From around 2-3 kg up to ~ 750 kg
Weight/Payload	Around 30-40
Axis	6 degree of freedom
Communications	Profibus, Canbus, devicenet, ethernet and serial channels (RS232 and RS485)
IO Capabilities	PLC like capabilities to handle digital and analog IO

Nevertheless, robotic GMAW has drawbacks in relation to real-time monitoring and sensing and control capabilities. Pre-setting of the geometrical parameters of the weld,

real-time monitoring of the welding operation, re-adjustment of the welding parameters and variables, and overall control of the entire welding operation present significant challenges in the application of robotic GMAW processes. The movement of the welding gun in corners, irregular wire feeding, unstable arc and weld discontinuities (porosity, lack of penetration, excessive melt-through, cracks) present further challenges (Ushio and Mao, 1994; Nomura, 1994). There is always the need to check, adjust or pre-program welding parameters before or after the welding operation. These routines, which are somewhat cumbersome, could be alleviated by adaptive welding systems based on data from sensing and monitoring systems.

2.2 Sensing and monitoring of the robotic GMAW process

Sensing and monitoring capabilities have advanced considerably in recent years. Integration of sensing and monitoring devices would enhance GMAW performance through motion control, monitoring of the entire welding process in real-time, joint detection and recognition, seam tracking (capture seam data and store weld data) while coordinating with other devices to respond appropriately in adjustment of output settings (Chen and Wu, 2009; Huanca and Adsi, 2010).

Sensors utilized for welding purposes measure parameters related to the welding process as they play a significant role as the major source of input to the control system that manage and control the behaviour and output of the welding system. The stored parameters are used to control the welding process in accordance with defined WPS (example shown in Appendix Table 4). In robotic GMAW, measured sensor information can be used for controlling both the welding power source and the robot manipulator. However, using only one sensor to perform these functions and additionally observe other parameters like joint geometry is not feasible. For these reasons, a robotic GMAW system needs multiple sensors and monitoring devices for optimum performance. Sensors for welding robots are divided into two groups, technological and geometrical sensors. Technological sensors measure parameters related to the welding process and geometrical sensors measure parameters related to weld joint geometry (Chen and Wu, 2009).

2.2.1 Sensing technological parameters

Sensors for technological parameters must be able to obtain information on arc voltage, current and wire feed rate. Measurement of the arc voltage can be done in several different ways. A reliable way is to measure the arc voltage on the wire inside the wire feeding system, which avoids errors from voltage drop (Rosheim, 1994; Pires, et al., 2006). The wire at this position does not carry any current so the voltage of the wire at the contact tube will be the same. For welding current measurements, two basic types of sensors are used: Hall effect and current shunt sensors. The principle of the Hall sensor involves a circular core of cast iron through which the cable that carries the current flows. The sensor device, consisting of a doped silicon plate, is placed in the gap in the iron core with two pairs of connecting cables. The first pair feeds the device with current and the device

responds by delivering a signal to the second pair of cables that is proportional to the magnetic field and the current. The benefit of the Hall sensor is that it is contactless and does not interfere with the current of the welding power source (Mvola, 2017). The current shunt sensor operates by letting current flow through a resistor and the voltage across the resistor is measured. Figure 8 shows the three sensor types for measuring technological parameters.

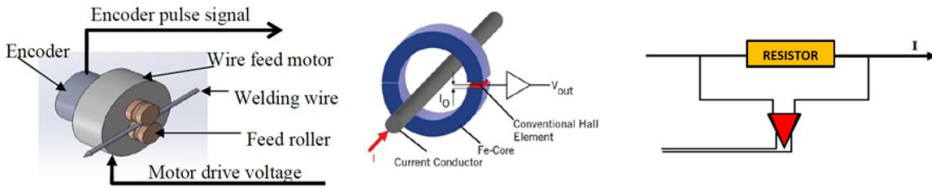

(a) (b) (c)

Figure 8. Technological sensing approaches: a) arc voltage, (b) Hall effect, (c) current shunt. Modified (Mvola, 2017).

2.2.2 **Sensing geometrical parameters**

Sensors used to obtain welding information about geometrical parameters primarily measure the geometry of the weld joint, deviation from a nominal path, position and orientation changes in joints, and workpiece and gap size. In some cases, location techniques can be applied for locating workpieces by using image recognition to detect the position of some plates of the workpiece. Such information is of great significance when performing seam tracking for use in quality control of the welding process. However, geometrical sensors face challenges arising from the harsh arc environment with high temperatures, fumes from the shielding gases, spatter from hot molten metal, electromagnetic fields and other driving forces, arc disturbance and noise, high current and intensive light radiations. These challenges affect the performance of the sensors, and purpose-built sensors must be utilized. The most common and frequently used sensors in this category are optical sensors and through-arc-sensors (Chen and Wu, 2009).

Most optical sensors, known as active direct visual sensors, use laser or light structures and an in-built camera. Laser beams are characterised by high intensity, directionality, monochromaticity and coherence (Chen and Wu, 2009). The laser light is applied on the weld joint under study and a camera with a narrow bandwidth filters the laser beam to extract the geometrical weld data of interest. In detection and recognition of weld data, the projected laser beam is moved in a scanning motion across the seam and a semiconductor charge-coupled device (CCD) camera or complimentary metal-oxide semiconductor (CMOS) is used to measure features of the weld joint from the laser strip. The laser strip in this case may not be a linear line on the joint but rather circular to detect weld joints also in corners from one location of the torch or point of view of the sensor.

The CCD camera measures the distance on the joint using the method of laser triangulation (Pires, et al., 2006; Chen and Wu, 2009).

The other common form of optical sensors, known as passive direct visual sensors, use the light of the arc without an additional secondary light source. Optical sensors are often mounted on the welding torch as a technique to have the weld joint in its field of view some distance ahead in the weld travel direction. Based on laser triangulation, optical seam trackers are capable of keeping the robot "on track" with the weld joint during welding in real-time. Added capabilities of optical sensors include recognition of joint volume, misalignment and tack welds based on a feature extraction algorithm. These capabilities of optical sensors can provide information for adaptive feed-back control of both the welding power source and the robot and can perform the defined tasks according to weld quality standards of the WPS (Pires, et al., 2006). Figure 9 shows the two geometric sensing approaches.

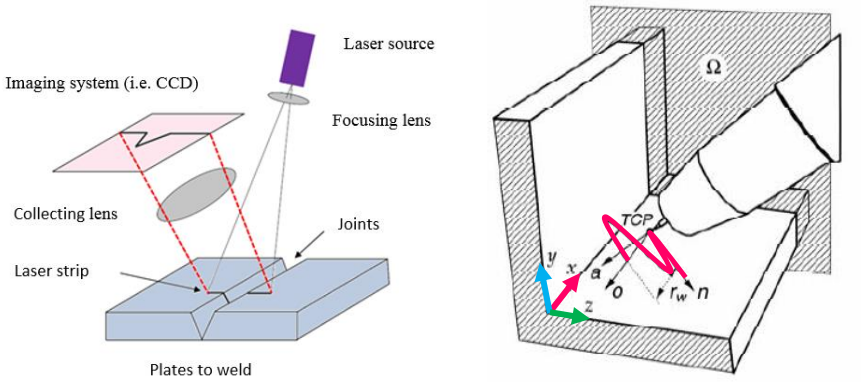

(a) (b)

Figure 9. Geometric sensing approaches: (a) Laser vision principle (Pires, et al., 2006), (b) definition of tool centre point and weaving direction during through-arc sensing (Fridenfalk, 2003).

Through-arc sensors, also known as seam tracking, use the weaving motion technique and the arc itself as the sensor. The technique relies on the change in current when the distance between the contact tube and the workpiece varies. The approach is commonly used for seam tracking methods in robotic GMAW due to it being cost-effective compared to optical sensors. Mathematically, the approximate relationship between arc voltage (U), arc current (I) and the CTWD (l) is expressed as:

$$U = \beta_1 I + \beta_2 + \beta_3 / I + \beta_4 l \tag{17}$$

where β_1 - β_4 are constants dependant on factors like wire diameter, gas flow and the characteristics of the welding power source. The welding power source is set to maintain

a constant voltage. When the *l* varies, the arc current *I* will also vary; therefore, a longer CTWD will result in a lower arc current given that all other parameters are kept constant. As the current is measured using the Hall effect or current shunt, a low-pass filter is employed to depress noise from the signal. Weld information from the through-arc sensor can be retrieved either through continuous measurement of the current or by measurement at the turning points of the weaving motion (Cook, et al., 1987).

Other arc welding sensing methods also exist: ultrasonic methods for sensing weld penetration (Hardt, 1984), arc pressure sensors to sense vibration information of the weld pool (Li, 1997), infrared thermography to sense the welding temperature field (Nagarajan 1989; Menaka, et al., 2005; Venkatraman, 2006; Gyasi, et al., 2017; Gyasi, et al., 2018), X-ray method to sense the shape of the welding pool, acoustic sensors, high speed CCD cameras and stroboscopic vision cameras (Chen and Wu, 2009). Sensors that do not have monitoring capabilities (feature recognition) should be complemented with monitoring systems when employed for a robotic GMAW process. Monitoring systems that record and capture welding data provide better observation and prediction of the behaviour of the welding process, as well as enhance total control of the welding.

2.2.3 Monitoring of process variables and parameters

Monitoring systems for arc welding have in-built feature recognition and extraction capabilities, which should be able to classify different weld parameters and or features that indicate the quality of the weld with respect to pre-set values and provide these as a basis for further control actions during the welding process. Commercially available monitoring systems for weld parameters include ADM III, Arc Guard, Analysator Hannover 10.1, and Weldcheck. These systems all work in a similar manner by measuring voltage, current and other process signals and comparing the measured values with pre-set nominal values. An alarm is triggered when there is a difference to the pre-set values that exceeds a given threshold. For WPS conformance, the alarm threshold is defined with respect to the WPS to maintain the welding process within nominal parameter limits and at the same time produce welds at the defined quality and productivity levels of the WPS (Pires, et al., 2006).

As mentioned earlier, some arc welding sensors have monitoring capabilities, which helps to reduce production cost and assure and improve weld quality and integrity. To be able to provide explicit information on weld quality, reference data (existing knowledge or information) must be available, including models or algorithms that describe and evaluate measured parameters (Pires, et al., 2006). A monitoring system with arc welding sensoring is necessary for control purposes of the entire welding process. Therefore, monitoring of a robotic GMAW process requires information about the mode of metal transfer, and using welding parameters, heat transfer and material flow equations must be formulated in development of algorithms for control purposes. For example, in a pulse-spray GMAW process, the criterion for detachment of one droplet per pulse is governed by the relationship:

$$I_p^n X T_p = K_2 \quad (18)$$

Where I_p is peak current, T_p is the pulse time, K_2 is a constant depending on the material, and n ≈ 2 (Amin, 1983; Pires, et al., 2006).

As an example, monitoring and processing of heat input signals, as shown in the block diagram in Figure 10, require special mechanical systems and devices, including analogue to digital converters and signal and noise filtering units. Heat input signals from the welding process sensed by the arc sensor in the form of analogue signals pass through an analogue-to-digital converter. Digital signals from the analogue-to-digital converter are directed through a digital signal processor and the output digital signals are filtered.

As the measurement conditions during sensing can be highly disturbed by electrical noise, a filtering unit is required to suppress such disturbance. The bandwidth required for monitoring systems is primarily determined by the short-circuit time, which is in the order of milliseconds, or about 500 Hz (Pires, et al., 2006). The rise time of the whole system should not exceed 10 % of the short-circuit time. Further processing of signals can be done through algorithm modelling (Pires, et al., 2006). For control purposes, specific modelling and control algorithms having the capability to map the monitored data with respect to quality and productivity specifications can be used. Feedback of the analogue signals ensures a close-loop system for full controllability of the welding processing for weld quality and assurance. Due to sensitivity to errors, integration of the monitoring systems with robotic GMAW is important also at the stage of defining the WPS. A model based control system is required when developing monitoring systems. This helps to use data from the monitoring system to control the entire welding process in real-time.

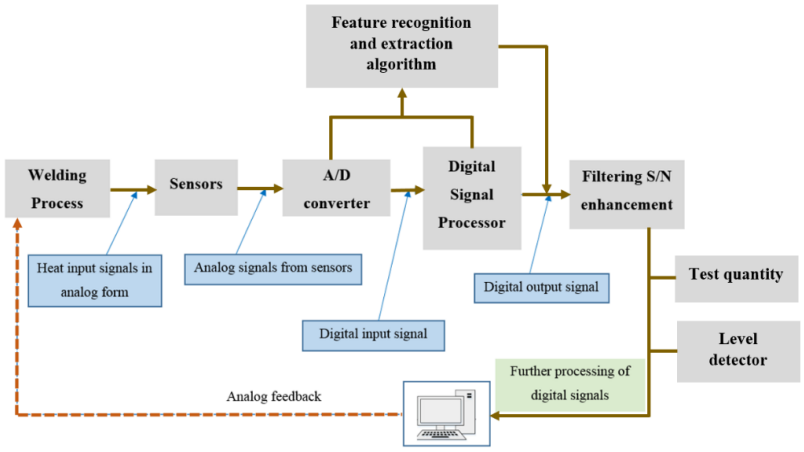

Figure 10. Architecture of a monitoring system for welding signal recognition and control.

2.3 Modelling the robotic GMAW process for control purposes

Modelling of the robotic GMAW process has to be done in two ways: a) using a theoretical approach, which involves solving the physical problems analytically; and b) using a technological approach, which takes understanding of the welding process from the theoretical perspective as a basis for performing empirical studies based on detailed experimentation to ascertain the governing models.

Due to the nonlinear nature of the GMAW process, many parameters need to be addressed theoretically and technologically before, during and after the welding process. Before welding, parameters denominated as fixed inputs need to be defined. The fixed inputs include the prepared joint geometry, plate thickness and physical properties of the material. Also welding parameters and variables such as shielding gas, gas flow rate, torch angle, and type and size of the wire need to be determined before welding. These secondary inputs rely on the primary inputs and any changes in these parameters will affect the welding process. In addition, any changes in the primary inputs (arc voltage, current, wire feed rate, torch travel speed) will affect the welding process greatly. Another essential set of parameters are the output parameters. Such parameters are metallurgically and geometrically defined and they are obtained after welding since they characterize the weld and are used to evaluate its quality.

2.3.1 Geometrical and theoretical modelling approaches

Geometrical parameters are classified according to weld penetration, weld bead width, weld bead height, length of the leg of the weld metal, weld metal throat thickness, weld toe contours, weld root penetration, etc. The welding standard EN ISO 5817 defines geometrical parameters for fillet and butt welded joints. Metallurgical characteristics which rely primarily on heat input for good metal fusion, penetration, temperature distribution and cooling rates, which affect weld solidification, play a major role in weld quality. They dictate and determine specific mechanical characteristics like hardness, tensile strength, residual stresses, and the integrity and reliability of the weld joint. These specific characteristics of the weld joint cannot be measured on-line, only after the welding process. Adaptive control could help achieve flawless welds by ensuring the desired mechanical and metallurgical properties of the weld and controlling the formation of the appropriate microstructure during solidification. Accurate definition of these requirements are dependent on an accurate model of the robotic GMAW process.

Sub-chapters 2.1.1 and 2.1.2 of this work introduced a theoretical (analytical) approach used in modelling of the GMAW process. The analytical study provides a foundation to further develop modelling for the GMAW process to enhance repeatability and consistency. This model development requires the findings of geometrical (empirical) study to refine the model to the accuracy desired. With robotic GMAW, a robust modelling system is very much needed due to the complexity and nonlinearity of the system integration between the robot and the GMAW process. Adopting the geometrical approach requires the following: a) a knowledge base, and b) sensors and interfaces.

A knowledge base in this case simply means following a rule-based approach (Bolmsjö, 1997; Pires, et al., 2006) to export information so that specific welding process boundary conditions can be modelled. Figure 11 shows an architecture of GMAW process modelling for control purposes.

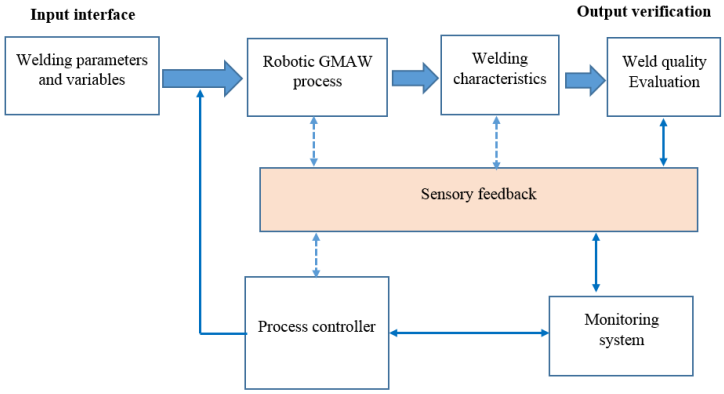

Figure 11. Architecture of GMAW process modelling for control purposes.

2.3.2 Welding process controllers

Several process controllers for welding applications exist. These controllers include PID controllers, fuzzy logic controllers, PSD controllers, expert system controllers, neural network self-learning controllers, and controllers utilizing a combination of these approaches (Chen and Wu, 2009). The controllers mostly work on closed-loop systems where output values are monitored and compared with input parameters (Burns, 2001). Basically, the function of a controller is to control the dynamic behaviour of the welding process by eliminating or reducing errors that occur due to process instability and disturbances. Errors in welding parameters such as arc voltage, current, arc length and weld attributes such as depth of weld penetration, joint gaps, and weld pool width can be controlled with a close-loop system.

Most commercial controllers provide PID (also called three-term) control actions (Burns, 2001), and due to the simplicity and robustness of PID, it is widely used in practice (Chen and Wu, 2009). PID is an acronym which stands for proportional, integral and derivation, and it defines the terms in which a control action is executed in responding to a non-zero error input to the controller. These three actions are executed in the same time domain and operate parallel to each other. The output sum, illustrated in Figure 12, is a result of adjusting the PID item of the error, which further regulates the steady-state deviation and transient deviation of the system so as to make the system stable (Chen and Wu, 2009). The error input signal in the first-order is directly multiplied by the proportional gain K_p, and the output is proportional to the error. The control action or signal is therefore proportional to the steady-state error. In the second-order, the error input signal is first integrated, and the integral action produces an output integral of the error.

This means that the error is integrated and multiplied by K_I. However, in some instances, the steady-state errors may be eliminated. The third-order, which is the derivative action, occurs when the error is first differentiated and multiplied with K_D (Owen, 2012). The control logic of the PID controller is implemented by finding suitable gain parameters of K_P, K_I, and K_D.

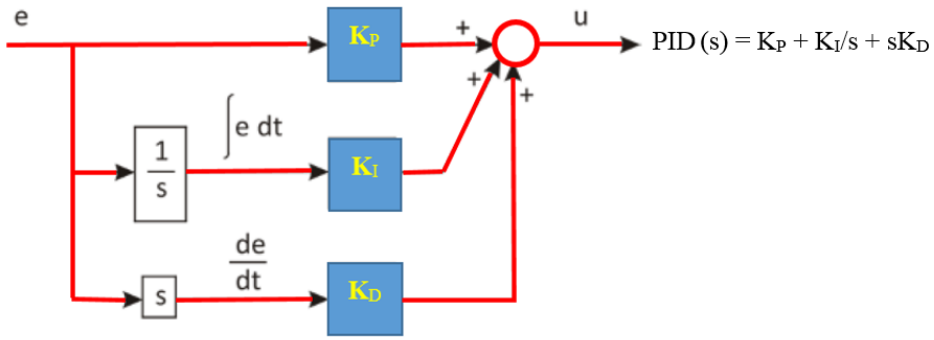

Figure 12. PID controller layout. Modified (Owen, 2012).

Despite its fast regulating speeds, simplicity and common use, the PID controller has problems when controlling nonlinear systems and systems having parameter variations. Their deficient performance leads to overshooting and instability in the system. GMAW operations, where a lot of parameters and variations have to be controlled, could pose challenges to PID controllers. Much research work in welding has combined PID with other artificial intelligent systems like fuzzy logic, ANN, etc. to eliminate the drawbacks of PID controllers and enable optimal control of the welding process (Chen and Wu, 2009). As most robots use PID controllers, there is a need to synchronize the PID control mechanism with an intelligent modelling system having control capabilities. Modelling a control system using artificial intelligence is presented in the next section. A framework of an intelligent PID controller system for robotic GMAW process is also described.

2.4 Artificial intelligence modelling and control of robotic GMAW

Artificial intelligence (AI) is a broad field that draws upon mathematics, computer science and other related subjects to develop approaches that enable machines to mimic the cognitive functions of humans. These functions include learning, reasoning, decision-making, retaining knowledge and problem solving. For some machines like robots, the ability to move and manipulate objects in a precise and repetitive manner is a desired function. In the GMAW domain, robotic systems that incorporate AI could perform functions similar to those carried out by human welders.

Some of the key approaches or systems of AI that are incorporated into robots include artificial neural networks (ANN), fuzzy logic, neural-fuzzy networks and adaptive neuro-

fuzzy inference systems (ANFIS). Such AI are already being utilized in other industries, for example, in medical technology (Holmes, et al., 2017; Lopez, et al., 2017) and for facial recognition in security applications (Aitkenhead and McDonald, 2003), and these well-known algorithmic and data modelling approaches are gaining significance in the welding manufacturing and production industries, with ANN systems being popular for robotic GMAW systems. Table 6 in *Publication II* provides a comparison between common artificial intelligence systems.

A typical robotic GMAW process for a fillet weld joint where ANN is favoured over other AI systems is shown in Figure 11 of *Publication II*. The ANN model considers nonlinear weldability factors associated with robotic GMAW in fillet joint weld configuration. Welding variables and parameters are denoted as the input requirements and the corresponding desired output requirements are mapped to various AI systems. As most research studies in welding simulation and modelling utilize the computational capabilities of ANN, it is important to elaborate its potential in this work.

2.4.1 **Artificial neural network (ANN)**

ANNs are developed based on identification/knowledge based approaches. These approaches are further used in developing the black-box model of the system because of their high precision and robustness. Practically, the ANN relies on input and output information such as experimental data and this information provides the basis on which the structure and parameters of the model are identified. The basic processor or processing element in the ANN is the artificial neuron. Each neuron receives one or more inputs carrying weight over connections called synapses and produces only one output. The activation of the neuron is computed by applying a threshold function (also known as an activation function) to the weighted sum of the inputs plus a bias. The output is therefore related to the state of the neuron and its activation function (Yadav, et al., 2015). The neuron behaves as a mapping function f (net) to produce an output y (either linear, sign, sigmoid or step function) which can be expressed as:

$$y = f(net) = f\left(\sum_{j=1}^{n} w_{ij} x_j + \theta\right) \tag{19}$$

where f is the neuron activation function, θ is the threshold value, x_j is the input, and w_{ij} is the weight. For nonlinear functions, the output y can be expressed using a sigmoid activation function (neuron transfer function), where input is mapped into values between +1 and 0.

$$y = \frac{1}{1 + e^{-Tx}} \tag{20}$$

ANNs can operate on several architectures, including the feed forward neural network (FFNN), recurrent neural network (RNN), radial basis function neural network (RBFNN), Hopfield network (HN) and the multi-layer perceptron (MLP) (Yadav, et al., 2015). Of these ANN architectures, MLP, which combines the capabilities of FFNN and RNN, is quite popular in welding research and practical welding cases. An ANN requires configuration such that the inputs will produce the desired set of outputs. The configuration process, termed learning, uses either prior knowledge or the network is trained by feeding it with data and allowing it to change its weights according to learning rules or algorithms. The learning classification can be in the form of supervised, unsupervised, reinforcement or competitive learning.

Supervised leaning, which is commonly used, is one in which weight adjustments are made from comparison with a target output. The MLP neural network is one of ANN systems requiring supervised learning. A teaching signal feeds into the neural network for the weight adjustments. These teaching signals are also termed a training sample (Yadav, et al., 2015). The MLP neural network architecture is composed of many simple perceptrons in a hierarchical structure forming a feed forward topology with one or more hidden layers between the input and output layers. Figure 12 in *Publication II* shows a MLP neural network with a 3-3-3 architecture.

When determining an optimized set of weights, the MLP neural network system uses learning algorithms such as the back propagation (BP), resilient propagation (RPROP), Levenberg-Marquardt, genetic algorithm (GA) and particle swarm optimization (PSO) algorithm (Yadav, et al., 2015). Generally, input data are weighted through sum biasing and are then processed through an activation function to produce the output. After each process, the output is matched to the output that is desired, and the difference between them gives an error signal. The weight is adjusted by presenting the error back to the neural network system in a manner which will decrease the error for every iteration. This process aims to reduce the error value and make the neural network system model approach the desired target. The adopted learning algorithm adjusts the weights as the iteration increases, thereby reducing the error and getting closer to the desired target (Juang, et al., 1998; Al-Faruk, 2010; Yadav, et al., 2015).

In an ANN system study related to welding, weld bead width characteristics were predicted as a function of key-process parameters in robotic GMAW (Kim, et al., 2004). The accuracy of the neural network model was verified by comparing the simulated data obtained from the neural network model with values obtained from actual robotic welding experiments. Figure 13 in *Publication II* illustrates the results of the study. It was concluded that the predictions obtained from the neural network model using a Levenberg-Marquardt learning algorithm agree closely with the actual values obtained from the robotic GMAW process.

In the study by Kim et al. (2004), adjustment of the weights and biases was derived according to the transfer function expressed in Equation 21 (Kim, et al., 2004). The Levenberg-Marquardt learning algorithm, also known as the damped least squares

method, provides numerical solutions by reducing error when solving complicated boundary value problems.

$$\Delta W = (J^T J + \mu I)^{-1} J^T e \quad (21)$$

where J is Jacobian matrix of derivation of each error, μ is a scalar, and e is error function. In other expressions, the Levenberg-Marquardt algorithm can be derived by considering the error E, after a differential change in the neural network weights from u_0 to u according to the second order Taylor series expansion, as shown in Equation 22. Additionally, the Jacobian matrix is used to define the Hessian for the special case of sum of squared error, as expressed in Equation 23 (Yadav, et al., 2015).

$$E(u) = E(u_0) + f^T(u - u_0) + \frac{1}{2}(u - u_0)^T H(u - u_0) + \cdots \quad (22)$$

$$H = 2\,J^T J + 2\frac{\partial J^T}{\partial u} F \quad (23)$$

The Levenberg–Marquardt algorithm improves the overall accuracy of neural network systems since it can provide a faster convergence than other learning algorithms such as the backpropagation algorithm (Yadav, et al., 2015). Therefore, in welding, where accurate setting of welding variables and parameters is imperative, adopting the Levenberg–Marquardt learning algorithm in artificial neural network systems could guarantee accurate predictions.

2.4.2 **Intelligent control using ANN**

Several control systems have combined the intelligence of a fuzzy logic controller with ANN, PID controller with ANN, fuzzy logic and PID with ANN, or ANN self-learning controller for controlling welding processes in real-time (Chen and Wu, 2009). Hirai (Hirai, 2001) used a fuzzy-ANN controller in robotic MIG welding for penetration control and weld penetration depth prediction. Andersen and Cook (1990) also used a fuzzy and PID controller combined with ANN to model and control weld bead geometry. The main objectives were to control instability in the welding system, eliminate nonlinear and steady-state errors, generate new results by formulating new rules, and obtain welding outputs as desired.

Chen (2004) developed a framework for an intelligent control system using ANN. The system features a PID controller, a robotic welding process, and a learning mechanism for ANN systems. A modified representation of his model is illustrated graphically in Figure 13. The model describes control of system errors through a feedback closed-loop system. Errors sensed in the system are fed back into the system. The system errors are distributed for control through the leaning mechanism of the ANN systems and also the proportional, integral and derivative controls of the PID controller. When the controlled signal leaves the PID controller, it passes to a second ANN system for further control while some level of signals go directly to the robotic welding process.

In instances where there are errors, the second ANN system feeds such errors in the system back to the learning mechanism. However, those signals which are in steady-state without errors go through the main output line from the robotic welding process.

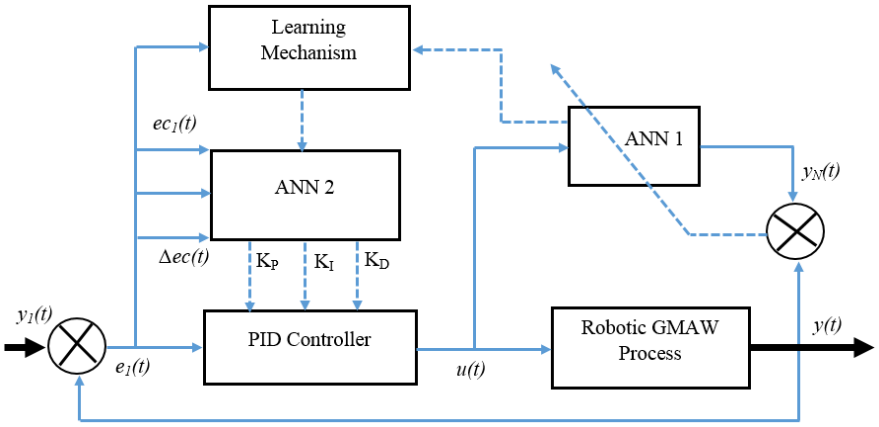

Figure 13. Framework of an ANN PID controller system for a robotic GMAW process (modified) Chen (2004).

The system integration of adaptive ANN with a PID controller for a robotic welding process illustrated based on Chen's framework serves as a model that could help in developing a new ANN-PID controller, in this case, the robotic GMAW process in this work. An ANN-PID controller similar to the framework shown in Figure 13 will help to overcome the drawbacks of "teach-and-playback" welding robots, which have no real-time sensing control of the welding process.

3 Research methods and summary of findings

This chapter presents the research methods used in this study. A more detailed description of the individual work can be found in the articles, *Publications I–V*. This chapter further summarizes the findings of *Publications I, II* and *V*, and presents the results of *Publication III* and *IV*.

3.1 Review of previous studies

Previous studies reviewed in this work include laboratory experiments and reports published in scientific journals and other scientific literature. In addition, industrial reports and interviews having scientific value are also included.

3.1.1 Publication I

Research aims

- *To explore the usability of HSS from both weldability and service performance viewpoints, paying critical attention to factors associated with weld quality.*
- *To identify methods which can be used to evaluate weld quality when welding HSS from a structural integrity viewpoint.*

A schematic framework which considers weldability factors (heat input, cooling rate, dilution and filler material); service performance factors (weld geometry, material grade and thickness, crack growth); machine factors; human factors; on-line process monitoring factors (pre-process monitoring, in-situ monitoring, post-process monitoring); failure analysis factors (design, stress data, fabrication details); and risk assessment options in determining structural integrity in welded HSS was designed and used as a tool in achieving the said objectives.

Findings

HSS could be identified in two main forms, that is, quenched and tempered (QT) steels and thermo-mechanical controlled process (TMCP) steels (Billingham and Sharp, 2003). The yield strength could be classified between 500–900 MPa. Carbon content is used as an important criteria in determining welding usability of HSS. The difference in carbon equivalence (CEV) influences the weldability of the steels. QT steels have higher carbon content than TMCP steels, making QT mostly easier to weld than TMCP steels, which have higher alloying elements (Wang and Liu, 2002; Zeman, 2009). Generally, HSS is susceptible to softening of the HAZ due to high welding heat input, which impairs tensile strength and joint strength properties like ductility and toughness (Billingham and Sharp 2003, Pirinen, 2013). Inter-critical reheating occurs at the two-phase zone, that is, between 700–900 ^{o}C. Therefore, HAZ softening occurs at high temperatures above tempering temperature (above 700 ^{o}C). A rapid cooling rate is required so that the

occurrence of softening of the HAZ is as minimal as possible. The risk of cold cracking in HSS is dependent on the choice of filler material used and the dilution rate together with the base metal. Low hydrogen filler materials are recommended since they prevent or limit the introduction of hydrogen into the weld (WTIA TN 15, 1999). Under appropriate welding conditions, a martensite-bainite microstructure is present in QT steels, while a ferrite-bainite microstructure is prevalent in TMCP steels (Wang, 2005). These microstructures must be present in welded HSS to ensure structural integrity.

Fatigue strength of HSS, a factor of its service performance, is reduced by the effects of welding, especially in the HAZ (Rantalainen, 2012; Meng, et al., 2013). Stress concentrations arise as the welded HSS structure is subjected to static or dynamic loading. Imperfections and weld defects, when present, increase crack growth. Undercut and porosity are typical examples that create notches and discontinuities, which give rise to further stress concentration. Crack initiation usually starts at the weld toe or weld root and is followed by crack propagation. The weld geometry is, therefore, critical to design, fabrication and welding method (Boardman, 1990; Hicks, 2001). The fatigue strength of HSS does not increase with increasing yield strength, but rather the strength properties of the material are associated with load carrying capacity (Jesus, et al., 2012; Rantalainen, 2012).

Machine and human considerations are also vital in welding manufacturing of HSS since these factors relate to conformance with standards and the ability to follow WPS defined for a specific HSS welding operation. When using SMAW, GMAW, GTAW, FCAW or SAW for welding HSS, the welding process must be examined for its suitability and the availability of appropriate consumables. Operators of such welding processes should be qualified and certified according to applicable welding standards.

To identify methods that could be used to evaluate weld quality of HSS welds from a structural integrity viewpoint, decision-making tools such as the analytical hierarchy process (AHP) (Saaty, 1980) and on-line monitoring systems (modelling and simulation approach) were found. Performing risk assessments on different driving factors and attributes was found to be essential for selecting the most suitable welding process for welding HSS (Balasubramanian, 2009). Although (AHP) was identified as being useful due to the variety of available welding machines, on-line process monitoring appears more promising as it matches well with modern-day welding manufacturing, where automation and digitization are increasing.

3.1.2 **Publication II**

Research aims

- *To explore the usability of UHSS from the weldability viewpoint.*
- *To identify relationships between nonlinear weldability factors of a robotic GMAW process in order to enable creation of an artificial intelligence model for welding UHSS material.*

Schematic frameworks which consider S960QC material properties (mechanical and chemical), welding parameters and variables (heat input, filler material, material thickness) and welding standards (EN ISO 5817; ISO 15609-1) and an artificial intelligence modelling system for fillet weld joints were designed and used to investigate UHSS weldability.

Findings

The UTS of S960QC is about 1000 MPa; the steel is thus suitable for applications where load carrying capacity is desired. Additionally, its reduced thickness and excellent load carrying capacity make it a suitable material for lightweight welded product manufacturing. Critical attention is required when selecting consumables for S960QC. Filler materials with high hydrogen content should be avoided because of the risk of hydrogen induced cracking. Hydrogen contents should be in the range of HD ≤ 5ml/100 g. Heat input of 0.5 kJ/mm should be used for material thickness > 4 mm. For material thickness ≤ 4 mm, the heat input should not exceed 0.4 kJ/mm due to the risk of HAZ softening. Cooling rates according to $t_{8/5}$ must be observed (Ruukki, 2007). In compliance with the EN ISO 5817 standard, surface imperfections and internal imperfections of fillet welded joints must meet quality levels designated by symbols B, C and D, where B corresponds to the highest requirement of the finished weld. Also, according to ISO 15609-1, for a given material thickness (t), the weld throat thickness should conform to: 0.5*t – 0.7*t.

Key process parameters and variables of robotic GMAW were identified by considering welding of S960QC in fillet joint configurations. Variables such as heat input, CTWD and torch angle were found to have a direct relationship with other welding parameters. For heat input, the direct parameters include arc current, arc voltage, welding speed and gas flow rate. For CTWD, the direct parameters include electrode extension, arc length, wire feed rate and wire diameter. For torch angle, the direct parameters include torch position, torch travel angle and torch movement technique (Hemmilä, et al., 2005; Jae-Woong, et al., 2008; Nele, 2013).

A schematic model of the AI system can help to understand the mechanisms underlying prediction and control of the output requirements of the fillet weld based on the input requirements. Due to the nonlinear characteristics of robotic GMAW and the considerations that need to be taken into account, the ANN approach was chosen as the

most suitable option for modelling and control of the welding performance of the welding system. A multilayer perceptron neural network architecture seemed feasible for practical implementation of the model, due to the multi input and multi output (MIMO) requirements. The Levenberg-Marquardt learning algorithm has been found to be valuable for reducing errors and adjusting weights and biases in the proposed ANN system for better and accuracy in convergence and prediction (Juang, et al., 1998; Fuller, 2000; Kim, et al., 2004; Yadav, et al., 2015).

3.1.3 **Publication V**

Research aim

- *This publication focused primarily on the practical usability of HSS grades for welded applications for Arctic operations. The study further considered quality and productivity aspects of welding processes used when welding HSS.*

Industrial interviews were conducted in the first phase of the research process. The second phase comprised review of previous studies on the usability of HSS. International welding standards and codes outlined by certification bodies were studied. In addition, scientific claims on the weldability of HSS were evaluated.

Findings

Selection of either quenched and tempered (QT) steels or thermomechanical controlled processing (TMCP) steels depends on the design (e.g. weld geometries) of the structure to be welded and the operational environment of the welded product. QT and TMCP steels of yield strength 500 MPa (grade E) are used for Arctic structural constructions. QT steel is mostly used in such constructions, but in recent times, the use of TMCP steel has become attractive because TMCP steels do not require preheating before welding as QT steels do. Welding productivity cycles are much higher when welding TMCP steels than QT steels. The plate thickness of these steels ranges between 5 mm – 40 mm, and they can operate in temperatures as cold as -40^{o}C (Nykänen, 1994).

Semi-automatic and automatic welding techniques are mostly used in hull production with the aim of increasing production rates. Flux-cored arc welding accounts for approximately 75% of welding processes used, while SAW and SMAW account for 15% and 10% respectively. The majority of the weld profiles are T-joints. Butt joints are also utilized, mostly one-side welded on ceramic or fixed backing. Higher efficiency in welding has been achieved through the use of automatic welding. The length of welded joint seams on side shells ranges between 400 mm – 500 mm. Welded joints account for about 3.5% of all the steel materials used in the hull assembly. Weld quality inspections are done either by ultrasonic tests or by radiography methods. These inspection processes are time consuming and result in delays in the production cycle. In addition to increased productivity, greater use of adaptive automated welding systems is seen as an attractive option to reduce labour cost.

Reviewing previous studies, it was found that QT and TMCP steels have somewhat similar physical properties, such as good strength-to-weight ratio, higher load carrying capacity and good weldability (Billingham and Sharp, 2003; Hill, 1991). QT steel grades such as E420 – E690, S390J6Q and S450J6Q can operate under very low temperatures between -50 to -60 ^{0}C at minimum impact energy of 27J (WTIA TN 15, 1999). TMCP steels also possess excellent toughness properties, and typical grades include S460ML, S500MC, S700MC, X100 and X120. However, TMCP steels are often more susceptible to softening of the HAZ (Kim, et al., 2009). The tendency to softening occurs when the HAZ of QT and TMCP steels are reheated at high temperatures above tempering temperatures (Nippon Steel and Sumitomo Metal, 2014) or as a result of the fusion welding processes and consumables used (Rodrigues, et al., 2004). It is reported that undermatched or matched filler metals are generally used in welding HSS (Porter, 2006), since the use of overmatched filler metal has not been economical in welding HSS (Pirinen, 2013).

Conventional welding processes such as shielded metal arc welding (SMAW), flux cored arc welding (FCAW), gas metal arc welding (GMAW) and submerged arc welding (SAW) have proven to be suitable for welding HSS (WTIA TN 15, 1999). Fillet joint configurations are mostly utilized for QT steels when the welded structure is to be subjected to fatigue loading. As QT steels are often loaded to higher stresses, it is essential that the welds be smooth, correctly contoured and well flared into the legs of the joined pieces. The runs of each fillet weld must have good penetration, particularly at the root, but must not undercut the joined pieces (WTIA TN 15, 1999).

3.2 Experimental study

Adaptive welding apparatus

The welding apparatus comprised equipment shown in Figure 14. The setup consisted of an adaptive GMAW process integrated with an industrial robot system. As shown in Figure 14, a pilot laser is positioned in front of the welding torch and finds and tracks the weld path as well as measures the groove geometry. A thermo-profile sensor (TPS), which is immediately behind the welding torch and in front of the second laser, captures the thermal profiles during solidification of the welding seam, before the seam is cooled. The second laser scanner, which trails behind the TPS, measures the bead height. All three sensors in the welding head, i.e. the two lasers and the TPS, send data to the monitoring and processing units.

The TPS non-contact monitoring system allows measurement of the weld seam at a sampling frequency of 400 Hz, permitting recording of the thermal distribution of the weld at high travel speeds up to 180 m/min. High measurement accuracy of about 0.2 % at a temperature of 1000 ºC is achievable. In-built band-pass filters are configured to mitigate the effect of welding spatter on data evaluation and to smoothen heat data in the lengthways and crossways direction. The TPS operates by measuring temperature distribution from infrared (IR) emissions emitted from the hot weld surface.

In the experimental works, the laser sensors were not used due to the fillet joint configurations used, and thus geometrical measurement with the laser sensors was not part of the aim of the experiments.

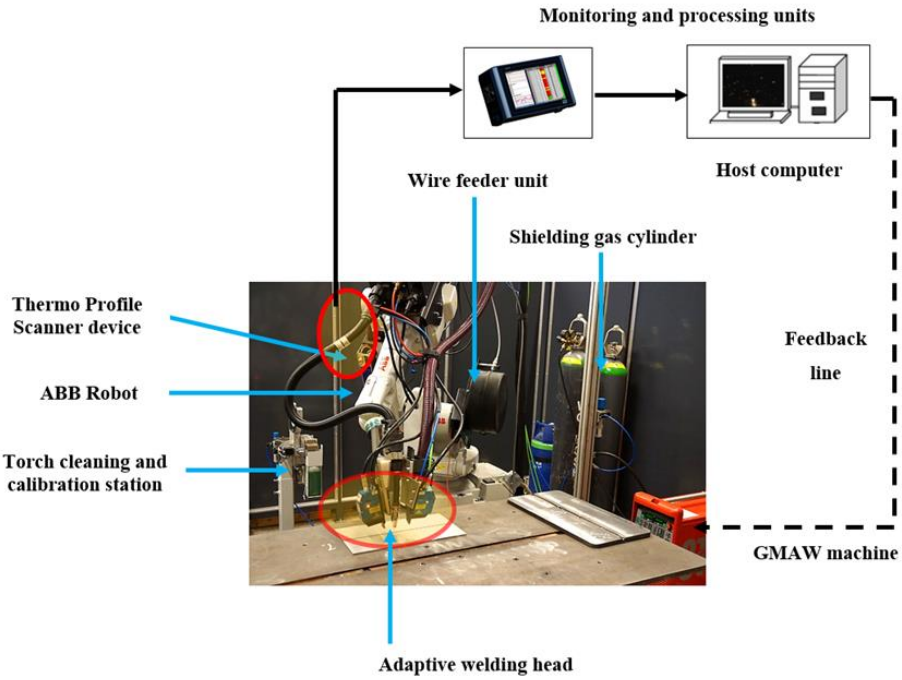

Figure 14. Setup of the adaptive intelligent robotic GMAW system.

Mechanical and chemical composition of the base metal (S960QC) and the consumables

The mechanical properties of S960QC UHSS are: yield strength (900 MPa), UTS (1000 MPa), impact strength of 33–50 J at operating temperature of -40 ^{o}C and elongation of 7%. The mechanical properties meet the applicable standards: EN ISO 148-1:2010 (impact strength test); EN ISO 10051 (thickness, width and length); EN 10029 (flatness, Class N, steel type H), and EN ISO 10149-1 (tensile test). The low alloyed solid wire electrode used conforms to EN 12534 (ISO 16834:2012) standard and matches with the chemical and mechanical properties of the base metal. The shielding gas conforms to EN 439:M21 standard. Table 6 and Table 7 show the composition of the base metal and the welding consumables respectively.

Table 6. Chemical composition of UHSS S960QC, wt.%

Items	C	Si	Mn	P	S	Al	Nb	Cu	Cr	Mo	Ni	Other
S960QC (t: 5 mm) (Ceq: 0.46)	0.09	0.21	1.05	0.01	0.004	0.030	0.003	0.025	0.82	0.158	0.04	0.008 (V) 0.032 (Ti) 0.0021 (B)

CEV = C + Mn/6+ (Cr + Mo + V)/5 + (Ni + Cu)/15

Table 7. Chemical composition and mechanical properties of consumables.

Filler metal	Union X 96 solid wire electrode (1.00 mm in diameter)		Chemical composition (wt. %)					
			C	Si	Mn	Cr	Mo	Ni
			0.12	0.80	1.90	0.45	0.55	2.35
Mechanical properties	f_y [MPa]	f_u [MPa]	A_5 [%]	KV [J]				
Nominal	930	980	14	40 (-40°C)				
Measured	990	1245						
Shielding gas for GMAW process 92% Ar + 8% CO_2								
Shielding gas for thermo-profile scanner 88% Ar + 12% CO_2								

3.2.1 **Publication III**

Research aims

- *To evaluate the accuracy of sensing systems such as infrared thermography based thermo-profile sensing in prediction of weld penetration as a weld quality attribute.*
- *To evaluate the effects of welding variables and parameters in attainment of full weld penetration in a fillet weld configuration.*
- *To introduce S960QC UHSS as a potential lightweight material applicable for offshore welded steel structures.*

This publication is based on empirical work. It also includes review of previous studies on lack of weld penetration at the weld root of fillet welded joints and possible repercussions for offshore welded steel structures. As a part of efforts to guarantee full

weld penetration to curb weld joint failures, the S960QC material was introduced, and the grade was proposed as a potential advanced steel applicable for offshore welded structures.

The empirical work comprises S960QC UHSS material of 5 mm thickness, welded in fillet joint configurations with the adaptive robotic GMAW system and the welding consumables mentioned earlier. Before welding, the S960QC material was machined and some of the samples were beveled to an angle of 60^{o} for full penetration welds. The configuration of the weld joint is shown in Figure 15. During welding, the TPS, attached and positioned at a distance of 30 mm behind the welding torch, was used to measure and record thermal heats from the solidified but still glowing hot surface of the weld seam. The welding of the prepared specimen was performed sequentially. Each specimen was mounted on a positioner, clamped and robot welded at an interval of 10 mm. This means that each specimen had 2 weld seams of length of about 120 mm.

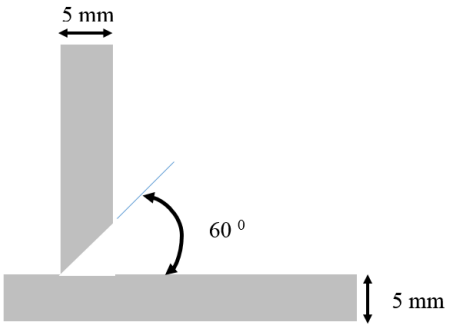

Figure 15. A 60^{o} fillet joint configuration for full penetration weld setup used in the experiments.

Welding parameters and variables were varied to aid comparison and analysis of the effects of varying welding heat input on weld penetration depth. Welded specimens were characterized by etching, microscopy and mechanical examination. Captured weld seam data were ascertained and imported to MATLAB for thermal profile distribution analysis. 9 samples were presented for analysis. Table 8 shows the welding parameters and variables used in the experiment. Detailed information about the welding operation can be found in *Publication III*.

Table 8. Welding parameters and variables for S960QC full penetration welds.

Specimen	*Heat Input*			*Contact tip-to-work distance (CTWD)*		*Torch angle*		
	I (**A**)	U (**V**)	v (***mm/sec***)	Electrode stick out ***mm***	Wire feed rate ***m/min***	Torch position (^{0})	Torch travel angle (^{0})	Torch movement technique
1	210.7	20.3	7.0	20.0	9.0	45	15	Pushing
2	236.4	24.3	7.0	20.0	10.0	50	15	Pushing
3	289.6	28.4	7.0	20.0	11.0	30	5	Pushing
4	245.7	28.0	7.0	18.0	11.0	45	0	Pushing
5	263.2	28.5	7.0	18.0	11.0	45	0	Pushing
6	269.6	25.6	7.0	15.0	11.5	35	0	Pulling
7	268.7	25.7	7.0	15.0	12.0	35	5	Pulling
8	269.4	27.0	7.0	15.0	11.0	35	0	Pushing
9	260.4	28.2	7.0	20.0	11.0	45	0	Pushing

Results and discussion

Macrostructure analysis

After macrostructure analysis, it was observed that, based on the welding heat input applied, full weld penetration could be achieved in some of the specimens, taking into consideration other factors like CTWD and the torch angle. However, defects detected include lack of weld penetration at the weld root, undercut and wide HAZ (see Figure 4 in *Publication III*). Throat thickness, which is a very significant weld attribute in fillet joints, in this case, was also affected in some of the specimens as a result of the nonlinear relation between welding parameters and welding variables. Table 9 shows the heat inputs obtained during the welding operation used in the welding of the various specimens.

Table. 9. Heat input obtained according to the performance of the welding operation.

Specimen	*Heat Input*			
	I (**A**)	U (**V**)	v (***mm/sec***)	Heat input value (Arc efficiency 0.8 %) kJ/mm
1	210.7	20.3	7.0	0.48
2	236.4	24.3	7.0	0.66
3	289.6	28.4	7.0	0.94
4	245.7	28.0	7.0	0.79
5	263.2	28.5	7.0	0.86
6	269.6	25.6	7.0	0.79
7	268.7	25.7	7.0	0.79
8	269.4	27.0	7.0	0.83
9	260.4	28.2	7.0	0.84

Heat inputs in the range 0.8–0.9 kJ/mm produced weld defects leading to undercut on the upright member of the fillet joint. Throat thickness of the weld was reduced as the heat washed off some of the material. Depending on the joint configuration, heat input of 0.79 kJ/mm produced the best weld penetration. The throat thickness when measured was ≥ 4 mm.

Behaviour of welding parameters and variables

The behaviour of the welding parameters, especially current, voltage, wire feed rate, temperature and infrared width of the weld seam, were detected during the welding operation. The thermal profile distribution based on temperature readings and infrared width readings are shown in Figure 5–10 in *Publication III*. The adaptive welding system was able to identify weld imperfections and defects that occurred in some of the specimens. By comparing these figures with macro images of the weld specimens, a clear correlation between weld penetration depth and weld defects was established. Heat input of 0.79 kJ/mm produced a uniform temperature reading of 1129 ºC without producing any defects in the weldment (see Figure 7 and 8 in *Publication III*).

Vickers hardness test

The Vickers hardness values across the weld metal were between 256 – 331 HV5, slightly lower than the hardness values across the surface of the base metal (351 – 356 HV5) at a load of HV5 between distances of 1 mm. This observation shows a mismatch between the weld metal hardness and the base metal. Moreover, the hardness values across the fusion line and HAZ show lower values than the hardness values of the weld metal. This difference is a result of the effects of heat input, which produces coarse grains across the fusion line and the HAZ. Figure 16 shows the hardness test results of the specimen welded with 0.79 kJ/mm heat input.

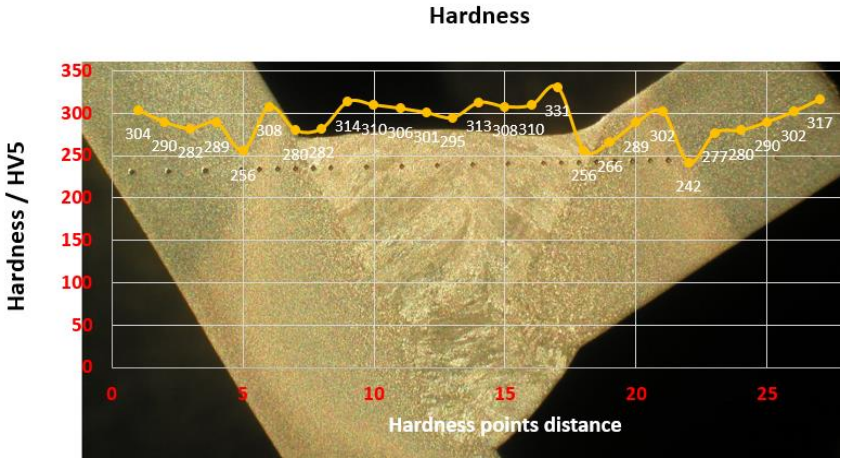

Figure 16. Hardness test of specimen welded with 0.79 kJ/mm heat input.

Using matched filler metal with high heat inputs can cause the weld metal strength to have mismatch with the base metal and consequently causes lower hardness and strength properties in the HAZ. The possible diffusion of alloying elements as impurities is also detrimental to HAZ properties.

3.2.2 **Publication IV**

Research aims

- *To explore the applicability of an adaptive intelligent robotic GMAW process in welding of S960QC UHSS, paying critical attention to the behavior of welding parameters and their effects on the joint geometries.*
- *To introduce S960QC UHSS as a potential lightweight material applicable for Arctic structural construction.*

This empirical study includes review of previous work on Arctic welding and construction and the need to construct lightweight welded structures. The review work gives an account of the requirements of weldable material for Arctic structural construction. An illustration of a welded Arctic structure was presented to indicate the various sections and parts that need to meet Arctic operation conditions and requirements. S960QC material was introduced and suggested as a potential advanced steel applicable for Arctic structural constructions.

The empirical work comprised investigation of S960QC UHSS material of 5 mm thickness, welded in fillet-joint configurations with the adaptive robotic GMAW system and the welding consumables mentioned earlier. Before welding, the S960QC material was machined for 20 samples. The plates were tacked together, forming 10 samples of fillet joints. For the welding experiments, 5 joints each were made to be welded in the PB and PA welding orientation and positions respectively. During welding, the TPS, which was attached and positioned at a distance of 30 mm behind the welding torch, was used to measure thermal zones from the hot weld surface of the cooling weld seam during the welding process. The adaptive welding system employed an existing artificial neural network (ANN) to model the behavior of welding parameters and variables. Figure 17 shows the various fillet weld configurations used in the experiment.

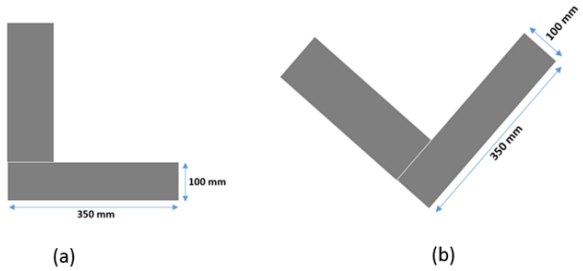

Fig. 17. Fillet weld configurations where a) is PB welding position and b) PA welding position.

The experimental work was done to determine the effects of varying heat inputs on the hardness properties of the weld metal, weld fusion zones and the HAZ. Results were compared with the base metal. Also, the effects of workpiece orientation on weld penetration were determined. In addition, the work evaluated the behavior of welding parameters and variables while using the intelligent adaptive welding system settings.

Out of the 10 tacked samples, only 2 samples were welded in the ANN environment. After initial evaluation, only 8 samples (including the 2 samples welded in the ANN environment) were utilized in analysis. The measured thermo-profile data were then imported into MATLAB for further analysis of the behavior of the welding parameters and variables. The welded specimens were etched with a 4% nital solution (95 ml C_2H_5OH + 5 ml HNO_3) to delineate the microstructure of the base metal and the macrostructure features of the welds and the HAZs of the specimen. Light microscopy and a Vickers hardness test machine were used for metallurgical and mechanical analysis of the effects of heat inputs on various weld specimens. Table 10 shows the welding parameters and variables used in the experiment. Detailed information about the welding operation can be obtained from *Publication IV*.

Table 10. Welding parameters and variables for S960QC deep penetration welds.

Specimen	*Heat Input*			*Contact tip-to-work distance (CTWD)*		*Torch angle*		
	I (**A**)	U (**V**)	v (***mm/sec***)	Electrode stick out ***mm***	Wire feed rate ***m/min***	Torch position (^{0})	Torch travel angle (^{0})	Torch movement technique
1 (PB ANN)	200.1	22.1	7.0	18.0	9.69	40	5	Pushing
2 (PA ANN)	202.2	22.3	7.0	18.0	9.37	90	0	Pushing
3 (PB 1)	213.6	24.3	7.0	18.0	10.31	40	5	Pushing
4 (PA 1)	232.1	26.2	7.0	18.0	10.27	90	0	Pushing
5 (PB 2)	204.7	26.2	7.0	18.0	8.90	40	5	Pushing
6 (PA 2)	211.7	26.1	7.0	18.0	8.87	90	0	Pushing
7 (PB 3)	195.7	24.6	7.0	18.0	8.90	40	5	Pushing
8 (PA 3)	208.9	24.6	7.0	18.0	8.90	90	0	Pushing

Results and discussion

Macrostructure analysis

The macrostructure of all the specimens welded in horizontal flat welding position (PA) showed deeper weld penetration at the weld root than those of horizontal welding position (PB). The finger weld characteristic of the GMAW process was well pronounced in the PA welding position.

Comparing weld specimens PB ANN and PA ANN, the heat input applied was the same value, with just slight variation. However, due to the welding position of PA ANN, the heat input produced high arc pressure causing deeper weld penetration. Contrarily, the cooling rate in PA ANN was much slower than PB ANN. This is, as a result of the amount of heat retained at the weld toe, caused slower dissipation of heat than in PB ANN. This phenomenon was observed in other specimens, too, such as PB 1, PA 1, PB 2, PA 2, PB 3 and PA 3. By visual examination, PB welding position shows non-uniform HAZ across the base member and the upright member. Although in PA the HAZs are also wide, there was uniformity in how the heat spreads across the joints. Another significant finding is that although PB 2 had higher heat input than PA 2, the cooling rates were quite similar. This observation affirms that there is much faster cooling rate in the PB welding position than the PA position for the same heat input or slightly higher input for PB (say, 0.05 kJ/mm difference).

The shape of the surface profile of the weld beads looked flatter from the top weld toe to the down weld toe, especially with the PA welding position. No major weld defect or imperfection was noticed in any of the specimens. The quality levels (surface and internal imperfections) of the specimens conform to EN 1SO 5817. Throat thickness, when measured with a weld bead gauge (calliper) falls within the range of 0.5*t – 0.7*t, where t is the thickness of the base metal (5 mm). Therefore, the weld throat thicknesses were ≥ 2.5 or ≤ 3.5 mm, showing acceptable throat thicknesses (see Figure 6 in *Publication IV*).

Behaviour of welding parameters and variables

The behaviour of the various welding parameters shows a direct effect on a temperature of the weld seam, thus causing non-uniform thermal cycles in the weld and surrounding zones. Comparing temperature graphs of all the PB welding positions (Figure 7 in *Publication IV*), it can be seen that the temperature readings did not exceed 1100 ^{o}C within heat input range from 0.50–0.65 kJ/mm. However, comparing all temperature graphs of PA within the same heat input range, the temperature captured from the surface of the weld seam peaked above 1100 ^{o}C. Heat input readings of PA 1 and PA 3 show better stability than PB 1 and PB 3. Nevertheless, arc length, wire feed, voltage and current reading were quite stable. It can be said that arc stability is very much achieved in the PA welding position, thus the mode of metal transfer from short-circuit arc to spray arc is smooth.

On the contrary, the behaviour of welding parameters as observed from PA ANN and PB ANN show unstable curves compared to other specimens. Figures 18 and 19 give a clearer view of the behaviour of the welding parameters (see Figure 7 of *Publication IV*). Although arc length and wire feed rate were quite stable, the severe fluctuations in voltage, current, and heat input readings could be a result of disturbances in the adaptive welding system. Such disturbances may have influenced the amount of heat input supplied during welding, thus keeping the weld seam temperature below 1100 ^{o}C. Secondly, such disturbance might be because the existing ANN system did not compensate or try to modify the mode of metal transfer from short-circuit arc to spray arc. It could also be because of lack of learning data or a compensating behavior to match target conditions of the ANN system. Generally, the driving forces in GMAW (electrostatic force, Marangoni force, buoyancy force, inertia, surface tension, and viscosity) might have influenced the behaviour of the welding parameters and variables in the different welding positions.

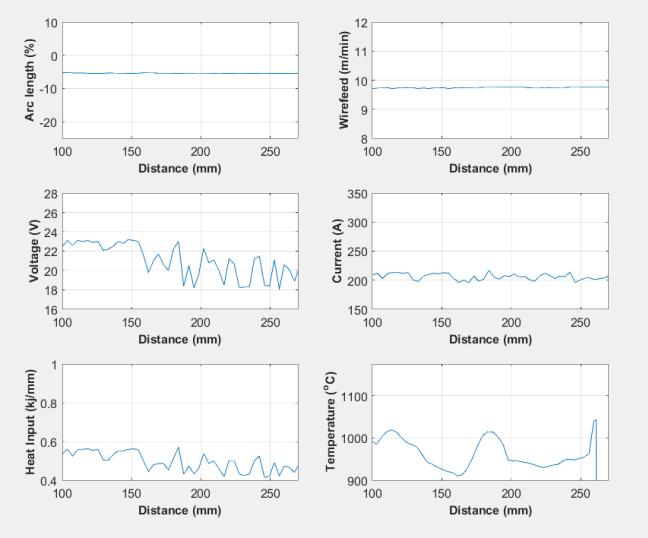

PA ANN

Figure 18. Behavior curves of welding parameters and heat input of specimen PA ANN.

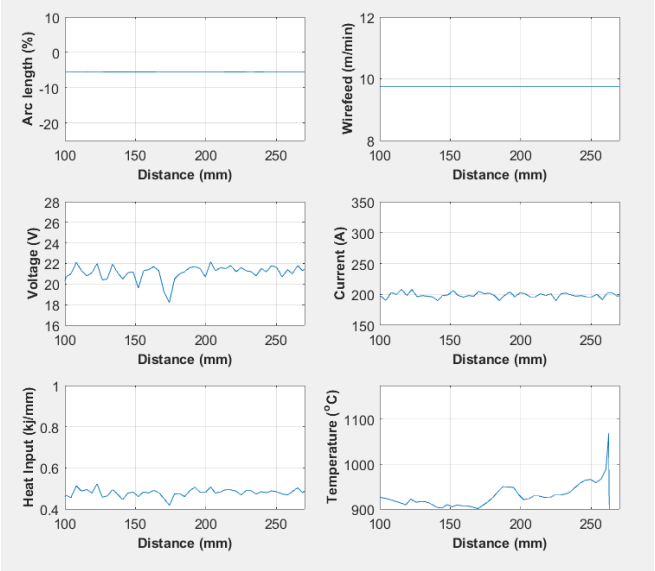

PB ANN

Figure 19. Behavior curves of welding parameters and heat input of specimen PB ANN.

Vickers hardness test

The Vickers hardness of the base metal varied between 351–356 HV at a load of HV5 between distances of 1 mm. The Vickers hardness values across the surface of the weld metal was found to be similar in both PA ANN and PB ANN. The highest hardness values obtained ranged between 375–397 HV. However, at the fusion boundaries, the hardness values of PA ANN dropped to about 295 HV to the left side and 303 HV to the right side of the joint geometry as shown in Figure 8 of *Publication IV*. Notably, at the fusion line of PB ANN, there was no significant drop in hardness, as depicted in Figure 9 of *Publication IV*.

At the HAZs, a drop in hardness was recorded in both welding positions. PA ANN recorded a more progressive drop in hardness towards the base metal. Considering the heat input applied in PA ANN and PB ANN, the maximum percentage drop in hardness across the fusion boundaries to the base metal is about 26 % to 24 %, respectively (using minimum hardness values). It can be seen from the graph of PA ANN from Figure 7 of *Publication IV* that when heat input was within the range of 0.50–0.65 kJ/mm, the temperature fluctuation reading did not peak above 1100 ^{o}C. This could be a result of the welding parameters being modified by the ANN system.

Comparing PA 3 and PB 3, it can be seen in Figure 10 and Figure 11 of *Publication IV* that PB 3 recorded higher hardness values at the surface of the weld metal than PA 3. Considering the heat input applied in PA 3 and PB 3, the maximum percentage drop in

hardness across the fusion boundaries to the base metal is about 21% to 16%, respectively (using minimum hardness values). However, in PA welding positions, that is Figure 8 and Figure 10 of *Publication IV*, the drop in hardness is quite uniform from the HAZ to the base metal on both sides of the welded joint. Hardness values across the surface of the weld metal is uniformly spread due to the flatness of the weld bead profile. In PB welding positions, that is Figure 9 and Figure 11 of *Publication IV*, a drop in hardness is more prone to the upright member than the base member, especially at the fusion boundary and in the HAZ. Although there is progressive drop in hardness towards the base metal, the upright member experienced greatest hardness drop.

Microstructure

The microstructure formed in specimens welded in the PA position is different from specimens welded in the PB position. The microstructure of the weld metal produced in the PA welding position is uniformly mixed bainite and martensite, as shown in Figure 20. However, the microstructure of the weld metal produced in the PB welding position is non-uniformly mixed, as shown in Figure 21. It is known that the electromagnetic force enhances mixing in the weld pool, causing liquid metal to flow downward in the middle of the weld pool and forming a counterclockwise circulation loop along the central longitudinal plane. However, at the top surface of the weld pool, the Marangoni force drives the melt from the center to the edge of the weld pool along the fusion boundary (Kou and Wang, 1986; Kumar and DebRoy, 2007). It can be said that, in the PA position, the combined forces of the electromagnetic and Marangoni produced a uniform mixing pass. However, in the PB position, the Marangoni force was stronger than the electromagnetic force so it could not sufficiently cause molten pool mix but rather drove the molten pool from the center to the edge of the weld pool along the fusion boundary.

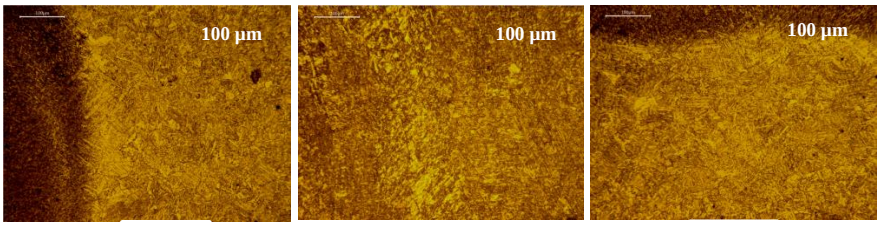

(a) (b) (c)

Figure 20. Micrograph of specimen PA ANN: a) HAZ of the upright member, b) weld metal, c) HAZ of the base member.

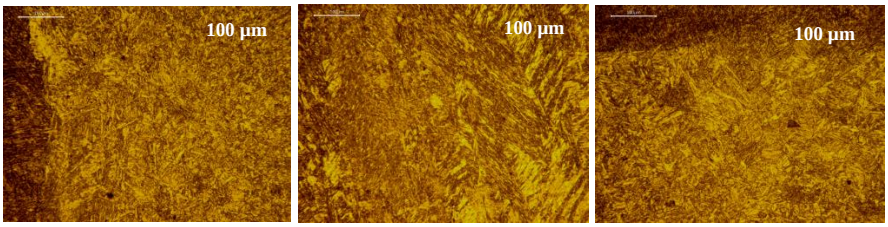

(a) (b) (c)

Figure 21. Micrograph of specimen PB ANN: a) HAZ of the upright member, b) weld metal, c) HAZ of the base member.

The grain sizes of the CGHAZ are larger in PA than in PB, as illustrated in Figures 22 and 23, respectively. Coarse bainite microstructure is more visible in Figure 22 than in Figure 23. This means that the PA weld has weaker HAZ than with PB. It is known that the HAZ or fusion line toughness of most carbon and low alloy steels transform to coarse bainitic or a mixture of coarse bainite and martensite in the CGHAZ. This extensive grain coarsening is due to heat inputs, even under moderate conditions (Akselsen, et al., 2017). The observations corroborate with the findings of Akselsen et al. (2017). However, it has also been reported that prevention of grain growth is essential to enhance fusion line toughness. The preventive mechanisms suggested include equal addition of Ti to form TiN precipitates to pin grain boundaries and control of intra-granular microstructure (Akselsen et al., 2017).

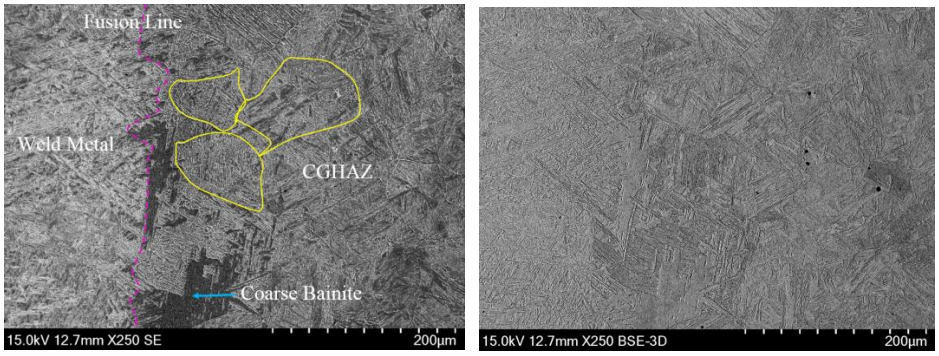

(a) (b)

Figure 22. Micrograph of specimen PA ANN: a) SEM micrograph, b) BSE micrograph.

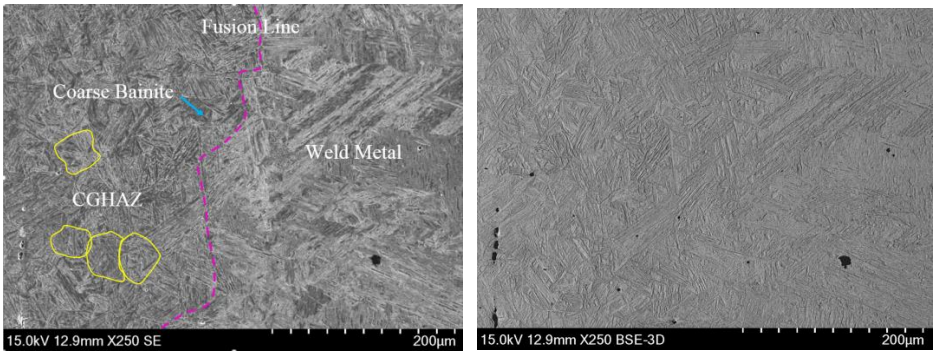

(a) (b)

Figure 23. Micrograph of specimen PB ANN: a) SEM micrograph, b) BSE micrograph.

It should be noted that the black dots on both the SE and BSE micrographs are dirt particles and are not related to the properties of the microstructures.

The illustration in Figure 24 shows a graphical description where grain growth prevention and intra-granular ferrite promotion causes a shift in the microstructure from coarse upper bainite to fine intragranular ferrite, resulting in a narrower CGHAZ. It has been presented that intra-granular nucleation occurs due to particles (Kojima, et al., 2004; Suzuki, et al., 2005), which can be oxides, sulfides, Ca, Mg or Ti, or high temperature stable nitrides (TiN), of size from 10 nm to 0.5 µm (Akselsen, et al., 2017).

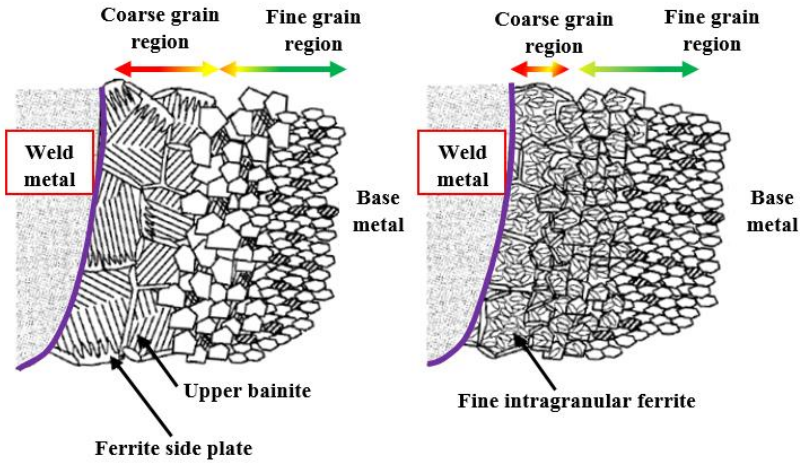

Figure 24. Possible microstructural changes under HAZ grain growth control. Modified. (Suzuki, et al., 2005).

Table 11. EDA compositional analysis of PA ANN and PB ANN weldments.

EDS compositional analysis	C K	Cr K	Mn K	Al K	Si K	Fe K	Ni K	Mo L	Mg K
PA ANN	0.0/10	0.0/2.09	0.0/3.89	0.0/3.8	0.0/1.52	85/99	0.0/4.78	0.0/2.26	
PB ANN	0.0/37	0.0/3.79	0.0/7.39	0.0/21	0.0/3.13	58/100	0.0/8.30	0.0/17	0.0/3.36

From Figure 23, it can be said that the CGHAZ shows an intra-granular microstructure with narrower polygonal shaped ferrite in addition to the martensite-bainite mix. The EDS compositional analysis performed revealed elemental variations in the weld metal, as shown in Table 11. It was observed that the microstructure of specimen PB ANN had traces of Mg. Therefore, the existence of Mg in the microstructure may have promoted intra-granular nucleation as depicted in Figure 23.

4 WQA model based on AIS

Among many practitioners there is a perception that implementation of robotic welding systems in welding factories is tedious and time consuming. Some small and medium-sized enterprises (SMEs) consider robotic welding uninteresting because their welding production is done in batches based on contractual work. This means that programming work has to be done for separate models of products before welding.

On the other hand, those welding companies who have made attempts to implement robotic welding systems also face weld quality related challenges. These challenges stem from the basic functionalities of robots. That is to say, robot manipulators are position-controlled devices that can receive a trajectory and run it continuously, but repeatability and precision is a challenge, as some margin of dimensional errors occur. Secondly, robot manipulators have closed-loop controllers, and for this reason, the system does not allow real-time position adjustment through programming by the user. Such robot controller systems, therefore, do not provide programming platforms to handle tasks that require complex techniques (learning, supervisory, monitoring, etc.). Additionally, remote control of the robot manipulator done from an external computer is not applicable.

To alleviate the repeatability and precision challenges of the robot manipulator, frequent calibration of the robotic welding system needs to be done, and this process does not fix the problem in the long term. To solve the programming challenges inherent with robot controllers, computational platforms suitable for handling complex non-linear operations are needed, and systems for guidance and inspection to handle monitoring and control tasks are also required.

For welding applications, the ability to start from one trajectory to another and essentially have the means to adjust the trajectory in real-time, as a function of the observed outcomes of the welding process, is very important. These functionalities and capabilities expected of a robotic welding system are a critical demand from welding factories as they pertain to welding productivity and quality assurance issues. Additional setup and computational work is required to guarantee that robots perform as expected with the required quality.

This chapter presents technological steps (assembly and programming capabilities) and new approaches in developing a welding quality assurance (WQA) model based on adaptive intelligent systems (AIS). The model is limited to the robotic GMAW process because of the system integration components involved. The reasons for developing a welding quality assurance model stem from the need to resolve the aforementioned complexities and challenges and a desire to resolve similar challenges surrounding the implementation of robotic GMAW systems in welding factories, be they in large or small and medium enterprises (SMEs). Key intelligent technologies and architecture (components, system integration protocols) for robotic GMAW will be discussed. Additionally, there is consideration of adaptive intelligent GMAW as an enabling technology for linking production across networks of companies.

4.1 Identification and selection of system hardware

The system hardware of an adaptive intelligent GMAW process should include components illustrated in Figure 25. The operational functionalities of these components, such as the sensors, robot manipulator, and monitoring systems, have been explained in Chapter 2 of this work. These components are commercially available and some of the components come with standardized programming languages, human-machine software, and hardware interfaces.

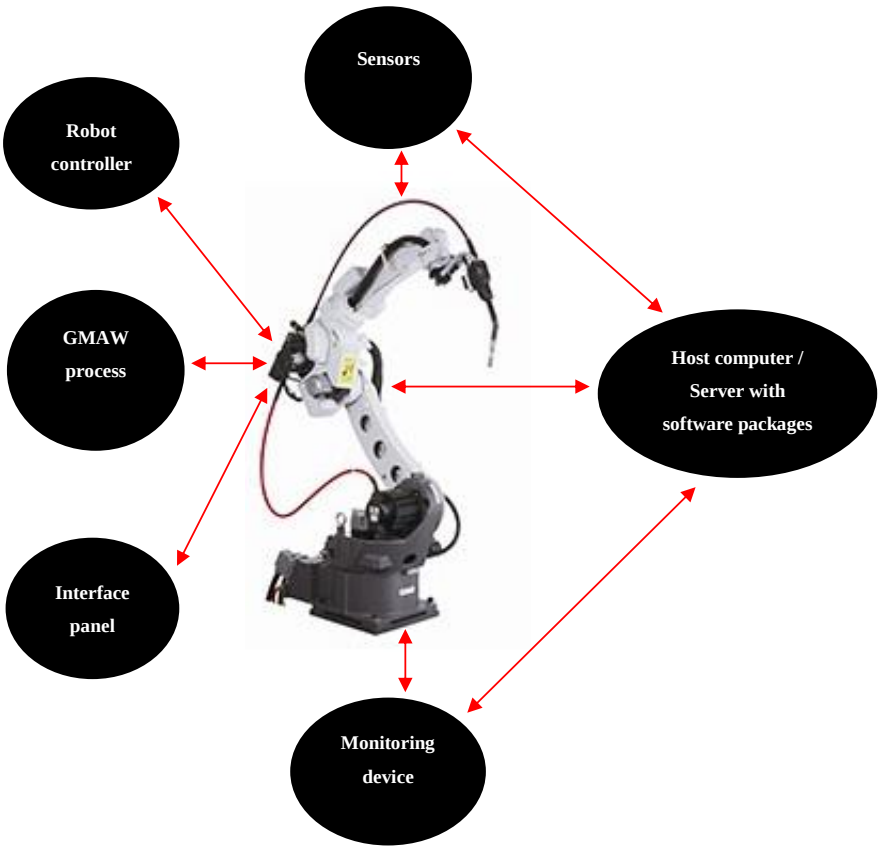

Figure 25. Hardware components for adaptive intelligent GMAW system.

However, identifying and selecting the right components to meet welding manufacturing and production needs is critical. When selecting the components, the following criteria must be observed:

- Components must have standardized features.
- Components must be compatible with system integration protocols.
- Components must be compatible with existing mechanical and engineering software packages.
- Components must have flexibility for configuration and programming.
- Components must have ease of connectivity with other system components.

4.2 System integration protocols

System hardware identified in Figure 25 require suitable, appropriate and standardized means to communicate with each other, either directly or indirectly, to execute single or multiple tasks. For these reasons, different forms of system integration protocols for diverse communication purposes are presented in this section.

A computer-based human-machine interface (HMI) is a fundamental requirement for communication between devices and components made of electro-mechanical systems. The teach pendant for robots basically serves the purpose of communicating input signals between other hardware and software units for a specific function to be performed. However, for such message signals to be communicated, system protocols like programmable logic controllers (PLC), Ethernet, application programmable interface (API) and fieldbus (IEC 61158) need to provide real-time distributed control and connectivity.

When connectivity between components is established, system protocols like the I/O controller (also called peripheral processor) receive the data and then communicate the signals between the central processing unit (CPU) and the motherboard. For communication between various software components, an API is required. For remote control of the components, message based protocols like transmission control protocol/internet protocol sockets (ICP/IP), and remote procedure call (RPC) sockets are needed.

Figure 26 shows a schematic structure of the connectivity between the various adaptive intelligent components and the system integration protocols. It can be seen that the HMI is connected to the PLC or desktop computer/personal computer by an Ethernet. However, a fieldbus is used to connect the HMI to the robot manipulator. Similarly, a fieldbus is used to connect the PLC or computer to the various sensing and monitoring systems. For connectivity between software systems of any of the components, an API interface is used. For remote control of any of the components, either the TCP/IP socket/server or RPC socket/server is used.

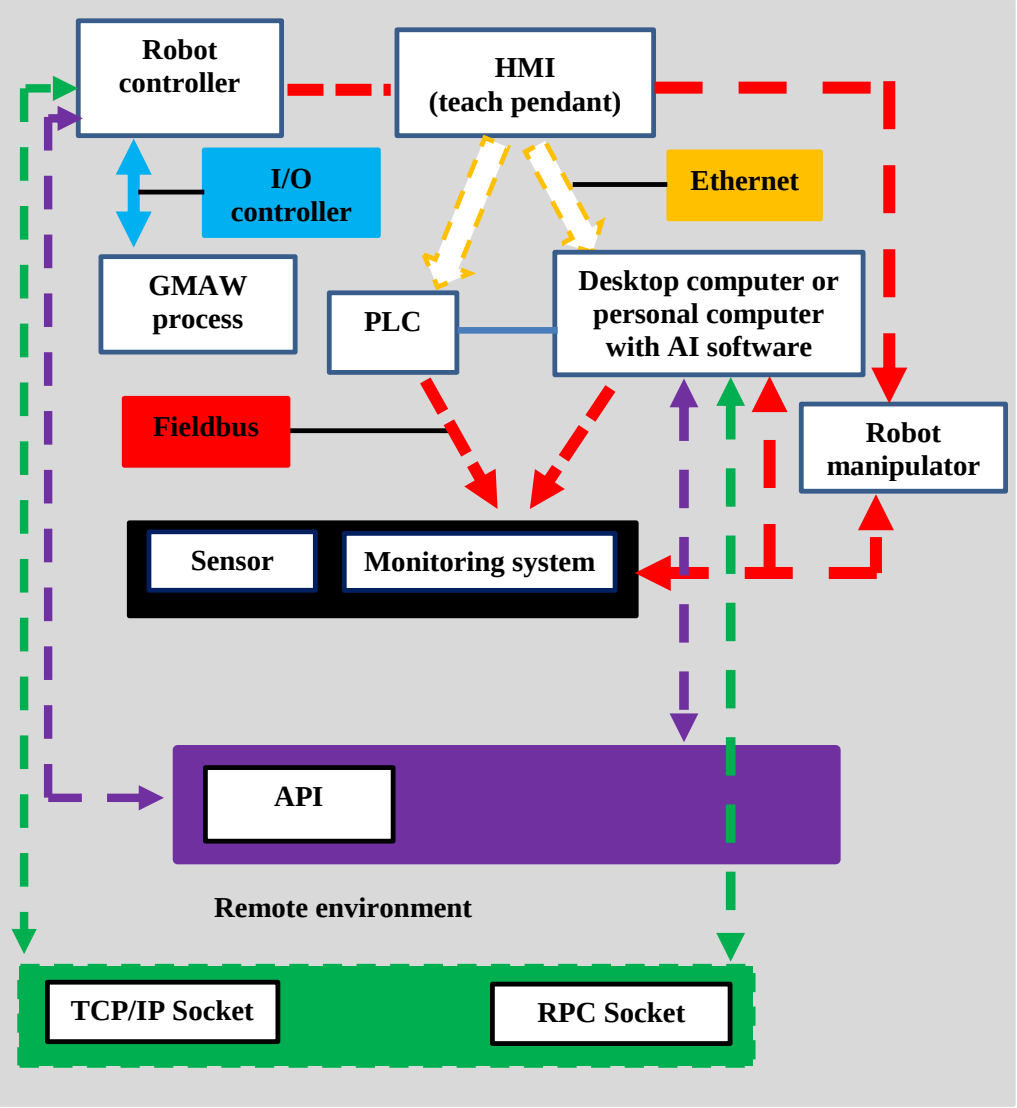

Figure 26. Systems architecture of components and protocols for adaptive intelligent robotic GMAW.

4.3 The AIS based WQA model

Programming and modelling of welding data can be done in a number of different ways, for instance: 1) by using existing engineering software packages like CAD/CAM with 3D tools to generate weld data; or 2) by performing empirical tests for weld data collection and exporting the data to software for further modelling and control. With software packages like CAD, the CAD interface is used to programme and guide the robot welding trajectories for execution of the welding operation in real-time (Chen and Wu, 2009). However, the rigidity of the system does not allow real-time adjustment of parameters and variables during welding. However, before or after welding, the welding parameters can be adjusted off-line or even from a remote environment.

For the above reasons, the integration of software components like adaptive intelligent systems to aid adjustment of welding parameters and variables through real-time monitoring and control can provide optimum welding solutions, especially from the perspective of weld quality and productivity. Adaptive intelligent systems, however, require prior information or data for modelling and control of the welding. Therefore, empirical tests are needed prior to designing the ANN model and control algorithm. Design of the ANN model and control algorithm comprises the following stages:

Stage 1: Data collection

The data collection stage entails creation of a knowledge base from material samples of welded metals. Figure 27 shows the schematics for data collection. With the adaptive intelligent system in place, the knowledge base is automatically updated by aggregating information generated during welding operations. The knowledge base includes information such as welding parameters and variables, and seam data from the welding process captured via the sensory and monitoring devices. The knowledge base can be retrieved from a desktop computer as a Microsoft Excel document in most cases. This process is vital because the transient details produced from the welding process have huge amounts of weld and seam information, which is captured in a time domain, and which needs to be validated through further modelling and control.

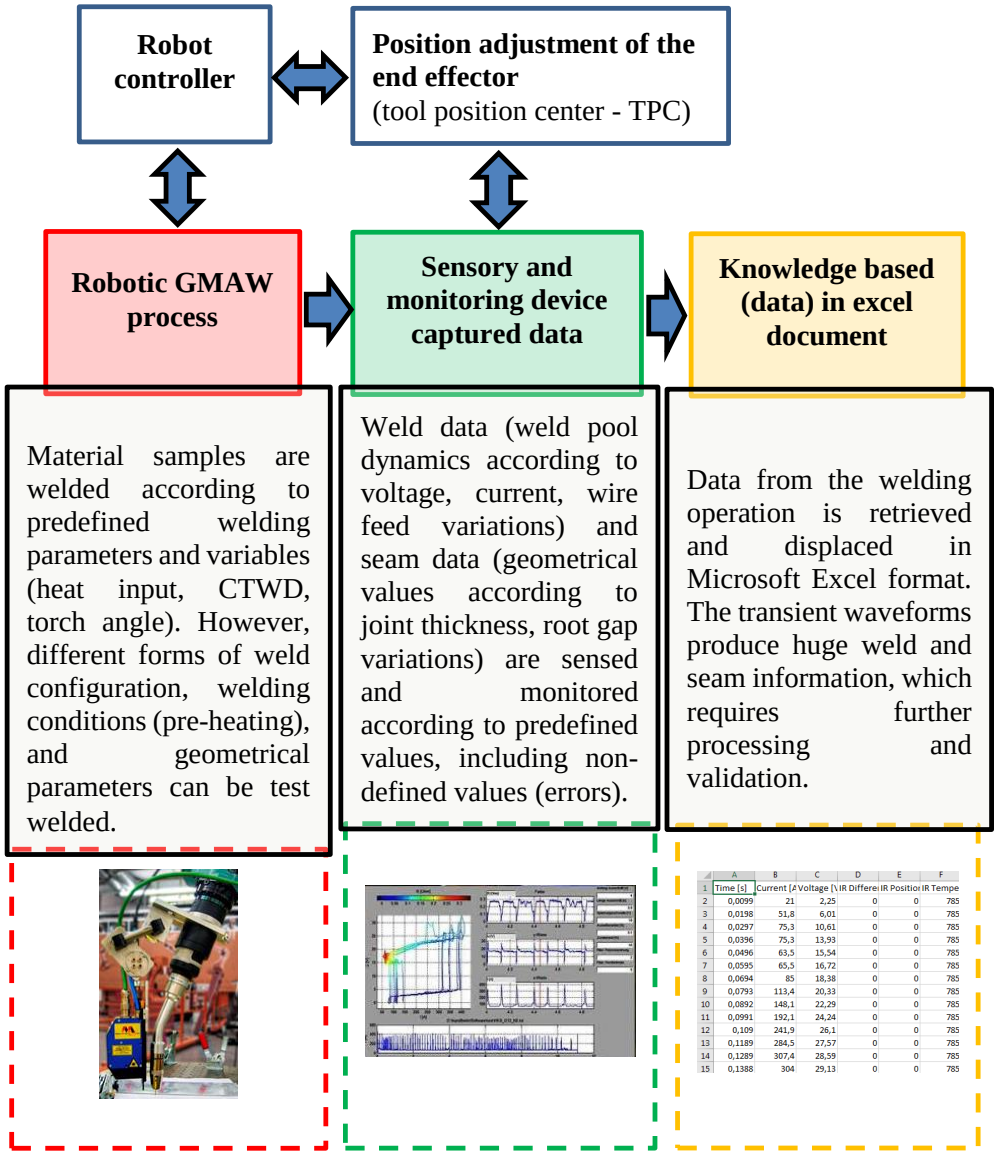

Figure 27. Schematics for data collection.

Stage 2: Data Validation

Welding data of the samples (in digital format) are examined by comparison with corresponding physical samples. Samples with excessive defects are discarded, as is their digital data. Those samples with minimal weld defects and acceptable according to welding standards like ISO 5817 and ISO 15609 are included together in the knowledge base with the good samples. This process helps in the creation of boundary conditions and the setting of desired targets when training the data set in the ANN system. Therefore, training of the data sets in the ANN system starts with an initiation process for data validation. All the input data defined and all the output data defined are together fed into the ANN system. Input data could be welding parameters like current, voltage and wire feed rate, or geometrical parameters like throat thickness, depth of weld penetration, air gap height, etc. Similarly, the output parameters can be either welding parameters or geometrical parameters depending on the learning algorithms to be used. However, all data items undergo an iteration process as part of the validation process to decrease data errors. The iteration process takes several minutes depending on the number of data sets, while the validation performance reaches a minimum error (mean square error). The performance of the system is validated by following set targets of the ANN.

Figure 28 shows data validation performance of the iteration process and the regression process. Iteration of the input-output data occurs in several time sequences. The regression plots show the performance of the ANN by fitting the various data to targets made with decisions by the ANN itself. Overfitting of the input-output data is bound to happen if the data has a lot of variation. In such cases, more iteration and validation has to be performed by the system through feeding back of error signals (re-training) into the hidden layers. If the overfitting is high, some of the data must be discarded. The behavior of the various welding parameters and variables can be analyzed by simulating the ANN system.

Stage 3: ANN welding verification

After data validation, welding data from the decision-making of the ANN is verified. In the verification process, the ANN welding data is used for empirical tests. If the tests produce desirable results then the system is maintained. In this regard, the system is assumed to be capable of adjusting itself automatically before, during and after the welding operation to eliminate any welding flaws as defined in the limits. However, if desirable results are not achieved, then Stage 2 is repeated.

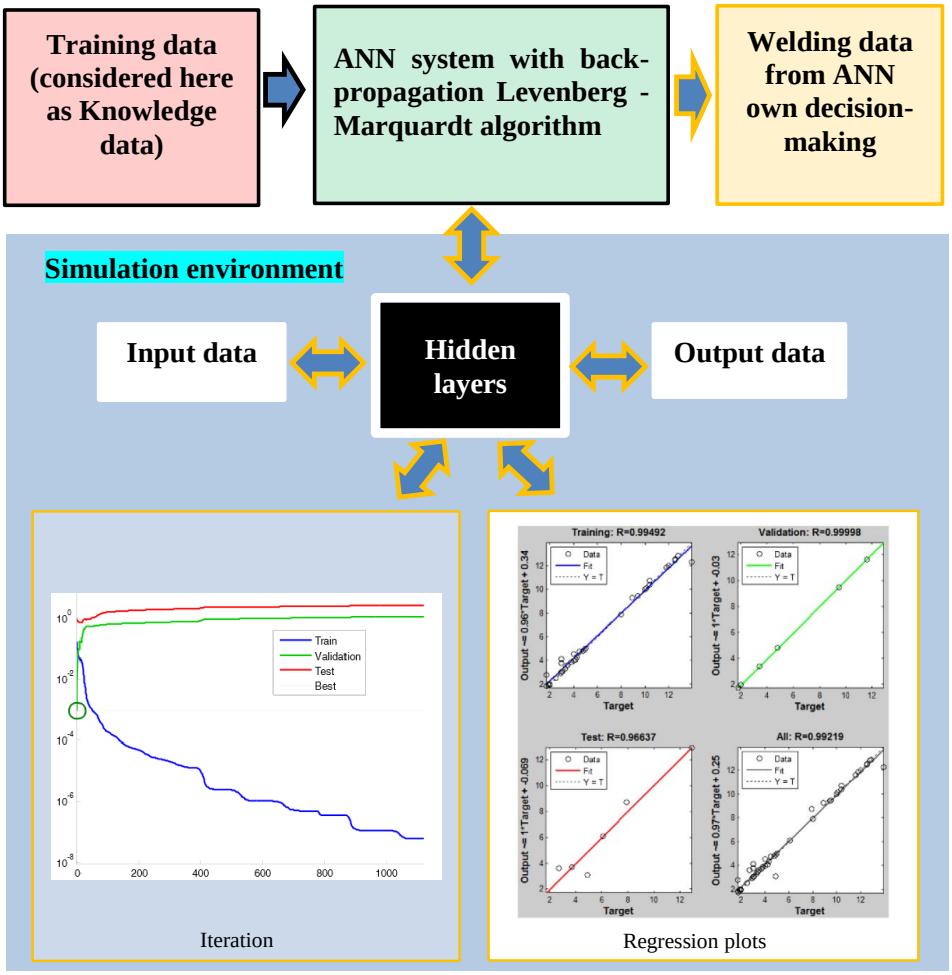

Figure 28. Data validation performance of the iteration process and regression process.

Although these stages are time-consuming, the possibilities of using AI methods for real-time operations could provide avenues for flexible offline welding as mentioned earlier. The use of sensors alone to guide and control welding robots in real-time has encountered some drawbacks leading to real-time malfunctions where the welding robot moves out of joint limits, collides with objects in the work space, or moves into singularities due to robot configuration changes (Cederberg, et al., 2002). With AI in place, the welding robot can be controlled remotely by planning its motion, optimizing its path and trajectories, and the robot can adapt to changes and unforeseen situations.

Most industrial robots are said to operate on CAR (Computer Aided Robotics) software that enables modelling, simulation and programming of robot operations within CAD

environments. To ensure optimum performance of real-time sensors with AI methods, a virtual sensor model (virtual twin/digital twin) of the real sensor must be created and implemented in the CAR virtual operating environment. The virtual sensor must be validated statically and dynamically. The static approach is performed by matching the virtual sensor with the real sensor through setup measurements and calibrations, while the dynamic approach is done by comparing a welding operation performed in real-time and a virtual work-cell created with a CAR application (Cederberg, et al., 2002).

Components to be welded are updated based on information provided by the virtual/real sensor in real-time. By going through these approaches, a feedback loop is created that makes full use of the sensor information (specific instructions used to define the robot task as set of motions) and integrates it to the world model and application process models. Real-time sensor feedback to the world model means that the information from the sensors will actually update the world model, including updating object positions in real-time as required or creating objects not included beforehand. Through this mechanism, the use of sensors can be validated in a CAR environment as similar tests should be made in a real physical setup (Cederberg, et al., 2002).

Development in remote welding has provided commercially available offline welding applications. Some of these offline welding platforms have open architecture, which needs to be customized to fit into the operationability of welding companies. Such offline welding platforms with AI capabilities help to resolve robot collision challenges, manipulator and end-effector reachability issues, and weld joint limit issues. Typical examples of these offline welding platforms include those of Delfoi and Visual Components. Together with other welding simulation platforms such as Simufact, SYSWELD, robust offline welding operations can be achieved geared towards weld quality and traceability.

Turnkey WQA Model

The turnkey WQA model in Figure 29 illustrates the steps required to design an adaptive intelligent welding system and develop a case-specific WQA document for implementation. The required steps and linkages are consolidated as preconditions for successful development of the model. For example, without first configuring/calibrating the controller and software according to systems specifications, the initial programming of the robotic GMAW process cannot be accomplished. Therefore, the WQA model provides generalized information to help large companies and especially SMEs to strategically plan how to integrate and speed up the implementation of adaptive intelligent welding systems into their manufacturing and production networks for weld quality purposes.

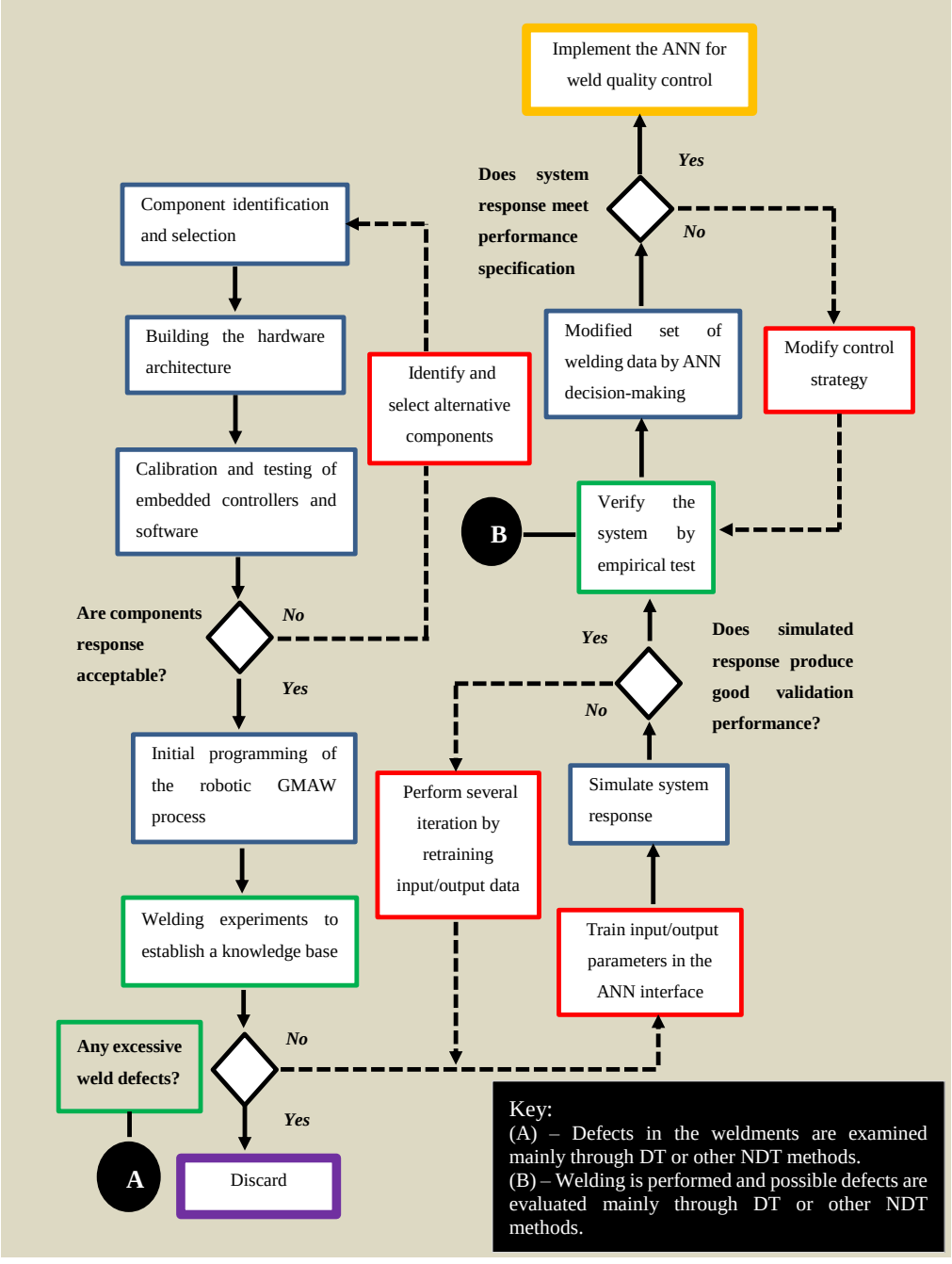

Figure 29. A weld quality assurance model based on adaptive intelligent systems.

5 Future research

Computational analysis of adaptive robotic GMAW of advanced steels needs to be investigated further since this work did not delve deeply into this subject. Special attention should be given to simulation tests on matched, undermatched and overmatched filler materials in welding of advanced steels where heat inputs, CTWD and torch angles are defined, visualized and observed with regards to their implications for weld quality (strength, toughness, ductility, and microstructure nucleation and segregation properties).

The developed WQA-AIS model is made according to critical observation of robot system integration and protocols, and a small number of empirical test observations. Practical integration of the framework of the model with engineering design platforms such as PDM systems to cover all factors related to welding manufacturing has not been done. The WQA-AIS model, therefore, presents a generalized model, which needs further study before it can be considered as acting as a proof of concept. Prior to implementation of the WQA-AIS model, much further work is required, especially as regards selection of system components, software, protocols, and intelligent systems.

5.1 Other research directions

This section presents general research directions based on the impact of AI and robotic systems on technological, economical, educational, societal and environmental advancement.

Networking of robot cells between large companies and SME's:

The possibilities for welding companies to connect and synchronize their robot cells to enhance welding throughput need investigation. Connection and synchronization can enable construction of a network between robot cells and specific welding operations can be performed even remotely. In addition, SMEs can network their robot cells to several robots cells in the factories of large companies to lessen the amount of programming and number of calibration tasks required before welding operations.

Collaboration between welding robots to expand job creation.

Several publications have stated that the use of robots for welding is a result of a global shortage of welding personnel. This claim seems unconvincing because, based on personal interactions and interviews, the unemployment rate among welding personnel appears to be increasing. A possible reason for a shortage of welders in certain areas may be because welding personnel have to go through several training courses, which are quite expensive, before accreditation and before being able to accept work from ISO 9000 certified organizations. For this reason, most welding personnel keep to basic welding skills when opening workshops offering welding services.

In the broader industrial context, there is a need to increase interaction between welding personnel and robots, to expand job creation and the range of welding applications, and to counteract the perception that robots steal human jobs. Robots should be seen as assisting humans to do their jobs in a safer, more productive and less stressful manner and as a way to improve quality. For SMEs with limited need for welding, welding robot stations could be built around cities (like gas fuel station points). Each user would have an ID card or a pass to go to the robot welding cell to order and weld a product. In such a scenario, the robot welding stations would have an interface with several products and specifications. Such robot welding cell stations could reduce unemployment among welders by providing greater flexibility. Clearly, some welding skills would be required, but SMEs would no longer have to set up specialist welding workshops with only limited usage rates. Furthermore, barriers to setting up small manufacturing businesses would be lowered by reducing the start-up capital required.

The use of universal robots in welding factory will promote human-robot collaboration because such robots have low inertia and payloads, thus risks associated with safety will be reduced. In addition, issues related with ergonomics is an area of concern. There is a need for further investigations of these health and safety aspects.

6 Conclusions

The thesis began with a review of weld integrity aspects of advanced steels. The focus was on weldability and service performance issues. These aspects constitute the key criteria when considering the usability of advanced steels in welding manufacturing and production. Heat input, cooling rate and filler material were considered when discussing weldability aspects, and when examining service performance, aspects related to weld geometry, material grade and crack growth were investigated. Other factors related to the GMAW process were also examined, such as the interaction between the forces in heat transfer and fluid flow. In addition to buoyancy, Marangoni and non-dimensional forces and properties associated with the GMAW process, the electromagnetic force was noted to play a major role in weld penetration and the formation of the weld pool. Also, sensing, monitoring and risk assessment systems were reviewed, and welding of ultra high strength steel (UHSS) material S960QC was evaluated from the control perspective to enable creation of an artificial intelligence model. Welding standards such as EN ISO 5817 and ISO 15609-1 were used as guidelines in the evaluation process.

An experimental study examining the applicability of an adaptive intelligent robotic GMAW system in welding of UHSS S960QC was presented. In addition, the study presented a new weld quality assurance model based on adaptive intelligence systems designed by utilizing the findings from the experimental study. The automation, robotics, sensory, monitoring and artificial intelligent systems reviewed and utilized in the experimental study aim to exploit the concept of Industry 4.0 and the “big data” involved in the systems integration process. One aim of the work is to support welding companies, both large and small and medium-scale enterprises (SME’s), in their decision-making and assist them in the implementation and integration of adaptive welding systems in their manufacturing and production networks. The new weld quality assurance model seeks to facilitate digitization of weld quality and assurance processes to improve weld quality, eliminate or reduce weldments with defects at the commissioning stages, generate a digital history of the welding operation for future analysis, reduce rework, trace weld defects digitally and in real-time, define and approve welding procedure specifications (WPS) in digital formats, and increase productivity.

The concluding remarks are based on the research hypotheses formulated as claims in chapter 1.8:

1. Advanced steels (structural steels having yield strength between 500-960 MPa and thickness $\geq$ 5 mm and $\leq$ 10 mm) can be considered as lightweight steels.

Comparing the physical and mechanical properties of UHSS and conventional steels, the potential savings from usage of UHSS become apparent; for example, the difference between plate thickness, for the same load carrying capacity/ bending strength, of 10 mm S 355 and 5 mm S960QC UHSS is about 66.7 %, and between weld seam volume about 95 % (Illustration in appendix Table 3).

2. When welding advanced steels, the selection of welding process and manufacturing setup, heat input levels, cooling rate, filler materials and consumables, weld geometry, weld orientation and control of the fusion process must be considered and critically observed.

Risks associated with welding of advanced steels include HAZ softening, cracking and embrittlement of the weld metal. HAZ softening is a result of microstructural changes that occur due to high heat inputs and the rate of cooling. Heat input is consequently a critical factor that affects significantly the strength and properties of welded joints of advanced steels. For instance, if heat input is too low, there is a risk of lack of fusion, and if the heat input is too high, the HAZ gets too wide as a result of grain growth and diffusion of alloying elements. HAZ softening leads to ductility, strength, and toughness problems, and the overall quality of welded joints may be affected. The risk of cracking is chiefly caused by the choice of filler materials.

The use of matched, undermatched or overmatched filler materials and the heat inputs involved must be critically considered when welding UHSS material with GMAW, as evident from Appendix Table 1 and 2. Low heat inputs have a tendency to produce weld defects like lack of fusion, incomplete penetration and poor weld quality. With moderate heat inputs, welds of acceptable quality (toughness, strength and microstructure properties) are produced. Unacceptable weld properties, softening of the HAZ and deterioration of strength, toughness and ductility across the weld occur when high heat inputs are used. The CTWD is an essential factor when considering the amount of heat that directly hits the surface of the base metal and the extent of weld depth penetration. The longer the electrode stick-out (between 18–28 mm), the less the effect of heat intensity on the weld, eventually resulting in a deeper weld depth penetration.

The matched filler metal used in the fillet welds produced acceptable hardness properties, especially when heat input was between 0.5–0.65 kJ/mm. It can be said that the hardness properties of the weld metal agree with the strength properties of the base metal, thus suitable for a complete joint penetration weld configuration due to the tensile properties of the weld strength. However, undermatched filler metal may have produced weld strength of acceptable hardness properties in relation to weld throat size and weld metal strength for fillet welds according to heat input range and cooling times shown in Appendix Table 1.

The orientation of the weld and the weld geometry have a significant influence on the rate of cooling. In situations where deeper weld penetration is achieved, the rate of heat dissipation may be slower and vice versa. A V-shaped fillet joint configuration produces deeper weld penetration, but slower cooling rates, than an L-shaped fillet joint. For load carrying purposes, the V-shaped fillet joint may be suitable to fulfil service requirements. Similarly, the L-shaped fillet joint could be suitable from a load carrying perspective, but the service performance must be evaluated.

3. An adaptive intelligent welding system is capable of providing real-time weld quality data because of the self-monitoring and control features embedded in the system.

Weld and seam data captured by sensory and monitoring systems integrated with the robotic GMAW process provide the means for real-time weld quality assurance data. Weld information is captured in the time domain and could be visualized during or after the welding process. Important parameters and variables of the welding process such as welding current, voltage, heat input can be accessed real-time and predictions of the outcome of the final weld can be made. Also, during welding, modifications can be made to the welding parameter and variables using the visualization opportunities provided by the adaptive welding system. Moreover, the automatic computation and analysis of temperature of the weld and width of the weld seam gives an indication whether the weld being produced will be of good or bad quality. Temperature readings up to about 1350 ^{o}C can be captured and defects such as discontinuity in the weld seam can also be captured by means of the thermal cycle readings across the weld seam. Weld and seam data captured as digital data and analysed in graphical forms correlates with macrographs produced from the weld specimens. It is possible to control the weld and seam data during welding, but not data related to unforeseen circumstances and dimensional distortion.

In addition to the limitation observed for the sensory and monitoring system, further processing of the data cannot be done using the same system, although play-back options are available. An intelligent system is always required for control purposes due to uncertainties and unforeseen conditions during welding. The welding process can produce sudden fluctuations in current and voltage values, leading to either high or low heat input being supplied to the weld. With an ANN system is place, the behaviour of the welding parameters and variables could be greatly influenced by modelling and controlling the output of the welding process. System parameters and variables can be smoothened and disturbances could be filtered off for efficient system response.

4. An adaptive intelligent welding system has the potential to be integrated with engineering design and manufacturing tools (CAD/CAM programs). By creating product data management (PDM) systems for fabrication of welded components, modular adaptive intelligent welding systems can be made for each bill of material (BOM) for fabricating specific products. Routines and modules in the welding process can be made for each product, and weld quality will be achieved with high assurance.

The possible integration of an adaptive intelligent welding system with engineering design platforms like CAD/CAM and PDM systems in welding manufacturing is noteworthy. This approach could facilitate offline welding possibilities and enable further modelling and control of welding parameters and variables. With such systems in place, the number of practical welding trials can be decreased, thus reducing waste and increasing productivity.

5. The proposed weld quality assurance model when implemented in factories of SME's and large companies will serve diverse purposes. Weld quality data in digitized format

can be achieved, digitized welding procedure specification (WPS) can be generated, wide range of modular products can be manufactured, and linking information to cloud-based systems for effective information sharing in welding operations can be achieved.

The implementation of the WQA-AIS model in welding manufacturing factories will facilitate digitization of weld quality and quality assurance processes in realizing the goals of sustainable future factories. The weld and seam data collection, and validation and verification process relies on digitization processes that can enhance analysis and interpretation of data related to weld quality. In addition, the adaptive system can improve communication, information sharing and can offer integration of product data information for reliable manufacturing. The WQA-AIS model, however, presents a generalized model which still requires further work to be considered a proof of concept. In particular, the WQA-AIS model requires further studies on implementation issues such as selection of system integration components, software, protocols and intelligent systems.

References

Akselsen, O.M., Lange, H.I., Ren, X., Alvaro, A., Nyhus, B. (2017). Evaluation of low temperature toughness in welding of 420MPa steel for Arctic application. *Proceedings of the Twenty-seventh International Ocean and Polar Engineering Conference*, San Francisco, CA, USA, June 25-30, pp. 274-281.

Aikenhead, M.J., McDonald, A.J.S. (2003). A neural network face recognition system. *Engineering Applications of Artificial Intelligence*, Vol. 16, pp. 167-176.

Al-Faruk, A., Hasib, Md. A., Ahmed, N., Kumar, U.D. (2010). Prediction of weld bead geometry and penetration in electric arc welding using artificial neural networks. *Int J Mech Mechatron Eng*, Vol. 10, pp. 19-24.

Amin, M. (1983). Pulse current parameters for arc stability and controlled metal transfer in arc welding. *Metal Construction*, Vol. 15(5), pp. 272-278.

Andersen, K., Cook, G.E. (1990). Artificial neural networks applied to arc welding process modelling and control. *IEEE Transaction Industry Application*, Vol. 26(9), pp. 824-830.

Balasubramanian, V., Ravisankar, V., Ramachandran, C.S., Muralidharan, C. (2009). Selection of welding process for hardfacing on carbon steels based on quantitative and qualitative factors. *Int J AdvManuf Technol*, Vol. 40, pp. 887-897.

Billingham, J., Sharp, J.V. (2003). Review of the performance of high strength steels used offshore. *Research report 105*. Cranfield University School of Industrial and Manufacturing Science, pp. 3.

Björk, T., Toivonen, J., Nykänen, T. (2012). Capacity of fillet welded joints made of ultra-high strength steel, *Weld World*, Vol. 57, pp. 71-84.

Bolmsjö, G. (1997). Knowledge based systems in robotized arc welding. Knowledge based systems - Advanced Concepts", Techniques and Applications, (Spyros Tzafestas, editor). Chapter 17, *World Scientific*, pp. 465-495.

Bowditch, W.A., Bowditch, K.E. (1997). Welding technology fundamentals, 2 nd ed. The Goodheart-Willcox company, Tinley Park, IL, pp. 64-82.

Burns, R.S. (2001). Advanced control engineering. Butterworth-Heinemann. A division of reed educational and professional publishing Ltd. ISBN 0750651008.

Cederberg, P., Bolmsjö, G., Olsson, M. (2002). Robotic arc welding - trends and developments for higher autonomy. *Ind. Robot*, Vol. 29, pp. 98–104

Chen, S.B., Wu, J. (2009). Intelligentized methodology for arc welding dynamical processes: Visual information acquiring, knowledge modelling and intelligent control of arc welding dynamical process. Vol. 29, pp.14.

Chen, W.J. (2004). Research on local autonomous intelligent welding robot system and its remote control. Doctoral dissertation. Shanghai Jiao Tong University.

Cheon, J., Kiran, D.V., Na, S-J. (2016). CFD based visualization of the finger shaped evolution in the gas metal arc welding process. *International Journal of Heat and Mas Transfer*. Vol. 97, pp. 1-14.

Cho, D.W., Na, S.J., Cho, M.H., Lee, J.S. (2013). A study on V-groove GMAW for various welding positions. *Journal of Materials Processing Technology*. Vol 213, pp. 1640-1652.

Cook, G.E., Andersen, K., Fernandez, K.R., Shepard, M.E., Wells, A.M. (1987). Electric arc sensing for robot positioning control. *Robotic Welding*. Editor: J. D. Lane. IFS Publications Ltd, UK, Springer-Verlag, pp. 181-216.

Dabiri, M., Skriko, T., Amraei, M., Björk, T. (2016). Effect of side grooves on plane stress fracture behavior of compact tension specimens made of ultra-high strength steel. *Key Engineering Materials*, Vol. 713, pp. 159-162.

Dabiri, M., Isakov, M., Skriko, T., Björk, T. (2017). Experimental fatigue characterization and elasto-plastic finite element analysis of notched specimens made of direct-quenched ultra-high strength steel. *Proc. Inst. Mech. Eng.*, Part C, Vol. 231, pp. 4209-4226.

Dabiri, M., Björk, T. (2017). Fatigue analysis of notched specimens made of direct-quenched ultra-high strength steel under constant amplitude loading. *Procedia Structural Integrity*, Vol. 5, pp. 385-392.

Essers, W., Walter, R. (1981). Heat transfer and penetration mechanisms with GMA and plasma-GMA welding. *Weld. J*. Vol. 60, pp. 37-42.

Fridenfalk, M. (2003). Development of intelligent robot system based on sensor control. Doctoral dissertation. Lund University, Dept. of Mechanical Engineering.

Fuller, R. (2000). Introduction to neuro-fuzzy systems: advances in soft computing. Physica-Verlag, New York, Heidelberg.

Garašić, I., Kožuh, Z., Remenar, M. (2015). Sensors and their classification in the fusion welding technology. *Technical Gazette*, Vol. 22:4, pp. 1069-1074.

Gyasi, E.A., Kah, P., Ratava, J., Kesse, M., Hiltunen, E. (2017). Study of adaptive automated GMAW process for full penetration fillet welds in offshore steel structures,

Proc. 27th International Ocean and Polar Engineering Conference, San Francisco, CA, USA June 2017, pp. 290-297.

Gyasi, E.A., Kah, P., Handroos, H., Layus, P., Lin, S. (2018). Adaptive welding of S960QC UHSS for Arctic structural applications. *International Review of Mechanical Engineering*, Vol. 12:4.

Hardt, D.E. (1984). Ultrasonic measurement of weld penetration. *Welding Journal*, Vol. 63(9), pp. 273-285.

Hemmilä, M., Laitinen, R., Liimatainen, T., Porter, D. (2005). Mechanical and technological properties of ultra high strength optim steels. Rautaruukki Corporation, Helsinki. Online: http://www.oxycoupage.com/FichiersPDF/Ruukki_Pdf/English/Ruukki-Technical-article-Mechanical-and-technological-properties-of-ultra-high-strength-Optim-steels.pdf.

Hemmilä, M., Hirvi, A., Kömi, J., Laitinen, R., Lehtinen, M., Mikkonen, P., Porter, D., Savola, J., Tihinen, S. (2010). Technological properties of direct-quenched structural steels with yield strengths 900 - 960 MPa as cut lengths and hollow sections. Rautaruukki Corporation, Helsinki. Online: https://oxycoupage.com/FichiersPDF/Ruukki_Pdf/English/Ruukki-Technical-article-Technological-properties-of-direct-quenched-structural-steels.pdf.

Hill, P. M. (1991). Cutting and welding in naval construction. *Welding and Metal Fabrication*, pp. 63-72.

Hirai, A. (2001). Sensing and control of weld pool by fuzzy-neural network in robotic welding system. *The 27th annual conference of the IEEE Industrial Electronics Society*, pp. 238-242.

Holmes, J.H., Sacchi, L., Peek, N. (2017). Artificial intelligence in medicine AIME 2015. *Artificial Intelligence in Medicine*, Elsevier, pp. 1-2.

Howard, B.C., Scott, C.H. (2005). Modern welding technology (6th edition, Pearson Prentice Hall, USA).

Huanca, C.E., Absi, A.S.C. (2010). Feasibility study of non-conventional parameters for disturbance monitoring and detecting in short circuit gas metal arc welding. *ABCM Symposium Series in Mechatronics*, Osa/vuosikerta 4, pp. 559-569.

International Federation of Robotics (2017). Executive summary world robotics 2017 industrial robots. Online: https://ifr.org/downloads/press/Executive_Summary_WR_2017_Industrial_Robots.pdf. Accessed: 10.10.2017.

ISO 5817 Welding (2014). Fusion-welded joints in steel, nickel, titanium and their alloys (beam welding excluded) - Quality levels for imperfections. International Organization for Standardization, Geneva, Switzerland.

ISO/TR 18491 (2015). Welding and allied processes – Guidelines for measurement of welding energies.

Jae-Woong, K., Jun-Young, L. (2008). A control system for uniform bead in fillet arc welding on tack welds. *J Mech Sci Technol* Vol. 22, pp. 1520-1526.

Jesus, M. P. A., Matos, R., Bruno, F. C., Rebelo, C., Silva, L. S., Veljkovic, M. (2012). A comparison of the fatigue behavior between S355 and S650 steel grades. *Journal of Construction Steel Research*, Elsevier, Vol. 79, pp. 140-150.

Juan, W., Yajiang, L., Peng, L. (2003). Effect of weld heat input on toughness and structure of HAZ of a new super-HSS. *Bulletin Material Science*, Vol 26, no 3, pp. 301-305.

Juang, S.C., Tarng, Y.S., Lii, H.R. (1998). A comparison between the back-propagation and counter-propagation networks in the modelling of TIG welding process. *J Mater Process Technol*, Vol. 75, pp. 54-62.

Kah, P., Pirinen, M., Suoranta, R., Martikainen, J. (2014). Welding of ultra high strength steels, *Advanced Materials Research*, Vol. 849, pp. 357-365.

Kah P., Shrestha M., Hiltunen, E., Martikainen, J. (2015). Robotic arc welding sensors and programming in industrial applications. *International Journal of Mechanical and Materials Engineering*. Vol.10:13, pp. 1-16.

Kim, K.N., Lee, S.H., Jung, K.S. (2009). Evaluation of factors affecting the fatigue behavior of butt-welded joints using SM520C-TMC steel. *International Journal of Steel Structures*, Vol. 9, pp. 185-193.

Kim, I.S., Son, J.S., Lee, S.H., Yarlagadda, P.K.D.V. (2004). Optimal design of neural networks for control in robotic arc welding. *Robot Comput Integr Manuf*, Vol. 20(1), pp. 57-63.

Kou, S., Wang, Y.H. (1986). Weld pool convection and its effect. *Welding Research Supplement*, March, pp. 63-70.

Kumar, A., DebRoy, T. (2007). Heat transfer and fluid flow during gas metal arc fillet welding for various joint configurations and welding positions. *Metallurgical and Materials Transactions A*, Vol. 38a, pp. 506-519.

Kumar, A., Zhang, W., Kim, C.H., DebRoy, T. (2005). A smart bi-directional model of heat transfer and free surface flow in gas metal arc fillet welding for practising engineers. *Welding in the Weld*, Vol. 49, pp.32-48.

Layus, P. (2017). Usability of the submerged arc welding (SAW) process for thick high strength steel plates for Arctic shipbuilding applications. Doctoral dissertation, Lappeenranta University of Technology. Acta Universitatis Lappeenrantaensis 742.

Li, J.P. (1997). Fundamental research on arc light sensing technology during welding process. Doctoral dissertation, Harbin Institute of Technology.

Liu, W.Y., Wang, L., Liu, J.B., Zhang, Y.Y., Li, P.H., Yuan, G.L. (2007). Microstructures and properties in simulated heat-affected zones of 685 MPa grade copper-bearing steel. *Proceedings of Sino-Swedish Structural Materials Symposium*.

Lopez, B., Martin, C., Vinas, P.H. (2017). Special section on artificial intelligence for diabetes. *Artificial intelligence in medicine*, Elsevier, pp. 26-27.

McFarlane, D., Sarma, S., Chirn, J.L., Wong, C.Y., Ashton, K. (2003). Auto ID systems and intelligent manufacturing control. *Eng Appl Artif Intel*, Vol. 16:4, pp. 365-376.

Menaka, M., Vasudevan, M., Venkatraman, B., Baldev, R. (2005). Estimating bead width and depth of penetration during welding by infrared thermal imaging, *Insight*, Vol. 47, pp. 564-568.

Mendez, P.F., Eagar, T.W. (2003). Penetration and defect formation in high-current arc welding. *Weld. J*. Vol. 82, pp. 296-306.

Meng, W., Li, Z., Huang, J., Wu, Y., Katayama, S. (2013). Microstructure and softening of laser-welded 960 MPa grade high strength steel joints. *Journal of Materials Engineering and Performance*. *ASM International*, Vol. 23, pp. 541.

Miller, D.K. (1997). Use undermatching weld metal where advantageous. *Welding Innovation*. Vol. 14, number 1.

Mvola, B. (2017). Effects of adaptive GMAW processes: Performance and dissimilar weld quality. Doctoral dissertation. Lappeenranta University of Technology. Acta Universitatis Lappeenrantaensis 750, pp. 30-41.

Nadzam, J., Armao, F., Byall, L., Kotecki, D., Miller, D. (2014). Gas metal arc welding. Online:*www.lincolnelectric.com/assets/global/Products/...SuperArc-SuperArcL-56/c4200.pdf*.

Nagarajan, S., Chen, W.H., Chin, B.A. (1989). Infrared sensing for adaptive arc welding. *Welding Journal*, Vol. 68(11), pp. 462-466.

Nele, L., Sarno, E., Keshari, A. (2013). Modelling of multiple characteristics of an arc weld joint. *Int J Adv Manuf Technol*, Vol. 69, pp.1331–1341.

Nestor, O. (1962). Heat intensity and current density distributions at the anode of high current, inert gas arcs. *J. Appl. Phys*. Vol. 33, pp. 1638-1648.

Nippon Steel and Sumitomo Metal. (2014). Steel plates A001en_04_2014f. Nippon Steel and Sumitomo Metal Corporation, Japan. [Online] http://www.nssmc.com/product/catalog_download/pdf/A001en.pdf.

Nomura, H. (1994). Sensor and control system in arc welding. Chapman & Hall. pp. 3-5.

Norrish, J. (2017). Recent gas metal arc welding (GMAW) process developments: The implications related to international fabrication standards. *Weld World*. Vol. 61, pp. 755-767.

Nykänen, E. (1994). Shipbuilding at Kvaerner Masa-Yards Helsinki New Shipyards. Hitsautekniikka 5/94, pp. 20-23.

Owen, F. (2012). Control systems engineering a practical approach. USA, California Polytechnic State University, pp. 1-25.

Pires, J.N., Loureiro A., Bölmsjo, G. (2006). Welding robots: Technology, system issues and applications. *Springer-Verlag London Limited*. pp.180.

Pirinen, M. (2013). The effects of welding heat input on the usability of high strength steels in welded structures. Doctoral dissertation, Lappeenranta University of Technology. Acta Universitatis Lappeenrantaensis 514.

Porter, D. (2006). Development in hot-rolled high-strength steel, *Nordic Welding Conference*, *New Trends in Welding Technology*, Tampere, Finland.

Rantalainen, T. (2012). Simulation of structural stress history based on dynamic analysis Doctoral dissertation. Acta Universitatis Lappeenrantaensis 494, Finland.

Rodrigues, D.M., Menezes, L.F., Loureiro, A. (2004). The influence of the HAZ softening on the mechanical behavior of welded joints containing cracks in the weld metal". *Engineering Fracture Mechanics*, Vol 71(13-14), pp. 2053-2064.

Rosheim, M. (1994). Robot evolution: The development of anthrobots. New York: John Willey & Sons, 1994.

Ruukki Metals (2007). Hot rolled steel plates, sheets and coils – Processing of materials-impact strength and through thickness properties. Helsinki.

Saaty, T.L. (1980). Analytical Hierarchy Process (McGraw-Hill, New York, 1980).

Suzuki, S., Ichimiya, K., and Akita, T. (2005). High tensile strength steel plates with excellent HAZ toughness for shipbuilding—JFEEWEL Technology for Excellent Quality in HAZ of High Heat Input Welded Joints. *JFE Technical Report*, No. 5, pp. 24-29.

Ushio, M., Mao, W. (1994). Sensors for arc welding: Advantages and limitations. *Transactions of JWRI*, Vol. 23(2), pp.135-141.

Venkatraman B., Menaka M., Vasudevan, M., Raj, B. (2006). Thermography for online detection of incomplete penetration and penetration depth estimation, In: *Asia-Pacific Conference on NDT*, 5th–10th November, Auckland, New Zealand.

Wahab, M.A. (1998). The prediction of the temperature distribution and weld pool geometry in the gas metal arc welding process. *Journal of Materials Processing Technology*. Vol. 77, pp. 233–239.

Wang, J., Li, Y., Liu, P. (2003). Effect of weld heat input on toughness and structure of HAZ of a new super-HSS, *Material Science*, Vol 26, No 3, pp 301-305.

Wang, S., Wan, J., Zhang, D., Li, D., Zhang, C. (2016). Towards smart factory for industry 4.0: A self-organized multi-agent system with big data based feedback and coordination. *Comput Netw*, Vol. 101, pp. 158-168.

Wang, W., Liu, S. (2002). Alloying and microstructure management in developing SMAW electrodes for HSLA-100 steel. *Welding Journal*, Vol. 81, pp. 132-145.

WTIA TN 15 (1999). Welding Technology Institute of Australia. Quenched and tempered Steels, Milsons point.

Yadav, N., Yadav, A., Kumar, M. (2015). An introduction to neural network methods for different equations. Springer Briefs in applied sciences and technology. *Computational intelligence*, Springer Science + Business Media B.V, Dordrecht.

Zeman, M. (2009). Properties of welded joints made of weldox 1100 steel. *Welding International*, Vol. 23, pp. 83-90.

Zhong, R.Y., Xu, X., Klotz, E., Newman, S.T. (2017). Intelligent manufacturing in the context of industry 4.0: A review. *Engineering*. Vol. 3, pp. 616-630.

APPENDIX

Table 1. Correlation of heat inputs and cooling rates of filler materials for UHSS material of 5 mm thickness.

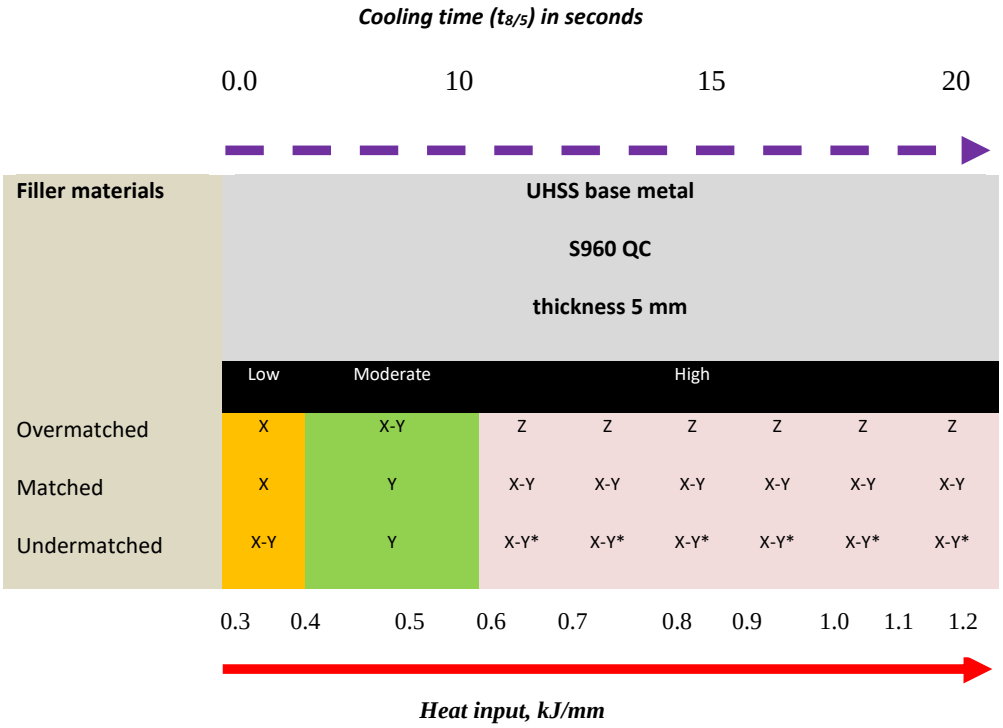

Key:

- Low heat inputs (in the yellow region).
- Moderate heat inputs (in the green region).
- High heat inputs (in the orange region).
- X means – tendency to produce weld defects like lack of fusion, incomplete penetration and poor weld quality.
- Y means – welds of acceptable quality (toughness, strength and microstructure properties) are produced.
- Z means – Unacceptable weld properties, softening of the HAZ and deterioration of strength, toughness and ductility across the weld occur.
- X-Y means – Weld properties between X and Y
- X-Y* means – Weld properties almost to Y.

Table 2. Types of filler metals and their effects on weld strength.

E.g. Using 12.64 filler metal for S960QC* *Filler metal 12.64* *A_5 = 26%* *Measured f_Y = 580 MPa* *Measure f_u = 690 MPa* 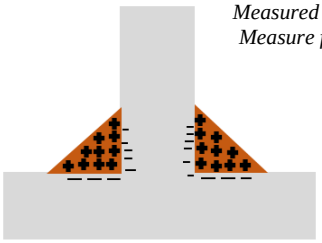 **Undermatched	Undermatched filler metal produces lower yield points resulting into less residual stresses on the base metal. Although the allowable strength level on the weld metal is the lowest when compared with matched and overmatched filler metals, the allowable strength levels on the base metal is highest since the weld metal controls the strength of the joint.
E.g. Using X96 filler metal for S960QC* *Filler metal X96* *A_5 = 14%* *Measured f_Y = 990 MPa* *Measure f_u = 1245 MPa* 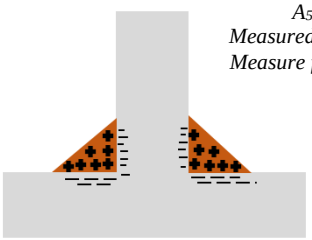 **Matching	Matched filler metal produces higher yield points than undermatched filler metals, thus resulting into higher residual stresses on the base metal. Although the allowable strength level on the weld metal is higher when compared with undermatched filler metals, the allowable strength levels on the base metal is lesser in comparison with undermatched filler metal. Nevertheless, the strength level of the weld metal is equally the same as that of the base metal.
E.g. Using X90 filler metal for Weldox 700 E* *Filler metal X90* *A_5 = 15%* *Measured f_Y = 890 MPa* *Measure f_u = 950 MPa* 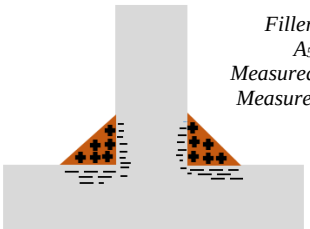 **Overmatched	Overmatched filler metal produces the highest yield points when compared with matched and undermatched filler metals. Residual stresses on the base metal are therefore very high. The allowable strength level on the weld metal is higher when compared with matched filler metals. Nevertheless, the allowable strength levels on the base metal is the lowest.

Table 3. Comparison between UHSS and S355 steels based on plate thickness and acting forces.

Steel Grades	**Maximum force to cause material to fracture at an angle of 30°** $F_{max} = 0.943btf_y$ Where **b** and **t** are the width and thickness of the plate, and $\mathbf{f_y}$ (MPa) is the yield strength of the material.	**Bending force** $F = CR_m bt^2/W$ Where **Rm** is tensile strength, **t** is plate thickness, **C** is a constant whose magnitude is 1.2 – 1.5, **b** is the bend length and **W** is the die gap. *The size of the punch is not considered, which leads to under-estimation of the bending force in the UHSS.
UHSS S960QC 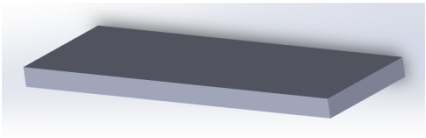 120 X 80 X 5 mm	F_{max} = 0.943 x 80 x 5 x 960 = 362 kN	Bending force = 1.5 x 960 x 1 x 5^2/ 1 = 36 kNm
S355 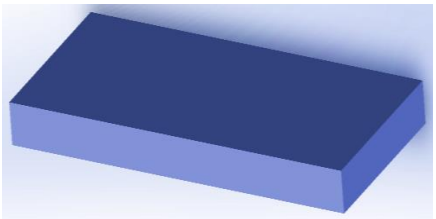 120 X 80 X 10 mm *A_5= 22%, hardness = 140 -190 HB, impact energy = 27J, ± 20°*	F_{max} = 0.943 x 80 x 10 x 355 = 267 kN	Bending force = 1.5 x 355 x 1 x 10^2/ 1 = 53 kNm

Table 4. Welding Procedure Specification (WPS) description according to ISO 15609-1.

Welding Procedure Specification:

WPQR No.:
Manufacturer:
Mode of metal transfer:
Joint type and weld type:
Weld preparation details (sketch)*

Method of Preparation and Clearing
Parent Material Designation:
Material thickness (mm):
Outside diameter (mm):
Welding position:

Joint Design	Welding Sequences

Welding Details

Run	Welding process	Size of Filler Material	Current (I)	Voltage (V)	Type of Current/Polarity	Wire Feed Rate	Run Out Length/Travel Speed	Heat Input

Filler material designation and make:
Any special baking or drying:
Designation gas/flux: *-Shielding*
-Backing

Gas flow rate *-Shielding*
-Backing
Tungsten electrode type/size:
Details of back gouging/backing:
Preheat temperature:
Interpass temperature:
Post-heating:
Preheat maintenance temperature:
Post-weld heat treatment and/or ageing:
(Time, temperature, method:
Heating and cooling rates*):

Other information*, e.g.
Weaving (max. width of run):

Oscillation: amplitude, frequency:
Pulse welding details:
Distance contact tube/work piece:
Plasma welding details:
Torch angle:

……
Manufacturer
(Name, signature, date)

Publication I

Gyasi, E.A. and Kah, P.
Structural integrity analysis of the usability of high strength steels (HSS)

Reprinted with permission from
Reviews on Advanced Materials Science
Vol. 46, pp. 39-52, 2016

Rev. Adv. Mater. Sci. 46 (2016) 39-52

STRUCTURAL INTEGRITY ANALYSIS OF THE USABILITY OF HIGH STRENGTH STEELS (HSS)

E. A. Gyasi and P. Kah

Laboratory of Welding Technology, Mechanical Engineering Department,
Lappeenranta University of Technology, P. O. Box 20, 53851 Lappeenranta, Finland

Received: November 05, 2015; in revised form: July 11, 2016

Abstract. High strength steels (HSS) of yield strength between 500 – 900 MPa are used in industries such as shipbuilding and automobile manufacturing and for applications like offshore structures due to their advantageous physical and mechanical properties, which surpass those of conventional steels. Although the strength levels of HSS make structural weight reduction possible, and corresponding reduction of transportation and other manufacturing costs, the usability of high strength steels is negatively affected by issues such as a susceptibility to cracking and heat affected zone (HAZ) softening due to the effects of welding heat input. These quality problems can have a detrimental effect on the structural integrity of HSS welded structures. This paper critically reviews the usability of high strength steels from a structural integrity viewpoint drawing attention to the key issues involved. A decision-making tool for risk assessment based on the analytical hierarchy process (AHP) is presented and its suitability for evaluation of structural integrity risk in welded HSS structures. Challenges regarding HSS usability from the weldability and service performance perspectives are related to factors such as heat input, cooling rate and type of filler material; and weld geometry and crack propagation, respectively. The potential of an on-line welding process monitoring system incorporating AHP as part of the risk assessment process is noted. Additionally, the study identifies a need for further research on neuro-fuzzy network systems as an optimization mechanism for mitigating potential flaws in welding usability of HSS and its variants (advanced high strength steels, and ultra-high strength steels).

1. INTRODUCTION

High Strength Steels (HSS) are in increasing demand since their superior physical and mechanical properties to conventional steels (e.g. grade S235, S355, etc.) permit their use in a wide range of industrial applications. However, a number of unfavorable characteristics, like susceptibility to cracking and heat affected zone (HAZ) softening, due to the effects of welding, limit the usability of high strength steels [1,2]. These undesirable characteristics can lower the integrity of structures constructed of HSS, making the structures weak, unstable and prone to fatigue failure, which in-turn can lead to catastrophic failure in some scenarios. It has been observed that HSS structures are sensitive to fatigue phenomena as a result of the welding heat input [3].

To be able to alleviate the detrimental effects of welding of HSS, thorough investigation of weldability and service performance, including effective, efficient and rigorous risk assessment, is required. This paper presents a framework that evaluates essential factors and processes in determining the structural integrity of welded HSS. As shown in Fig. 1, many elements associated with weldability, service performance, machine factors and human factors have effects on structural integrity. Also as depicted in Fig. 1, these elements need to be evaluated through structured risk assessment, for example, by use of

Corresponding author: E. A. Gyasi, e-mail: emmanuel.gyasi@student.lut.fi

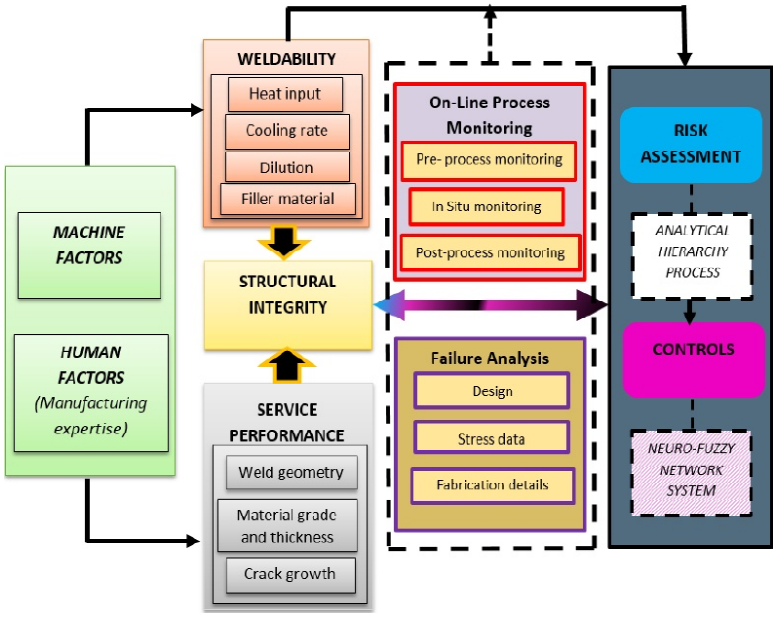

Fig. 1. Schematic framework for determining sound structural integrity in welded HSS structures.

a decision-making tool such as the analytical hierarchy process (AHP).

In addition to the risk assessment process, the framework includes on-line process monitoring and failure analysis procedures. These procedures serve as a new approach to facilitate the risk assessment process. The elements, factors, processes and procedures presented in the framework are elaborated in the paper.

Furthermore, the cross link shown in Fig. 1 represents a feedback loop system between the effects on structural integrity and the entire risk assessment and control process. Based on this cross link "feedback loop system", the adoption of a neuro-fuzzy network system approach is proposed as an optimization mechanism for eliminating potential flaws when welding HSS. This paper attempts to bridge a research gap observed in the literature pertaining to risk assessment of HSS for structural applications as well as expanding the knowledge base on the consequences of welding on fatigue in HSS welded structures.

2. STRUCTURAL INTEGRITY OF HSS

2.1. Weldability

HSS are often produced and delivered as quenched and tempered (Q&T) or thermo-mechanical controlled process (TMCP) steels. These steels are distinct due to their chemical properties, which are mainly determined by the addition of particular alloying elements, such as aluminum, vanadium, silicon, zirconium, and copper, to increase or decrease hardenability. The chemical composition of Q&T steels may contain alloying elements such as nickel, titanium, molybdenum and boron, and thus their qualities may differ slightly from those of TMCP steels. Moreover, carbon equivalent values (CEV) for Q&T and TMCP steels also differ significantly due to the carbon content, which contributes greatly to the hardness of the steels [4]. Table 1 shows examples of chemical composition of Q&T and TMCP steels.

Some typical Q&T steels for structural applications are the steel grades S500, S550, S620, S690, S890, and S960 [EN10025-6] [5]. Q&T high strength structural steels (usually up to S690) are ideal for applications with heavy sections and heavy live loads (e.g. long span bridges), where weight reduction is important.

Generally, the alloying composition of Q&T steels increases with increasing plate thickness in order to ensure sufficient hardening of the plate in the core region. Therefore, the CEV of a Q&T plate increases with increasing thickness. It is known that Q&T and TMCP steels have fairly similar physical properties such as good strength to weight ratio and high load carrying capacity [5,6].

Table 1. Chemical composition of Q&T and TMCP steels for low temperature applications.

	Typical Composition (wt.%)	Thickness (mm)	CE IIW	Typical Mechanical Yield Strength / CVN range
TMCP Steels	C, Mn, Si, S, P, Nb, V, Al, Cu, Ni, Cr	30	0.35	400 MPa/190J @ -40°C
		32	-	398 MPa/300J @ -20°C
		32	0.32	400 MPa/>300J @ -20°C
		30	0.37	460 MPa/220J @ -40°C
Q&T Steels	C, Mn, Si, S,P, Nb, V, Al, Ti, Cu, Ni, Cr, Mo, B	6-140	0.81	550 – 690 MPa/80J @ -84°C
		30	0.45	450 MPa/>35J @ -40°C
		50-64	0.43 (Ti)	480 MPa/>40J @ -40°C
		50	0.64 (Ti, Mo, B)	690 MPa/>40J @ -40°C
		30	0.64 (B)	960 MPa/>40J @ -40°C

Table 2. Thermal cycles influencing HAZ softening of HSS characteristics and examples.

Inter-critical reheating occurring at the two-phase zone, i.e. between 900-700 ^{0} C, produces martensitic microstructure during rapid cooling, which undermines toughness in the HAZ. But when slowly cooled, a pearlitic microstructure with good toughness is achieved in the HAZ. However, HAZ softening occurs when HSS is heated at high temperature above tempering temperature (above 700 ^{0}C). As HSS is a heat treated steel, welding conditions must be determined carefully so that changes to the maximum hardness or softness of the HAZ may be as minimal as possible.	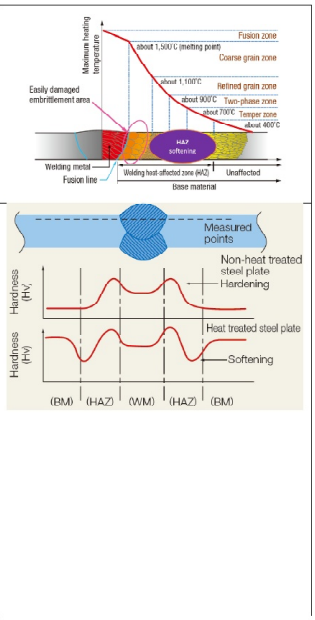

Exploring the use of HSS makes it possible to reduce construction weight and cost, lower consumption of welding consumables, and reduce welding time as a result of decreased thickness of the material [7,8].

Conventional welding processes such as shielded metal arc welding (SMAW), flux cored arc welding (FCAW), gas metal arc welding (GMAW), and submerged arc welding (SAW) have proven to be suitable for welding HSS. Nevertheless, the characteristic softening phenomenon due to uncontrolled heat input and cooling time [9] impairs tensile strength [10-11] and joint strength properties [6,12], as well creating weld crack tendencies, and leaves HSS weldability issues unsolved. Table 2 illustrates the thermal cycles influencing the heat affected zone softening phenomenon of HSS.

The risk of cracking and HAZ softening phenomena during welding of HSS places limitations on both the maximum and minimum total heat input, as illustrated schematically in Fig. 2 [14]. The shaded region shows the permissible heat input. The risk of cold cracking and excessive hardening, as depicted on the left side of the diagram, occurs when mini-

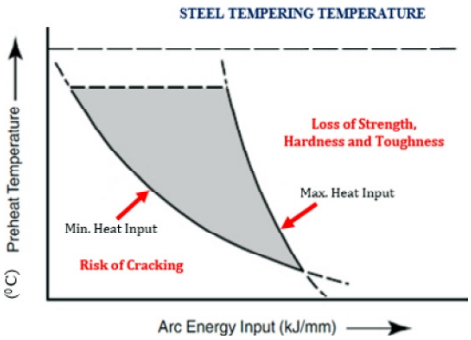

Fig. 2. Total weld heat input relations for welding Q&T steels characteristic. Reprinted with permission from Welding Technology Institute of Australia, Quenched and Tempered Steels, WTIA (Technical Note 15, Milsons Point, 1985). © 2016 WTIA.

mum heat inputs are used. Also, loss of strength and hardness due to over-tempering and possible loss of toughness as a result of re-transformation to upper bainitic microstructures during cooling occurs when high or maximum heat inputs are used [13,14].

For Q&T steels, the harder the microstructure, the greater is the cold cracking risk [15]. For TMCP steels, due to their low carbon equivalent content (CEV), there is high tendency of decreased welded joint strength as a result of the softening of the HAZ caused by uncontrolled heat input. As an important variable governing cooling rate/time, the higher the heat input the slower the cooling rate. This phenomenon has a key role in the phase balance and mechanical properties of HAZ and the weld [16]. In practice, the cooling rate is dependent on many factors: heat input, process efficiency, material properties, preheat temperature, material thickness and wire feeding rate [17,18]. The total weld heat input involving preheat temperature, interpass temperature and arc energy input has to be considered when determining appropriate cooling times [14].

It has been shown [16] that martensite-bainite microstructural transformation is prevalent when welding HSS of the Q&T type under appropriate welding conditions and when using suitable filler materials. For TMCP steels, a ferrite-bainite microstructure is obtained. Therefore selection of undermatched, matched or over-matched filler material must be done with accuracy since wrong judgments can lead to low toughness properties in the HAZ or weld metal (dilution of the base metal and the filler material) and consequently affect the microstructural transformation. Nevertheless, the microstructural formations in both Q&T and TMCP steels exhibit excellent ductility, and higher strength and toughness properties [16]. Therefore to ensure sound structural integrity of a welded HSS structure, such microstructures aforementioned should be obtained. Considering cold cracking in Q&T steels, low hydrogen filler materials are used to prevent or limit the introduction of hydrogen into the welded joints or HAZ [19]. Furthermore, it has been reported that welding of Q&T steels often require pre-weld or post-weld heat treatment in order to also minimize susceptibility of hydrogen-induced cracking thereby promoting sound microstructural formation [20]. On the other hand, TMCP steels exhibit sufficient strength and toughness, and they do not require hot working and post-weld heat treatment (PWHT), as they can create strength problems [21-23]. However, service performance conditions also revile the need to lessen weldability problems of HSS.

2.2. Service performance

The usability of HSS in the contest of service lifetime is influenced by effects of welding. For this reason, factors related to service performance of HSS, such as static strength, ductility, fatigue life, and corrosion resistance require particular attention, because, as a structural detail, a weld is initially prone to fatigue as a result of fatigue stresses, discontinuities, and welding defects. Therefore pre-existing cracks from welding defects promote crack formation, which has repercussions on fatigue life. Welded HSS have been observed to be more sensitive to fatigue phenomenon and more likely to experience fatigue failure [3].

Traditionally, fatigue life has been expressed as the total number of stress cycles required for a fatigue crack to initiate and grow large enough to produce catastrophic failure [24]. Generally, fatigue phenomena occur as a result of fatigue stresses and discontinuities. Fatigue stress therefore increases as a result of stress components (nominal stress, bending stress, nonlinear stress peak) whereas discontinuities occur mainly due to effect of notches, crack initiation, and crack propagation. Fatigue failure is common in welded structures due to notch geometries, which act locally as stress concentrator. Thus, the fatigue life of a notched specimen depends on the material and the notch geometry [3]. On the other hand, the geometry of a weld determines its fatigue strength whereas the static strength of the parent material (and of the filler metal) is of less importance in determining the fatigue strength [25,26].

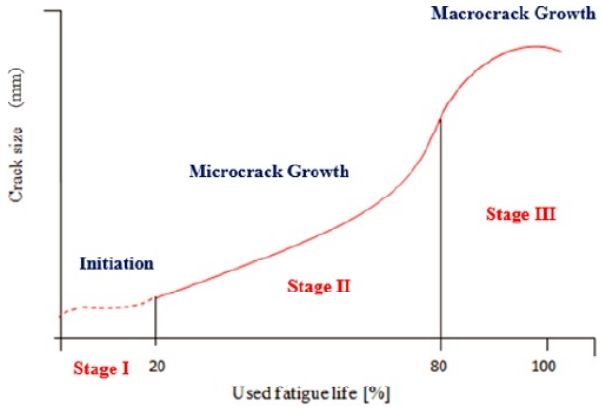

Fig. 3. Phases of crack growth in fatigue cracking. Reprinted with permission from T. Rantalainen, Simulation of Structural Stress History Based on Dynamic Analysis (Acta Universitatis Lappeenrantaensis 494, Finland, 2012). © 2012 Acta Universitatis.

Structural fracture and failure is divided into two phases: the crack initiation phase and the crack propagation phase. In the crack initiation phase, one or more small cracks begin to form in the material, while in the crack propagation phase, the initial crack propagates until it results in the failure of the structure. Fig. 3 illustrates the three fatigue cracking stages. Microcrack initiation and microcrack growth are together referred to as Stage I crack growth. Once the Stage I crack achieves a critical length, it will become a Stage II crack. In stage III, crack growth changes direction and begins propagating normal to the maximum principal stress [3].

For loaded welded structures, fatigue damage is caused by the simultaneous action of cyclic stress, tensile stress and plastic strain. If any one of these three elements is not present, a fatigue crack will not initiate and propagate [24]. Cyclic stress initiate cracks, the tensile stress propagates crack growth, and together they produce plastic strain. In the case of a brittle material, the released energy exceeds the absorption capacity of the material, and the crack propagation continues unstably, and hence the material fractures in a brittle way [3].

Some studies have shown that the fatigue strength of steels is usually proportional to their yield strength [27]. This generalization is not true for all cases because for high tensile strength values, toughness and critical flaw size may govern ultimate load carrying ability. Therefore, fatigue tests performed on small specimens are not always sufficient to precisely establish the fatigue life of a part. These small specimen tests are, however, useful for rating the relative resistance of a material to cyclic stressing and ascertaining the baseline properties of the material.

For example, a recent experiment compared the fatigue behavior of mild steel (S355) and high strength steel (S690) [28]. The two specimens were experimented using strain control, fatigue crack propagation and cyclic elastoplastic tests. The results indicated that although the S690 steel grade showed higher resistance to fatigue crack initiation than the S355 steel, its resistance to fatigue crack propagation was lower. Fig. 4 compares the fatigue crack propagation rates between the two steels. It is evident that the S690 steel shows the highest fatigue crack growth rates for all four tested stress ratios of 0.0, 0.25, 0.50, and 0.75 respectively. This finding was explained as being due to the finer grain of the S690 steel promoting fatigue crack propagation.

These results confirm an inverse dependence between static strength and fatigue life of HSS. Therefore utilizing HSS for applications where fatigue crack propagation is the governing phenomenon requires critical design consideration [28].

The superior fatigue crack initiation resistance of the HSS may not be relevant in HSS welded joints, since fatigue life is often affected by fatigue crack propagation. Data found in literature shows that fatigue resistance of welded high and ultra-high strength steel structural parts is similar to that of conventional steels with much lower yield stress [29].

This is due to short fatigue crack initiation period caused by stress concentration and weld defects. Nevertheless, crack propagation plays a key role on fatigue life [30]. Therefore when subjecting

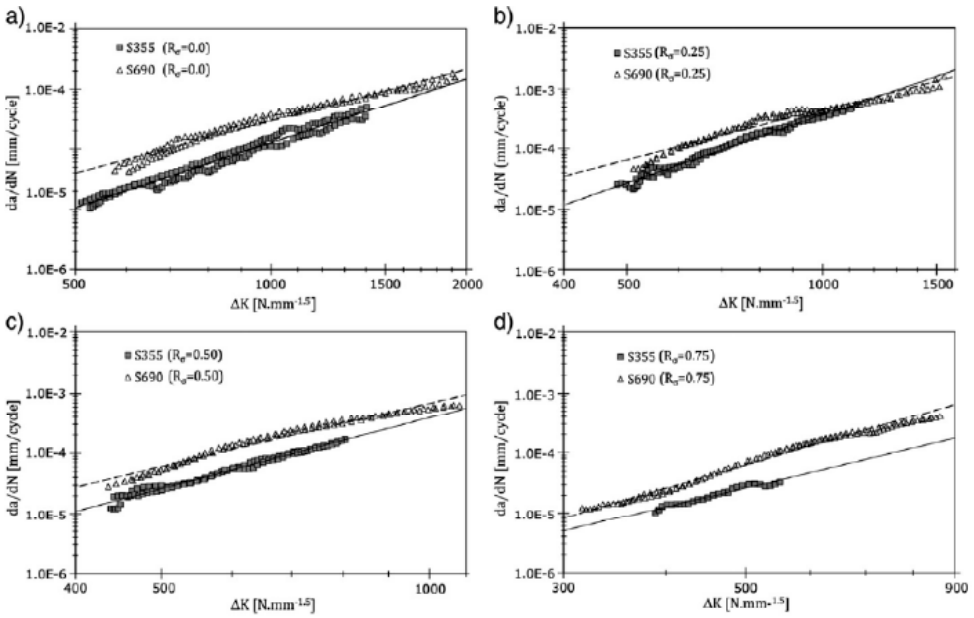

Fig. 4. Comparison of crack propagation growth between S355 and S690 steel grades. Reprinted with permission from M. P. A. Jesus, R. Matos, F. C. Bruno, C. Rebelo, L. S. Silva and M. Veljkovi // Journal of Construction Steel Research, Elsevier. **79** (2012) 140. © 2012 Elsevier Ltd.

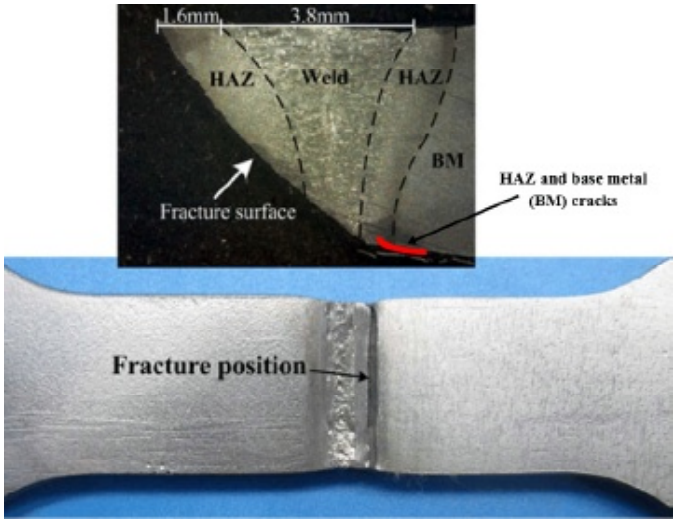

Fig. 5. Weld profile of a laser-welded 960 MPA high strength steel joint. Reprinted with permission from W. Meng, Z. Li, J. Huang, Y. Wu and S. Katayama // JMEPEG 23:538-544, ASM International. **23** (2013) 541. © 2014 ASM International.

welded HSS structures to fatigue loads, it should be noted that the fatigue strength does not increase proportionally to the static strength of the base metal [28,31]. Fig. 5 shows an example of a laser-welded 960 MPA high strength steel joint. The study concluded that the weld joint profile was affected by welding heat input leading to HAZ softening and cracks, and also base metal cracks, as shown in Fig. 5. The HAZ exhibited lower yield and tensile strength properties in the weld joint than the base

material. However, on occurrence of fatigue failure, the weld joint fractured along the HAZ soft zone and cracked areas [32].

Research has shown that fatigue life of HSS can be improved by it fatigue strength. Several researchers have proposed a number of techniques for improving the fatigue strength of welded joints. Techniques suggested include: high frequency mechanical impact (HFMI) [33-35] and low transformation temperature filler materials [36]. Although these repair methods contribute to improving weld quality, from economic point of view they slow down productivity, which in turn affects profitability, and affects quality if wrongly executed.

2.3. Machine and human factors consideration

Machine factors involving the selection of welding processes play a vital role when establishing procedures to ensure the structural integrity of an HSS structure. With arc welding processes such as SMAW, GMAW, gas tungsten arc welding (GTAW), SAW, and FCAW, the electrode coating, shielding gases and mode of transfer of the filler materials are contributing factors in determining the strength of a welded joint as they affect porosity, and hydrogen inclusion in the weld. Since most arc welding processes employ either manual, semi-automatic, automatic, or robotic welding techniques, the welding position and directional formation of the weld puddle plays a key role in determining the strength of a welded joint since lack of fusion, undercut, etc. are potential flaws. For an HSS structure, these combined effects account for the structural integrity as these affect the quality of welded joints.

From the human factors viewpoint, the skills and knowledge of the welder/operator are influential in determining if the structural integrity of a welded HSS structure meets required standards and specifications. Therefore considering risk assessment and controls as a holistic approach in assuring accuracy, consistency and flawless parameters when defining and implementing welding procedure specifications for HSS welding is vital and demands attention.

3. RISK ASSESSMENT

This part of the paper presents a methodological approach for assessing risk and structural integrity of welded HSS structures. As an effective management tool, the analytical hierarchy process (AHP) [37] is used in the risk assessment process, as shown in Fig. 6. From Fig. 6, the layout depicts a scheme of risk assessment using the AHP approach as follows:

- Risk assessment based on quantitative factors and qualitative factors.
- Converting quantitative and qualitative factors into attribute and alternative factors.
- Decision making using the AHP for selection preferences. Thus selecting the most suitable process based on total priority weight.

The scheme as illustrated in Fig. 6 is to ensure that all relevant aspects and steps are considered in the risk assessment process. The risk assessment process therefore considers the identification of both intrinsic and extrinsic factors that might have an impact on the structural integrity. For each of these impacts, identification of the criteria and quantifiable indicators for the criteria that could be used as a measure for decision making and risk assessment is vital. Developing a graphical representation of the problem in terms of the overall goal, the factors, the criteria, and the decision alternatives is also essential.

From Fig. 6, the qualitative component, as described in Table 3, and the quantitative component, i.e. welding processes, are converted into attributes and alternative factors respectively in order to establish criteria that could be used as a measure for risk assessment. For the alternative factors, the criteria that could be used as measures include weld bead profile/geometry evaluations (i.e. percentage of dilution obtained from the various welding processes), destructive test values (bend test, hardness test, impact test, microstructural evaluations), or non-destructive test values (ultrasonic test, radiography test, penetrant test).

For the attribute factors, the criteria that could be used as a measure involve the establishment of priorities through the use of a pairwise comparison procedure. This is done to determine the relative importance of the attributes, to determine the relative importance of each of the alternatives with respect to each attribute, and to determine the overall priority weight of each of the alternatives. The scale for pairwise comparison used for preparing the pairwise comparison matrix elements for each criterion is as shown in Table 4.

From Fig. 6, the first level shows that the overall goal is to minimize risk through decision making in selecting the most suitable welding process available to ensure sound structural integrity of a welded HSS structure. At the second level, factors such as the welder's skill requirement, operator fatigue and

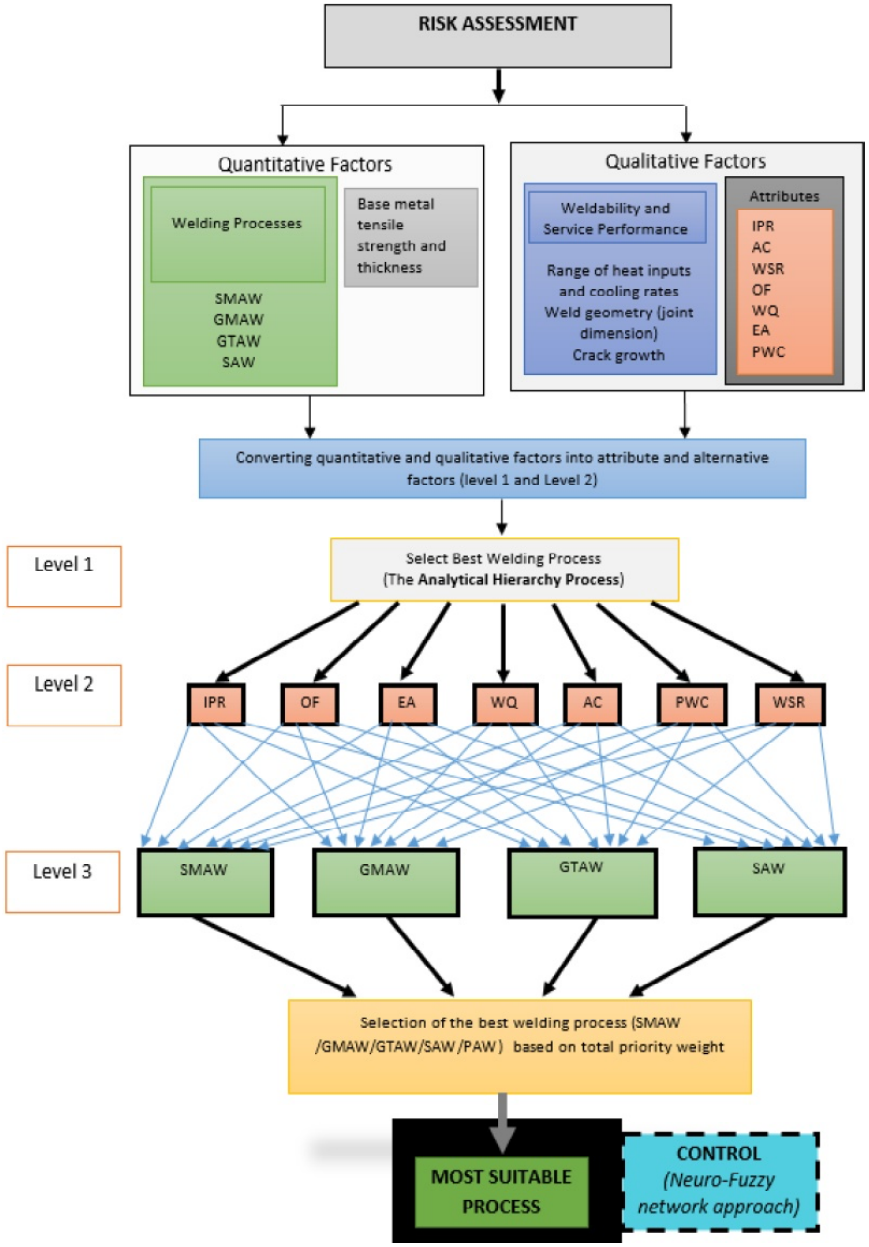

Fig. 6. Schematic diagram in performing Risk Assessment.

availability of consumables contribute to the achievement of the overall goal. At the third level, the alternatives (SMAW, GMAW, GTAW, and SAW) are presented and these must be evaluated through the criteria with respect to each attribute.

The following steps describe the arithmetic behind the AHP model [37]:

1. Assign weights to each alternative on the basis of the relative importance of its contribution to each decision criterion. This is carried out through a pairwise comparison of the alternatives based on the decision criterion.
2. Once the pairwise comparison matrix has been formed for a criterion, the normalized priority of each

Table 3. Description of process attributes considered.

No	Attributes	Description
1	Initial preparation required (IPR)	Preparation of joint, fit-ups and clamping in fixtures, setting welding parameters (voltage, current, welding, speed, gas flow rate, wire feed, etc.), and electrode/filler metal preparation, cleaning the base metal.
2	Availability of consumables (AC)	Electrodes, filler wires, shielding gases
3	Welder skill requirements (WSR)	Pre-heating requirement, root pass requirement, number of passes required, interpass temperature maintenance, and post-heating requirements.
4	Operator fatigue (OF)	Arc glare, smoke and fumes, electrode changing, and nozzle cleaning.
5	Weld Quality	Weld bead appearance, percentage of rejects due to welding defects (e.g. distortion, misalignment, porosity, lack of penetration, etc.).
6	Ease of automation (EA)	Manual, semi-automatic, fully automatic, robotics
7	Positional welding capacity (PWC)	Horizontal welding, vertical welding, overhead welding, and root pass welding.

Table 4. Scale for pairwise comparison characteristics and example.

Degree of importance	Definition
1	Equal (no preference)
2	Intermediate between 1 and 3
3	Moderately preferable
4	Intermediate between 3 and 5
5	Strongly preferable
6	Intermediate between 5 and 7
7	Very strong preferable
8	Intermediate between 7 and 9
9	Extremely strong preferable
Reciprocal of above numbers (1/2, 1/3, 1/4, etc.)	If a criterion is assigned to one of the above numbers when it is compared with another, the second will be assigned the reciprocal of the number when it is compared with the first

alternative is synthesized. The procedure for this is as follows: (a) sum up the values in each column, (b) divide each element in the column by its column total, which results in a normalized pairwise comparison matrix, and (c) compute the average of the elements in each row of the normalized comparison matrix, thus providing an estimate of the relative priorities of the alternatives.

3. In addition to the pairwise comparisons of the alternatives, use the same pairwise comparison procedures to set the priorities for all the criteria in terms of the importance of each in contributing towards the overall goal.

4. The priority is synthesized in a manner similar to Step 2.

5. Calculate the overall priority for each alternative.

6. Select the alternative having the highest priority.

The basic algorithm to forming the *M* X *N* pairwise comparison matrix is shown in Table 5. Depending on the nature of the assessment to be made, a set of well-defined algorithms is used for arithmetic processing of the data. The AHP model has been implemented for risk assessment and decision making in the field of science in diverse disciplines through different algorithmic approaches. Typical examples are sited in the paper to buttress the implications of this paper. However, risk assessment methods such as fault tree analysis, bow tie analysis, and preliminary hazard analysis methods for qualitative analysis; and risk level analysis, quantitative risk analysis, and Monte Carlo Simulation methods for quantitative risk analysis also are available. Nonetheless, the AHP method was chosen in this paper due to data consistencies.

Table 5. Pairwise comparison matrix for AHP computation.

$A = \begin{bmatrix} a_{11} & a_{12} & \cdots & a_{1j} & \cdots & a_{1n} \\ a_{21} & a_{22} & \cdots & a_{2j} & \cdots & a_{2n} \\ \vdots & \vdots & & \vdots & & \vdots \\ a_{i1} & a_{i2} & \cdots & a_{ij} & \cdots & a_{in} \\ \vdots & \vdots & & \vdots & & \vdots \\ a_{m1} & a_{m2} & \cdots & a_{mj} & \cdots & a_{mn} \end{bmatrix}$ *M X N* matrix	After establishing the *M X N* matrix, a reciprocal matrix is formed. This step is preceded by normalizing the matrix by totaling the numbers in each column. To check for consistency of original preference rating, a consistency analysis is made through consistency index and ratio calculations [37,38].

Table 6. Pairwise comparison of attributes. Reprinted with permission from V. Balasubramanian, V. Ravisankar, C. S. Ramachandran and C. Muralidharan // Int J Adv Manuf Technol, Springer-Verlag, London. **40** (2009) 887. © 2008 Springer-Verlag London Limited.

Process	SMAW	GMAW	GTAW	SAW	PTAW	Priority
SMAW	1 (0.559)	5 (0.535)	3 (0.0642)	9 (0.333)	7 (0.382)	0.491
GMAW	1/5 (0.112)	1 (0.107)	1/3 (0.071)	7 (0.259)	5 (0.273)	0.164
GTAW	1/3 (0.185)	3 (0.321)	1 (0.0214)	7 (0.259)	5 (0.273)	0.251
SAW	1/9 (0.062)	1/7 (0.015)	1/7 (0.030)	1 (0.037)	1/3 (0.018)	0.032
PTAW	1/7 (0.079)	1/5 (0.021)	1/5 (0.043)	3 (0.111)	1 (0.055)	0.062
	1.787	9.342	4.675	27	18.333	1.000

Table 7. Pairwise comparison of welding processes on initial preparation requirement. Reprinted with permission from V. Balasubramanian, V. Ravisankar, C. S. Ramachandran and C. Muralidharan // Int J Adv Manuf Technol, Springer-Verlag, London. **40** (2009) 887. © 2008 Springer-Verlag London Limited.

#	Attributes	IPR	AC	WSR	OF	PC	EA	PWC	Priority weight
1	IPR	1 (0.031)	1/2 (0.022)	1/7 (0.015)	1/9 (0.045)	1/3 (0.013)	1/5 (0.022)	1/6 (0.033)	0.025
2	AC	2 (0.061)	1 (0.043)	1/5 (0.021)	1/7 (0.058)	1/2 (0.021)	1/3 (0.036)	1/5 (0.039)	0.038
3	WSR	7 (0.212)	5 (0.213)	1 (0.104)	1/3 (0.136)	4 (0.161)	1/2 (0.054)	1/3 (0.065)	0.135
4	OF	9 (0.273)	7 (0.298)	3 (0.3130)	1 (0.408)	5 (0.201)	3 (0.327)	3 (0.589)	0.344
5	PC	3 (0.091)	2 (0.085)	1/4 (0.261)	1/5 (0.082)	1 (0.041)	1/7 (0.016)	1/7 (0.028)	0.085
6	EA	5 (0.152)	3 (0.128)	2 (0.209)	1/3 (0.136)	7 (0.282)	1 (0.109)	1/4 (0.049)	0.152
7	PWC	6 (0.182)	5 (0.213)	3 (0.313)	1/3 (0.136)	7 (0.282)	4 (0.436)	1 (0.196)	0.251
		33	23.5	9.59	2.453	24.83	9.18	5.09	1.000

In the field of welding, several studies have utilized AHP for decision-making. Selection of a welding process to fabricate a butt joint of high strength aluminum alloy of AA 7075 grade using AHP was investigated in [39]. In the work, several activities and cost drivers were used as the criteria to measure the alternating factors of GMAW, GTAW and plasma arc welding (PAW). With reference to Table 3, the results of the experiment revealed that weld quality was the most important attribute, thus giving rise to GTAW as the process with the higher priority weight.

In a recent study [40], AHP was used for selection of a welding process for hardfacing on carbon steels. In the work, a number of carbon steel specimen were hardfaced with varying heat inputs from welding processes such as SMAW, GMAW, GTAW, SAW and plasma transfer arc welding (PTAW). Percentages of dilution were used as the criteria to measure the alternating factors. Table 6 shows the pairwise comparison matrix for the attribute factors. In Table 7, the pairwise comparison matrix of the welding processes on initial preparation requirement is illustrated. The tables of the pairwise comparison matrix for the other attributes (AC, WSR, OF, PC, EA, and PWC) are omitted in this paper. However, Table 8 shows the final composite rating of the welding processes.

Based on the quantitative factors (percentage of dilution), the PTWA process was preferred since it produced the lowest percentage of dilution level as a result of the low percentage of the base metal in the deposited weld metal. Moreover, from the qualitative factors, it was noticed that operator fatigue was the most important attribute with the highest priority weight. Based on this result, the welding

Table 8. Final composite rating of the welding processes. Reprinted with permission from V. Balasubramanian, V. Ravisankar, C. S. Ramachandran and C. Muralidharan // Int J Adv Manuf Technol, Springer-Verlag, London. **40** (2009) 887. © 2008 Springer-Verlag London Limited.

Specimen no.	Attributes	Attributes priority weight	Process priority weight									
			SMAW		GMAW		GTAW		SAW		PTAW	
1	IPR	0.025	0.491	(0.0123)	0.164	(0.0004)	0.251	(0.0063)	0.032	(0.0008)	0.062	(0.0016)
2	AC	0.038	0.246	(0.0093)	0.072	(0.0027)	0.132	(0.0051)	0.038	(0.0014)	0.502	(0.0191)
3	WSR	0.135	0.121	(0.0163)	0.081	(0.0109)	0.036	(0.0049)	0.258	(0.0348)	0.504	(0.0681)
4	OF	0.344	0.068	(0.0234)	0.134	(0.0461)	0.035	(0.0121)	0.260	(0.0894)	0.503	(0.1730)
5	PC	0.085	0.074	(0.0063)	0.031	(0.0026)	0.247	(0.0209)	0.162	(0.0138)	0.486	(0.0413)
6	EA	0.152	0.058	(0.0088)	0.164	(0.0249)	0.038	(0.0058)	0.251	(0.0382)	0.489	(0.0743)
7	PWC	0.251	0.491	(0.1232)	0.164	(0.0412)	0.251	(0.0630)	0.032	(0.0081)	0.062	(0.0156)
Total				0.1996		0.1288		0.1181		0.1865		0.3930
Rating			2	2	4	4	5	5	3	3	1	1

process selected was PTAW, since it had the highest composite weight of 0.503 with the highest priority weight of 0.3930 as shown in Table 8.

The scientific relevance of the AHP therefore serves as a step beyond the conventional way of determining structural integrity where destructive and non-destructive tests are solely performed. In addition, the AHP create new ways for expressing variables and welding parameters when defining and implementing welding procedure specification. Moreover, it create avenues to develop new approaches like the utilization of on-line process monitoring and fatigue analysis systems to facilitate risk assessment process when considering structural integrity in welding.

4. ON-LINE PROCESS MONITORING AND FATIGUE ANALYSIS

A practical developmental case is the utilization of machine-human interface equipment such as sensor and camera based systems for on-line process monitoring, as indicated in the framework and introduction part of this paper. Fig. 7 describes on-line process monitoring and failure analysis layout for the risk assessment process. In on-line process monitoring, the key aspects are pre-process monitoring, in-situ monitoring and post-process monitoring. Seam tracking, groove volume and groove shape are observed with pre-process monitoring, and temperature, metal vapor, back reflection and metal pool

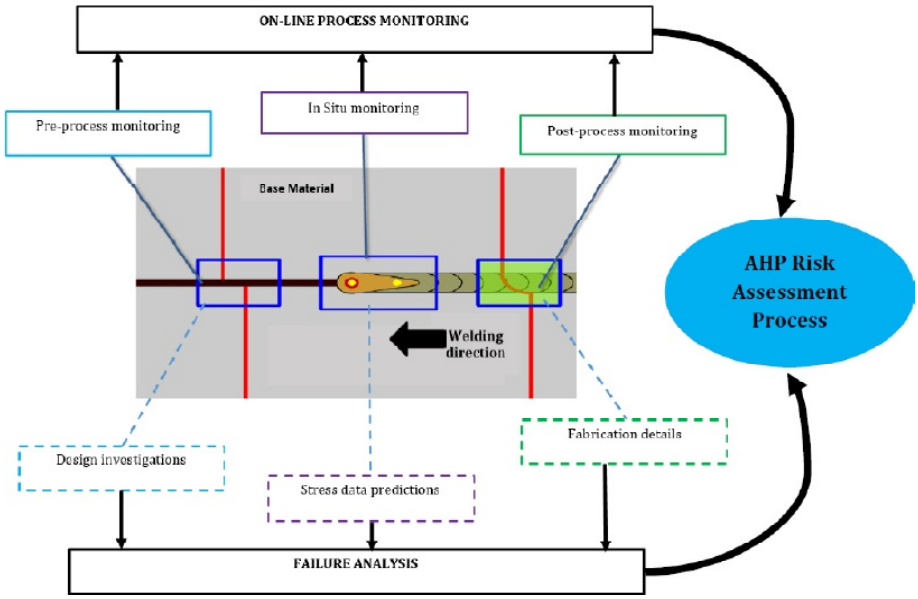

Fig. 7. On-line process monitoring and failure analysis layout for risk assessment process.

shape are monitored with in-situ monitoring. Post-process monitoring is used to monitor the shape of the weld bead, and to evaluate surface flaws. Failure analysis involving design investigations of weld profile/geometry, stress data predictions from thermal history of microstructural transformations, and fabrication detail assessment rely on feedback information obtained from the on-line process monitoring system.

The on-line process monitoring and failure analysis system with AHP risk assessment process system enables effective structural integrity analysis of weldability and service performance as it helps to identify flaws before, during and after welding. Therefore incorporating the digitalized computational system with AHP risk assessment process system would provide a high degree for quality improvement and assurance when establishing procedures to ensuring structural integrity of an HSS structure.

5. DISCUSSION

From the weldability viewpoint, risks associated with welding of HSS include HAZ softening, cracking, and brittleness in the weld bead. HAZ softening is a result of microstructural changes that occur when high heat inputs are applied. Heat input is consequently a critical factor which significantly affects the strength and properties of HSS welded joints. For instance, if heat input is too low, there is a risk of lack of fusion, and on the other hand if the heat input is too high, the heat affected zone gets too wide, which can cause HAZ softening and brittleness in the weld bead [41]. Although such risks lead to ductility, strength, and toughness problems, they also affect the quality of weld joints and bring about low welding productivity. In addition, risk of cracking is a factor in the choice of filler materials. This occurrence is usually due to improper weld metal (base metal plus filler material) dilution. As heat-input plays a significant role in such phenomenon thereby causing low toughness in the HAZ and the weld metal, care must be taken when selecting or choosing matched, under-matched or over-matched filler materials in welding HSS. Productivity wise, this situation leads to consumable wastage and also lots of repair work due to low quality welds which are also prone to fracture toughness failure.

Secondly, from the viewpoint of service performance, fatigue strength of HSS does not increase with increasing yield strength, but strength properties of the material are associated with load carrying capacity. Fatigue strength is consequently reduced by means of welding as a result of the softening phenomenon of the HAZ. Risk factors associated with service performance of a welded HSS include weld geometry, material grade and thickness, and crack growth. For weld geometry, design and fabrication play a critical role as both variables are closely dependent on each other. Therefore poor design leads to wrong fabrication and vice versa. The process of fabrication and welding create levels of stress on the geometric profile of the weld. Additionally, stress concentration arises as the welded structure is subjected to static or dynamic loading, thus reducing fatigue life. Furthermore, the risk of crack growth is highly pronounced when there are imperfections in the weldment. For instance, defects such as undercut, porosity, etc. create notches and discontinuities which give rise to further stress concentrations. In such events, crack initiation, usually located at the weld toe or at the weld root, begins, followed by crack propagation.

In order to alleviate such potential flaws, risk assessment and controls should be performed. Using the AHP model could yield satisfactory results in decision making since qualitative and quantitative factors can be assessed in detail. Several criteria with relative importance could be used as measures in the risk assessment process. The ability to lower risk to ensuring sound structural integrity in the process of welding HSS could be high. As part of HSS weldability predictions, on-line welding process monitoring system could be employed for seam and groove tracking, weld pool shape monitoring, and weld bead and weld metal surface flaws monitoring as a measure to identify flaw before, during and after welding

For service performance of HSS, the design and fabrication aspects must be precise. In addition, despite the limitations of correcting weld flaws with the on-line process monitoring system, obtaining digital feedback from the system would help in the computation and controllability of welding parameters to level with fatigue strength and also fatigue life of the parent metal. Minimization of elastic stress concentration and decrease of fatigue notch factor becomes achievable. These procedures when critically examined and practiced would also serve a great deal to reduce extra costs in HSS welding.

6. CONCLUSIONS

Potential benefits from utilization of HSS for industrial applications cannot be under-estimated despite the material's drawbacks due to welding effects. As new applications are emerging in the metal indus-

try, the weldability and service performance of HSS proves to be an intriguing issue which needs to be understood from industrial and scientific point of views. Therefore, a rigorous risk assessment process needs to be performed, considering the metallurgical, physical and mechanical flaws observed in previous studies, when selecting welding processes and filler material in welding HSS of different material grade and thickness.

Adapting the AHP system would be an effective approach for evaluating the selection of welding processes and filler material in HSS welding. The AHP system therefore creates a paradigm shift from the conventional method of selecting and assessing welding processes and filler materials in welding HSS. Likewise, design and fabrication processes need to be pre-assessed under welding conditions to lessen flaws in weld geometry, crack formation, and to prevent fatigue failure in order to ascertain considerable fatigue life. This is achievable by employing sensor and camera based systems for on-line welding process monitoring and advanced simulation tools for failure analysis during and after design and fabrication phases.

However, the limitations of the on-line welding process monitoring system mean that further research is required, for example, on neuro-fuzzy network system as an optimization mechanism for identifying, correcting and eliminating potential flaws before, during and after welding. The arguments presented in this paper not only emphasize on weldability and service performance of HSS, but also provides effective new ways of developing justifiable variables for welding procedure specifications. Therefore the neuro-fuzzy system when developed and incorporated with AHP and on-line welding process monitoring would create a new trend for ensuring quality and assuring structural integrity in welding usability of materials for demanding applications.

REFERENCES

[1] M. Pirinen, *The Effects of Welding Heat input on the Usability of High Strength Steels in Welded Structures* (Acta Universitatis, Lappeenrantaensis 514, Finland, 2013).
[2] V. Bertram and T. Lamb, *Ship Design and Construction*, *Volume 1-2* (Society of Naval Architects and Marine Engineers - SNAME, Jersey City, 2003-2004).
[3] T. Rantalainen, *Simulation of Structural Stress History Based on Dynamic Analysis* (Acta Universitatis Lappeenrantaensis 494, Finland, 2012).
[4] J. Billingham and J.V. Sharp, *Review of the Performance of High Strength Steels used Offshore* (Research Report 105, Cranfield University School of Industrial and Manufacturing Science, 2003).
[5] W. Wang and S. Liu // *Welding Journal* **81** (2002) 132.
[6] M. Zeman // *Welding International* **23** (2009) 73.
[7] P. Dainelli and F. Maltrud, *Etudes Et Recherche* (Institut de Soudure, France, 2012).
[8] *Hot Rolled Steel Plates, Sheets and Coils* (Ruukki Metals, Processing of Materials, Helsinki, 2007).
[9] *Quenched and Tempered Steels* (Technical Note 15, Welding Technology Institute of Australia, Milsons Point, 1999).
[10] F. Ade // *Welding Journal* **70** (1991) 53.
[11] P. K. Ghosh, P. C. Gupta, R. Avtar and B. K. Jha // *ISIJ International Journal* **30** (1990) 233.
[12] M. Xia, E. Biro, Z. Tian and Y. N. Zhou // *ISIJ International Journal* **48** (2008) 809.
[13] K. Hakansson, *Weld Metal Properties for Extra High Strength Steels* (The Royal Institute of Technology, KTH, Stockholm, 2002).
[14] *Quenched and Tempered Steels* (Technical Note 15, Welding Technology Institute of Australia, Milsons Point, 1985).
[15] G. H. Ryder, *Fundamentals of Welding Metallurgy* (Jaico Publishing House, Bombay, 1994).
[16] H. S. Wang // *Materials Transactions* **46** (2005) 593.
[17] *Welding Hand Book* (American Welding Society, Miami, 1981).
[18] T. Terasaki and T. G. Gooch // *ISIJ International* **35** (1995) 1272.
[19] P. Kah, M. Pirinen, R. Suoranta and J. Martikainen // Advanced Materials Research **849** (2014) 357.
[20] M. J. Cieslak, In: C*racking Phenomena Associated with Welding: ASM International Handbook* (ASM International, Materials Park, 1997), p. 71.
[21] B. A. Graville, In: *Welding of HSLA (Micro-alloyed) Structural Steels: American Society for Metals* (Rome, Italy, 1976), p. 85.
[22] M. Toyosada, In: *Proceedings of the Twelfth International Offshore and Polar Engineering Conference* (Kitakyushu, Japan, 2002), p. 365.

[23] S. Imai, In: *Proceedings of the Twelfth International Offshore and Polar Engineering Conference* (Kitakyushu, Japan, 2002), p. 392.
[24] B. Boardman, In: *ASM Handbook: Properties and Selection: Irons, Steels, and High-Performance Alloys*, ed. by AWS committee (ASW International, Ohio, 1990), p.673.
[25] J. Hicks, *Welded Design – Theory and Practice* (Woodhead Publishing, England, 2001).
[26] K. Weman, *Welding Processes Handbook* (Woodhead Publishing, England, 2012).
[27] Y. Bai and Q. Bai, Subsea Pipelines and Riser (Elsevier, Oxford, 2005).
[28] M. P. A. Jesus, R. Matos, F. C. Bruno, C. Rebelo, L. S. Silva and M. Veljkovi // *Journal of Construction Steel Researc* **79** (2012) 140.
[29] C. Miki, K. Homma and T. Tominaga // *Journal of Construction Steel Research* **58** (2002) 3.
[30] J. D. M. Costa, J. A. M. Ferreira and L. P. M. Abreu // *Procedia Engineering* **2** (2010) 697.
[31] S. Beretta, A. Bernasconi and M. Carboni // *International Journal of Fatigue* **3** (2009) 102.
[32] W. Meng, Z. Li, J. Huang, Y. Wu and S. Katayama // *ASM International* **23** (2013) 541.
[33] G. B. Marquis and Z. Barsoum // *Procedia Engineering* **66** (2013) 98.
[34] C. H. Yildirim and G. B. Marquis // *International Journal of Fatigue* **44** (2012) 168.
[35] C. H. Yildirim, G. B. Marquis and Z. Barsoum // *International Journal of Fatigue* **52** (2013) 57.
[36] A. A. Bhatti, Z. Barsoum, V. van der Mee, A. Kromm and T. Kannengiesser // *Procedia Engineering* **66** (2013) 192.
[37] T. L. Saaty, *Analytical Hierarchy Process* (McGraw-Hill, New York, 1980).
[38] T. S. Shores, In: *Applied Linear Algebra and Matrix Analysis*, ed. by S. Axler and K.A Ribet (Springer Science and Business Media, LLC, New York, 2007), p. 24.
[39] V. Ravisankar, V. Balasubramanian and C. Muralidharan // *Materials and Design* **27** (2006) 373.
[40] V. Balasubramanian, V. Ravisankar, C. S. Ramachandran and C. Muralidharan // *Int J Adv Manuf Technol* **40** (2009) 887.
[41] R. Raunch, S. Kapl, G. Posch and K. Radlmayr // *BHM.* **157** (2012) 102.

Publication II

Gyasi, E.A., Kah, P., Wu, H. and Kesse, M.A.
Modelling of an artificial intelligence system to predict structural integrity in robotic GMAW of UHSS fillet welded joints

Reprinted with permission from
International Journal of Advanced Manufacturing Technology
Vol. 93, pp. 1139-1155, 2017

Int J Adv Manuf Technol (2017) 93:1139–1155
DOI 10.1007/s00170-017-0554-0

ORIGINAL ARTICLE

Modeling of an artificial intelligence system to predict structural integrity in robotic GMAW of UHSS fillet welded joints

Emmanuel Afrane Gyasi[1] · **Paul Kah**[1] · **Huapeng Wu**[1] · **Martin Appiah Kesse**[1]

Received: 27 August 2016 / Accepted: 10 May 2017 / Published online: 7 June 2017

Abstract The use of welded lightweight steels in structural applications is increasing due to the greater design possibilities offered by such materials and the lower costs compared to conventional steels. Ultra-high-strength steels (UHSS) having tensile strength of up to 1700 MPa with a high strength-to-weight ratio offer a unique combination of qualities for diverse industrial applications. For productivity and quality reasons, gas metal arc welding (GMAW) is usually utilized for welding of UHSS. However, for full penetration fillet welded joints, the need for high heat input to gain acceptable weld penetration is problematic when welding UHSS. This is due to UHSS sensitivity to heat input and possible heat-affected zone (HAZ) softening. In this paper, an attempt is made, on the basis of analysis of experimental reviews, to identify and define relationships between nonlinear weldability factors to enable creation of an artificial intelligence model to predict full penetration in robotic GMAW fillet welded joints of UHSS S960QC. Welding variables and parameters associated with GMAW are first evaluated by reviewing scientific literature. The possibility of employing an artificial neural network (ANN) to predict full penetration fillet weld characteristics is then examined. It is noted that nonlinear variables associated with the GMAW process, such as heat input, contact tip to work distance (CTWD), and torch angle, and their related parameters, which pose weldability challenges, can be modeled by applying artificial intelligence systems. Ensuring full penetration in fillet welded joints of UHSS using artificial intelligence is thus feasible. Further, an optimized control system could potentially be developed by incorporating adaptive robotic GMAW with an artificial intelligence-based system to guarantee sound structural integrity that conforms to EN ISO 5817. The paper increases awareness of welding aspects of UHSS S960QC and presents an approach for overcoming existing limits to GMAW via adaptive robotic welding and artificial intelligence systems.

Keywords Ultra-high-strength steel (UHSS) · Robotic GMAW · Artificial intelligence · Structural integrity · Artificial neural network · Full penetration · Weld quality

1 Introduction

Nowadays, manufacturing industries are increasingly employing lightweight steels of high tensile strength in welded structural applications as a response to the need to reduce structural weight and attain cost reductions in welding manufacturing and production. These needs stem from demands for increased energy efficiency, which has become critical from the environmental point of view. Ultra-high-strength steel (UHSS) is one material choice for lightweight manufacturing. UHSS has superior strength-to-weight ratio and excellent physical, mechanical, and low-temperature properties, which enable lower fuel consumption and lower carbon emissions [1–4] than when using conventional steels. Industries that produce and operate mobile structures such as offshore platforms, floating production, storage, and offloading (FPSO) units, heavy-duty vehicles for mining or lifting purposes, and alternative energy industries operating in the fields of solar power, wind power, and liquefied natural gas (LNG) production stand to benefit from increased use of UHSS.

✉ Emmanuel Afrane Gyasi
emmanuelgyasi.giw@gmail.com; emmanuel.gyasi@student.lut.fi

[1] School of Energy Systems, Mechanical Engineering Department, Laboratory of Welding Technology, Lappeenranta University of Technology, P.O. Box 20, 53851 Lappeenranta, Finland

A major challenge facing manufacturing industries is to guarantee that full penetration is achieved in fillet welded joints of structural applications. Increased heat input is generally utilized to ensure acceptable full weld penetration in fillet joints.

As a result of the alloying elements and production process used in its manufacture, UHSS possesses a dual-phase microstructure consisting of bainite and martensite [1]. Its microstructure, similar to advanced high-strength steels (AHSS), is sensitive to high heat input, and exposure to elevated temperature can change its mechanical properties. More critical effects of heat input are heat-affected zone (HAZ) softening and an increased propensity to fatigue failure, which affect the toughness and strength of welded joints of UHSS [2, 3].

For productivity and quality reasons, fusion welding processes, especially gas metal arc welding (GMAW), have been favored for joining lightweight high tensile strength steels. A number of studies have been presented where GMAW has been employed for welding of UHSS S960QC [1–3]. Successful implementation of robotic GMAW in UHSS welding would have a significant effect on the profitability of manufacturing industry, where repeatability, precision, cost, time, and quality are key drivers in manufacturing and production. However, utilizing robotic GMAW in an uncontrolled manner poses weldability challenges for the structural integrity of UHSS fillet welded joints. The outcome of the GMAW process is dependent on a number of nonlinear variables, such as heat input, contact tip to work distance (CTWD), and torch angle, and their related parameters, e.g., arc current, arc voltage, welding speed, gas flow rate, arc efficiency, electrode stick out, wire feed speed, electrode diameter, torch position, and torch travel angle.

Development in artificial intelligent system for robotic welding shows that adaptive features such as sophistically sensory, monitoring, and control systems could be incorporated in the entire robotic artificial intelligent welding system to help the robot to adjust to its operating environment to enable monitoring, detection, measurement, inspection, and recording welding process parameters, and other features such as joint geometry and weld pool geometry. A typical example like infrared thermography-based sensors could be used in adaptive robotic artificial intelligent system to measure thermal profiles during welding to check susceptibility to heat inputs and temperature variations to assure weld integrity. However, for the robot to be capable to self-adjust to its functions and operations, artificial intelligent systems such as artificial neural network (ANN), fuzzy logic system, neural-fuzzy network (NFN), adaptive neuro-fuzzy inference system (ANFIS), genetic algorithm (GA), or swam particle optimization (SPO) need to be used as a data modeling tool. These artificial intelligent systems not only adapt, aid prediction of desired outcomes, and operate real time but are also capable to learn new input and output relationships and previously unknown situations and environments.

Therefore, development of a system able to account for and control the nonlinear factors associated with GMAW would alleviate weldability problems and guarantee sound structural integrity and full penetration in fillet welded joints of UHSS, enabling the joints to conform to the EN ISO 5817 standard, and would be a valuable scientific contribution to welding science, and manufacturing and production industries.

In this paper, an attempt is made, on the basis of analysis of experimental reviews, to identify and define relationships between nonlinear weldability factors to enable creation of an artificial intelligence (AI) model to predict full penetration in robotic GMAW fillet welded joints of UHSS S960QC. Figure 1 illustrates the concept of modeling an AI system for robotic welding of UHSS. It is assumed that all required inputs and the relationship between the inputs and the corresponding output requirements must be identified and considered. In addition, it is anticipated that the AI system should be able to predict desirable weld characteristics, such as weld bead penetration depth and weld geometry, based on the input data and expected outcomes.

A further requirement for the system is the ability to predict, during the welding process, possible weld flaws or errors in data modeling, as outputs, on receiving input requirements like welding parameters. In situations where undesirable outcomes and defects are likely to occur, the intelligent system should be able to capture, control, and correct the errors. This important adaptive function requires an optimized control system, whose discussion is beyond the scope of this work.

2 Material and welding considerations for welding of UHSS S960QC

Experimental studies have shown that welding of UHSS is challenging due to several nonlinear factors that affect weldability [1]. For example, weldability problems can occur as a result of inappropriate heat input and choice of filler materials [2], and problems can arise from fatigue effects related to weld geometry/profiles [3]. Figure 2 presents and

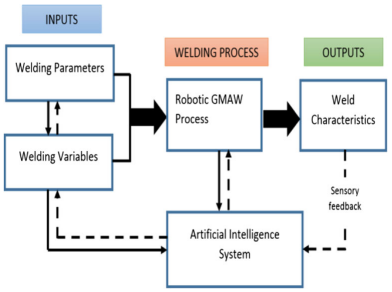

Fig. 1 Schematic diagram of modeling of an artificial intelligence system for a robotic GMAW process

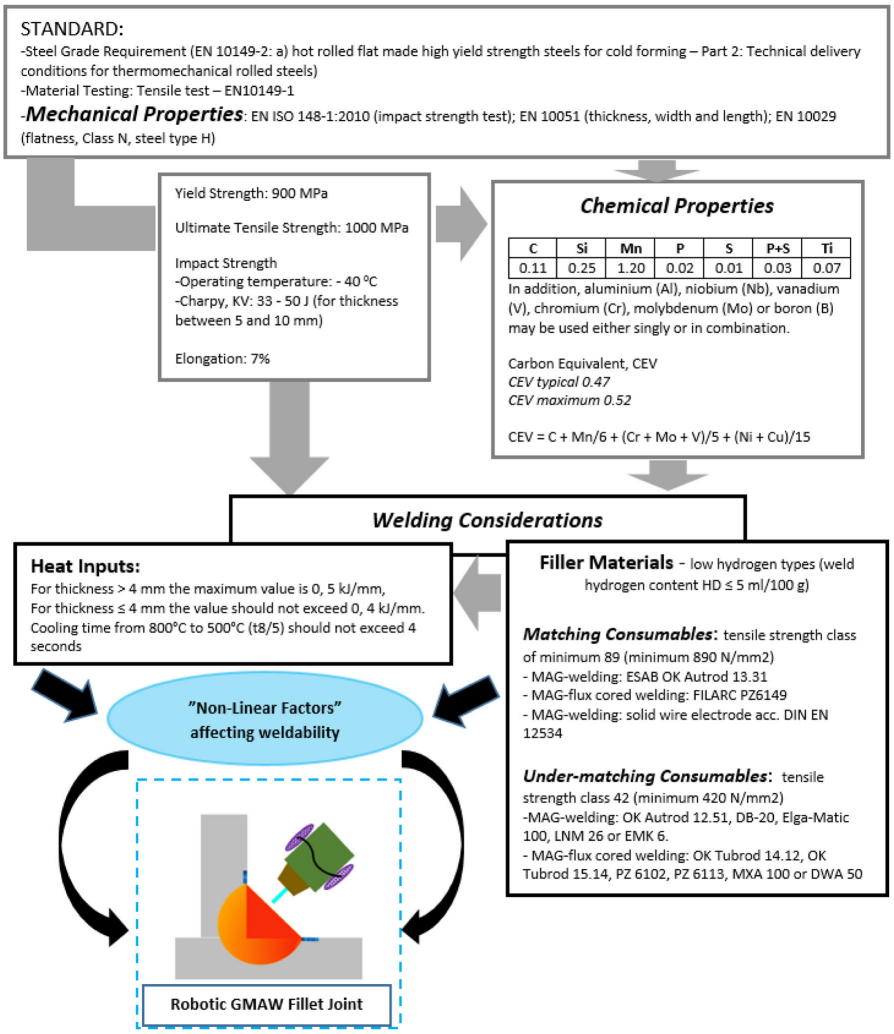

Fig. 2 Schematic representation of UHSS S960QC material data and robotic GMAW process fillet joint

summarizes information regarding standard requirements, material properties, and welding of UHSS S960QC. The schematic data representation does not provide a complete welding procedure specification (WPS) since items such as welding position, type of polarity, size of filler material, need for preheating or post-heating, and procedure sequence are missing. Such information is case-specific to the particular structure being welded, and it thus cannot be generalized but must be validated for the specific welding procedure. Nevertheless, the schematic data serves as relevant technical information when considering UHSS S960QC for experimental study.

For fillet welded joints, higher levels of structural integrity cannot be guaranteed due to susceptibility to a lack of full penetration [5]. In most cases, extra material preparations such as beveling have to be done, especially on the upright member of the fillet joint profile. This requirement increases material preparation costs and such pre-welding preparation cannot be utilized in many applications. Tables 1 and 2 show quality levels and critical imperfections in fillet welded joints according to EN ISO 5817. The quality levels are designated by symbols B, C, and D, where B corresponds to the highest requirement on the finished weld. The load types evaluated

Table 1 Surface imperfections in fillet welded joints [6]

No.	Reference to ISO 6520-1	Imperfection designation	Drawings and Remarks	t, mm	Limits of imperfections for quality levels		
					D	C	B
1.	**Surface imperfections**						
1.7	5011	Continuous undercut	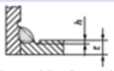 Smooth transition is required. This is not regarded as a systematic imperfection	0,5 to 3	Short imperfections: $h \le 0{,}2$ t	Short imperfections: $h \le 0{,}1$ t	Not permitted
	5012	Intermittent undercut		> 3	$h \le 0{,}2$ t, but max. 1 mm	$h \le 0{,}1$t, but max. 0,5 mm	$h \le 0{,}05$ t, but max. 0,5 mm
1.10	503	Excessive convexity		≥ 0,5	$h \le 1$ mm + 0,25 b, but max. 5 mm	$h \le 1$ mm + 0,15 b, but max. 4 mm	$h \le 1$ mm + 0,1b, but max. 3 mm
1.12	505	Incorrect weld toe	 $\alpha_1 \ge \alpha$ and $\alpha_2 \ge \alpha$	≥ 0,5	$\alpha \ge 90°$	$\alpha \ge 100°$	$\alpha \ge 110°$
1.16	512	Excessive asymmetry of fillet weld (excessive unequal leg length)	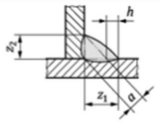 In cases where an asymmetric fillet weld has not been prescribed	≥ 0,5	$h \le 2$ mm + 0,2 a	$h \le 2$ mm + 0,15 a	$h \le 1{,}5$ mm + 0,15 a
1.20	5213	Insufficient throat thickness	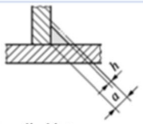 Not applicable to processes with proof of greater depth of penetration	0,5 to 3	Short imperfections: $h \le 0{,}2$ mm + 0,1 a	Short imperfections: $h \le 0{,}2$ mm	Not permitted
				> 3	Short imperfections: $h \le 0{,}3$ mm + 0,1 a, but max. 2 mm	Short imperfections: $h \le 0{,}3$ mm + 0,1 a, but max. 1 mm	Not permitted
1.21	5214	Excessive throat thickness	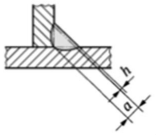 The actual throat thickness of the fillet weld is too large	≥ 0,5	Permitted	$h \le 1$ mm + 0,2 a, but max. 4 mm	$h \le 1$ mm + 0,15 a, but max. 3 mm

in definition of these quality levels include static load, thermal load, corrosion load, and pressure load [6].

Tables 1 and 2 serve as a guide for the objective of creating an AI model to predict full penetration in robotic GMAW fillet welded joints of UHSS S960QC. Surface imperfections such as excessive convexity, incorrect weld toe, excessive asymmetry of the fillet weld, insufficient throat thickness, and excessive throat thickness must fall within the acceptable quality level range in accordance with the EN ISO 5817 standard for material thickness greater than or equal to 0, 5, to 3 mm. Similarly, in Table 2, the quality level range in accordance with EN ISO 5817 standard for material thickness greater than or equal to 0, 5, to 3 mm must be observed for internal, joint geometry, and multi-imperfections.

2.1 Case study 1

Hemmilä et al. [1] investigated the weldability of Optim 960QC, which is the same as UHSS S960QC, for 3- and 6-mm-thick plates. In order to establish a basis for comparison of the effects of heat input, 3-mm-thick plates were prepared for laser welding and MAG welding, and 6-mm-thick plates were prepared for hybrid laser welding (CO_2 laser and MAG welding using shielding gas: 50% He + 45% Ar + 5% CO_2) and MAG welding using shielding gas: 80% Ar + 20% CO_2. Experimental data from the study is shown in Table 3. The MAG welding equipment employed was ESAB LAH 630 from Ruukki Productions, nowaday a division of SSAB. The laser and laser-hybrid welding equipment used were,

Table 2 Surface imperfections in fillet welded joints [6]

No.	Reference to ISO 6520-1	Imperfection designation	Drawings and Remarks	t, mm	Limits of imperfections for quality levels		
					D	C	B
2. Internal imperfections							
2.13	402	Lack of penetration	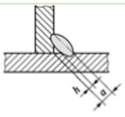	> 0,5	Short imperfection: $h \leq 0,\ 2a$, but max. 2 mm	Not permitted	Not permitted
			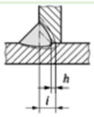 T-joint (partial penetration)	≥ 0,5	Short imperfections: butt joint: $h \leq 0,2\ s$ or i, but max. 2 mm T-joint: $h \leq 0,2\ a$, but max. 2 mm	Short imperfections: butt joint: $h \leq 0,1\ s$ or i, but max. 1,5 mm fillet joint: $h \leq 0,1\ a$, but max. 1,5 mm	Not permitted
3. Imperfections in joint geometry							
3.2	617	Incorrect root gap for fillet welds	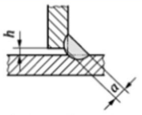 Gap between the parts to be joined. Gaps exceeding the appropriate limit may, in certain cases, be compensated for, by a corresponding increase in the throat thickness.	0,5 to 3 > 3	$h \leq 0,5$ mm + 0,1 a $h \leq 1$ mm + 0,3 a, but max. 4 mm	$h \leq 0,3$ mm + 0,1 a $h \leq 0,5$ mm + 0,2 a, but max. 3 mm	$h \leq 0,2$ mm + 0,1 a $h \leq 0,5$ mm + 0,1 a, but max. 2 mm
4. Multiple imperfections							
4.1	None	Multiple imperfections in any cross section	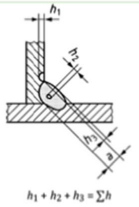 $h_1 + h_2 + h_3 = \sum h$	0,5 to 3 > 3	Not permitted Maximum total height of imperfections: $\sum h \leq 0,4\ t$ or $\leq 0,25\ a$	Not permitted Maximum total height of imperfections: $\sum h \leq 0,3\ t$ or $\leq 0,2\ a$	Not permitted Maximum total height of imperfections: $\sum h \leq 0,2\ t$ or $\leq 0,15\ a$

respectively, a Rofin-Sinar 6000 and ESAB ARISTO 2000 welding system.

In the laser-hybrid welding, the joints were tack welded using the MAG process and the distance between tacks was approximately 100 mm. In the other MAG welding, the 6 mm plate was milled and a V-groove cut. The welding was carried out without preheating using interpass temperatures of 25 °C and arc energies of 0.5 and 0.8 kJ/mm.

Non-destructive visual and X-ray examination conforming to EN ISO 15614-1 showed that class B (stringent) was generally achieved in the MAG-welded joints, but class C dominated in the laser and laser-hybrid welded joints. The lower quality class of the laser and laser-based methods was due to higher porosity, incomplete filling of grooves and roots, and local lack of fusion. Figures 3 and 4 show Vickers hardness profiles across the welds.

It was concluded that the HAZ showed a significant drop in hardness below that of the base plate in the MAG welding of the 3-mm plate, as can be seen in Fig. 3. The narrow, shallow soft HAZ in the autogenous laser weld of the 3-mm plate did not lower the tensile strength of the joint compared to that of the base plate. The use of laser or laser-hybrid welding could therefore help to reduce the width and depth of the HAZ softened zone.

Weld metal was even-matching in the case of the laser-based methods, but slightly under-matching in the MAG weld of the 3-mm plate. However, in both the 3- and 6-mm plates, the MAG welds demonstrated cross-weld tensile strength that was lower than that of the base plate. For a constant heat input (0.5 kJ/mm), the reduction in tensile strength increased as the plate thickness decreased from 6 to 3 mm, as can be seen by comparison of Figs. 3 and 4.

A similar effect was obtained when increasing the arc energy in the case of the 6-mm-thick MAG-welded butt joints: higher arc energy (0.8 kJ/mm) produced greater under-matching. Cross-weld tensile strength decreased as arc energy and cooling time increased.

Table 3 Experimental data for different plate thicknesses and welding processes

Plate thickness	Dimension	Laser welding	Hybrid laser welding	MAG welding
3 mm	500 × 150 mm	Laser type: CO_2 laser		Heat input—0.5 kJ/mm
		Laser power—6 kW		Wire type: matching
		Shielding gas: helium		Wire grade: PZ6149
		Gas flow rate—25 l/min		Shielding gas: 80% Ar + 20% CO_2
		Air gap—0 mm		Root gap—1.5–2 mm
6 mm	500 × 150 mm		Laser type: CO_2 laser	Heat input—0.5 kJ/mm
			Laser power—6 kW	Electrode type: matching
			Shielding gas: 50% He + 45% Ar + 5% CO_2	Electrode grade: OK Autod 13.31
			Gas flow rate—30 l/min	Shielding gas: 80% Ar + 20% CO_2
			Electrode grade: OK Autrod 13.31	Root gap—1.5–2 mm
			Electrode stick out—15 mm	Electrode stick out—15 mm
			Electrode diameter—1.0 mm Air gap—0.25 mm	Electrode diameter—1.0 mm

Laser-based welding processes gave the best combinations of strength and toughness. The impact toughness of the HAZ was better in the laser-hybrid welded joint than in the MAG-welded joint. This improved impact toughness is a result of the finer lath martensitic-bainitic microstructure found in the HAZ of the laser-hybrid joint as a resultant effect of the higher cooling rate. With the MAG weld, the toughness of the fusion line (FL/HAZ) is the limiting factor, whereas in the laser-hybrid weld, the weld metal toughness is the limiting factor.

The susceptibility to HAZ softening of S960QC when MAG welded is a challenge. Although it has been stated that welding of S960QC should be done with as low an arc energy as possible, and that high hydrogen content filler materials should be avoided to prevent hydrogen-induced cracking in the weld metal [2], the precise factors involved and the relationships between the welding variables and parameters have not been clearly established. Therefore, predicting and ensuring toughness and hardness properties in the HAZ similar to those of the base material and achieving even-matching properties of the weld metal to the base material when using GMAW need further research. Welding variables and parameters pertaining to GMAW are discussed more thoroughly in Section 3.

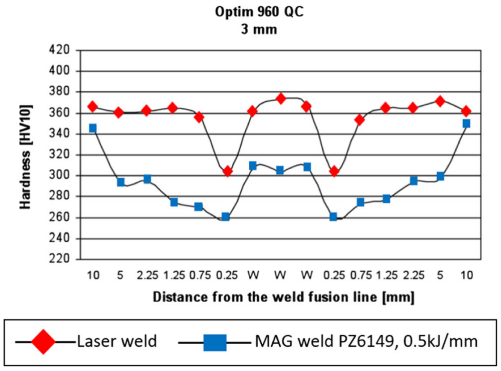

Fig. 3 Hardness profiles across 3-mm-thick laser and MAG-welded butt joints in Optim 960 QC (note that the distance scale is nonlinear) [1]

2.2 Case study 2

In another study, Björk, Toivonen, and Nykänen [3] investigated the ultimate load-bearing capacity of typical fillet welded joints made of UHSS S960. Validations of current design rules (Eurocode 3 Parts 1–12) covering steel grades up to S700 were done for fillet welded joints fabricated from direct quenched (un-tempered) UHSS S960. Throat thickness and other dimensions for the fillet welds were validated through experimental testing and nonlinear finite element analysis (FEA). The studied joints were load-carrying (denoted by L-, T-, LT, and X-series) and non-load-carrying (X0 series) joints. Several parameters were considered for each joint type, such as filler metal, and

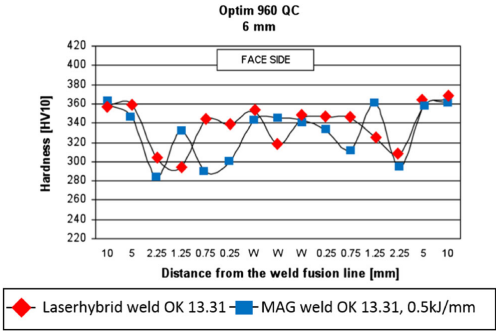

Fig. 4 Hardness profiles across 6-mm-thick laser and MAG-welded butt joints in Optim 960 QC (note that the distance scale is nonlinear) [1]

length and throat thickness of the welds. A fully mechanized GMAW process (MAG) was used for joining the plates of 8 mm thicknesses. The test results showed that ductile rupture occurred in all the joints when tested at room temperature. Additionally, the optimal cooling rate was difficult to reach; low heat input increased the risk of incomplete fusion. In the X0 series, however, the failure and capacity of the non-load-carrying joints seemed to depend on the heat input due to welding. When heat input was low, the softening was local, and it had no effect on the load-bearing capacity of the joint, and the failure occurred outside the joint (typically at an angle of 30°) as shown in Fig. 5. When heat input was increased, the softened width/plate thickness ratio increased and the critical ratio, experimentally about 0.2, was exceeded. Consequently, the failures occurred in the HAZ next to the weld.

It can be seen from Fig. 5 that heat input of 0.61 kJ/mm generated low throat size of 4.5 mm and smaller HAZ than with heat inputs of 0.77 and 0.94 kJ/mm. Based on measured ultimate strength of the base material, strain hardening seems not to compensate the softening effect. Therefore, in addition to ensuring that the load-carrying capacity of the fillet weld agrees with the design rules (Eurocode 3 Parts 1–12), heat input must be considered due to the softening effect on the HAZ. S960 tolerates very high cooling rates and strength properties for the welded joint are reached if the *t8/5*-time is less than 10 s. Consequently, the strength properties of the HAZ will drop by more than 10% of the strength of the base material when the optimal cooling rate is not reached. In addition, for matched filler materials, the weakest strength appears in the HAZ, but for under-matched electrodes, the weakest strength appears in the weld itself. However, utilizing under-matched filler materials can improve the deformation capacity of fillet welds if critical heat input limits are observed.

3 Robotic GMAW process parameters and variables

Development in industrial robotics has had a profound effect on modern welding, and industrial welding geared towards high quality and high productivity is nowadays often carried out using state-of-the-art robots. The GMAW process is most often used as the joining technique for robotic welding, mainly because of its flexibility and adaptability. Industrial GMAW is commonly a semi-automatic welding process since it utilizes an inert or active gas to shield a consumable and continuously fed filler material.

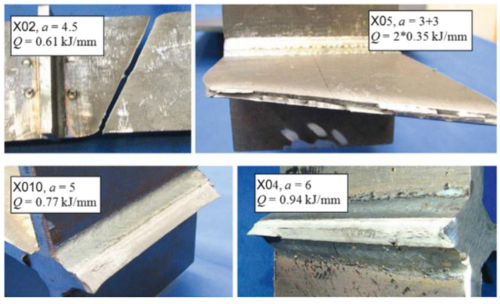

Fig. 5 Failure modes in non-load-carrying joints of UHSS S960 [3]

The GMAW process is defined by the shielding gases used, that is, metal inert gases in MIG welding, which are argon and helium gases, and metal-active gases in MAG welding, generally argon and carbon dioxide.

A large number of welding experiments have been conducted with the GMAW process. Table 4 presents key welding variables and parameters and indicates studies in which they were investigated. The defining welding parameters are heat input, contact tip to work distance, and torch angle. The studies listed in the right-hand column of Table 4 are utilized for the purposes of this work. In the studies, some welding parameters were assumed to be constants, for example arc length. The listed welding variables and parameters affect the weld geometry characteristics and properties of the weld and are considered in more detail in the following sections.

3.1 Heat input

Heat input influences the way molten filler material is transferred to the workpiece, arc stability, generation of spatter, weld bead profile formation, and weld quality. Most importantly, the terminology heat input is used because only part of the welding energy as established from these welding parameters enters the workpiece [17]. The expression for heat input is presented in Eq. (1) [18].

$$\text{Heat input (kJ/mm)} = \frac{\text{Arc voltage } (E) \times \text{Arc current } (I) \times 60 \times \text{Arc efficiency } (\eta)}{\text{Welding speed } (V) \times 1000} \quad (1)$$

As can be seen from Eq. (1), the relationship between current and voltage greatly influences the heat input value. Arc characteristics under conditions of stable arc and uniform arc length give synergetic control of voltage and current. Ohm's law therefore does not satisfy the current and voltage relationship in welding, where increase in current results in voltage increase [19].

In GMAW, it has been observed that the arc mode, and thus the weld quality, is greatly influenced by the arc current [20] as a heat input parameter. The depth of penetration is significantly influenced by the arc current; depth of penetration increases with increase in current [21]. However, increased joint penetration also increases the possibility of burn-through and solidification cracking. Experiments have shown that a higher

Table 4 GMAW welding variables and parameters used in reviewed experiments

Welding variables	Welding parameters	References
Heat input	Arc current	[7–15]
	Arc voltage	[7–16]
	Welding speed	[7–16]
	Gas flow rate	[7, 8, 11, 13, 15, 16]
Contact tip to work distance (CTWD)	Electrode extension	[11, 15]
	Arc length	[7–15]
	Wire feed speed	[11, 15]
	Wire diameter	[7, 8, 10, 11, 13–16]
Torch angle	Torch position	[8]
	Torch travel angle	[11]

current leads to a higher electromagnetic force, which causes the droplet to detach from the electrode and transfer to the weld pool. Furthermore, with a higher current, the size of the molten droplet is smaller and there is a higher droplet frequency.

Arc penetration depends also on electrode polarity. The penetration characteristic of GMAW with direct current electrode positive (DCEP), i.e., reverse polarity, and direct current electrode negative (DCEN), i.e., straight polarity, are depicted in Fig. 6. DCEP is mostly utilized because it produces good weld bead geometry and depth of weld penetration, and generates only low levels of spatter [20].

The current for a given GMAW solid or metal-cored electrode will reach a maximum density level and once this level is attained, no additional current can be carried by the electrode; thus, the electrode has reached its maximum current density [22]. Notably for a given heat source, the extent to which energy is absorbed by the workpiece depends on the rate of heat absorption of the material, the type of heat source, and the parameters of the welding process (voltage, current, and welding speed) [17]. Thus, from the arc efficiency expression shown in Eq. (2), it is imperative to determine the rate of heat absorption of the material when considering the relation between the current and voltage values.

$$\eta = 1 - \frac{(1-n)q_{p+}mq_w}{EI} \tag{2}$$

where

- η arc efficiency, expressed as a fraction, %
- n proportion of the energy radiated and convected from the arc column per unit of time and transferred to the workpiece, expressed as a fraction, %
- q_p energy radiated and convected from the arc column per unit of time, Btu/min (cal/s)
- m proportion of heat radiated away from the workpiece, expressed as a fraction, %
- q_w rate of heat absorbed by the workpiece, Btu/min (cal/s)
- E voltage, V
- I welding current, A

Experiments reveal that arc efficiency is higher for consumable electrode processes than for non-consumable electrode processes due to heat losses from the arc to the surroundings. With consumable electrodes, heat loss from the electrode can often be ignored as the energy transferred to the electrode

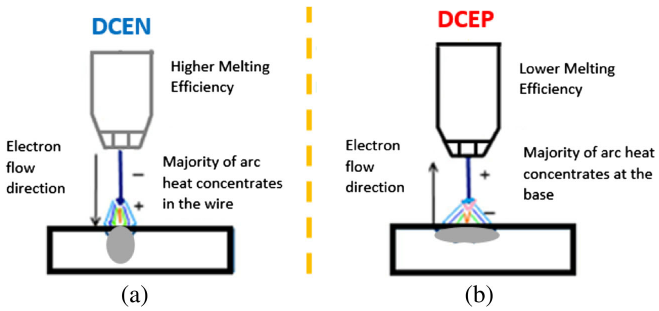

Fig. 6 Arc penetration characteristics of GMAW with **a** DCEN and **b** DCEP electrode polarity

is eventually absorbed by the workpiece. Arc efficiency in GMAW falls within the range 66–85% [17, 23]. It has been observed that gas tungsten arc welding (GTAW) loses substantially more heat from the arc to the surrounding environment than GMAW, shielded metal arc welding (SMAW), and submerged arc welding (SAW). It must be noted that this generalization can result in supplying too high or too low heat input since specifications of material grade and strength are not given [17]. This observation, though, gives an indication of how to determine the rate of heat absorption of a material when establishing welding heat inputs, as in the case of UHSS. It should however be noted that the higher the heat conductivity of a material, the lower the penetration [21].

For the GMAW process, arc voltage is proportional to arc length. Welding with a high voltage produces a wide and flat weld bead with possible undercuts, and welding with too low voltage produces a low-quality weld bead with high concave reinforcement [24, 25] and decreased depth of penetration [21]. Arc voltage can be controlled by altering the arc length [26]. Too small arc length may give rise to poor penetration if the arc power is very low [21].

Gas flow rate and welding speed play major roles in determining heat input. The electric arc is stabilized by the arc plasma as a result of ionization of the shielding gas. In addition, the mode of metal transfer from the consumable electrode is determined by the arc type and also depends on the gas flow rate. In GMAW, binary shielding gas blends (argon + helium, argon + CO_2, or argon + oxygen) or ternary shielding gas blends (helium + argon + CO_2, or argon + CO_2 + oxygen) are mostly utilized [22, 27]. Table 5 shows GMAW arc types, descriptions, and material application.

The extent of convective loss depends on the nature of the shielding gas, its flow rate, and its configuration system [17]. It must be noted that the percentage mixture of CO_2 in both binary and ternary blends has an effect on heat input, and defining the relationship between CO_2 percentage and control of current and voltage values is imperative. Extensive research on arc types has shown that in many applications, greater benefit accrues from spray and pulsed arcs than short and globular arc modes [27]. Moreover, enhanced arc processes such as controlled short arc, heavy deposition rate arc, and controlled spray arc offer significant improvements in efficiency and usability [27].

Welding speed contributes to determining the cooling rate during and after welding. The variation of temperature with time as a function of the cooling rate, often referred to as the *thermal cycle*, affects microstructures, residual stresses, and the extent of distortions in weldments. On the surface of the weld pool, the temperature distribution affects the loss of alloying elements by evaporation as well as absorption and desorption of hydrogen and other gases. The chemical composition of the weldment is affected correspondingly.

The cooling rate of a weldment is a function of the rate of energy dissipation. Fast welding speed generates fast cooling and vice versa. As weld penetration increases with decreasing

Table 5 GMAW arc descriptions and material applications

Type of arc	Shielding gas	Metal transfer	Material application	Material thickness
Short arc	100% CO_2 or a mixture of 75–80% argon, plus 25–20% CO_2	Short-circuiting	Ferrous	0.5–2.6 mm
Globular arc	100% CO_2, and argon/CO_2 blends	Globular	Ferrous	3 mm and beyond
Axial spay arc	Argon + 1–5% oxygen or argon + CO_2, where the CO_2 levels are 18% or less	Axial spray	Ferrous and non-ferrous	5 mm and above
Pulse spray arc	Argon + 18% CO_2	Pulse spray	Ferrous, non-ferrous, and dissimilar	0.3 mm and beyond
Controlled short circuiting arc	Argon and CO_2 based	Short-circuiting	Ferrous, non-ferrous, and dissimilar	0.3 mm and beyond
Controlled globular arc	Argon and CO_2 based	Globular with short arc length (buried arc)	Ferrous	3 mm and beyond
Controlled spray arc	Argon and CO_2 based	Spray	Ferrous, non-ferrous, and dissimilar	1.5 mm and above
High-power arc	Argon and CO_2 based	Stream and rotating	Ferrous, non-ferrous, and dissimilar	3 mm and beyond

welding speed, the final metallurgical structure of the weld zone can be determined by the cooling rate from the maximum, or peak temperature achieved during the weld cycle. The average cooling rate from 1472 to 932 °F (800 to 500 °C, $t_{8/5}$) is particularly significant when welding heat treatable steels, and especially in the case of UHSS. The critical cooling rate for the formation of martensite in these steels is often commensurate with $t_{8/5}$ [17].

The boundary conditions derived from heat transfer equations, which are governed primarily by the time-dependent transport of heat by conduction and convection, may specify the temperature at various locations on the surface of the workpiece. For a large workpiece, the surface temperatures distant from the heat source can be taken as room temperature. However, near the heat source, the surface temperatures are much higher and are unknown in most situations [17].

Monitoring temperature variations across the weldment is important in the welding of UHSS due to its susceptibility to elevated temperatures.

Welding dilution plays a major role when considering heat input and its resultant effect on depth of penetration of the weld metal through the melting and fusion of the filler material with the base material. The selected filler material must be compatible with the base material such that four major areas of requirements are met by welds produced within a range of acceptable dilution rates: metallurgy compatibility, mechanical properties, physical properties, and corrosion properties. The percentage of dilution can be determined by the expression in Eq. (3).

$$\%\text{of dilution} = \frac{\text{Area of penetration}}{\text{Area of reinforcement} + \text{Area of penetration}} \times 100 \tag{3}$$

Figure 7 illustrates a fillet weld bead geometry with HAZ traces. In Fig. 7, (a_1) is area of reinforcement, (a_2 + a_3) is area of penetration, and (a) is the throat thickness. Based on EN ISO 15609-1, throat thickness (a) is expressed as 0.5 * t − 0.7 * t, where t is the thickness of the base material.

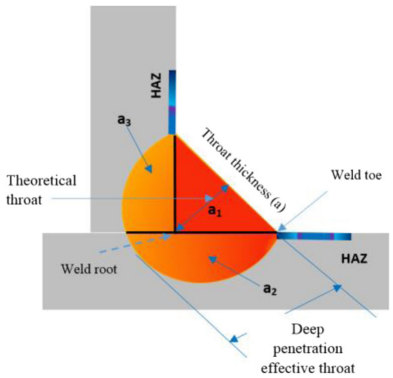

Fig. 7 Fillet weld bead geometry

In order to predict weld penetration, several factors must be considered and related. The relationship between weld penetration, arc voltage, arc current, and welding speed using a welding technique performance factor (WTPF) is expressed in Eq. (4) as follows:

$$\text{WTPF} = \left(I_S^4 / F_1 \times V_S\right)^{1/3} \tag{4}$$

where I_s is arc-current in amperes, F_1 is the arc-travel rate in centimeters per minute, and V_s is the arc-voltage in volts [28]. Knowledge of the relationship between these and other variables and parameters such as contact tip to work distance and the torch angle could lead to better prediction of depth of penetration.

3.2 Contact tip to work distance

In GMAW, the output characteristics of the arc are controlled by two main power sources: the constant current (CC) power source and the constant voltage (CV) power source. Considering these power sources, the CTWD greatly influences the arc length during welding. With constant current, the CTWD determines the arc length. As the CTWD increases, the arc length increases, and as the CTWD decreases, the arc length decreases. The problem of maintaining a constant arc length when using CC has been resolved by incorporating wire feed speed control. Thus, as the CTWD decreases, the wire feed speed increases, and as the CTWD increases, the wire feed speed decreases. The arc voltage is proportional to the arc length. The arc voltage can therefore be controlled by changing the arc length [22]. Hence, an increase in arc length will generate an increase in arc voltage [29].

With CV power source, however, the CTWD controls the welding current as a function of the arc length. As the CTWD increases, the welding current decreases, and as the CTWD decreases, the welding current increases. Moreover, in the CV scenario, the arc becomes a series circuit, and the CTWD provides resistance to current. Therefore, voltage remains unchanged and the arc length is unchanged despite changes to wire extension dimensions, as shown in Fig. 8. Furthermore, the relationship between CTWD and current, voltage, welding speed, and gas flow rate influences arc penetration. From Fig. 8, the arc penetration can be determined by identifying the arc position, which is the sum of wire extension and arc length [22].

Electrode extension ranges from 5 to 15 mm for dip transfer and up to 25 mm in other transfer modes [24, 25]. Weld properties and geometry can be predicted based on relationships between welding current, arc voltage, gas flow rate, wire feed speed, and CTWD. Electrode diameter varying from 0.8 to

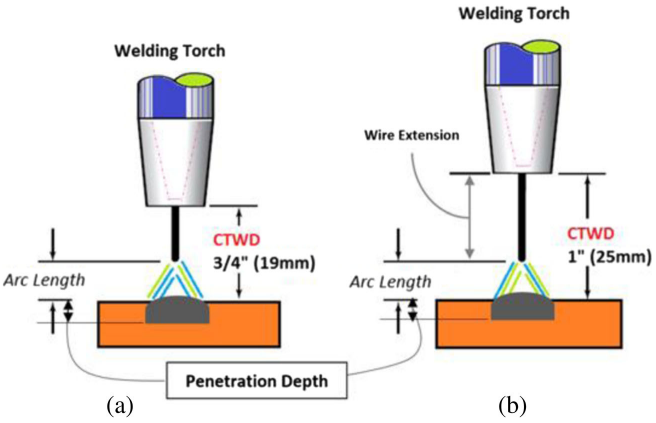

Fig. 8 Arc length representations in GMAW process contact tip to work distance. **a** 3/4″ (equivalent to 19 mm). **b** 1″ (equivalent to 25 mm)

1.6 mm has effects on melting depending on heat input relationships. As smaller diameter electrodes are used for thin materials and vice versa, operational difficulties arise when electrodes are selected wrongly, thus affecting weld joint quality [24, 25].

3.3 Torch angle

The torch angle has an influence on the quality of the weld bead and the weld geometry. The torch angle is characterized by its orientation (torch travel angle) and its linearity (torch position). The deposition rate is lower when the torch angle is off-set or not in correct alignment with the cross-section of a groove. Generally, in fillet weld welding positions such as horizontal down-hand (PB or 2F), it has been estimated that the torch angle with respect to torch position should be 45–50° and the torch travel angle should be 10–15° in the welding direction as illustrated in Fig. 9.

Torch angle discrepancies result in undercut and insufficient fusion, mostly in the upright member of the fillet weld. This phenomenon leads to quality problems and lack of penetration between the upright member and the base member. Investigation of the effect of torch position and torch angle on

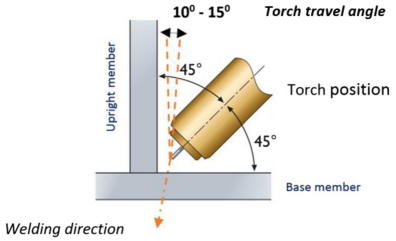

Fig. 9 GMAW torch angle (torch travel angle and torch position) representation

welding quality and welding process stability in pulse-on-pulse MIG welding–brazing of an aluminum alloy to stainless steel in a lap configuration reaches a similar conclusion [30]. In the experiment, direct current with a positively charged electrode (DCEP) was used to weld 6061 aluminum alloy (200 × 60 × 3 mm) and 304 stainless steel (200 × 60 × 2 mm). Images of the arc, electrical signals of the welding current, and welding voltage were acquired in synchronous modes by a high-speed camera and electrical signal acquisition system, respectively. It was concluded that arc shape, macrostructure, microstructure, and mechanical properties are sensitive to torch travel angle and torch position (work angle) for settings of 20° and 0°, respectively. A fracture occurred in the HAZ as a result of the effect of uneven heat distribution. However, when torch travel angle was 20° and work angle was 20°, the effects of torch position with respect to heat distribution were insignificant.

In robotic GMAW, the torch travel angle and torch position can be altered by manually controlling the manipulator and the end effector attached to the welding torch. Incorporation of adaptive features such as sophisticated sensory and monitoring systems make robots adaptive to their operating environment and enable monitoring, detection, measurement, inspection, and recording of welding process parameters and other features such as joint geometry and weld pool geometry [31]. The ability to maintain torch linearity and orientation, follow the desired trajectory, as well as the ability to perform seam tracking, which emulates the behavior of manual welders, is achievable in robotic welding systems [32]. However, an ideal sensor that combines all the aforementioned functionalities with respect to seam finding, seam tracking, quality monitoring, through-arc sensing, and control of welding parameters does not yet exist [33].

Artificial intelligent systems provide possible alternative solutions for adaptive robotic welding. For example, infrared

thermography-based sensors could be used in adaptive robotic GMAW and incorporated with an artificial intelligent system to measure thermal profiles when welding UHSS S960QC to check heat input and temperature variations and assure full penetration welds. In addition, motion control also creates a need to incorporate artificial intelligent systems in adaptive robotic welding for accurate trajectory planning as "teach and play" technique used in robotic programming today has repeatability and precision errors.

Figure 10 shows arc shape and arc characteristic based on torch angle, work angle, and arc length. The arc characteristic in Fig. 10 (y) indicates that adequate fusion and low susceptibility to HAZ are achieved. The dumbbell shape of the arc in Fig. 10 (y) indicates good arc characteristics in terms of its stability. In contrast, Fig. 10 (x) suggests that uneven heat distribution is likely to occur and thus high HAZ susceptibilities in one sample than another.

4 Artificial intelligence system application in welding

Modeling of an artificial intelligence system for robotic GMAW can be done usually by mathematical approaches. AI systems such as artificial neural networks (ANN), fuzzy logic systems, neural-fuzzy networks, adaptive neuro-fuzzy inference systems (ANFIS), genetic algorithms, and swam particle optimization (SPO) systems, which are mathematically based, can be used as data modeling tools to predict desired outcomes. These mathematically based and well-known algorithmic systems are gaining significance in the welding manufacturing industries. In the field of welding, for example, research work has considered the use of one or more artificial intelligence systems to predict weld characteristics such as weld bead strength, weld surface weld surface quality, weld penetration, and weld size for GMAW [34–36]. Different types of artificial intelligence systems to control arc welding processes have been investigated in a recent study on adaptive gas metal arc welding control and optimization of welding parameter output [37]. The study identified the effects and benefits of AI system predictions on metallurgical and geometric qualities in T-joint welds. It was concluded that the quality and properties of welded joints, weld deposition rate, microstructure, and weld geometry can be improved since welding parameters can be predicted by AI systems like ANN [37]. Table 6, supported by references [37–39], provides a comparison between frequently used AI systems in modeling and simulation of welding.

The computational abilities of AI systems, as shown in Table 6, comprise decision-making and/or linguistic performance. Depending on the type of AI system adopted and the output requirement expected, modeling a robust artificial intelligent system for weld characteristic predictions in robotic GMAW process should have enough input data. It should be noted that the output requirement can be limited but the input must have enough data to enable accuracy in predictions. Figure 11 illustrates a framework of a schematic model of an AI system for robotic GMAW. The model considers nonlinear weldability factors associated with robotic GMAW in the welding of UHSS S960QC. Welding variables and parameters are denoted as the input requirements and the corresponding desired output requirements are mapped to various AI systems.

In addressing UHSS S960QC weldability challenges, it is assumed that the output requirements given in Fig. 11 should conform to EN ISO 5817 for fillet weld quality levels as described in Table 1 and Table 2. The HAZ is expected to demonstrate consistent microstructural properties equal to the base material. If softening in the HAZ does occur, hardness should not drop considerably below the hardness value of the base material, and, additionally, toughness, ductility, and tensile strength should not deteriorate. As moderate strength properties for welded joints are reached if the cooling rate ($t_{8/5}$) is less than 10%, then the strength properties of the HAZ should not drop by more than 10% relative to the nominal strength properties of the base material [3]. Monitoring thermal cycles with a thermal profile senor/scanner while welding the UHSS S960QC material would be beneficial for cooling rate evaluation.

It is claimed that an optimal cooling rate is difficult to achieve when using GMAW (MAG) to weld 8-mm-thick

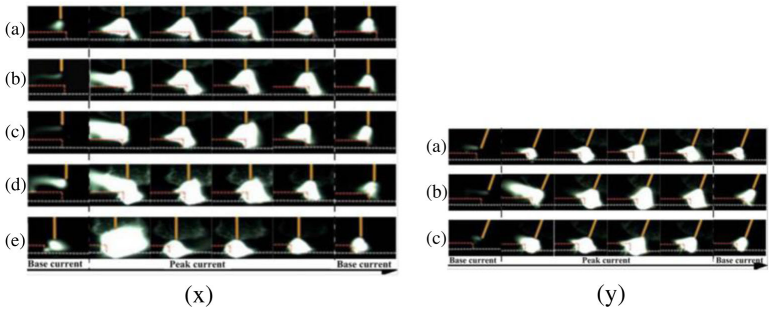

Fig. 10 Arc shape with different torch positions: In image (x), the torch angle is 20° and work angle is 0° and the lengths are (*a*) = −2 mm, (*b*) = −1 mm, (*c*) = 0, (*d*) = 1 mm, and (*e*) = 2 mm; In image (y), the torch angle is 20° and the work angle is 20° and the lengths are (*a*) = 0 mm, (*b*) = 1 mm, and (*c*) = 2 mm [30]

Table 6 Artificial intelligent systems for arc welding

Artificial intelligence systems	Principles	Advantages	Limitations
Artificial neural network systems	- Operates on feed forward back propagation system - Represents interconnected groups of artificial visible and hidden neurons - Develops models that depict interrelation characteristics between input data and desired output data	- Has learning and training capabilities for nonlinear system modeling - Has pattern recognition, signal processing, data prediction and control, and time series analysis capabilities - Has adaptability abilities where free parameters can be adapted to changes in surrounding environment - Has knowledge discovery and data mining abilities - Has uncertainty tolerance and imprecision abilities	- Lack of linguistic/explanatory ability - Lack of knowledge representation abilities
Fuzzy logic systems	- Operates on a set of linguistic fuzzy rules - Relies on rule-based systems	- Has linguistic/explanatory abilities -Has good knowledge representation abilities, good uncertainty tolerance abilities, and good imprecision tolerance	Lack of self-learning abilities; lack of adaptive and pattern recognition abilities, and rather bad knowledge discovery and data mining abilities
Neuro-fuzzy systems	- Operates by hybridizing fuzzy logic qualitative approach and adaptive neural network system capabilities	- Combines the advantages of both paradigms and conquer their own shortcomings concurrently to produce improved intelligence system	- It is typical for Mamdani fuzzy inference system with a single output defuzzification
Adaptive neuro-fuzzy inference systems	- Uses a hybrid learning algorithm by combining least squares estimators and the gradient descent method	- Both antecedent and consequent parameters are optimized, has the ability to generalize and converge rapidly particularly in online learning, and applicable in adaptive control	- It is typical for Sugeno systems, i.e., for constant and linear output membership functions and single output defuzzification

plates of UHSS S960QC. Moreover, a high risk of incomplete fusion is bound to occur when small heat input is employed [3]. To alleviate HAZ softening and susceptibility to a lack of fusion when welding UHSS S960QC, adaptive robotic GMAW incorporating AI systems for real-time modeling provides an alternative and holistic approach.

Due to its operational functionalities and benefits, an ANN system is selected as a case schematic model (Fig. 11). The schematic model represents an ideal situation to serve as a practical step to design a neural network system modeling input/output data for a given set of parameters from input and output requirements. It is assumed that the neural network model when validated by comparing the predicted results with actual practical results should agree with the results obtained through real-time experiments on UHSS S960QC with a robotic GMAW process.

4.1 Artificial neural network

Considering the schematic model for ANN modeling, the input and output requirements can be represented as data functions in the neural network system. In the model, there are multiple input requirements and multiple output requirements which are mapped in a multilayer perceptron (MLP) neural network architecture as shown in Fig. 12.

The MLP neural network requires supervised learning. Weight adjustments are made based on comparison with some target output. A teaching signal feeds into the neural network for the weight adjustments. These teaching signals are also termed the training sample [40]. The MLP neural network architecture is composed of many simple perceptrons in a hierarchical structure forming a feed forward topology with one or more hidden layers between the input and output layers.

4.2 Multilayer perceptron learning algorithms

In determining an optimized set of weights, the MLP neural network system uses learning algorithms such as back propagation (BP), resilient propagation (RPROP), the Levenberg–Marquardt algorithm, genetic algorithm (GA), or particle swarm optimization (PSO) [40]. Generally, input data are weighted through sum biasing and are then processed through an activation function to produce the output. After each process, the calculated output is matched to the desired output, and the difference between the two gives an error signal. The weight is adjusted by presenting the error back to the neural network system in a manner that will decrease the error for every iteration. The process aims to reduce the error value and drive the neural network system model towards the desired target. The learning algorithm adjusts the weights as the iteration increases, thereby reducing the error and getting closer to the desired target [41, 42].

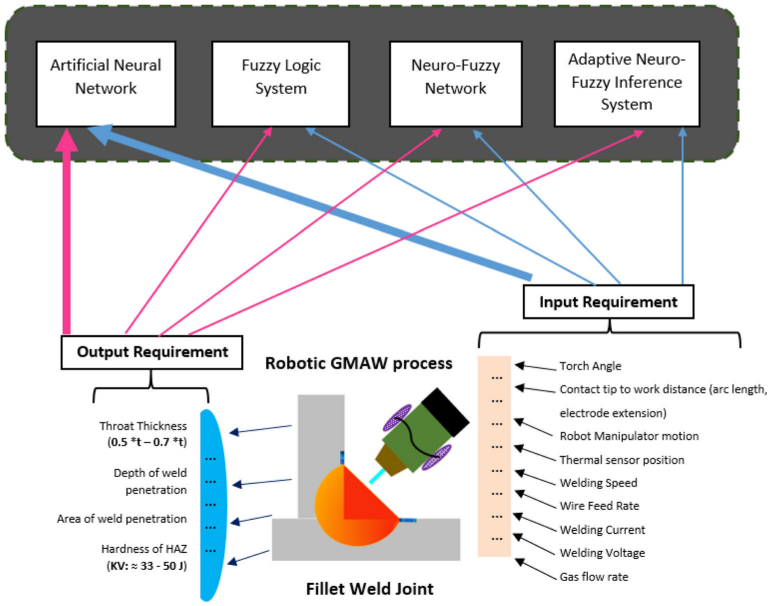

Fig. 11 A schematic model of artificial intelligence system for robotic GMAW process

In an ANN system development study [34], weld bead width characteristics were predicted as a function of key process parameters in robotic GMAW. The accuracy of the neural network model was verified by comparing the simulated data obtained from the neural network model with values obtained from actual robotic welding experiments. In the study, BV-AH32 steel of 12 mm thickness was multi-pass welded with GMAW.

The process parameters were the following: number of passes—3; welding current—170, 220, and 270 A; arc voltage—23, 26, and 28 V; and welding speed—12–50 cm/min. All other parameters were fixed. These process parameters were considered as input data and the required weld bead width was the output for the neural network system [34].

A back propagation learning algorithm and Levenberg–Marquardt learning algorithm were employed to train the neural network based on both the input and output data. A training set of 500 cycles was employed for the training of the network with an initial error of 1.0×10^6 [34].

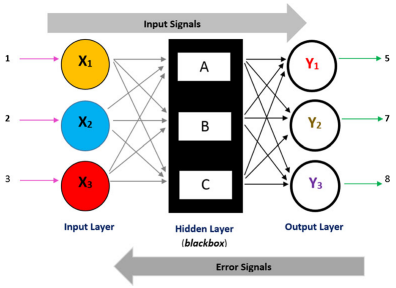

Fig. 12 A 3-3-3 multilayer perceptron neural network architecture

The training was carried out using MATLAB. It was observed that the Levenberg–Marquardt algorithm gave the lowest root mean square (RMS) error of about 0.0000845 with four neurons in hidden layers in 500 training cycles [34]. Figure 13 illustrates the performance of the back propagation algorithm and the Levenberg–Marquardt approximation algorithm for prediction of bead width [34]. From Fig. 13, it can be seen that the points obtained from the Levenberg–Marquardt predictions correlate with those of the actual experiment.

With back propagation, although the plotted points were not that far from values from the actual experiment, the predictions were not as exact as those of the Levenberg–Marquardt algorithm.

The Levenberg–Marquardt learning algorithm, also known as the damped least squares method, provides numerical solutions by reducing error when solving complicated boundary value problems. In the ANN system study [34], adjustment of the weights and biases was done according to the transfer function expressed in Eq. (5):

$$\Delta W = \left(J^T J + \mu I\right)^{-1} J^T e \tag{5}$$

where J is the Jacobian matrix of derivation of each error, μ is a scalar, and e is the error function. In other expressions, the Levenberg–Marquardt algorithm could be derived by

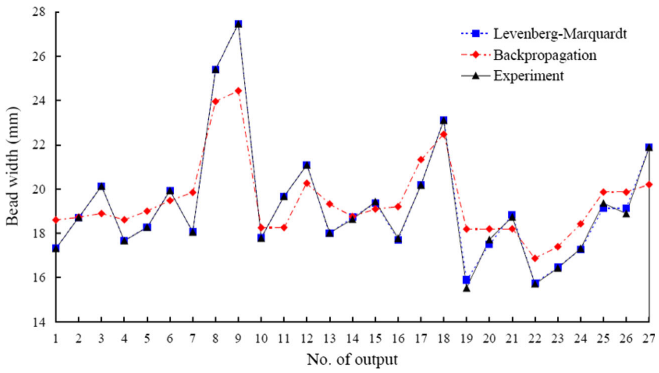

Fig. 13 Performance of learning algorithm prediction data against actual weld bead width data [34]

considering the error E after a differential change in the neural network weights from u_0 to u according to the second-order Taylor series expansion as shown in Eq. (6). Additionally, the Jacobian matrix is used to define the Hessian for special case of sum of squared error as expressed in Eq. (7) [40].

$$E(u) = E(u_0) + f^T(u{-}u_0) + \frac{1}{2}(u{-}u_0)^T H(u{-}u_0) + \ldots \quad (6)$$

$$H = 2\,J^T J + 2\frac{\partial J^T}{\partial u} F \quad (7)$$

Levenberg–Marquardt algorithm improved the overall accuracy of the neural network systems since it could provide a faster convergence. Therefore, for welding, where accurate setting of welding variables and parameters are imperative, the use of the Levenberg–Marquardt learning algorithm in ANN systems could guarantee accurate predictions.

5 Discussions

UHSS is becoming more usable for structural applications especially in mobile equipment industries. However, in applications where there is high fatigue loading on the structural welded load-carrying member, UHSS may not satisfy service performance requirements due to weldability challenges that arise from welding heat input, causing HAZ softening effects, lack of fusion, and susceptibility to cracking and fatigue failure. Previous study of structural integrity and the usability of high-strength steels (HSS) has emphasized the need for risk assessment when considering HSS and its variants such as UHSS and AHSS, especially as regards weldability and service performance following high heat input [43].

In this paper, UHSS S960QC material data presented in Fig. 2 shows welding considerations that require risk assessment. Adhering to heat input values and filler material recommendations can ensure sound welded joint characteristics. Nevertheless, weldability challenges clearly exist when manufacturing full penetration fillet welded joints of UHSS S960QC. Weldability challenges are increased where the UHSS S960QC weldments need to conform to ISO 5817.

Previous studies of online welding process monitoring [43] have shown the necessity of using sensing systems like infrared thermography in pre-process monitoring, in situ monitoring, and post-process monitoring for adaptive robotic GMAW. This sensory system will allow temperature differences to be measured and enable the required amount of heat needed for full penetration to be monitored. Despite the ability to acquire this data, such sensory systems are unable to control temperature variations dynamically in tandem with robotic GMAW process variables and parameters. Thus, an AI system for data modeling and process control should be embraced.

The AI model discussed and the welding information presented can provide a useful basis for real-time experimentation on UHSS S960QC. Actual experimentation data can then be compared with data values predicted from different learning algorithms like back propagation (BP), resilient propagation (RPROP), Levenberg–Marquardt, genetic algorithm (GA), and particle swarm optimization (PSO) to ascertain the accuracy of predicted AI values against actual experimental values. As neural network systems can learn new associations, new functional dependencies, and new patterns based on teaching and learning via input data and expected output, accurate prediction of desired outcomes is feasible [44].

6 Conclusion

Modeling of welding systems to guarantee sound structural integrity in lightweight-welded materials is relevant to modern welding manufacturing and production. In the current economic environment, structural weight must be reduced, stability of the welded structure must be assured, manufacturing

must be cost effective, and overall production must be profitable. Lightweight materials of high yield strength like UHSS S960QC are a possible material choice for lightweight manufacturing. UHSS S960QC has a superior strength-to-weight ratio, and excellent physical, mechanical, and low-temperature properties. From the environmental viewpoint, welding usability of UHSS translates into improved energy efficiency through low fuel consumption and low carbon emissions, especially in welded mobile equipment and structures.

In this paper, a schematic model of an AI system has been created by considering identified nonlinear factors associated with UHSS S960QC weldability and robotic GMAW. High heat input, which can result in HAZ softening and greater propensity to fatigue failure, thus affecting toughness and strength properties, is the most critical weldability issue with UHSS-welded joints. The multiple welding variables associated with robotic GMAW, such as heat input, CTWD, and torch angle, and related parameters like arc current, arc voltage, welding speed, gas flow rate, arc efficiency; electrode stick out, wire feed speed, electrode diameter, and torch position and torch travel angle, make accurate prediction of weld characteristics very challenging. Other nonlinear factors connected with the robot manipulator and end effector trajectory bring repeatability and precision errors, which further complicates prediction of the outcome of robotic GMAW.

One possible way to address or alleviate weldability challenges associated with nonlinear factors is by deploying AI systems. The welding information presented together with the neural network schematic model show that it is possible to accurately predict welding parameters and process outputs using learning algorithms. The schematic case model can provide a basis for future experimental study of UHSS S960QC welding in conformance with ISO 5817. Additionally, an optimized control system using infrared thermography-based sensors can be developed, which would enable an adaptive approach in robotic GMAW to be incorporated into the neural network modeling and control system. This paper increases awareness of the potential of UHSS S960QC and presents a scenario for using an AI system to overcome current limits on adaptive robotic GMAW.

Acknowledgements The authors would like to thank Mr. Peter Jones for his comments and assistance with the English language. Special thanks to the Finnish State for the financial support.

References

1. Hemmilä M, Laitinen R, Liimatainen T, Porter D (2010) Mechanical and technological properties of ultra high strength Optim steels. Rautaruukki Oyj, Ruukki Production, Helsinki. http://www.oxycoupage.com/FichiersPDF/Ruukki_Pdf/English/Ruukki-Technical-article-Mechanical-and-technological-properties-of-ultra-high-strength-Optim-steels.pdf. Accessed 20 April 2016
2. Kah P, Pirinen M, Suoranta R, Martikainen J (2014) Welding of ultra high strength steels. Adv Mater Res 849:357–365
3. Björk T, Toivonen J, Nykänen T (2012) Capacity of fillet welded joints made of ultra-high strength steel. Weld World 57:71–84
4. Laitinen R, Valkonen I, Kömi J (2013) Influence of the base material strength and edge preparation on the fatigue strength of the structures made by high and ultra-high strength steels, 5th Fatigue Design Conference, Fatigue Design. Science Direct. Procedia Eng 66:282–291
5. Hicks J (2001) Welded design—theory and practice, Woodhead Publishing Ltd, Cambridge. Elsevier. Chapter 4, p 36–41
6. Finnish Standards Association (SFS): welding—fusion-welded joints in steel, nickel, titanium and their alloys (beam welding excluded)—quality levels for imperfections (ISO 5817:2014)
7. Hemmilä M, Laitinen R, Liimatainen T, Porter D (2005) Mechanical and technological properties of ultra high strength Optim steels. Rautaruukki Corporation, Helsinki
8. Jae-Woong K, Jun-Young L (2008) A control system for uniform bead in fillet arc welding on tack welds. J Mech Sci Technol 22: 1520–1526
9. Shi L, Tian X, Zhang C (2015) Automatic programming for industrial robot to weld intersecting pipes. Int J Adv Manuf Technol 81: 2099–2107
10. Ahiale GK, Oh Y-J, Choi W-D, Lee K-B, Jung J-G, Nam SW (2013) Microstructure and fatigue resistance of high strength dual phase steel welded with gas metal arc welding and plasma arc welding processes. Met Mater Int 19:933–939
11. Nele L, Sarno E, Keshari A (2013) Modeling of multiple characteristics of an arc weld joint. Int J Adv Manuf Technol 69:1331–1341
12. Jaime A-V F, Reyes R-C, Ismael L-J (2016) On-line learning of welding bead geometry in industrial robots. Int J Adv Manuf Technol 83:217–231
13. Moon H-S, Na S-J (1997) Optimum design based on mathematical model and neural network to predict weld parameters for fillet joints. J Manuf Syst 16:13–23
14. Son JS, Kim IS, Kim HH, Kim IJ, Kang BY, Kim HJ (2007) A study on the prediction of bead geometry in the robotic welding system. J Mech Sci Technol 21:1726–1731
15. Xiong J, Zhang G, Hu J, Wu L (2014) Bead geometry prediction for robotic GMAW-based rapid manufacturing through a neural network and a second-order regression analysis. J Intell Manuf 25: 157–163
16. Lin H-L, Yan J-C (2014) Optimization of weld bead geometry in the activated GMA welding process via a grey-based Taguchi method. J Mech Sci Technol 28:3249–3254
17. DebRoy T, Kou S, Tsai C (2001) Heat flow in welding: welding handbook chapter committee. Chapter 3, American Welding Society (AWS)
18. Gunaraj V, Murugan N (2002) Prediction of heat-affected zone characteristics in submerged arc welding of structural steel pipes. Weld J 81:94–98
19. Ibrahim Khan M (2007) Welding science and technology. New Age International Publishers, New Delhi
20. Howard BC, Scott CH (2005) Modern welding technology, 6th edn. Pretice Hall, United States of America
21. Nagesh DS, Datta GL (2002) Prediction of weld bead geometry and penetration in shielded metal arc welding using artificial neural networks. J Mater Process Technol 123:303–312
22. Nadzam J (2014) Gas metal arc welding: production and procedure selection—The Lincoln Electric Company. http://www.lincolnelectric.com/assets/global/products/consumable_miggmawwires-superarc-superarcl-56/c4200.pdf. Accessed 20 April 2016

23. Robert Messler Jr W (2004) Principles of welding: processes, physics, chemistry and metallurgy. WILEY-VCH Verlag GmbH & Co. KGaA, Weinheim
24. Weman K, Gunnar L (2006) MIG welding guide. Woodhead Publishing and Maney Publishing, Cambridge
25. Weman K (2003) Welding process handbook. Woodhead Publishing Limited, Cambridge
26. Naidu DS, Ozcelik S, Moore K (2003) Modeling, sensing and control of gas metal arc welding, 1st edn. Elsevier, Kidlington
27. Kah P, Latifi H, Suoranta R, Martikainen J, Pirinen M (2014) Usability of arc types in industrial welding. Int J Mech Mater Eng 9(15):1–12
28. Jackson CE, Shrubsall AE (1953) Control of penetration and melting ratio with welding technique. Weld J 32(4):172–178
29. Kovacevic R, Zhang YM, Li L (1996) Monitoring of weld joint penetration based on weld pool geometrical appearance. Welding Research Supplement 317-s, University of Kentucky, Lexington, KY
30. Li J, Li H, Wei H, Gao Y (2016) Effect of torch position and angle on welding quality and welding process stability in pulse on pulse MIG welding–brazing of aluminum alloy to stainless steel. Int J Adv Manuf Technol 84:705–716
31. Pires JN, Loureiro A, Bölmsjo G (2006) Welding robots: technology, systems issues and applications. Springer-Verlag, London Limited, p74
32. Kah P, Shrestha M, Martikainen J (2015) Robotic arc welding sensors and programming in industrial applications. Mater Eng 10:13
33. Bolmsjö G, Olsson M (2005) Sensors in robotic arc welding to support small series production. Ind Robot Int J 32(4):341–345
34. Kim I-S, Son J-S, Lee S-H, Yarlagadda PKDV (2004) Optimal design of neural networks for control in robotic arc welding. Robot Comput Integr Manuf 20(1):57–63
35. Chan B, Pacey J, Bibby M (1999) Modelling gas metal arc weld geometry using artificial neural network technology. Can Metall Q 38(1):43–51
36. Sreeraj P, Kannan T (2012) Modelling and prediction of stainless steel clad bead geometry deposited by GMAW using regression and artificial neural network models. Adv Mech Eng. doi:10.1155/2012/237379
37. Mvola B (2016) Adaptive gas metal arc welding control and optimization of welding parameters output: influence of welded joints. Int Rev Mech Eng 20:67–72
38. S-R JJ (1993) ANFIS: adaptive network-based fuzzy inference systems. IEEE Trans Syst Man Cybern 23:665–685
39. Negnevitsky M (2002) Artificial intelligence: a guide to intelligent systems. Addison-Wesley, Pearson Education Limited
40. Yadav N, Yadav A, Kumar M (2015) An introduction to neural network methods for different equations. Springer Briefs in Applied Sciences and Technology. Computational Intelligence. Springer Science + Business Media B.V, Dordrecht
41. Al-Faruk A, Md AH, Ahmed N, Kumar Das U (2010) Prediction of weld bead geometry and penetration in electric arc welding using artificial neural networks. Int J Mech Mechatron Eng 10:19–24
42. Juang SC, Tarng YS, Lii HR (1998) A comparison between the back-propagation and counter-propagation networks in the modeling of TIG welding process. J Mater Process Technol 75:54–62
43. Gyasi EA, Kah P (2016) Structural integrity analysis of the usability of high strength steels. Rev Adv Mater Sci 46:39–52
44. Fuller R (2000) Introduction to neuro-fuzzy systems: advances in soft computing. Physica-Verlag, New York, Heidelberg

Publication III

Gyasi, E.A., Kah, P., Ratava, J., Kesse, M.A. and Hiltunen, E.
Study of adaptive automated GMAW process for full penetration fillet welds in offshore steel structures

Reprinted with permission from
International Society of Offshore and Polar Engineers (ISOPE)
pp. 290-297, 2017

Proceedings of the Twenty-seventh (2017) International Ocean and Polar Engineering Conference **www.isope.org**
San Francisco, CA, USA, June 25-30, 2017

ISBN 978-1-880653-97-5; ISSN 1098-6189

Study of Adaptive Automated GMAW Process for Full Penetration Fillet Welds in Offshore Steel Structures

Emmanuel Afrane Gyasi, Paul Kah, Juho Ratava, Martin Appiah Kesse and Esa Hiltunen
Lappeenranta University of Technology (LUT), School of Energy Systems, Laboratory of Welding Technology
Lappeenranta, Finland

ABSTRACT

Offshore steel structures are prone to disasters as a result of failures of welded joints due to fatigue, lack of load bearing capacity and, stability. As fillet-welded joints are susceptible to these major causes of failure, the manufacturing industries, such as offshore manufacturing companies are compelled to adopt techniques to guarantee full penetration in fillet-welded joints in steel structures for offshore applications. This paper presents the possibilities of achieving full penetration fillet welds through an adaptive automated GMAW process. It discusses a case study of a UHSS S960QC material welded by adaptive robotic GMAW with varying welding parameters and variables. In the welding experiment, an adaptive system, which comprises a thermo-profile scanner, was used to measure thermal profiles from the hot surface of the solidifying and still glowing weld bead during the welding process. Optical microscopy and a weld bead gauge were further used for metallurgical and mechanical characterizations of the various weld specimens after etching. The analyzed results of thermographic and macrostructural images show full penetration fillet welds in some of the specimens. Defects, such as lack of penetration, undercut and a large heat affected zone were noted. The results imply that with adaptive welding systems, where thermo-profile scanners using infrared thermography are employed, full penetration fillet welds can be predicted through thermal profile cycle outputs. As thermo-profile scanning serves as a technique for weld quality assurance, utilizing adaptive welding systems with the GMAW process seems to be beneficial in offshore steel structural construction since it provides the possibilities of achieving fillet welds of high quality in full penetration scenarios.

KEY WORDS: Adaptive Automated GMAW Welding, Thermo-Profile Scanner, Offshore Structures, Ultra High-Strength Steel, Weld Quality.

INTRODUCTION

Fillet welds are used in a wide range of structural joints due to geometry and fabrication reasons such as ease of welding. However, operating conditions prevalent in offshore pose challenges to the structural integrity of fillet-welded components, especially in situations where the fatigue phenomenon is likely to occur. In such cases, fatigue cracks can be initiated and grow not only from the weld toe to the base material, but, also from the weld root through the fillet weld or into the section under welding (Fricke 2003). It is noted that fatigue failure occurs in an area where stress concentration is higher than the average stress in the surrounding regions. As fillet weld happens to generate additional local stress concentrations in the weld root, this further means that for welds not fully penetrating the material, cracks may grow from the weld root in addition to the weld toe (Fricke et al. 2006; Kainuma et al. 2008). Fig. 1 shows a typical case of a fillet-welded joint with possible failure susceptibility regions.

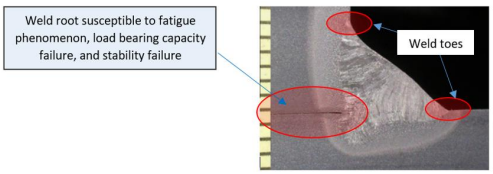

Fig. 1. Transverse view of a fillet-weld showing longitudinal throat thickness and possible failure susceptibility regions.

The weld root in Fig. 1 depicts high susceptibilities to fatigue, load bearing capacity failure, and stability failure. In addition, the weld toes are likely to be subjected to geometry failures, which arise from crack initiation and the softening or embrittlement of the heat affected zone (HAZ). The less reliable test results at the weld root compared to the weld toes also pose a challenge, as weld quality cannot be guaranteed (DNV 2012). For these failure reasons, the manufacturing industries like offshore manufacturing companies are compelled to adopt techniques to guarantee full penetration in fillet-welded joints in steel structures for offshore applications in conformance with EN ISO 5817 weld quality standard. Fatigue life calculations such as normal stress, structural hot spot stress, and effective notch stress, have been used during welding design phases to decrease the possibility of failures that arise from the weld root and weld toe in fillet weld joint in offshore structures (Rajad 1996; IIW 2008).

Apart from fatigue life calculation interventions, however, the new era of digitalized welding systems is becoming popular as a possible technique for weld quality assurance. Incorporated into automated robotic and artificial intelligent systems, monitoring systems with thermo-profile scanning using infrared thermography could be adopted as a method to predict the integrity of welded structures. Researchers have discussed on-line process monitoring to improve the structural integrity of welded steels (Gyasi, EA and Kah, P 2016) and some have used infrared thermography experimentally for weld penetration monitoring (Venkatraman, B et al. 2006; Chokkalingham, S et al 2010).

Similarly, in the field of non-destructive testing, thermo-profile scanning using infrared thermography is utilized as a temperature/heat transfer detector for thermo-graphic image interpretations (Meola et al. 2002; Ibarra-Castanedo, C et al. 2013; ASTM International). Thermo-profile scanning using infrared thermography could therefore, serve as a promising alternative predicting tool for fillet-welded joints in full penetration scenarios for quality and productivity assurance. The schemata in Fig. 2. illustrates thermo-profile scanning in a digitalized welding system framework for weld quality assurance.

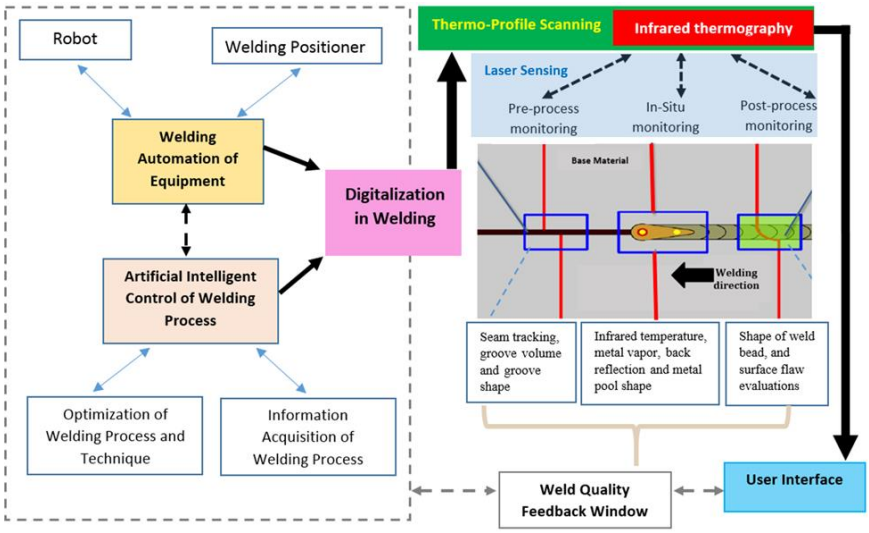

Fig. 2. Thermo-profile scanning in a digitalized welding framework.

In a digitalized welding framework, thermo-profile scanning can identify and monitor the on-line thermal profiles of welding processes. In situations where laser sensors are employed, on-line welding methods such as pre-process monitoring, in situ monitoring and post-process monitoring, can be applied. Considering optimized process feedback situations, artificial intelligent systems coupled with automated welding systems could be integrated into a user interface platform as an approach to fully monitor and control welding process parameters for flawless welds.

The purpose of this study is to investigate the possibilities of achieving full penetration fillet welds with the adaptive automated robotic gas metal arc welding (GMAW) process based on thermo-profile scanning using infrared thermography. This paper presents an experiment on ultra high-strength steel (UHSS) S960QC welded with adaptive automated robotic GMAW by varying the welding parameters and variables. In the experiment, an adaptive system, which comprises a thermo-profile scanner, is attached and positioned at a distance of 30 mm behind the welding torch to measure electromagnetic emissions in near infrared band (NIR) as thermal profiles from the hot weld surface of the weld bead during the welding process. The welded specimens were etched with a 4% nital solution to delineate the macrostructural features of the welds and the HAZs of the specimen. Optical microscopy and a weld bead gauge were used for metallurgical and mechanical analysis of the various weld specimens. The measured thermo-profile data were imported into MATLAB for further analysis. The effects, taking into account the temperature cycles from the heat input, contact tip-to-work distance, and torch angle are further analyzed based on thermographic and macrostructural images.

EXPERIMENTAL PROCEDURE

Welding Apparatus

The welding apparatus consists of an adaptive GMAW process installed around an ABB industrial robot, featuring: a robot controller (ABB IRC5 M2004), robot manipulator (ABB IRB-A1600), power supply with network connections (Fronius Trans Puls Synergic 5000), a wire feeder (Fronius), welding torch (Dinse DIX METZ 542), collision sensor (Dinse DIX SAS 100), positioner (NewFiro 800 HHT), torch cleaning and calibration station (ABB TSC), two laser sensors (Meta SLS 50 V1 with Meta Smart Laser Pilot system), an HKS-Prozesstechnik Thermo-Profile Scanner and WeldQAS monitoring system, a process sensor with current/voltage measurement (HKS-

Prozesstechnik P1000), gas sensor (HKS-Prozesstechnik GM30L 10B), wire feed sensor (HKS-Prozesstechnik DV 25 ST), master computer with ABB RobotStudio, meta laser tools, an SQL-server, and a custom-made real-time welding parameter adjustment program. The process monitoring system coupled with the thermo-profile scanner receives and records the current, voltage, gas flow, wire feed, and temperature, and thermal profile data are incorporated in the entire adaptive system.

Material Characteristics and Preparation

The as-received plates of UHSS Optim 960 QC were machined to the dimensions of 350×100×5 mm (ISO 10051) for 10 samples. V-grooves were prepared on 5 samples at an angle of 60° with a zero air gap and root-face in fillet joint configuration as illustrated in Fig. 3. The chemical compositions of the base and filler metals are presented in Table 1. On welding consumables, the solid wire electrode used in the experiment conforms to EN 12534 (ISO 16834:2012) standard and matches with the chemical and mechanical properties of the base material. The shielding gas conforms to EN 439: M21 standard. Table 2 shows the consumables used in the experiment.

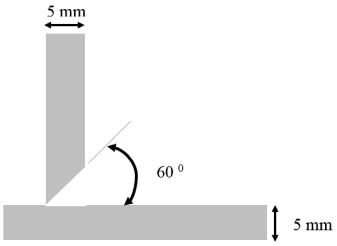

Fig. 3. A 60 ° fillet joint configuration for full penetration weld setup used in the experiments.

Table 1. Chemical composition (wt.%) of the base material UHSS S960QC and filler

Items	C	Si	Mn	P	S	Al	Nb	Cu	Cr	Mo	Ni	Other
S 960 QC (t: 5 mm) (Ceq: 0.46)	0.09	0.21	1.05	0.01	0.004	0.030	0.003	0.025	0.82	0.158	0.04	0.008 (V) 0.032 (Ti) 0.0021 (B)

Table 2. Welding consumables composition

Filler metal	Union X 96 solid wire electrode (1.00 mm in diameter)	Chemical composition (wt.%)					
		C	Si	Mn	Cr	Mo	Ni
		0.12	0.80	1.90	0.45	0.55	2.35
Shielding gas for GMAW process	92% Ar + 8% CO_2						
Shielding gas for thermos-profile scanner	88% Ar + 12% CO_2						

Welding Procedure

The welding of the prepared specimen was performed sequentially. Each specimen was mounted on a positioner, clamped and robotic welded at an interval of 10 mm. This means that each specimen had 2 weld beads of length of about 120 mm. The variables observed were heat input; contact tip-to-work distance (CTWD); and torch angle, and the respective parameters used were current, voltage, welding speed, gas flow rate; electrode stick-out, arc length, wire diameter; and torch position (work angle), torch travel angle, and torch movement technique. Welding parametric values pertaining to welding speed and arc length were maintained in the experiment to ease evaluations, comparisons, and interpretation of data. It must be noted that, each welding sequence was programmed differently per the welding parameters indicated in Table 3.

An adaptive system which comprises a thermo-profile scanner attached and positioned at a distance of 30 mm behind the welding torch was used to measure and record thermal profiles from the solidified but still glowing hot surface of the weld bead during the welding process.

Metallurgical and Mechanical Characterization of Weldments

After visual investigations, only 9 weld beads were selected for metallurgical and mechanical characterization, since they represented the preferred weld quality cases for investigation. Metallography specimens were rough-grinded with SiC foil number 120 for 4 minutes and fine-grinded with 9 µm diamond paste by an MD-Allegro Struers machine for 4 minutes.

Table 3. Welding variables and parameters for the experiment include: arc current (I), arc voltage (U), and welding speed (v).

	Welding variables and parameters										
Specimen	*Heat Input*				*Contact tip-to-work distance (CTWD)*				*Torch angle*		
	I (**A**)	U (**V**)	v (***mm/sec***)	Gas flow rate ***l/mm***	Electrode stick out ***mm***	Arc length ***mm***	Wire feed rate ***m/min***	Wire diameter ***mm***	Torch position (^{0})	Torch travel angle (^{0})	Torch movement technique
1	210.7	20.3	7	17	20	1	9	1	45	15	Pushing
2	236.4	24.3	7	17	20	1	10	1	50	15	Pushing
3	289.6	28.4	7	17	20	1	11	1	30	5	Pushing
4	245.7	28	7	17	18	1	11	1	45	0	Pushing
5	263.2	28.5	7	17	18	1	11	1	45	0	Pushing
6	269.6	25.6	7	17	15	1	11.5	1	35	0	Pulling
7	268.7	25.7	7	17	15	1	12	1	35	5	Pulling
8	269.4	27	7	17	15	1	11	1	35	0	Pushing
9	260.4	28.2	7	17	20	1	11	1	45	0	Pushing

The specimens were finally polished with 3 µm diamond paste by the Tegra Force-5 machine for 5 minutes. The specimens were rinsed under running tap water and cleansed with ethanol solution to prevent water molecules from corroding the specimens.

A 4% nital solution (95 ml C_2H_5OH + 5 ml HNO_3) was used for etching the specimen for 15 s, in compliance with EN ISO 17639 standard for microscopic examination of welds and ISO/TR 16060 for etchants. Optical microscopy (also called light microscopy) was used to delineate the macrostructural features of the welds and HAZs of the specimen. With the aid of a weld bead gauge (caliper), the throat thickness of the specimens were also measured.

RESULTS

Macrostructure of Weldment

An optical microscopy and visual analysis of the macrostructures of the specimens is presented in Fig. 4. For specimen 1, defects detected include lack of penetration and lack of fusion at the weld root. The HAZ's, as observed are narrower in comparison to other specimens. The throat thickness is undersized (< 4 mm) due to irregular weld bead from the weld toes. In specimen 2, lack of penetration and fusion at the weld root, and wide HAZ's are the major defects. Throat thickness matches with the required size (≥ 4 mm) due to regular weld bead formation at the weld toes. In specimen 3, lack of fusion at the weld root, undercut and wide HAZ's are the major defects. Although a regular weld bead at the weld toes was obtained, the throat thickness was quite below the required size (< 4mm). Similar effects were obtained and observed for specimens 4 and 5. With specimens 6 and 7, full penetration fillet welds were achieved, despite wide HAZ's were observed in both specimens. Throat thicknesses matched with the required size (≥ 4 mm) due to regular weld bead formation at the weld toes. Besides, quite a bit of over-penetration was obtained in specimen 6. For specimen 8, although full penetration fillet weld was achieved, an undercut defect was observed in addition to wide HAZ's. Throat thickness was quite below the required size (< 4mm) despite an even weld bead formation at the weld toes. Specimen 9 showed similar defects as specimens 4 and 5.

Thermal Profile Distribution

The infrared thermography produced a large amount of weld and seam data as feedback signals from the thermal profile scanner. The measured thermo-profile data, imported into MATLAB for further analysis, have been represented as thermal distribution signal graphs. The graphs of specimens 1, 3, 7 and 8 illustrated in Figures 5, 6, 7, 8, 9, and 10, are discussed in this section since they represent the most likely scenarios for investigation. The thermo-profile scanner identified and recorded parameters, such as time, current, voltage, gas flow, wire feed speed, infrared (IR) difference, IR position, IR temperature, IR width, IR symmetry and temperature. As IR temperatures correlate and depend on heat input values, the relation between arc current, voltage, the wire feed rate and welding speed parameters accounts for the minimum and maximum IR temperatures. Although the thermo-profile window was 1350 ^{o}C, in the experiment the maximum IR temperature was set at 1200 ^{o}C because of the UHSS material under investigation which requires a heat input of 0.4 - 0.5 KJ/mm (Hemmila, M et al. 2010; Bjork, T et al. 2015). For specimens 1, 3, 7 and 8, the IR temperatures, the most important signal indicator of the heat input were recorded at 785 ^{o}C, 1162 ^{o}C, 1129 ^{o}C and 1252 ^{o}C respectively.

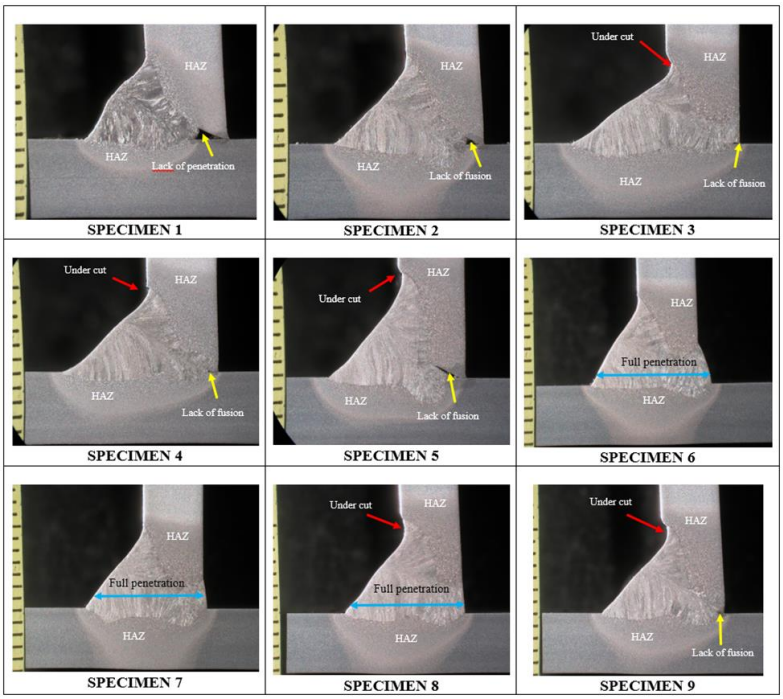

Fig. 4. Full penetration fillet weld with test specimens showing a transverse view of macro-sections, possible defects and longitudinal throat thickness with the aid of optical microscopy.

Analysis of Thermo-Profile Signals per Process Parameters

Specimen 1

The thermal profile at a temperature of 785 ^{o}C produced a blank thermographic image of the weld bead. This is due to the heat input (0.48KJ/mm) supplied, with low heat energy reaching the minimum IR temperature. With the IR temperature/IR width graph, the IR width signal, which depicts the depth of weld penetration, was virtually zero. These observations were in agreement with the optical macroscopic image obtained for specimen 1 in Fig. 4, which showed a lack of weld penetration and incomplete fusion. Arc current, as a factor of the heat input was not adequate enough to produce acceptable weld penetration. The synergic effect of both the arc voltage and current also produced shallow weld penetration. It has been said that the depth of penetration or joint penetration, and the weld deposition rate are significantly influenced by the arc current, hence the depth of penetration increases with an increase in the arc current (Nagesh, DS and Datta, GL 2002). On the other hand, electrode stick-out, the wire feed rate, welding speed, torch angle and the torch movement technique were contributing factors for inadequate weld penetration, especially where the torch angle was set at 45^{o} and a leading travel angle was employed (refer to Table 3).

Technically, the trailing travel angle (pulling welding) provides maximum penetration, and narrow and convex weld beads, whereas the leading travel angle (pushing welding) provides flatter bead profile and adequate weld pool protection (Olson, DL et al. 1993; Cornu, J 1988).

Specimen 3

In Fig. 5, it can be seen that the thermal profile climbed to an appreciable temperature of 1162 ^{o}C, indicating that the heat input (0.94 KJ/mm) supplied was adequate. The thermographic image of the weld bead produced gives a clue of possible weld defects as shown in the thermal profile pixels. Moreover, from the IR temperature/IR width graph in Fig. 6, it can be noted that the IR width signal, which depicts the depth of weld penetration, is above the IR temperature curve with excessive perturbation. The relationship between Fig. 5, Fig. 6, and the optical macroscopic image obtained for specimen 3, as depicted in Fig. 4, agrees with the defect of incomplete fusion and undercut of the weld. In addition to this, factors such as electrode stick-out, the wire feed rate, welding speed, and most of all the torch angle position and the torch movement technique (pushing) could also contribute to the observations noted.

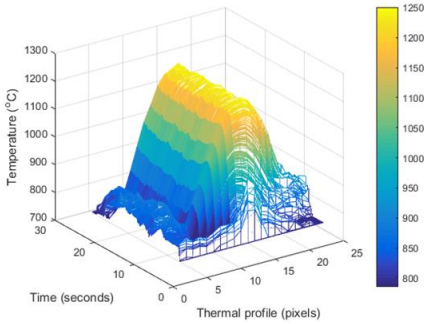

Fig. 5. Thermal profile distribution signals for specimen 3.

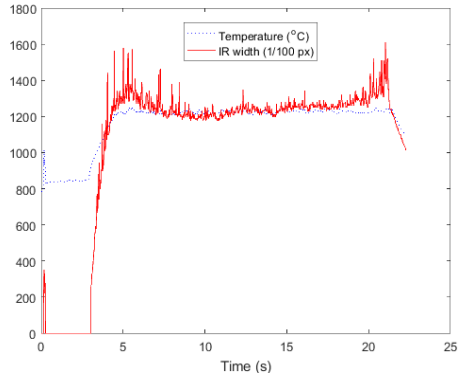

Fig. 6. Weld penetration versus IR temperature for specimen 3.

Specimen 7

Fig. 7 shows that the thermal profile at a temperature of 1129 °C closely agrees with the pre-set IR temperature due to the adequacy of the heat input (0.79 KJ/mm) supplied. The thermographic image of the weld bead produced gives an indication of a smooth thermal profile distribution with no major defect as shown in the thermal profile pixels. Also, from the IR temperature/IR width graph in Fig. 8, it can be noted agrees well with the IR temperature curve. The relationship between Fig. 7, Fig. 8, and the optical macroscopic image obtained for specimen 7, as shown in Fig. 4, confirms the full weld penetration obtained. Other contributing factors such as electrode stick-out, the wire feed rate, and welding speed were set right, especially, the torch position at 35° and the trailing travel angle at 5° (pulling welding), which provided maximum full weld penetration.

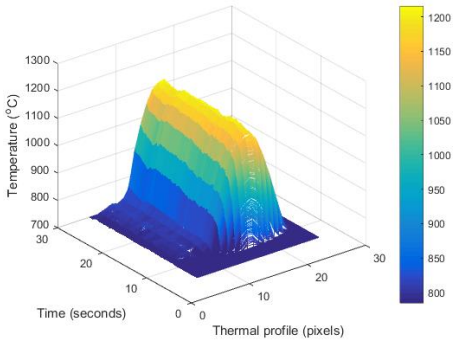

Fig. 7. Thermal profile distribution signals for specimen 7.

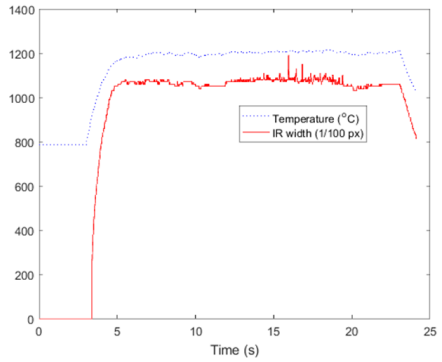

Fig. 8. Weld penetration versus IR temperature for specimen 7.

Specimen 8

In Fig. 9, it can be seen that the thermal profile at a temperature of 1252 °C was above the maximum pre-set IR temperature, although the heat input (0.83 KJ/mm) supplied was quite good. The thermographic image of the weld bead produced indicates a clipping effect at the peak of the profile and also shows possible weld defects in the thermal profile pixels. Therefore, when the maximum measurement temperature of the equipment was exceeded, in the case of any splashes, the IR width of the weld exceeded the measurement width of the thermo-profile scanner. In the IR width graph in Fig. 10, these sections have been replaced with a linear interpolation between the closest known successful measurements, clearly seen as straight line segments. It can also be noted that the IR width signal is above the IR temperature curve with excessive perturbation due to feedback signal fluctuations from the thermal profile. The relationship between Fig. 9, Fig. 10, and the optical macroscopic image obtained for specimen 8, as depicted in Fig. 4, agrees with the defect of weld undercut.

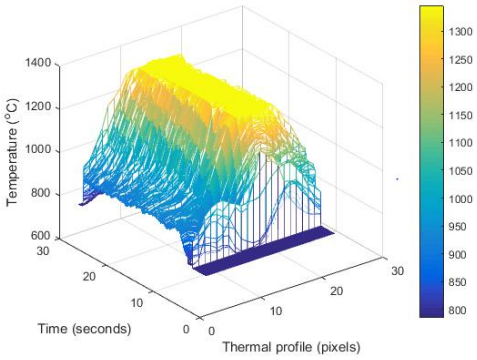

Fig. 9. Thermal profile distribution signals for specimen 8.

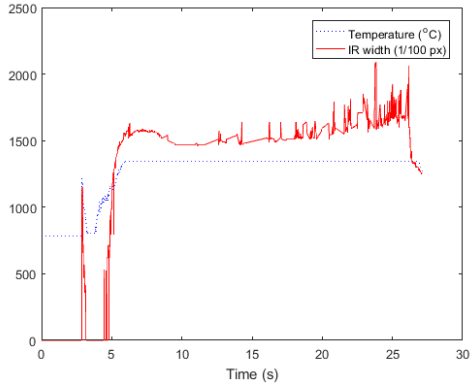

Fig. 10. Weld penetration versus IR temperature for specimen 8.

DISCUSSION

Full penetration weld configuration can be one of the geometric designs when considering possibilities to assure weld quality in fillet-welded joints of steel structures. For offshore fillet-welded structures, full penetration fillet-weld could serve as a possible remedy to prevent or minimize load bearing capacity and stability problems, and fatigue failure especially in situations where the fatigue phenomenon is likely to occur. Although most fillet-welded joint evaluations are based on fatigue life assessment through finite element analysis, the alternative to harness thermo-profile scanning using infrared thermography provides real-time possibilities for quality assessment and results. With its digital capabilities, thermo-profile scanning using infrared thermography has been extensively employed in welding.

Venkatraman, B et al. (2006) used infrared thermography for weld bead monitoring techniques through on-line detection of incomplete penetration. A thermal imaging sensor for detection of defects, such as lack of penetration, and estimation of depth of penetration during tungsten inert gas (TIG) welding was used in the experiment. It was claimed that the infrared thermography technique can detect any lack of penetration and depth of penetration on-line and further establish a linear relationship between the surface thermal profile and depth of penetration. Chandrasekhar, N et al. (2015) also used infrared thermography to estimate the bead width and depth of penetration in an artificial neural network (ANN) modeling of adaptive tungsten inert gas welding (A-TIG) process. In the ANN modeling process, image features extracted from the infrared thermal images together with A-TIG process parameters were used. It was established that all the ANN models predicted for the weld bead and depth of penetration were accurate and correlated with the measured weld bead and depth of penetration as depicted in the infrared thermal images.

The capabilities of the infrared thermography method through thermo-profile scanning cannot be under-estimated, practically due to its adaptability with intelligent automated welding systems where robots are utilized. In this study, full penetration fillet-welded joints of UHSS S960QC have been achieved by the aid of automated robotic GMAW with thermo-profile scanning using the adaptive features of infrared thermography. Observations, particularly from the peak temperature and weld penetration width curves, which were monitored and captured through infrared thermography, have created avenues for weld quality assessment. It has become evident that the depth of weld penetration and the area under the temperature distribution curves either depend on the heat input or correspond to it. As the gap between the peak temperature curve and the weld penetration width curve widens, and the area below these two curves decreases, it is an indication of a low heat input with possible welding flaws, like a lack of penetration or insufficient fusion. Similarly, an excessive perturbation of peak temperature and weld penetration width curves indicates the likelihood of high a heat input with possible welding flaws like under-cut. Menaka, M et al. (2005) estimated that as the depth of penetration increases, the weld width and area under the temperature distribution curve also increase, when the peak temperature is attained. The metallographic images obtained from both optical microscopy and visual weld bead gauge (caliper) measurements corroborate these observations.

The effects of welding temperature variations and other variables and parameters on the microstructure of UHSS under study were not investigated in this work. However, due to the susceptibility of UHSS to elevated temperatures, the effects of temperature variations on the weldment of UHSS S960QC need further studies. UHSS S960QC has a superior strength-to-weight ratio, as well as excellent physical, mechanical, and low-temperature properties, which enable influencing lower fuel consumption and lower carbon emissions (Hemmila, M et al. 2010; Bjork, T et al. 2015; Kah, P et al. 2014; Laitinen, R et al. 2013) in comparison with conventional steels. The manufacturing industries that produce mobile offshore structures, such as offshore platforms, floating production, storage and offloading (FPSO) units, mooring vessels and crane vessels for lifting purposes, stand to benefit from the use of UHSS.

CONCLUSIONS

A new study on full weld penetration in fillet-welded joints in steel structures, possibly for offshore structural applications, has been presented in this research paper. The novelty of this work has been realized by incorporating thermo-profile scanning using infrared thermography with automated robotic systems in the experimental process. Analytical predictions and observations based on infrared thermal distribution curves and metallographic images clearly show some correlation and linear effects of GMAW process parameters and

variables, such as heat input, contact tip-to- work distance, and torch angle, on full weld penetration in fillet-welded joints. The effects are seen from the magnitude of the temperature curves, the depth of weld penetration, and the area under the temperature distribution curves.

As the depth of weld penetration and the area under the temperature distribution curves correspond to the amount of heat input supplied, a further study to optimize the process parameters could be done through feedback controls. In addition, the effects of welding temperature variations and other variables and parameters on the microstructure of the UHSS material under study could be investigated. These aspects are relevant when considering the effects of welding temperature variations and other parameters on the microstructure of UHSS S960QC for offshore structural use.

Finally, in the context of digitalized welding, the ease of monitoring, capturing, predicting and detecting weld defects, such as lack of weld penetration, through thermal profile imaging as presented in this study, means great potential for weld quality assurance. Thermo-profile scanner using infrared thermography could therefore serve as a promising alternative predicting tool for fillet-welded joints in full penetration scenarios for quality and productivity assurance.

ACKNOWLEDGEMENT

This work was completed at the Laboratory of Welding Technology, Lappeenranta University of Technology. The authors would like to express their gratitude to Antti Kakkonen and Sakari Penttila for the experiment setup. Special thanks to Antti Heikkinen for his assistance in conducting the optical microscopy analysis and to Jukka Martikainen for his support.

REFERENCES

ASTM International. "Standard Practice for Infrared Flash Thermography of Composite Panels and Repair Patches used in Aerospace Applications," ASTM E2582-07.

Björk T, Toivonen J, Nykänen T (2015). "Capacity of Fillet Welded Joints made of Ultra-High Strength Steel," Doc IIW-2210, Recommended for Publication by Commission XV Design, Analysis and Fabrication of Welded Structures. Springer, 71-84.

Chandrasekhar, N, Vasudevan, M, Bhaduri, AK, Jayakumar, T (2015). "Intelligent Modeling for Estimating Weld Bead Width and Depth of Penetration from Infra-red Thermal Images of the Weld Pool," *Journal of Intelligent Manufacturing*, 26(1), 59-71.

Chokkalingham, S, Chandrasekhar, N and Vasudevan, MK (2010). "Artificial Neural Network Modeling for Estimating the Depth of Penetration and Weld Bead Width from the Infrared Thermal Image of the Weld Pool during A-TIG Welding," Springer-Verlad Berlin Heidelberg, LNCS 6457, 270-278.

Cornu, J (1988). Advanced Welding Systems. Welding Automation, Consumable Electrode Processes. IFS Publications Ltd, UK. 2, 301.

DNV-RP-C203 (2012). "Fatigue Design of Offshore Steel Structures," Det Norske Veritas AS.

Finnish Standards Association (2014). "Welding - Fusion-Welded Joints in Steel, Nickel, Titanium and their Alloys (Beam Welding Excluded)," Quality Levels for Imperfections (ISO 5817:2014).

Finnish Standards Association (2012). Welding Consumables – Wire Electrodes, Wires, Rods and Deposits for Gas Shielded Arc Welding of High Strength Steels – Classification (ISO 16834:2012).

Finnish Standards Association (2010). Continuously Hot-Rolled Strip and Plate/Sheet cut from Wide Strip of Non-Alloy and Alloy Steels - Tolerances on Dimensions and Shape (EN-10051:2010).

Finnish Standards Association. (2013). Destructive Tests on Welds in Metallic Materials - Macroscopic and Microscopic Examination of Welds (ISO 17639:2003).

Finnish Standards Association (2003). Destructive Tests on Welds in Metallic Materials - Etchants for Macroscopic and Microscopic Examination (ISO/TR 16060:2003).

Fricke, Wolfgang (2003). "Fatigue Analysis of Welded Joints: State of Development," *Marine structures*, 16(3), 185-200.

Fricke, W, and Doerk, O (2006). "Simplified Approach of Fatigue Strength Assessment of Fillet-Welded Attachment Ends," *International Journal of Fatigue*, 28,141-150.

Gyasi, EA and Kah, P (2016). "Structural Integrity Analysis on the Usability of High Strength Steels", *Rev. Adv. Mater. Sci.*, 46, 39-52.

Hemmilä, M, Laitinen R, Liimatainen, T, Porter D (2010). "Mechanical and Technological Properties of Ultra-High Strength Optim Steels," Rautaruukki Oyj, Ruukki Production, Finland: Ruukki-Technical Article-Mechanical-and-Technological Properties- of-Ultra-High-Strength-Optim-Steels.pdf. http://www.oxycoupage.com/FichiersPDF/Ruukki_Pdf/English/. Accessed 20 April 2016.

Ibarra-Castanedo, C, Tarpani JR, Maldague XP (2013). "Non-Destructive Testing with Infrared Thermography," *Eur J Phys*, 34, 91–109.

International Institute of Welding (2008). "Recommendations for Fatigue Design of Welded Joints and Components," doc XIII-1539-96 / XV845-96, Paris, France.

Kah, P, Pirinen, M, Suoranta, R, Martikainen J (2014). "Welding of Ultra High Strength Steels," *Advanced Materials Research*, 849, 357-365.

Kainuma, S, and Mori, T (2008). "A Study on Fatigue Crack Initiation Point of Load Carrying Fillet Welded Cruciform Joints," *International Journal of Fatigue*, 30(9), 1669-1677.

Laitinen, R, Valkonen, I, Kömi J (2013). "Influence of the Base Material Strength and Edge Preparation on the Fatigue Strength of the Structures made by High and Ultra-High Strength Steels," *5th Fatigue Design Conference, Fatigue Design. Science Direct, Procedia Engineering*, 66, 282 – 291.

Menaka, M, Vasudevan, M, Venkatraman, B and Baldev R (2005). "Estimating Bead Width and Depth of Penetration During Welding by Infrared Thermal Imaging," *Insight*, 47(9), 564-568.

Meola, C, Boccardi, S, Carlomagno, GM, Boffa, ND, Ricci, F, Simeoli, G, Russo, P (2017). "Impact Damaging of Composites Through Online Monitoring and Non-Destructive Evaluation with Infrared Thermography," NDT&E International, Elsevier, 85, 34–42.

Nagesh, DS, Datta GL (2002). "Prediction of Weld Bead Geometry and Penetration in Shielded Metal Arc Welding using Artificial Neural Networks," *Journal of Materials Processing Technology*, 123, 303-312.

Olson, D L, Siewert, TA, Liu, S and Edwards, G R (1993). "Welding, Brazing and Soldering ASM Handbook,"ASM International, 10th edition, 6, 2872.

Radaj, D (1996). "Review of Fatigue Strength Assessment of Non-welded and Welded Structures Based on Local Parameters," *International Journal of Fatigue*, 18(3), 153-170.

Venkatraman, B, Menaka, M, Vasudevan, M, Raj, B, (2006). "Thermography for Online Detection of Incomplete Penetration and Penetration Depth Estimation," In: *Asia-Pacific Conference on NDT*, 5th–10th November, Auckland, New Zealand.

Publication IV

Gyasi, E.A., Kah, P., Handroos, H., Layus, P. and Lin, S.
Adaptive welding of S960QC UHSS for Arctic structural applications

Reprinted with permission from
International Review of Mechanical Engineering (I.RE.M.E)
Vol. 12, No. 4, 2018

Adaptive Welding of S960QC UHSS for Arctic Structural Applications

Emmanuel Afrane Gyasi[1], Paul Kah[2], Heikki Handroos[3], Pavel Layus[4], Sanbao Lin[5]

Abstract – *The construction of welded structures capable of withstanding the harsh operating conditions found in the Arctic region is essential for effective exploitation of the area. This paper examines the usability of S960QC UHSS as potential weldable material for lightweight Arctic structural constructions. The paper concurrently explores the applicability of an adaptive robotic GMAW process in welding the UHSS material. The adaptive welding system featured an infrared thermo-profile scanner. S960QC UHSS was welded in two different fillet joint orientations employing PA and PB welding positions. Using the adaptive welding system, the behavior of welding parameters such as current, voltage and heat input and their effect on the temperature of the weld seam were monitored in relation to the metallurgical properties of the welds. It was observed that the orientation of the joint geometry influences weld penetration and the shape of the weld. Metallurgical tests performed across the weld metal revealed that, using heat inputs between 0.5–0.65 kJ/mm, weld hardness between 375–397 HV5 can be achieved. The hardness values together with impact strength of 33–50 J at an operating temperature of -40 °C demonstrate material properties suitable for Arctic structural applications where excellent strength-to-weight ratio and high load carrying capacity are required. The paper contributes to the field of lightweight steel construction and digitization in welding where adaptive intelligent systems are harnessed in sensing, monitoring, predicting and modelling of the welding process for weld quality control and assurance purposes.*

Keywords: *Adaptive Welding, Arctic Welded Structures, Heat Inputs, Robotic GMAW Process, Ultra High Strength Steels (UHSS), Weld Hardness*

I. Introduction

The Arctic region is known for its remote, harsh and extremely cold climatic conditions. It is estimated that the Arctic possesses enormous natural resources and holds about 22% of world oil and gas reserves [1]. Other resources such as the strong Arctic wind provide viable opportunities for wind power industries [2]. Moreover, global warming effects, which have resulted in shrinking of Arctic sea ice, provide other opportunities in the region [3]. For example, the gradual opening of the Northern Sea Route (NSR) and the Northern passage offer new transportation routes [4].

Tapping these resources and harnessing the opportunities that they offer demands construction of welded structures capable of withstanding the harsh conditions of the Arctic. This paper examines the usability of S960QC UHSS as weldable material for lightweight Arctic structural constructions. The paper further explores the applicability of an adaptive intelligent robotic GMAW process in welding of the S960QC UHSS material. Experimental work was carried out to determine the effects of varying heat inputs on the hardness properties of the weld metal, weld fusion zones and the HAZs by comparison with the base metal. Additionally, the effects of workpiece orientation on weld penetration and weld shape were determined. The experimental work was also used to evaluate the behavior of welding parameters and variables while using the adaptive intelligent welding system settings. The adaptive welding system included an infrared thermo-profile scanner attached and positioned at a distance of 30 mm behind the welding torch to measure thermal zones from the hot surface of the cooling weld seam during the welding process. The adaptive welding system employs an artificial neural network (ANN) configuration to model the behavior of the welding parameters and variables. Two samples were welded in the ANN environment. The measured thermo-profile data were then imported into MATLAB for further analysis of the behavior of the welding parameters and variables. The welded specimens were etched with a 4% nital solution (95 ml C_2H_5OH + 5 ml HNO_3) to delineate the microstructure of the base metal and, additionally, the macrostructural features of the welds and the HAZs of the specimens. Light microscopy and a Vickers hardness test machine were used for metallurgical and mechanical analysis of the effects of heat inputs on various weld specimens.

The paper contributes to the field of lightweight steel construction for Arctic welded structures by study of utilization of S960QC UHSS and digitization in welding where adaptive intelligent systems that integrate sensors,

Manuscript received March 2018, revised June 2018

monitoring systems and artificial intelligence are used for weld quality control and assurance purposes.

II. Requirements of an Arctic Welded Structure

Typical welded Arctic offshore structures, as illustrated in Fig. 1, are sophisticated assemblies consisting of many sections with different functions [5]. Different sections of the structure usually have different material requirements and experience different environmental conditions. A wide range of materials with different properties are employed in the construction of such structures. The various sections of an Arctic offshore platform can be classified into elements with special requirements, general construction elements and secondary construction elements [6]. The elements with special requirements are responsible for the overall strength of the structure and have to be capable of withstanding heavy loads. Such elements include, for example, waterline construction elements, ice-resistant girders, connection elements of platform body parts, and elements whose cross-section area changes considerably.

The general construction elements are used to provide overall strength to the platform and ensure the safety of operations. These elements include the outer cover plates of body parts, structural frame beams, general deck cover plates and bulkhead covers. The secondary construction elements do not significantly influence operational safety. Materials for the most critical and important parts of Arctic offshore structures require special attention to ensure that they have the necessary strength to be able to withstand rigorous operation conditions [6].

Sections located above the waterline experience extremely low temperatures down to -60°C, a moderately corrosive environment (sea air) and various loads as described in Fig. 1.

These sections have to meet the following criteria [7-9]:

- Low temperature toughness down to -60°C.
- Yield strength requirements up to 690 MPa.
- Isotropy of properties across material dimensions to ensure high strength.
- Resistance to brittle fracture at low operational temperatures.
- Reasonable weldability with minimal preheat and post-heat temperature required to ease the assembly process.
- Moderate corrosion resistance in sea air.
- Ability to withstand static and dynamic wind and wave loads according to the operational parameters.

When considering transportation and installation, weldable steels that have lightweight properties while simultaneously meeting the above-listed requirements are preferable for construction of the upper sections of Arctic structures. Use of lightweight steel brings benefits from not only reduced structural weight and cost in welding manufacturing and production [10] but also improved energy efficiency, which would be beneficial from the environmental point of view. Other structures that could harness the potential of lightweight cold-resistant materials include knuckle-boom cranes, mobile cranes, and Arctic vessels and icebreakers [10].

Currently, industrial Arctic offshore stationary structures and floating drilling units typically use steel plates up to 70 mm thickness, although some elements can be up to 130 mm in thickness. Some icebreakers are built of plates of thicknesses up to 60–70 mm [11]. The use of ultra high strength steels, whose thickness is about 30-50% less than conventional steels for the same strength [12], would make construction of welded Arctic structures more productive and cost efficient without sacrificing weld quality and the integrity of the whole structure.

Fig. 1. A welded Arctic offshore platform showing the various sections and environmental conditions based on data from [5,13]

III. Ultra High Strength Steels

Selection of weldable materials for the Arctic environment has to be rigorous due to the low temperature conditions, which can fall below -60 °C [14]. In addition to the cold temperatures, strong wind speeds of about 5-15 m/s with peaks up to 50 m/s [15] can be encountered, which makes for challenging working conditions. Metals tend to increase in yield strength, hardness and ultimate tensile strength, but lose their ductility in conditions when operating temperatures drop to sub-zero degrees [16,17] and prolonged exposure to the cold climatic conditions of the Arctic has resulted in a number of serious accidents in the region [16]. Advanced structural steels like UHSS must therefore fulfil stringent requirements, such as those listed in the previous section, to be eligible for use in the Arctic region.

To resist brittle fracture, advanced structural steels such as UHSS materials have to demonstrate high impact and fracture toughness at operating and working conditions [18]. Table I shows a typical chemical composition of UHSS. The weldability is moderately good since the carbon equivalent is typically 0.47 minimum and 0.52 maximum [19, 20].

UHSS exists as heat-treated steel, in other words, as hardened steel. The process of direct quenching results in the formation of metastable martensite, a percentage of which is reduced to the desired amount during tempering. UHSS thus possesses a dual-phase microstructure consisting of fine-grained martensitic-bainitic microstructure [19, 20].

Its microstructure, similar to advanced high-strength steels (AHSS), is sensitive to high heat input, and exposure to elevated temperature can change its mechanical properties. Other critical effects of heat input are HAZ softening and an increased propensity to fatigue failure, which has been found to affect the toughness and strength of welded joints of UHSS [21, 22].

Greater susceptibility to fatigue failure occurs because during welding, where the UHSS is exposed to elevated temperatures, the steel composition assumes an annealed state, which leaves a softened zone in the HAZ. This softened zone becomes over-ductile, and hardness reduces considerably.

A typical grade of UHSS like S960QC is suitable for lightweight manufacturing. The steel grade is hot-rolled flat plate made of high yield strength steel for cold forming and delivered under thermomechanical rolled steel conditions.

The mechanical properties of S960QC are: yield strength (900 MPa), ultimate tensile strength (1000 MPa), impact strength of 33–50 J at operating temperature of -40 °C, and elongation of 7%. S960QC satisfies various standards: EN ISO 148-1:2010 (impact strength test); EN ISO 10051 (thickness, width and length); EN 10029 (flatness, Class N, steel type H) and EN ISO 10149-1 (tensile test) [19, 20, 23]. A potential saving from utilizing UHSS in place of conventional steel derives from the difference between the plate thicknesses, for equivalent properties, of 15 mm for S 355 and 4 mm for S 960 UHSS, which is about 73% for thickness and 93% for weld seam volume. Similarly to a 15 mm S 355 plate, a 4 mm S 960 UHSS steel plate is able to withstand a bending moment under static load of 50 kNm [12].

A wide range of consumables for welding UHSS are available. Filler materials of low hydrogen type (weld hydrogen content HD $\leq$ 5 ml/100g) are suitable for welding UHSS. Filler materials having such hydrogen content are produced to meet standards like DIN EN 12534, thereby avoiding hydrogen inclusion in the weld and ensuring low susceptibility to cold cracking. Tensile strength class of minimum 89 (890N/mm^2) is suitable for matched consumables; while tensile strength class of minimum 42 (minimum 420/mm^2) is suitable for under-matched consumables in welding of UHSS. Most importantly, the maximum heat input for plate thickness > 4 mm should be 0.5 kJ/mm and for plate thickness $\leq$ 4 mm should not exceed 0.4 kJ/mm. The cooling time from 800 °C to 500 °C should not exceed 4 s for high-strength matching welds [23]. For high-strength undermatched welds, cooling time from 800 °C to 500 °C for plate thickness of 8 mm should not exceed 10 s [22]. Based on its mechanical properties and chemical composition, UHSS is prone to ductile-brittle transition (DBT), which is a factor to be considered when evaluating welding usability for Arctic conditions. It is reported that at DBT temperature regions, fracture occurs as a combination of both brittle and ductile behavior [24, 25, 26]. This behavior is similar to fracture toughness or impact energy temperature dependency of ferritic steels [24].

TABLE I
CHEMICAL COMPOSITION OF UHSS S960QC, wt.% : CEV = C + Mn/6+ (Cr + Mo + V)/5 + (Ni + Cu)/15; 5 mm THICKNESS

C	Si	Mn	P	S	Al	Nb	Cu	Cr	Mo	Ni	Other
0.09	0.21	1.05	0.01	0.004	0.030	0.003	0.025	0.82	0.158	0.04	0.008 (V) 0.032 (Ti) 0.0021 (B)

Fracture toughness remains almost constant at both lower and upper shelves. In the transition area, fracture often starts as ductile tearing, followed by cleavage fracture. Since there is no exact value for the transition temperature, some studies advise that DBT be defined using the average temperature of both the upper and lower limits, using a temperature that causes the fracture mode to be 50% cleavage, or using a temperature of a specific impact energy such as 20 J [26, 27].

Interactions between ductile collapse and brittle fracture in DBT are important phenomena when considering welded UHSS for Arctic applications. Charpy-V impact tests on four martensitic UHSS specimens with different grain sizes were performed in [28]. The results of the study are shown in Fig. 2. It can be seen that the sample with the smallest grain size had the highest resistance to impact energy, about 200 J, and the slowest ductile-to-brittle transition with respect to low temperatures. Other research [29] also found that UHSS experiences ductile-to-brittle transition, and it was noted that the transition temperature might be as low as -105 °C.

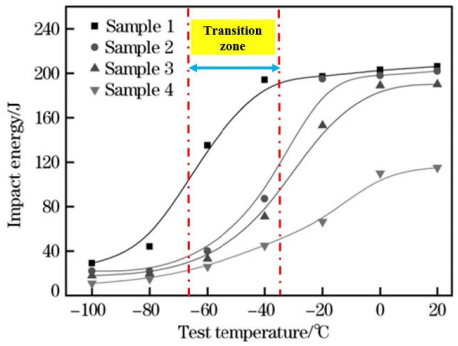

Fig. 2. UHSS impact energy temperature dependency. All samples have different grain sizes; Sample 1 has the smallest and Sample 4 the largest grain size [28]

IV. Experimental Procedure

IV.1. Welding Apparatus

The welding apparatus consists of an adaptive GMAW process integrated with an industrial robot. The main features of the apparatus comprise: a robot controller, robot manipulator, power supply with network connections (Pulse Synergic 5000), a wire feeder, welding torch, collision sensor, positioner, torch cleaning and calibration station, a thermo-profile scanner sensor monitoring system, wire feed sensor, master computer with Robot Studio, an SQL-server, and a custom made real-time welding parameter adjustment program. The process monitoring system coupled with the thermo-profile scanner receives and records the current, voltage, gas flow, wire feed, temperature and thermal profile data. Fig. 3 shows the experimental setup of the GMAW intelligent adaptive welding system.

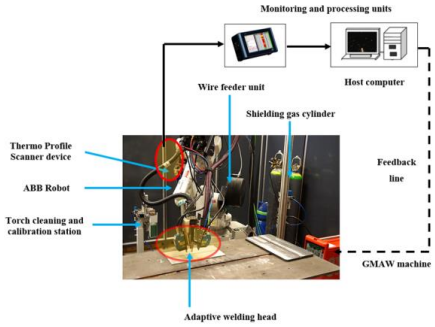

Fig. 3. GMAW adaptive intelligent setup

IV.2. Material Characteristics and Preparation

As-received plates of UHSS Optim 960 QC were machined to the dimensions of 350×100×5 mm (ISO 10051) to produce 20 samples. The preparation of the fillet joint configurations is as illustrated in Fig. 4. For welding, 5 joints each were made to be welded in the PB and PA positions respectively. The composition of the welding consumables used is as given in Table II. The solid wire electrode used in the experiment conforms to EN 12534 (ISO 16834:2012) and matches with the chemical and mechanical properties of the base material. The shielding gas conforms to the EN 439: M21 standard.

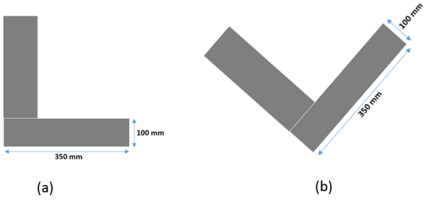

Fig. 4. Fillet weld configurations where a) is the PB welding position and b) the PA welding position

TABLE II
COMPOSITION OF WELDING CONSUMABLES

		Chemical composition (wt. %)					
Filler metal	Union X 96 solid wire electrode (1.00 mm in diameter)	C	Si	Mn	Cr	Mo	Ni
		0.12	0.80	1.90	0.45	0.55	2.35

Shielding gas for GMAW process
92% Ar + 8% CO_2
Shielding gas for thermos-profile scanner
88% Ar + 12% CO_2

IV.3. Welding Procedure

Welding of the prepared samples was performed sequentially. Each welding sequence was programmed differently per the welding parameters indicated in Table III. Each specimen was mounted on a positioner, clamped and welded with the adaptive robotic GMAW process. Welding parametric values pertaining to welding speed, gas flow rate, electrode stick, arc length, wire diameter, torch position and torch travel angle were maintained constant to ease evaluation, comparison and interpretation of data. Key welding parameter values were gas flow rate, 17.7 l/mm; arc length, 1.0 mm; and wire diameter, 1.0 mm. The arc efficiency of the GMAW process used for determination of the heat input values was 0.8. The adaptive GMAW process included a thermo-profile scanner attached and positioned at a distance of 30 mm behind the welding torch, which was used to measure and record thermal heat from the solidified but still glowing hot surface of the weld seam during the welding process. After visual examination, eight (8) samples were presented for analysis.

The adaptive welding system employs an ANN configuration to model the behavior of the welding parameters and variables. Welding parameters for two samples were fed into an already-existing ANN modelled system and the parameters were adjusted by a few welding trails.

The measured thermo-profile data were then imported into the MATLAB environment for further analysis of the behavior of the welding parameters and variables. Two samples, denoted PA ANN and PB ANN, were welded using the ANN modelled system.

IV.4. Metallurgical and Mechanical Characterization

Metallography specimens were rough-ground for 4 minutes with SiC foil number 120 and fine-ground with 9 µm diamond paste for 4 minutes using an MD-Allegro Struers machine. The specimens were finally polished with 3 µm diamond paste for 5 minutes using a Tegra Force-5 machine. The specimens were rinsed under running tap water and cleansed with ethanol solution to prevent water molecules from corroding the specimens.

A 4% nital solution (95 ml C_2H_5OH + 5 ml HNO_3) was used to etch the specimens for 15 s, in compliance with EN ISO 17639 standard for microscopic examination of welds and ISO/TR 16060 for etchants. Light microscopy was used to delineate the microstructure of the base metal and the macrostructure features of the welds and HAZs of the specimen.

TABLE III.
WELDING VARIABLES AND PARAMETERS FOR THE EXPERIMENT INCLUDE: ARC CURRENT (I), ARC VOLTAGE (U), AND WELDING SPEED (v)

Specimen	*Heat Input*			*Contact tip-to-work distance (CTWD)*		*Torch angle*		
	I (**A**)	U (**V**)	v (***mm/sec***)	Electrode stick out ***(mm)***	Wire feed rate ***(m/min)***	Torch position (^{0})	Torch travel angle (^{0})	Torch movement technique
1 (PB ANN)	200.1	22.1	7.0	18.0	9.69	40	5	Pushing
2 (PA ANN)	202.2	22.3	7.0	18.0	9.37	90	0	Pushing
3 (PB 1)	213.6	24.3	7.0	18.0	10.31	40	5	Pushing
4 (PA 1)	232.1	26.2	7.0	18.0	10.27	90	0	Pushing
5 (PB 2)	204.7	26.2	7.0	18.0	8.90	40	5	Pushing
6 (PA 2)	211.7	26.1	7.0	18.0	8.87	90	0	Pushing
7 (PB 3)	195.7	24.6	7.0	18.0	8.90	40	5	Pushing
8 (PA 3)	208.9	24.6	7.0	18.0	8.90	90	0	Pushing

V. Results

V.1. Microstructure of the Base Metal

The microstructure of the base metal S960QC UHSS is illustrated in Fig. 5. The presence of martensite in the crystal lattice is reflected as needlelike microstructure, while the presence of bainite is seen as dark portions in the crystal lattice [30]. Under welding conditions, the basic microstructure can change significantly depending on the heat inputs applied, the type of consumables used, transformation or dislocation of the crystalline structure, and diffusion of the alloying elements.

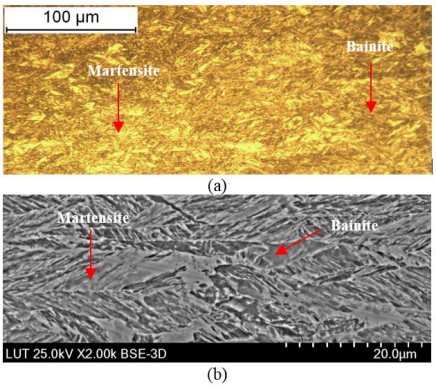

Fig. 5. Fine-grained martensite-bainite morphologies of UHSS S960QC: a) Light micrograph, length of micron bar 100 µm. b) SEM analysis using back-scattered electron approach.

V.2. Macrostructure of weldments

Light microscopy images of the macrostructures of chosen specimens are given in Fig. 6. Generally, the macrostructure of the specimens for horizontal flat welding position (PA) show deeper weld penetration at the weld root than with horizontal welding position (PB). The finger weld characteristics of the GMAW process is well pronounced in the PA welding position. Also, the shape of the surface profile of the weld beads look flatter from the top weld toe to the down weld toe, especially with the PA welding position. No major weld defect or imperfection is noticed in the specimens. The quality levels (surface and internal imperfections) of the specimens conform to EN 1SO 5817. Throat thicknesses, measured with a weld bead gauge (caliper), fall within the range of 0.5*t – 0.7*t, where t is the thickness of the base metal (5 mm). Therefore, the weld thicknesses were $\geq$ 2.5 or $\leq$ 3.5. The percentage of dilution of the filler wire and the base metal, based on the heat inputs supplied, was commensurate with the throat thicknesses achieved.

Comparing weld specimens PB ANN and PA ANN, the heat input applied was of the same value, with slight variation. However, due to the welding position of PA ANN, the heat input produced high arc pressure causing deeper weld penetration. Contrarily, the cooling rate in PA ANN was much slower than PB ANN. This slower cooling is a result of the amount of heat retained at the weld toe, causing slower dissipation of heat than with PB ANN. The same phenomenon was observed in the other specimens (PB 1, PA 1, PB 2, PA 2, PB 3 and PA 3). By visual examination, the PB welding position shows non-uniform HAZs across the base member and the upright member. Although in PA the HAZs are also large, there was uniformity in how the heat spreads across the joints. Another significant finding is that although PB 2 had higher heat input than PA 2, the cooling rates were quite similar. This observation affirms that there is a much faster cooling rate in the PB welding position than the PA position for the same or slightly higher heat input (say, 0.05 kJ / mm difference).

V.3. Behavior of the Welding Parameters and Variables

The behavior of the various welding parameters has a direct effect on the temperature of the weld seam, thus causing non-uniform thermal cycles in the weld and surrounding zones. By comparing the temperature graphs of the PB welding positions in Fig. 7, it can be seen that the temperature readings did not exceed 1100 °C with a heat input range from 0.50–0.65 kJ/mm. However, from the temperature graphs of PA for the same heat input range, it can be seen that the temperature captured from the surface of the weld seam peaked above 1100 °C. Heat input readings of PA 1 and PA 3 show similar stability to readings for PB 1 and PB 3. Arc length, wire feed, voltage and current reading were quite stable. It can be said that arc stability is very much achieved in the PA welding position, and thus change of the mode of metal transfer from short-circuit arc to spray arc is smooth.

The behavior of the welding parameters observed for PA ANN and PB ANN shows more unstable curves than with the other specimens. Although arc length and wire feed rate were quite stable, there are severe fluctuations in voltage, current, and heat input readings, which could be a result of disturbances in the adaptive welding system. Such disturbances may have affected the amount of heat input supplied during welding, thus keeping the weld seam temperature below 1100 °C. The observed behavior might also be due to the change in the mode of metal transfer from short-circuit arc to spray arc, which the ANN system tried to modify, or to which it did not compensate. The driving forces (electrostatic force, Marangoni force, buoyancy force, inertia, surface tension and viscosity) involved in the GMAW process [31] might have influenced the behavior of the welding parameters and variables in the different welding positions.

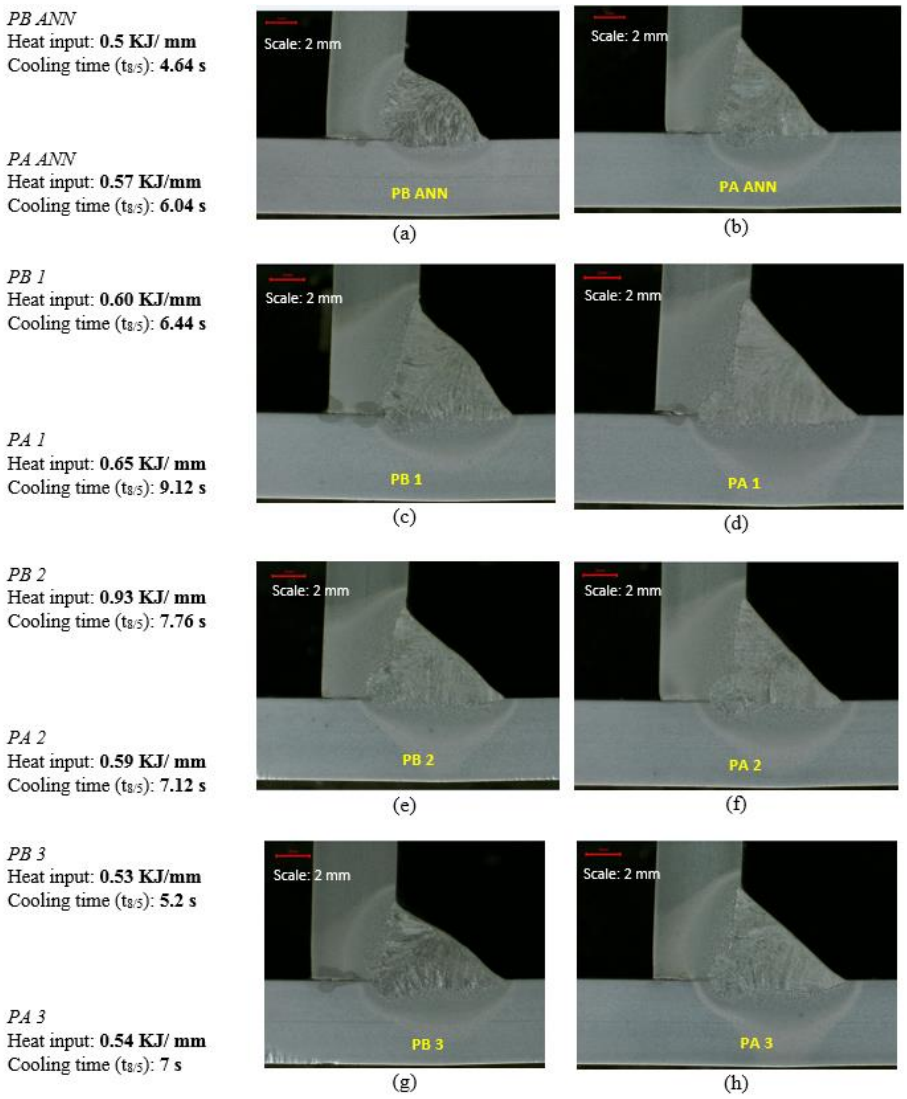

Fig. 6. Light microscopy images (2 mm scale) of test specimens showing a transverse view of macro-sections and longitudinal throat thickness.

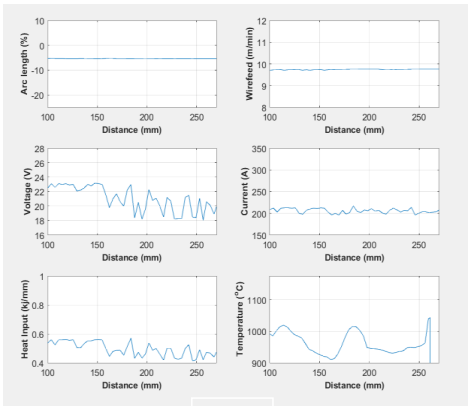

(a)

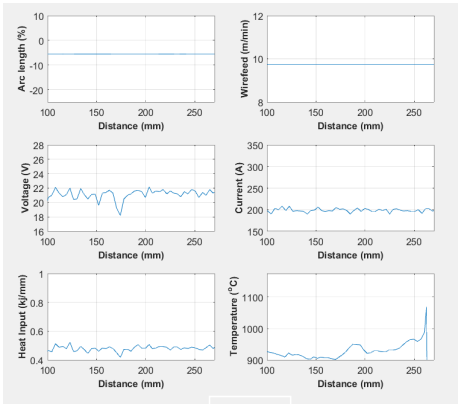

(b)

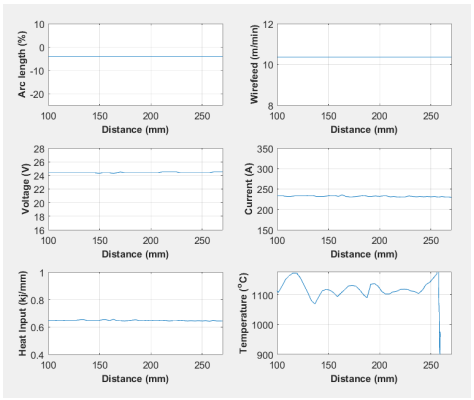

(c)

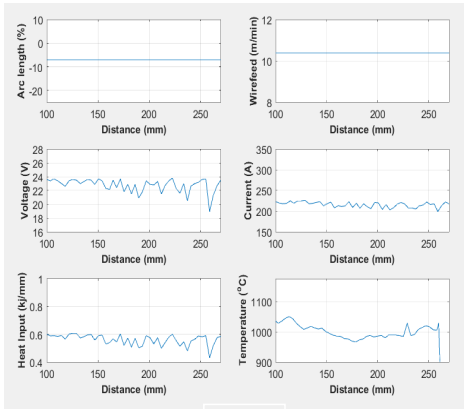

(d)

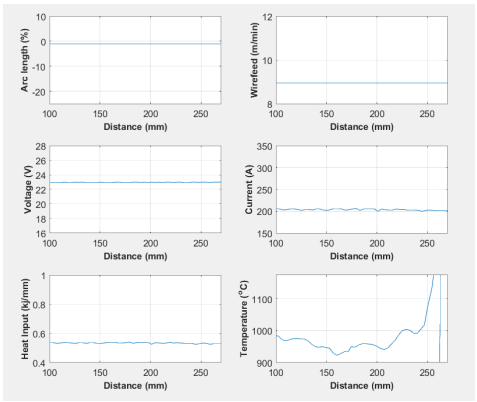

(e)

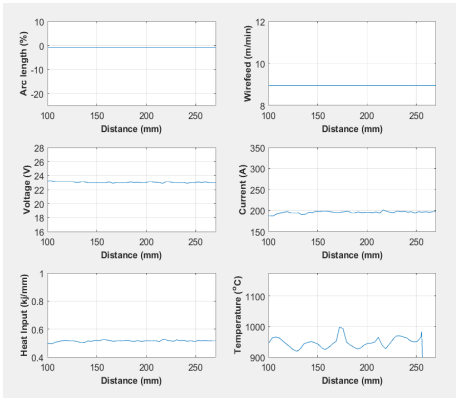

(f)

Fig. 7. Behavior curves of welding parameters of selected specimens: (a) PA ANN, (b) PB ANN, (c) PA 1, (d) PB1, (e) PA 3 and (f) PB 3

VI. Hardness Analysis

The Vickers hardness of the base metal at a load of HV5 varies from 351–356 HV measured at intervals of 1 mm. For comparison, the Vickers hardness values across the surface of the weld metal is similar in the PA ANN and PB ANN specimens. The highest hardness values obtained ranged from 375–397 HV5. However, at the fusion boundaries, the hardness values of the PA ANN specimen dropped to about 295 HV5 on the left side and 303 HV5 on the right side of the joint geometry, as shown in Fig. 8. Notably, there was no significant drop in hardness at the fusion line of the PB ANN specimen, as seen in Fig. 9.

A drop in hardness was recorded at the HAZs in both welding positions. PA ANN recorded a more pronounced drop in hardness towards the base metal (non-HAZ). Considering the heat input applied, it can be seen that in the PA ANN and PB ANN specimens, the maximum percentage drop in hardness across the fusion boundaries to the base metal is about 26% to 24%, respectively (using minimum hardness values). Interestingly, it can be seen from the graph of PA ANN in Fig. 7 that when heat input was within the range of 0.50–0.65 kJ/mm, the temperature fluctuation reading did not peak above 1100 ^{o}C. This could be a result of the welding parameters being modified by the ANN system.

Comparing PA 3 and PB 3, it can be seen in Fig. 10 and Fig. 11 that PB 3 had higher hardness values at the surface of the weld metal than PA 3. Considering the heat input applied, it can be seen that in PA 3 and PB 3, the maximum percentage drop in hardness across the fusion boundaries to the base metal is about 21% to 16%, respectively (using minimum hardness values).

In PA welding positions, that is Fig. 8 and Fig. 10, the drop in hardness is quite uniform from the HAZ to the base metal on both sides of the welded joint. Moreover, hardness values across the surface of the weld metal are uniform due to the flatness of the weld bead profile. In PB welding positions, that is Fig. 9 and Fig 11, the drop in hardness is more pronounced towards the upright member than the base member, especially at the fusion boundary and also in the HAZ. Although there is progressive drop in hardness towards the base metal (non-HAZ), the upright member experienced the greatest drop in hardness.

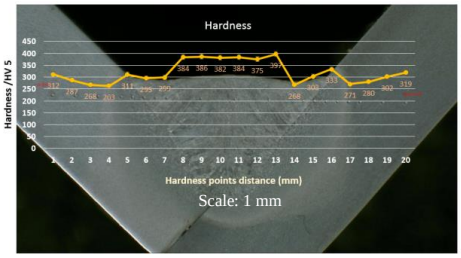

Fig. 8. Hardness test of specimen PA ANN

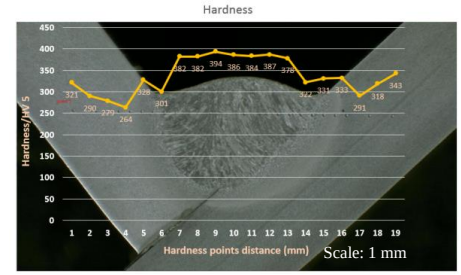

Fig. 9. Hardness test of specimen PB ANN

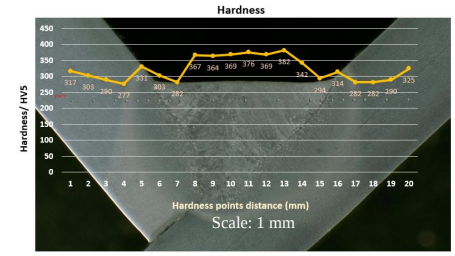

Fig. 10. Hardness test of specimen PA 3

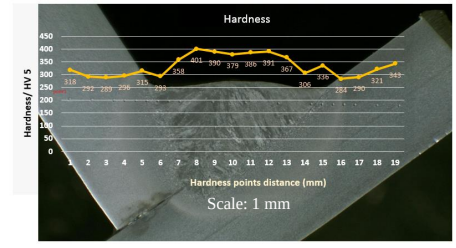

Fig. 11. Hardness test of specimen PB 3

VII. Discussions

Having an impact strength between 33–50 J at an operating temperature of -40 ºC, the UHSS under study meets the requirements of materials for use in Arctic structures. However, to ensure that such material can be used successfully in the Arctic environment, there is a need to consider controlled and intelligent approaches in welding of UHSS. Welding operations with uncontrolled heat inputs introduce high stress concentrations in welded UHSS, especially when there are imperfections and defects such as softening of the HAZ [22]. In such cases, the grain sizes of the weld fusion line and the HAZ may become large and service performance will be compromised. Research on UHSS materials with different grain sizes [28] attests to this phenomenon.

Two fillet weld joint configurations of UHSS S960QC are studied in this paper and their suitability for Arctic structural applications considered. The adaptive robotic GMAW system employed provided opportunities for monitoring, predicting and modifying the behavior of the welding parameters and variables. Some of the specimens were welded while the system was operating from an ANN configuration. The results of the welding experiment produced meaningful findings on the effects of varying heat inputs on the hardness properties of the weld geometry and the influence of the behavior of the welding variables and parameters on weld temperature.

It was observed that the ANN configuration had a great influence on the behavior of the welding parameters and variables, which changed without showing a significant effect on temperature. However, those specimens that were welded without the ANN system experienced susceptibility to high temperatures even though the heat inputs supplied during welding were quite similar. High temperatures as a result of heat input effects could produce HAZ softening tendencies and low cooling rates, which is a risk and, moreover, detrimental to the welded structure.

Although all the welded joints had satisfactory weld fusion, PA welds had deeper weld penetration than welds welded in the PB position. In hardness tests performed for both fillet joint configurations, PB welded joints produced more satisfactory hardness values across the weld geometry than PA. This suggests that PB welded joints should be preferred for Arctic structural constructions where considerable load carrying capacity is required. However, the base member of the PB welded joint should be the load carrying member since the drop in hardness was lower in this region. Alternatively, PA welded joints could be used where stiffening of an Arctic structural member is required because the hardness properties were uniform across the weld geometry. Nevertheless, PA could also be used where load carry capacity is required due to the deeper weld penetration achieved.

Based on this work, it can be seen that using an adaptive intelligent GMAW system is beneficial for welding of lightweight materials like UHSS for Arctic structural constructions. Other work has also reported the applicability of the adaptive GMAW process for UHSS [32, 33]. Implementation of adaptive GMAW processes in the future welding industry looks promising as the approach brings benefits from digitalization (online and offline welding) [34] and interaction between robots, humans and intelligent system protocols that increase productivity and quality [35].

In future work, further investigation and analysis of the microstructure of the welded metal and the HAZs is required. Additionally, from the perspective of system integration, a control algorithm could be developed to control the amount of heat input supplied to the weld or to optimize the entire welding system.

VIII. Conclusion

The objective of this work was to examine the usability of S960QC UHSS as weldable material for lightweight Arctic structural constructions and, further, to explore the applicability of intelligent adaptive techniques in welding of S960QC UHSS. Adaptive robotic GMAW of 5 mm S960QC UHSS plates in two fillet joint configurations was performed. The fillet joints were welded in PA and PB welding positions. 8 specimens were analyzed to assess the effects of varying heat inputs on the hardness properties of the weld metal, weld fusion zones and the HAZs. In addition, the behavior of welding parameters and variables while using the adaptive intelligent welding system settings was appraised. Applied heat inputs in the range 0.5–0.65 kJ/mm produced weld hardness values between 375 HV5 and 397 HV5. The hardness values together with impact strength of 33–50 J, at operating temperature of - 40 ºC, indicate that S960QC UHSS has properties suitable for Arctic structural applications where excellent strength to weight ratio and high load carrying capacity is required. However, the susceptibility of S960QC UHSS to HAZ softening is a critical issue that needs attention. Careful selection of consumables, welding processes and techniques, and the adoption of appropriate control mechanisms for the welding process is recommended. It is also important to consider the cooling rate of the weld since it affects the microstructural properties. In assessment of the applicability of intelligent adaptive welding, it was found that the system was beneficial for monitoring, capturing, predicting, detecting and modifying the behavior of the welding parameters and variables. After further development, the adaptive intelligent welding system could potentially be used to control and optimize welding operations and thus increase welding productivity and weld quality.

Acknowledgements

This research was carried out at Lappeenranta University of Technology in collaboration with the State Key Laboratory of Advanced Welding and Joining, Harbin Institute of Technology, China. The work received financial support from an Academy of Finland grant awarded to Lappeenranta University of Technology, Laboratory of Welding Technology project 'Monitoring and Modelling of Advanced Adaptive Welding Process Systems for Ultra High Strength Steel (UHSS)' and Laboratory of Intelligent Systems project 'Manufacturing 4.0 – Strategies for Technological, Economical, Educational and Social Policy Adoption'. The authors would like to thank Peter Jones for his comments and assistance with the English language, and Esa Hiltunen and Sakari Pentillä for their support during the experimental work.

References

[1] P. Budzik, Arctic Oil and Gas Potential, Publications of US Energy Information Administration Office of Integrated Analysis and Forecasting Oil and Gas Division, 2009.

[2] J. Lancaster, *Handbook of Structural Welding Processes, Materials and Methods Used in the Welding of Major Structures, Pipelines and Process Plant* (3rd edition, Cambridge, 2003).

[3] O.N. Knut, The Arctic – A Region of Opportunities and Interest. Stiftelsen Det Norske Veritas Germanischer Lloyd (DNV.GL), 2012.

[4] K. Paananen, Opportunities for Finland – the Arctic and Russia, *Baltic Rim Economics*, Quarterly Review 3, Expert Article 1267, 2013.

[5] A. Khaustov, New cold-resistant steel for shipbuilding, *Sudostroenie*, Vol 4, pp 57-58, 2006.

[6] I. Novitsky, A. Portnoy, V. Razuvaev, V, *Handbook of Design of Offshore Platforms*: *Requirements of Standards* (Teoksessa, Saint Petersburg, Russia: SPbGMTU, 2009) (in Russian).

[7] I.V. Gorynin, V.V. Rybin, V.A. Malyshevskii, E.I. Khlusova, Alloying principles, phase transformation, structure and properties of low-temperature weldable shipbuilding steels, *Metal Science and Heat Treatment*, Vol. 49, n. 1-2, pp. 3-9, 2007.

[8] P.D. Odessey, Microalloying of steels for the North and unique metal structures, *Intermet Engineering*, pp.176, 2006.

[9] P. Layus, P. Kah, M. Kesse, E.A. Gyasi, *Submerged Arc Welding Process in Welding Thick High Strength Steel Plates Used for Arctic Applications*, Proc. 27th International Ocean and Polar Engineering Conference, San Francisco, CA, USA June 2017, pp. 92-98.

[10] P. Layus, P. Kah, J. Martikainen, V. Gezha, Advanced SAW processes for Arctic structures and ice-going vessels, *Proceedings of the Institution of Mechanical Engineers, Part B: Journal of Engineering Manufacture*, Vol.232(1), pp.1-14, 2018.

[11] A. Ilyin, Presentation at Prometheus seminar, Saint Petersburg, 2013.

[12] Alform, Superior Solutions in High-Strength and Ultra-High-Strength TM steel, Voestalpine Steel Division, 17th edition. [Online] alform_Produktfolder_Hochfeste_und_Ultrahochfeste_TM_EN_1401.pdf. Accessed 5.1.2018.

[13] P. Layus, P. Kah, J. Martikainen, *Peculiarities of Welding Technical Requirements for Arctic Applications*, Proc. 25th International Ocean and Polar Engineering Conference (Hawaii, USA June 2015), pp. 285-288.

[14] M.C. Serreze, R.G. Barry, The Arctic Climate System (2nd edition, Cambridge University Press, 2005).

[15] R. Przybylak, *The Climate of the Arctic*, Springer, pp. 288, 2003.

[16] J.P. Kaushish, *Manufacturing Processes*, PHI Learning Pvt. Ltd, 1007, 2008.

[17] T.L. Anderson, H.I. McHenry, Interim Progress Report: Fracture Toughness of Steel Weldments for Arctic Structures, NBSIR 83-16980, Colorado 80303, 1982.

[18] P. Layus, P. Kah, E. Khlusova, V. Orlov, Study of the sensitivity of high-strength cold-resistant shipbuilding steels to thermal cycle of arc welding, *International Journal of Mechanical and Materials Engineering*, Vol.13(3), pp.1-9, 2018.

[19] D. Porter, *Development in Hot-Rolled High-Strength Steel*, Nordic Welding Conference, New Trends in Welding Technology, Tampere, Finland, 2006.

[20] M. Hemmilä, R. Laitinen, T. Liimatainen, D. Porter, Mechanical and Technological Properties of Ultra High Strength Optim Steels, Rautaruukki Oyj, Helsinki. [Online] http://www.oxycoupage.com/FichiersPDF/Ruukki_Pdf/English/Ruukki-Technical-article-Mechanical-and-technological-properties-of-ultra-high-strength-Optim-steels.pdf. Accessed 18.1 2018.

[21] P. Kah, M. Pirinen, R. Suoranta, J. Martikainen, Welding of ultra high strength steels, *Advanced Materials Research*, Vol. 849, pp. 357-365, 2014.

[22] T. Björk, J. Toivonen, T. Nykänen, Capacity of fillet welded joints made of ultra-high strength steel, *Weld World*, Vol. 57, pp. 71–84, 2012.

[23] Ruukki Metals, Hot Rolled Steel Plates, Sheets and Coils – Processing of Materials- Impact Strength and Through Thickness Properties. Helsinki, 2007.

[24] Z.A. Chen, Z. Zeng, Y.J. Chao, YJ, Effect of crack depth on the shift of the ductile–brittle transition curve of steels, *Engineering Fracture Mechanics*, Vol. 74, n.15, pp. 2437–2448, 2007.

[25] N.E. Dowling, *Mechanical Behavior of Materials. Engineering Methods for Deformation, Fracture, and Fatigue* (3rd edition, Upper Saddle River, New Jersey: Pearson Education, Inc., 912, 2007).

[26] F. Dominique, P. Andre, Z. Andre, *Mechanical Behaviour of Material". Volume II: Fracture Mechanics and Damage*, Dordrecht Springer, pp. 662, 2013.

[27] W.D. Callister, D.G. Rethwisch, *Materials Science and Engineering* (6th edition, John Wiley & Sons, 2007).

[28] F. Zhen, K. Zhang, Z. Guo, J. Qu, Effect of martensite fine structure on mechanical properties of an 1100 MPa grade ultra-high strength steel, *Journal of Iron and Steel Research, International*, Vol.22, pp. 645–651, 2015.

[29] X. Wu, H. Lee, Y.M. Kim, N.J. Kim, Effects of processing parameters on microstructure and properties of ultra high strength line-pipe steel, *Journal of Materials Science & Technology*, Vol. 28, pp. 889–894, 2012.

[30] B.C. Howard, C.H. Scott, *Modern Welding Technology* (6th edition, Pearson Prentice Hall, USA, 2005).

[31] A. Kumar, T. Debroy, Heat transfer and fluid flow during gas-metal-arc-fillet welding for various joint configuration and welding positions, *Metallurgical and Materials Transactions A*, Vol. 38A, pp. 506-519, 2007.

[32] E.A. Gyasi, P. Kah, J. Ratava, M. Kesse, E. Hiltunen, *Study of Adaptive Automated GMAW Process for Full Penetration Fillet Welds in Offshore Steel Structures*, Proc. 27th International Ocean and Polar Engineering Conference, San Francisco, CA, USA June 2017, pp. 290-297.

[33] E.A. Gyasi, P. Kah, H. Wu, M.A. Kesse, Modeling of an artificial intelligence system to predict structural integrity in robotic GMAW of UHSS fillet welded joints, *Int J Adv Manuf Technol.* Vol. 93, pp. 1139-1155, 2017.

[34] E.A. Gyasi, P. Kah, Structural integrity analysis of the usability of high strength steels. *Rev. Adv. Mater. Sci*, Vol. 46, pp: 39-52, 2016.

[35] J.N. Pires, A. Loureiro, G. Bölmsjo, Welding robots: Technology, system issues and applications. Springer-Verlag London Limited. pp.180, 2006.

Authors' information

[1]Laboratory of Welding Technology, Department of Mechanical Engineering, School of Energy Systems, Lappeenranta University of Technology, Lappeenranta, Finland.
emmanuelgyasi.giw@gmail.com; emmanuel.gyasi@student.lut.fi
[2]Laboratory of Welding Technology, Department of Mechanical Engineering School of Energy Systems, Lappeenranta University of Technology, Lappeenranta, Finland.
paul.kah@lut.fi
[3]Laboratory of Intelligent Systems, Department of Mechanical Engineering, School of Energy Systems, Lappeenranta University of Technology, Lappeenranta, Finland.
heikki.handroos@lut.fi
[4]Laboratory of Welding Technology, Department of Mechanical Engineering, School of Energy Systems, Lappeenranta University of Technology, Lappeenranta, Finland.
pavel.layus@lut.fi
[5]State Key Laboratory of Advanced Welding and Joining, Harbin Institute of Technology, Weihai, China.
sblin@hit.edu.cn

Emmanuel Afrane Gyasi was born in Accra, Ghana. He earned a B.Eng. (Industrial Management) in 2010 from Savonia University of Applied Sciences, Finland, and M.Sc. (Mechanical Engineering) in 2013 from Lappeenranta University of Technology, Finland.
He has published 7 scientific journals and conference papers in the field of welding technology. His current research interests include automation, robotics, artificial intelligence, steel structures and advanced welding processes.
Mr. Gyasi is a member of the Finnish Welding Society (SHY) and serves on the International Institute of Welding (IIW) technical commissions (C-II, C-IX and C-XII). Mr. Gyasi is the founder of the Ghanaian Institute of Welding, and currently acts as the President and CEO of the organization.

Paul Kah obtained a professional Master's degree certificate, DIPET II, from ENSET at the University of Douala, Cameroon, in 2001 and graduated from Lappeenranta University of Technology, Finland with a second MSc (Tech) in 2007.
He completed his doctoral studies at Lappeenranta University of Technology in 2011. He has a position of Associate Professor and has published about 150 scientific papers in peer-reviewed scientific journals and conference proceedings.
Docent Kah is an expert in the International Institute of Welding (IIW) Commission IX, XII, C-XII-A, and a guest editor of Welding in the World and a reviewer in IEEE. Docent Kah is the President (Chairman) of Cameroon Welding Association.

Heikki Handroos was born in Tampere, Finland. He earned an M.Sc. (Eng.) in 1985 and a D.Sc. (Tech.) in 1991 in Hydraulics and Automation from Tampere University of Technology, Finland.
He has published 250 journal and conference papers in the field of mechatronics and robotics.
Professor Handroos is a member of ASME and IEEE. Currently he is an Associate Editor of ASME Journal of Dynamic Systems, Measurement and Control. Professor Handroos is a Full Professor in Machine Automation in the Department of Mechanical Engineering, Lappeenranta University of Technology

Pavel Layus was born in St. Petersburg (Russia). He earned his doctoral degree from Lappeenranta University of Technology (Finland) in the field of welding technology for low temperature shipbuilding applications (2017).
He is the first author of about 15 academic and conference papers on various topics related to welding and material science.
Dr. Layus has been a member of Finnish Welding Society (SHY) since 2013 and received a SHY silver medal for outstanding doctoral dissertations in the field of welding.

Sanbao Lin obtained a B.S., M.S., and Ph.D. degrees from Harbin Institute of Technology, Heilongjiang, China in 1994, 1996, and 2000, respectively.
He has been working at the State Key Laboratory of Advanced Welding and Joining at Harbin Institute of Technology since 2000.
He has authored and co-authored over 150 papers in peer-reviewed journals.
Professor Lin research interest includes are welding procedure and process control. Professor Lin has had research stay at the University of Cambridge in UK.

Publication V

Gyasi, E.A., Pirinen, M., Nallikari, M. and Martikainen, J.
Transforming Arctic welding with Finnish technological know-how

Reprinted with permission from
Canadian Welding Association (CWA) Journal - Special CWA-IIW Conference Edition
pp. 82-91, 2015

Transforming Arctic Welding with **FINNISH TECHNOLOGICAL KNOW-HOW**

The Arctic region is known for its remote, harsh, and extremely cold climatic conditions. It is estimated that, the Arctic region which possesses enormous natural resources hold about 22% of oil and gas reserves [1]. Other resources such as the strong Arctic wind also provide viable opportunities for wind power industries [2]. Moreover, global warming situations which have resulted in Arctic ice shrinking provide other opportunities in the region [3]. The gradual opening of the Northern Sea Route (NSR), due to climate changes, thus offer new transportation routes in the region [4].

In recent times, the Arctic region is increasingly being seen as a potentially sustainable area for infrastructural and product development due to continuous efforts to tap resources which were once considered commercially unrecoverable. The development of the Arctic region has become necessary in other to exploit the un-tapped opportunities, whiles protecting the fragile ecosystem [5]. The entire development of the Arctic region, however, demands huge investment to facilitate construction of structures such as ships, tankers, vessels, pipelines, communication and energy production structures capable to resist brittle fracture in the harsh Arctic conditions. As these structures are mostly constructed with metals and predominantly joined through welding, the accurate selection of weldable materials such as high strength steels, and suitable welding processes are stringent requirements. There is a need for corporate effort through cooperation and partnerships to developing the Arctic region. Finland

Icebreaker at sea

demonstrates high technological and undoubtable expertise in welding due to exceptions made in material and welding process selections for Arctic structural construction. Following long tradition in shipbuilding, about 60% of all icebreakers in the world have been designed and built in Finland [6], based on strong expertise in research and development, specialities in the construction of technically demanding vessels, systematic industrial innovative processes, networking, and procedures for welding of structures for Arctic operations [6, 7].

This paper evaluates Finland's welding expertise and technological know-how relevant to development of the Arctic region. The study emphasizes the need for business partnerships to harness un-tapped opportunities in the Arctic region and also draws attention to international cooperation and networking for multidisciplinary research in the field of Arctic Welding, as economic activities and infrastructure in Arctic condition have become paramount. It is such that Finland's position in Arctic operations is strong and thus serves as a safe and reliably bridge for other nations to participate in developing Arctic welding activities.

1. WELDABLE METALS FOR ARCTIC STRUCTURES

The selection of weldable materials for the Arctic environment has been rigorous due to the low temperature conditions which could fall below -60 ^{0}C [8]. Weldable materials selected for applications in the Arctic region must therefore fulfill stringent requirements such as: low temperature toughness down to -60 ^{0}C; yield strength up to 690 MPa; Isotropy properties across dimensions [9, 10]. Additionally, as the natural environment of the Arctic region is harsh with strong wind velocity of about 5-15 m/s up to 50 m/s [11], the selection of weldable materials are required to fulfill working conditions as well since continual exposure of materials to the cold climatic conditions has resulted in several detrimental accidents in the region [12].

As a phenomenon, metals tend to increase in yield strength, hardness and ultimate tensile strength but lose their ductility in conditions when operating temperatures go down to sub-zero degrees [12, 13]. In view of this, weldable materials for the Arctic region are expected to demonstrate high impact and fracture toughness at operating and working condition to resistance brittle fracture. While impact toughness is determined by Charpy V-notch test, fracture toughness is either determined by the crack tip opening displacement (CTOD) test or the crack tip opening angle (CTOA) [14,15].

Due to the wider range of materials and consumables available for selection for Arctic applications, this section of the paper will focus on high strength steels.

Table 1. Typical composition of Q&T and TMCP steels (modified) [16].

Q&T Steels / TMCP Steels	Thickness (mm)	Typical composition (by weight %)	CE_{IIW}	Typical mechanical yield strength/ CVN range
Typical composition and mechanical properties of thermochemical controlled processed steel – yield strength range 400 to 500MPa, typical average plate thickness 30mm	30	C, Mn, Si, S, P, Nb, V, Al, Cu, Ni, Cr	0.35	400MPa/190J @ -40°C
	32		-	398MPa/300J @ -20°C
	32		0.32	400MPa/>300J @ -20°C
	30		0.37	460MPa/220J @ -40°C
Typical composition and mechanical properties of quenched and tempered steel – yield strength range 400 to 500MPa, typical average plate thickness 30mm	6 - 140	C, Mn, Si, S, P, Nb, V, Al, Ti*, Cu, Ni, Cr, Mo*, B*	0.81	550 to 690MPa/80J @ -84°C
	30		0.45	450MPa/>35J @ -40°C
	50 - 64		0.43 (Ti*)	480MPa/>40J @ -40°C
	50		0.64 (Ti*,Mo*, B*)	690MPa/>40J @ -40°C
	30		0.64 (B*)	960MPa/>40J @ -40°C

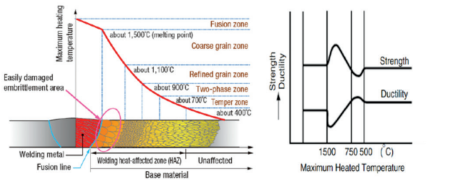

A) Fe-C equivalent state and its relationship with the welding thermal cycle

B) Strength and Ductility Distribution of Welds in Q&T Steels

Figure 1. Effect on Strength and Ductility of Q&T Steels during Welding Thermal Cycle [20, 23].

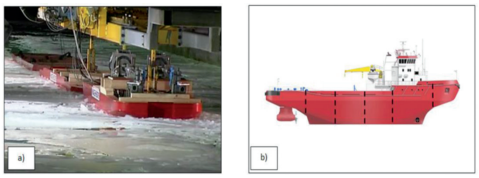

Figure 2. Arctic Structure a) Pulling Barges in Floe Ice; b) Icebreaker Hull Block Sections [31].

High Strength Steels

Due to the imprecise definition for high strength steels (HSS) as a result of differences in steel classifications for each industrial field, in this paper, steels with yield strength above 355 MPa are denoted as HSS. The production and delivery of HSS are mainly quenched and tempered (Q&T) or as thermomechanical controlled processing (TMCP) steels [16]. It is known that Q&T and TMCP steels have slight similar physical properties such as good strength to weight ratio, higher load carrying capacity, good weldability and improved service life [16, 17]. Exploring the use of HSS therefore makes it possible to reduce construction weight and cost, lower consumption of welding consumables, and reduce welding time as a result of decreased thickness of the material [18, 19]. However these steels are very distinct with regards to their chemical properties, especially the equivalent carbon contents as shown in *Table 1*.

Depending on chemical composition, most Q&T steels operate under very low temperatures down to -40 ^{0}C than TMCP steels of the same yield strength and thickness [16]. Q&T steels with minimum yield strength between 460 - 690 MPa therefore possess high toughness, good ductility properties at very low temperatures.

It is scientifically proven that Q&T steel grades such as E420 – E690; S390J6Q; S450J6Q could operate under very low temperatures between -50 to -60 ^{0}C at minimum impact energy of 27J [20]. TMCP steels also possess excellent toughness properties, thus prevents brittle fracture in ships at a design temperature of 0 0C [21]. Typical grades of TMCP steel grades include S460ML; S500MC; S700MC; X100; X120. However each steel grade has a range of yield strengths, a factor which is not fully recognized in designing [16].

Although both Q&T and TMCP steels offer good weldability, TMCP steels are often more susceptible to softening of the heat affected zone (HAZ) [22], whiles Q&T steels in most cases require preheating and often post-heating. However, Longitudinal or transverse cold cracking in weld metal and the heat affected zone (HAZ), and poor ductility or toughness due to loss of strength are typical welding problems of HSS [18]. The tendency of softening of the base metal therefore occurs when the HAZ of Q&T and TMCP steels are heated at high temperatures above tempering temperatures [23], or as a result of fusion welding processes and consumables used [24]. Nevertheless, the formation of martensite-bainite in Q&T steels indicates excellent ductility properties and higher toughness than TMCP steels which produce ferrite-bainite microstructure during welding. Thus the HAZ of TMCP tends to be softer than Q&T steels of the same yield strength under the

same welding parameter, say high heat input [25].

Figure 1 depicts the effect of welding on strength and ductility of Q&T steels. Although the strength and hardness of welded joints in Q&T steels attain a maximum in the HAZ towards the fusion boundary and drops to a minimum in the base material beyond the visible HAZ where overtempering occurs, ductility reaches a minimum in the coarse grained HAZ and rises to a maximum in the softened base material, before dropping somewhat to a level representative of the base material [20].

Using weldable materials for structural applications in the Arctic environment requires accurate identification of welding consumable grades either by test temperature or by strength level. These identifications should, however, correspond with the impact test temperature or the strength level of the high strength steel grade's energies [26]. It is proven that undermatched or matched filler metals are generally used in welding HSS [27], since the use of overmatched filler metal has not been economical in welding HSS [25].

2. WELDING PROCESSES USED FOR ARCTIC STRUCTURES

Welding of HSS requires critical consideration of heat inputs, cooling times and filler materials as a factor of thickness of the steel, preheating, current, voltage, post heating, and speed of welding. In addition, the welding method, technique and work piece geometry also demands consideration. The overall selection of correct welding procedures is therefore vital to guaranteeing satisfactory sound welds by major welding processes for HSS [25, 28].

Conventional welding processes such as shielded metal arc welding (SMAW), flux cored arc welding (FCAW), gas metal arc welding (GMAW), and submerged arc welding (SAW) have proven to be suitable for welding HSS [20]. Current research have also shown that advanced welding methods such as multilayer-multipass-multiwire narrow- gap submerged arc welding process (Multi-SAW-NG), dual-tandem narrow gap pulsed-spray MIG/MAG welding process, and laser-tandem MIG/MAG hybrid welding process combined with narrow gap welding techniques are efficient for welding HSS Arctic structures [29].

The gas shielded FCAW process is particularly suitable for welding Q&T steels owing to the low hydrogen content. The flux cored wires are normally used with CO_2 gas shielding or argon- CO_2 mixtures with dew point of -35 ^{0}C or lower [20]. Also the addition of titanium-boron in FCAW wires increases weld strength and improves weld impact toughness when nickel is added. In SAW wires, the addition of molybdenum helps to increase weld strength. In a recent study, 550 MPa yield strength for both SAW and FCAW in welding HSS have shown adequate weld toughness, with upper shelf values >150 J and the 50 J impact transition temperature below -60 ^{0}C. All the welds depicted low hardness values and showed no indication of hydrogen cracking. The major microstructure of the welds was acicular ferrite, but microstructure coarsened with increasing heat input [30].

Weld profiles such as butt and fillet joints are considerable in the welding of HSS. Butt joints could be used for plate thickness > 12mm together with symmetrical double-vee groove. This configuration minimizes angular distortion as back-gouging facilitates the two sides of the weld deposit almost equal in thickness. However, if good fit up and appropriate welding techniques are employed then back-gouging is generally not necessary. Fillet joint profiles are important in welding Q&T steels when the structure is to be subjected to fatigue loading. As Q&T steels are often loaded to higher stresses, it is essential that welds be smooth, correctly contoured, and well flared into the legs of the joined pieces. The runs of each fillet weld must have good penetration, particularly at the root, but must not undercut the joined pieces [20].

3. FINNISH ARCTIC WELDING EXPERTISE AND TECHNOLOGICAL KNOW-HOW

Material selection as well as designing weldable structures to operate in the Arctic environment is Finland's core expertise. As conditions in the Arctic environment differ considerably from each location on the Arctic Circle, Finland's technological know-how include specialities in welding of materials to withstand diverse conditions in the Arctic region. Even though maintenance of welded Arctic structures has not been peculiar with Finland's Arctic experience, its core expertise does not create room for catastrophic failures in the Arctic environment. This is because failures which are bound to occur are already foreseen and thus corrected on time to prevent its happening.

CASE COMPANY: Arctech Helsinki Shipyard

3.1 DESIGN FOR WELDING

One of the essential aspects in the construction of Arctic structures is designing. The technological relevance here is the ability to know the various forms of load imposed on the structures and how the strength of the structure could withstand those loads. Additionally, the influence of ice pressures on welded structures in different locations in the Arctic environment is another compelling technological know-how.

Designing of Arctic structures is done together with partners in most cases. The whole constructional work involves cooperative activities in conformance with design rules

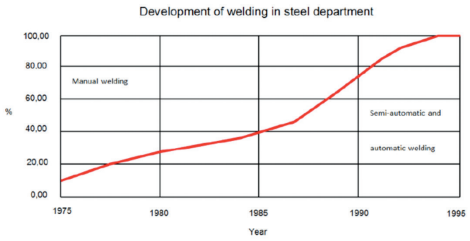

Figure 3. The Development of Wire Welding in Hull Assembly [6].

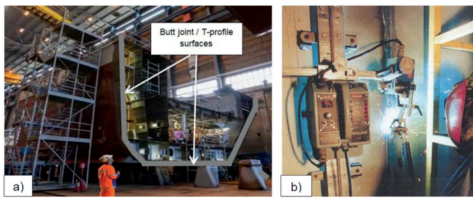

Figure 4. a) Joint Surfaces of an Arctic Structure Block Section; b) Mechanized Vertical FCAW in Hull Production [6].

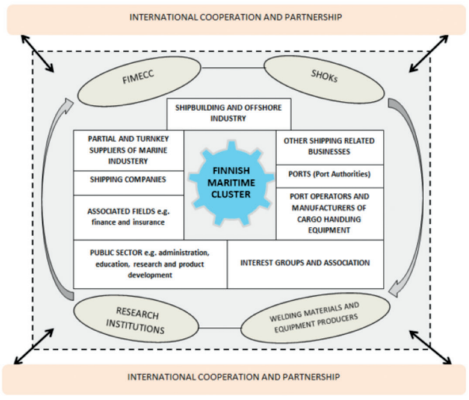

Figure 5. A schematic of Finnish Arctic Development framework for International Cooperation and Partnership.

required in constructing structure in order to operate in a specific location or capable for operation in other locations. Structural designs are model tested in laboratories for evaluation to ascertain performance of the actual structure when subjected to the Arctic environment as shown in *Figure 2a*. Arctic structure such as an icebreaker is composed of a number of blocks with several structural members forming a complete hull assemblage as shown in *Figure 2b*. The hull production is optimized through sophisticated design processes to enhance efficiency in joining of the materials selected with suitable and effective welding techniques.

3.2 MATERIAL SELECTION

Due to different conditions, materials and consumables available from variety of rules instituted by classification societies and manufacturers for diverse applications in the Arctic region have wider range of yield strengths depending on their chemical composition. The core expertise relies on the ability to make exceptions of the classification rules towards the selection of effective, efficient and suitable materials and consumables available. Therefore Arctic structures such as icebreakers, offshore vessels, icebreaking cargo vessels, and icebreaking special vessels are constructed with HSS. The permissible yield strength of HSS used is 500 MPa (grade E), which is in accordance with rules enacted by the classification society. These structures are therefore able to operate in temperatures as cold as – 40 ^{0}C.

The steel type used in the building of the aforementioned structures is mostly Q&T, but TMCP has been an attractive choice in recent times. Although these steel types exhibits the required weldability and toughness properties according to today standards, only a margin of its strength have been essential since benefits accruing from its full strength have not been realized in practical sense. However, TMCP steels have been utilized in recent constructions since they are less prone to the need of preheating, which practically has significant effect on productivity in welding production. The plate thickness of HSS selected for the construction of such Arctic structures ranges between 5mm – 40mm.

3.3 WELDING TECHNIQUES AND PROCESSES UTILIZED

The development of wire welding in hull assembly of Arctic structures has been tremendous due to the enormous value placed on the use of automatic and semi-automatic welding techniques. This transition as shown in *Figure 3* has influenced the use of different types of welding processes and also the environment were the welding processes are used have raised the preference level. Therefore since most of the welding jobs are performed

in-doors, the flux-cored arc welding (FCAW) has been the most prominent welding process used among others such as the submerged arc welding (SAW), and the shielded metal arc welding (SMAW) process. The FCAW accounts for approximately 75% of filler material consumption while that of SAW and SMAW accounts for about 15% and 10% respectively. The percentage usage of these welding processes is as a result of development procedures aimed to increase the utilization of wire welding in hull production to 100%. The progress in this developmental process still leaves a share between 5 – 10 % for stick electrode since SMAW is used in ship installation in outfitting production.

Welded Joints in Section and Hull Production

The major weld profiles utilized in the production of hulls of the Arctic structures are butt joints and T-joints. In a way to completely exclude one working phase, avoid difficult overhead welding and eliminating the need for back gouging, butt joints are carefully planned and welded as one sided welds on ceramic or fixed backing. This set-up improves installation and welding of section limits in the dock phase, and thus decreases installation time to achieving efficient use of automatic welding.

Pre-assembly lines are equipped with double-head FCAW tractors with metal-cored wires and SAW tractors. Butt welds of the deck at the panel line are welded at the welding station as one-sided welding in a three wire SAW station. However, deck beam welding is made with double-head FCAW tractors with metal-cored wires. Other parts such as the section limits are semi-automatic welded with FCAW from one side either by using ceramic or fixed backing at the grand section and hull phase. Besides, T-profiles are also welded on a separated beam line by twin-arc SAW. *Figure 4* illustrates the joint surfaces of an Arctic structure block section and a mechanized vertical FCAW in hull production.

The length of welded joints of block seams on side shells ranges between 400mm – 500mm. Welded joints therefore accounts for about 3.5% of all steel materials used in the assembly of several block sections for hull production. Metal and flux-cored tubular wires are therefore used as filler material if the welding position so requires.

Weld Quality

Welding operations are carried out by welding personnel with EN 287 (steel), EN 9606-2 (aluminum) or EN 1418 (operators) qualifications, and thus certified by a classification society. This system ensures and assures high quality of welding in welded joints made. Quality levels of welded joints meeting EN ISO 5817 standard however, are approved through inspection by non-destructive test (NDT) personnel with EN 473 (ISO 9712) qualification.

Most importantly, the root sides of welded joints are inspected in-house by NDT procedures and principles which also involve traceability of welds. About 70% of internal inspection is done by ultrasonic test method while 30% is done by radiography method. The normal rate of weld defect is between 1 – 5%. In addition, very high welding quality control processes such as Q.HKI.C.R.734 (dimensional control at block supplier) and Q.HKI.C.R.723 (block deliveries to another production place) implemented in-house are also used. This control process helps in minimizing weld defect in a complete weld length of about 400mm to 1 - 2%, thus re-welding of the joints accounts for the same level of defects. The entire system serves as strong expertise and technological know-how for quality welding of Arctic structures.

Welding Assembly Productivity and Economy

Block assembly for hull production is greatly influenced by the duration of block delivery from suppliers, and welding processes and techniques utilized in the whole construction process. Blocks are auditioned to meeting the EN 3834-2 standard. Accuracy in the assembly process is highly ensured, thus providing the platform to deploy mechanization in welding for semi-automatic and automatic welding processes. Reducing the use of SMAW by 10% and increasing the use of FCAW and SAW by 75% and 15% respectively, as already indicated, serves as a means to improving productivity in welding of Arctic structures. With economy of welding, labor cost accounts for about 82.5% of the production cost. Although other cost also account for total production cost, the cost of consumable accounts for about less than 10%. The need to increasing the use of mechanization in welding has been imperative to reducing the cost of production especially with regards to labor cost.

4 FINNISH ARCTIC WELDING VALUE CHAIN

The Finnish Arctic maritime industry in its strategic interest to transforming the Arctic region combine the skills and competences of other industries under one association termed as the Finnish Maritime Cluster [32]. The various industries within the Finnish Maritime Cluster, as shown in Figure 5, are well networked and particularly have strong cooperation activities with steel producers and foundries, technology centers, research institutions, and original equipment manufacturers such as the Finnish Strategic Centres for Science, Technology and Innovation (SHOKs), Finnish Metals and Engineering Competence Cluster (FIMECC), Finnish universities and Finnish welding machines and equipment producers.

The execution of Arctic operations by members and affiliates of the Finnish Maritime Cluster include transportation, construction of ice-friendly structures and manufacturing

of other pertinent energy-efficient products. Within the shipbuilding and offshore industry, shipbuilding processes from concept development to product building has been a traditional Finnish strength [31]. However, the establishment of the whole infrastructures for Arctic operation thus necessitates corporate efforts from several interest groups. Currently, developmental and research activities on breakthrough steels, and hybrid materials for demanding applications such as for Arctic environments are ongoing within the facets of the Finnish Arctic maritime industry [33].

Taking a closer look, it is evident that the Finnish Arctic welding value chain is prominent within the networks of the Finnish Maritime Cluster. Thus, from the Finnish perspective, the development of structural products and the establishment of infrastructure in the Arctic environment are somewhat not technically and economically feasible without considering welding as a prime joining technique for diverse Arctic materials. This is so because there is high dependency among the industries and the cooperating institutions in aspects of welding research, technology and its implementation.

Considering Arctic welding value chain from international perspective, it appears that the Arctic region offers enormous welding business possibilities for both Arctic and non-Arctic nations, thus the Finnish Arctic welding value chain goes beyond this regard. It has become an open need for new business models to be developed for profit-sharing within the Arctic welding value chain through international cooperation and partnerships. Notably, the Finnish maritime cluster in its corporate activity to streamline and optimize new building processes based on modularity in design and production targets to reduce the build time for maritime products by 30% by 2020 [32]. Arctic welded products market trends would therefore transition from slow-to-market to fast-to-market within this paradigm shift. The creation of Arctic welding network value would support the productivity and optimization of welded products during the transition. The Finnish Maritime Cluster and its affiliates therefore serve as an effective international platform for businesses already involved in Arctic operations as well as new possible entrants to penetrate and involve immensely in the Arctic welding value chain for the development of the Arctic region. This network integration model as depicted in Figure 5 would facilitate more welding research and technology development activities towards the transformation of welding in the Arctic region. The Arctic Council in its effort to establishing a “task force” work group towards improving scientific research cooperation among the eight Arctic States [34] serves as a strong need for cooperation and partnership for the development of the Arctic region.

5 DISCUSSIONS

Welding in the Arctic cannot be fully elaborated without acknowledging the need to discuss materials suitable for constructing Arctic structures with regards to designing, efficient welding technologies, and cooperation and partnership networks for the development of the region.

As the Arctic region is known for its remote, harsh, and extremely cold climatic conditions, the selection of suitable materials, especially metals is paramount for the construction of Arctic structures. Beside the designing aspects, material properties of selected metals for Arctic structural applications demand to fulfill stringent requirements to prevent brittle fracture failures during operation. Studies show that HSS steels such as Q&T and TMCP steels have the suitable material properties considering their weldability and ability to withstand Arctic operating temperatures down to -40 °C [16, 20].

Nevertheless, the softening of the HAZ of TMCP more than Q&T steels as a factor of welding, which could be as a result of uncontrolled heat input and cooling rate parameters make Q&T steels more preferable [25]. Moreover, the material properties of Q&T steel grade E have proven to be suitable for operating in Arctic conditions down to -60 0C [20, 26]. This finding corroborates with Finnish technological know-how in utilizing such steel grade in constructing Arctic structures, for example ice-breakers. Although grade of filler materials were not explicitly indicated, the selection of appropriate filler materials to suit base materials is an obvious Finnish expertise considering the know-how in making exceptions for choices of materials for Arctic structural applications.

Obtaining a sound quality welded joint from suitably selected base and filler materials require utilizing efficient welding processes and techniques. Although suitable welding processes have been mentioned in this paper, the use of FCAW in welding HSS, i.e. Q&T steels has been satisfactory beyond research [20]. Adapting the use of FCAW, which is Finnish technological know-how to utilizing mechanization and automation in welding have indicated high productivity, cost reduction, and minimal-to-zero weld defects in welding production of Arctic structures.

Finland's welding technological know-how relevant to transforming the Arctic region spans through and across its Arctic maritime industry. Relaying on this and other Arctic technological know-how, the Finnish Arctic maritime industry needs to create effective business models to attract investments towards developing the Arctic region. Although Finland has indulged in cooperation and partnerships activities regarding shipbuilding and or construction of Arctic structures with countries such as Russia, Canada, China, USA, Norway and Germany in recent past [35], it is quite critical for Finland to reconsider new business models in Arctic welding while making efforts to protect and retain the intellectual property to Finland.

However, establishing cooperation and partnership networks among the eight Arctic states and other nations in aspects of research and business in Arctic welding would serve as a strong backbone to developing the Arctic region efficiently and economically. This issue cannot be overlook as the Arctic council also tries to push the agenda through its "task force" working group to address improving scientific research cooperation for the development of the Arctic region [34]. Nevertheless, Finland's strategy for the Arctic region [36] highlight to needs to develop the region through interdisciplinary research, thus making welding in the Arctic a more relevant issue in this present time.

6 CONCLUSIONS

In this paper, Finnish technological know-how relevant to transforming welding in the Arctic has been evaluated. With reference to a number of established research works, it is evident that the expertise and advanced technological know-how needed for accurate selection of materials and consumables, and utilization of suitable welding processes and techniques, which are requirements for Arctic structural constructions and development is Finland's strength, particularly in view of expertise and high quality in welding for low-temperature environments. In addition, the extensive and active network within and beyond Finland's Arctic maritime industry makes Finland a potential forerunner in Arctic welding business development. Additionally, it is such that Finland's position in Arctic operations is strong and thus serves as a safe and reliably bridge for other nations to participate in developing Arctic welding activities. Businesses interested in maximizing their market share and eager to broaden their international horizon should devise cooperation strategies with key members in the Finnish Arctic development framework to access other reliable networking possibilities so as to become part of the international Arctic welding value chain.

Emmanuel Afrane Gyasi, Markku Pirinen, & Jukka Martikainen - *Laboratory of Welding Technology, Department of Mechanical Engineering, Lappeenranta University of Technology, Finland.*

Matti Nallikari - *STX Finland, Arctech Helsinki Shipyard*

Emmanuel Afrane Gyasi is a researcher and affiliated to the welding department of Lappeenranta University of Technology in Finland. He has several years of work experience in the welding industry and has been involved in research and development activities for both onshore and offshore welding development. He is practically oriented in welding and has adequate knowledge in welding management applicable to the Arctic region.

As an incorporated engineer and a graduate member of The Welding Institute, his engineering competence is highly recommendable. His strong leadership capabilities make him the first president of the Ghanaian institute of welding.

REFERENCES

[1] Energy Information Administration (EIA), (2009), "Arctic Oil and Natural Gas Potentials".

[2] *Lancaster, J (1997), Handbook of Structural Welding: Processes, Materials and Methods Used in the Welding of Major Structures, Pipelines and Process Plant, Woodhead Publishing, pp 448.*

[3] *Knut, O.N., (2012), "The Arctic – A Region of Opportunities and Interest", Stiftelsen Det Norske Veritas Germanischer Lloyd (DNV.GL). [Online] http://www.dnv.com/industry/oil_gas/publications/updates/arctic_update/2012/01_2012/The_Arctic__a_region_of_opportunity_and_interest.asp. Accessed on 10.05.2014.*

[4] *Paananen, K. (2013), "Opportunities for Finland – the Arctic and Russia", Baltic Rim Economics. Quarterly Review 3, Expert Article 1267.*

[5] *Royal Dutch Shell plc, (2011), "Developing Arctic Oil and Gas". [Online] http://s04.static-shell.com/content/dam/shell/static/future-energy/downloads/arctic/developing-arcticoilandgas.pdf. Accessed on 15.05.2014.*

[6] *Nykänen, E. (1994), "Shipbuilding at Kvaerner Masa-Yards Helsinki New Shipyards". Hitsauatekniikka 5/94, pp 20-23.*

[7] *Viitanen, M. et al., (2003), "The Finnish Maritme Cluster", TEKES Technology Review 145/2003, ISSN 1239-758X. Paino-Center Oy, Helsinki.*

[8] *Serreze, M.C. and Barry, R.G., (2005), "The Arctic Climate System, Cambridge University Press, pp 385.*

[9] *Gorynin, I.V. et al., (2007), "Alloyinh Principles, Phase Transformation, Structure and Properties of Low-temperature Weldable Ship building Steels", Metal Science and Heat Treatment, Vol 49, No. 1-2, pp 3-9.*

[10] *Odessey, P.D., (2006), " Microalloying of Steels for the North and Unique Metal Structures (in Russia), Intermet Engineering, pp 176.*

[11] *Przybylak, R., (2003), "The Climate of the Arctic, Springer, pp 288.*

[12] *Kaushish, J.P., (2008), "Manufacturing Processes, PHI Learning Pvt. Ltd, pp 1007.*

[13] *Anderson, T.L. and McHenry, H.I., (1982), " Interim Progress Report: Fracture Toughness of Steel Weldments for Arctic Structures, NBSIR 83-16980, Fracture and Deformation Division National Measurement Laboratory, National Bureau of Standard, US Department of Commerce, Boulder, Colorado 80303.*

[14] *KOBELCO, "CTOD", (2005), KPBELCO Welding Today, Vol 8, No. 1.*

[15] *SFS-EN 1993-1-1. 2005. Eurocode 3: Design of Steel Structures. Part 1-1: General Rules and Rules for Building. Finnish Standards Association, Helsinki.*

[16] *Billingham, J. and Sharp, J.V., (2003), "Review of the Performance of High Strength Steels used Offshore" Research Report 105. Cranfield University School of Industrial and Manufacturing Science, pp 3*

[17] *Hill, P. M., (1991), "Cutting and welding in naval construction", Welding and Metal Fabrication, pp 63-72*

[18] *Dainelli, P. and Maltrud, F., (2012), "Management of Welding Operations with High Strength Steels", Etudes Et Recherche, Institut de Soudure, pp 37.*

[19] *Ruuki Metals, (2007), "Hot Rolled Steel Plates, Sheets and Coils – Processing of Materials- Impact strength and through thickness properties, Helsinki.*

[20] *WTIA TN 15 1999e, Welding Technology Institute of Australia, "Quenched and Tempered Steels", Milsons Point.*

[21] *Daidola, J.C. et al., (1996), "Residual Strength Assessment of Pitted Plate Panels", Ship Structure Committee, Report Number SSC-394, Washington, DC.*

[22] *Kim, K.N., et al., (2009), "Evaluation of Factors Affecting the Fatigue Behavior of Butt-Welded Joints using SM520C-TMC Steel", International Journal of Steel Structures, Vol. 9, pp. 185-193.*

[23] *Nippon Steel and Sumitomo Metal, (2014), "Steel Plates" A001en_04_2014f. Nippon Steel and Sumitomo Mteal Corporation, Japan. [online] http://www.nssmc.com/product/catalog_download/pdf/A001en.pdf. Accessed 13.05.2014.*

[24] *Rodrigues, D.M. et al., (2004), "The Influence of the HAZ Softening on the Mechanical Behaviour of Welded Joints Containing Cracks in the Weld Metal". Engineering Fracture Mechanics, 71, Issue 13-14, pp 2053-2064.*

[25] *Pirinen, M., (2013), "The Effects of Welding Heat Input on the Usability of High Strength Steels in Welded Structures". Doctor of Science Thesis, Lappeenranta University of Technology, Lappeenranta, Finland.*

[26] *Russian Maritime Register of Shipping, (2012), "Rules for the Classification, Construction and Equipment of Mobile Offshore Drilling Units and Fixed Offshore Platforms.*

[27] *Porter, D., (2006), "Development in Hot-Rolled High-Strength Steel", Nordic Welding Conference 06. New Trends in Welding Technology, Tampere, Finland.*

[28] *Kah, P., et al., (2014), "Welding of Ultra High Strength Steels", Advanced Materials Research, Vol. 849, pp 357-365.*

[29] *Aderinola, O.O. et al., (2013), "Efficient Welding Technologies Applicable to HSS Arctic Offshore Structures", Proceedings of the Twenty-third International Offshore and Polar Engineering Anchorage, Alaska, USA, pp 257-264.*

[30] *Billingham, J. et al., (1998), "Further Assessment of High Strength Weld Metals for use in Offshore Engineering Applications". Cranfield Finla Report, pp 30.*

[31] *Arpiainen, M. et al., (2001), "Model Tests with Icebreaking Barges for Operation in the Northern Caspian Sea", POAC 2001, Ottawa. [Online] http://www.akerarctic.fi/publications/pdf/Poac01XModel Barges.pdf. Accessed on 05.05.2014.*

[32] *Meriteollisuus, Smart Maritime Technology Solution – Strategic Research Agenda for Finnish Maritime Cluster 2014-2020. [Online] http://www.teknologiateollisuus.fi/file/15518/strategic_research_agenda.pdf.html. Accessed on 04.05.2014.*

[33] *Heino, M., (2013), "Breakthorugh Steels and Applications", Finnish Metals and Engineering Competence Cluster.*

[34] *Arctic Council, (2014), "Interview from the Scientific Cooperation Task Force Meeting". [Online] http://www.arctic-council.org/index.php/en/resources/news-and-press/news-archive/871-interview-from-the-scientific-cooperation-task-force-meeting. Accessed on 20.05.2014.*

[35] *Aker Arctic Technology Inc, (2013), "The state of Finland Acquires Majority of Shares in Aker Arctic Technology INC", Press Release, Helsinki.*

[36] *Finland's Strategy for the Arctic Region 2013. Government Resolution on 23 August 2013. Prime Minister's Publication 16/2013. ISBN (PDF) 978-952-287-062-9.*

ACTA UNIVERSITATIS LAPPEENRANTAENSIS

767. KASURINEN, HELI. Identifying the opportunities to develop holistically sustainable bioenergy business. 2017. Diss.

768. KESKISAARI, ANNA. The impact of recycled raw materials on the properties of wood-plastic composites. 2017. Diss.

769. JUKKA, MINNA. Perceptions of international buyer-supplier relational exchange. 2017. Diss.

770. BAYGILDINA, ELVIRA. Thermal load analysis and monitoring of doubly-fed wind power converters in low wind speed conditions. 2017. Diss.

771. STADE, SAM. Examination of the compaction of ultrafiltration membranes with ultrasonic time-domain reflectometry. 2017. Diss.

772. KOZLOVA, MARIIA. Analyzing the effects of a renewable energy support mechanism on investments under uncertainty: case of Russia. 2017. Diss.

773. KURAMA, ONESFOLE. Similarity based classification methods with different aggregation operators. 2017. Diss.

774. LYYTIKÄINEN, KATJA. Removal of xylan from birch kraft pulps and the effect of its removal on fiber properties, colloidal interactions and retention in papermaking. 2017. Diss.

775. GAFUROV, SALIMZHAN. Theoretical and experimental analysis of dynamic loading of a two-stage aircraft engine fuel pump and methods for its decreasing. 2017. Diss.

776. KULESHOV, DMITRII. Modelling the operation of short-term electricity market in Russia. 2017. Diss.

777. SAARI, JUSSI. Improving the effectiveness and profitability of thermal conversion of biomass. 2017. Diss.

778. ZHAO, FEIPING. Cross-linked chitosan and β-cyclodextrin as functional adsorbents in water treatment. 2017. Diss.

779. KORHONEN, ILKKA. Mobile sensor for measurements inside combustion chamber – preliminary study. 2017. Diss.

780. SIKIÖ, PÄIVI. Dynamical tree models for high Reynolds number turbulence applied in fluid-solid systems of 1D-space and time. 2017. Diss.

781. ROMANENKO, ALEKSEI. Study of inverter-induced bearing damage monitoring in variable-speed-driven motor systems. 2017. Diss.

782. SIPILÄ, JENNI. The many faces of ambivalence in the decision-making process. 2017. Diss.

783. HAN, MEI. Hydrodynamics and mass transfer in airlift bioreactors; experimental and numerical simulation analysis. 2017. Diss.

784. ESCALANTE, JOHN BRUZZO. Dynamic simulation of cross-country skiing. 2017. Diss.

785. NOKKA, JARKKO. Energy efficiency analyses of hybrid non-road mobile machinery by real-time virtual prototyping. 2018. Diss.

786. VUORIO, ANNA. Opportunity-specific entrepreneurial intentions in sustainable entrepreneurship. 2018. Diss.

787. PULKKINEN, AKI. Towards a better understanding of activity and selectivity trends involving K and O adsorption on selected metal surfaces. 2017. Diss.

788. ZHAO, WENLONG. Reliability based research on design, analysis and control of the remote handling maintenance system for fusion reactor. 2018. Diss.

789. IAKOVLEVA, EVGENIA. Novel sorbents from low-cost materials for water treatment. 2018. Diss.

790. KEDZIORA, DAMIAN. Service offshoring industry: systems engineering approach to its transitional challenges. 2018. Diss.

791. WU, JING. Soft computing methods for performance improvement of EAMA robot in fusion reactor application. 2018. Diss.

792. VOSTATEK, PAVEL. Blood vessel segmentation in the analysis of retinal and diaphragm images. 2018. Diss.

793. AJO, PETRI. Hydroxyl radical behavior in water treatment with gas-phase pulsed corona discharge. 2018. Diss.

794. BANAEIANJAHROMI, NEGIN. On the role of enterprise architecture in enterprise integration. 2018. Diss.

795. HASHEELA-MUFETI, VICTORIA TULIVAYE. Empirical studies on the adoption and implementation of ERP in SMEs in developing countries. 2018. Diss.

796. JANHUNEN, SARI. Determinants of the local acceptability of wind power in Finland. 2018. Diss.

797. TEPLOV, ROMAN. A holistic approach to measuring open innovation: contribution to theory development. 2018. Diss.

798. ALBATS, EKATERINA. Facilitating university-industry collaboration with a multi-level stakeholder perspective. 2018. Diss.

799. TURA, NINA. Value creation for sustainability-oriented innovations: challenges and supporting methods. 2018. Diss.

800. TALIKKA, MARJA. Recognizing required changes to higher education engineering programs' information literacy education as a consequence of research problems becoming more complex. 2018. Diss.

801. MATTSSON, ALEKSI. Design of customer-end converter systems for low voltage DC distribution from a life cycle cost perspective. 2018. Diss.

802. JÄRVI, HENNA. Customer engagement, a friend or a foe? Investigating the relationship between customer engagement and value co-destruction. 2018. Diss.

803. DABROWSKA, JUSTYNA. Organizing for open innovation: adding the human element. 2018. Diss.

804. TIAINEN, JONNA. Losses in low-Reynolds-number centrifugal compressors. 2018. Diss.

Acta Universitatis
Lappeenrantaensis
805

LUT
Lappeenranta
University of Technology

ISBN 978-952-335-251-3
ISBN 978-952-335-252-0 (PDF)
ISSN-L 1456-4491
ISSN 1456-4491
Lappeenranta 2018